# A DETAILED MECHANISTIC INVESTIGATION OF THE EXOGLYCANASE FROM *CELLULOMONAS FIMI*

By

DEDREIA TULL

B. Sc., McGill University, 1989

M. Sc., University of British Columbia, 1991

A THESIS SUBMITTED IN PARTIAL FULFILLMENT OF

THE REQUIREMENTS FOR DEGREE OF

DOCTOR OF PHILOSOPHY

in

THE FACULTY OF GRADUATE STUDIES

**DEPARTMENT OF CHEMISTRY**

We accept this thesis as conforming

to the required standard:

THE UNIVERSITY OF BRITISH COLUMBIA

July, 1995

In presenting this thesis in partial fulfilment of the requirements for an advanced degree at the University of British Columbia, I agree that the Library shall make it freely available for reference and study. I further agree that permission for extensive copying of this thesis for scholarly purposes may be granted by the head of my department or by his or her representatives. It is understood that copying or publication of this thesis for financial gain shall not be allowed without my written permission.

(Signature)

Department of CHEMISTRY

The University of British Columbia
Vancouver, Canada

Date AUG 4/95

DE-6 (2/88)

## ABSTRACT

The exoglycanase from *Cellulomonas fimi* catalyses the hydrolysis of cello-oligosaccharides to cellobiose as well as the hydrolysis of xylan and aryl β-glycosides (Gilkes et al (1984) *J. Biol. Chem. 259*, 10455). Its mechanism of action is thought to involve a double displacement reaction which is investigated here through detailed kinetic studies of the native enzyme and point mutants with a range of aryl β-glycosides, and through inactivation studies with 2-deoxy- and 2-deoxyfluoro-glycoside mechanism-based inactivators and the affinity label, *N*-bromoacetyl cellobiosylamine.

A pH study of the native enzyme revealed ionisations of $pK_a$ = 4.1 and 7.7 in the free enzyme, likely corresponding to the catalytic nucleophile and the acid-base catalyst, respectively. The large secondary deuterium kinetic isotope effects measured on both steps for the glucosides and on the deglycosylation step for the cellobiosides reveal significant oxocarbonium ion character at the corresponding transition states, thus suggesting substantial C-O bond cleavage and little nucleophilic preassociation. By contrast, the relatively small secondary deuterium kinetic isotope effect and the small Broensted constant measured on the glycosylation step for the cellobiosides suggest that the cellobiosylation transition state is less highly charged than the glucosylation transition state. These studies suggest that the primary function of the distal glucosyl moiety of the cellobiosides is to increase the rate of glycosylation, likely through improved acid catalysis and greater nucleophile preassociation, without affecting its rate of deglycosylation. The greater rates of hydrolysis of the xylo-sugars, relative to those for the gluco-sugars, indicate that the substrate preference of *C. fimi* exoglycanase increases in the order glucosides < xylosides < cellobiosides < xylobiosides and that the C-5 hydroxymethyl group is slightly inhibitory to catalysis. The role of the C-2 hydroxyl group was probed using 2,4-dinitrophenyl 2-deoxy-2-fluoro cellobioside (2F-DNPC) and cellobial (a 2-deoxycellobiose analogue). Rates of hydrolysis of the 2-deoxyfluorocellobiosyl- and 2-deoxycellobiosyl-enzymes are $10^7$ and $10^6$-fold lower respectively, than that for the cellobiosyl-enzyme, indicating that the

C-2 hydroxyl group is necessary for catalysis and that it contributes a minimum of ~9 kcal/mole of stabilisation energy to the transition state.

Electrospray ionisation mass spectrometry (ESI-MS) of the 2F-DNPC-inactivated enzyme provided evidence for the covalent nature of the glycosyl-enzyme intermediate while $^{19}F$ NMR analysis of this 2FCb-enzyme and the 2-deoxy-2-fluoro 4-O-(β-glucosyl)-β-mannosyl fluoride (2F-GMF) -inactivated enzyme provided evidence for the α- anomeric stereochemistry of the intermediate.

The catalytic nucleophile involved in *C. fimi* exoglycanase-catalysed hydrolysis of the cellobiosides was identified as Glu 233 by use of tandem MS techniques and 2F-DNPC and cellobial. Kinetic analysis of the Glu233Asp mutant revealed that pulling the catalytic nucleophile 1 Å away from the reacting anomeric centre reduces the rates of glycosylation and deglycosylation ~4 x $10^3$-fold.

ESI-MS analysis of N-bromoacetyl cellobiosylamine-inactivated *C. fimi* exoglycanase reveals that one mole of N-acetyl cellobiosylamine is incorporated per mole of enzyme. The labeled residue was identified as Glu 127 by use of a combination of MS techniques. This residue has recently been suggested to be the acid-base catalyst based on kinetic analysis of mutants (MacLeod et al (1994) *Biochemistry 33*, 6571). More detailed kinetic analysis of the Glu127Ala mutant revealed rate reductions of 200-300 fold on the deglycosylation step while the rate reductions on the glycosylation step are dependent on the leaving group ability of the phenolate. The larger Broensted constant seen with the Glu127Ala mutant compared to that for the native enzyme reflects greater negative charge accumulation on the leaving phenolate at the glycosylation transition state for the Glu127Ala mutant. These results are consistent with the role of Glu 127 as the acid-base catalyst.

These structural findings are completely consistent with the recently solved X-ray crystal structure of the catalytic domain of *C. fimi* exoglycanase (White et al (1994) *Biochemistry 33*, 12546).

# TABLE OF CONTENTS

## LIST OF TABLES

## LIST OF FIGURES

## LIST OF ABBREVIATIONS AND DEFINITIONS

### Glucosides

| | |
|---|---|
| 2,4-DNPG | 2,4-Dinitrophenyl β-D-glucoside |
| 2Cl,4NPG | 2-Chloro-4-nitrophenyl β-D-glucoside |
| 3,4-DNPG | 3,4-Dinitrophenyl β-D-glucoside |
| 2,5-DNPG | 2,5-Dinitrophenyl β-D-glucoside |
| PNPG | 4-Nitrophenyl β-D-glucoside |

### Cellobiosides

| | |
|---|---|
| 2,4-DNPC | 2,4-Dinitrophenyl β-cellobioside |
| 3,4-DNPC | 3,4-Dinitrophenyl β-cellobioside |
| 2,5-DNPC | 2,5-Dinitrophenyl β-cellobioside |
| PNPC | 4-Nitrophenyl β-cellobioside |
| ONPC | 2-Nitrophenyl β-cellobioside |
| 3,5-DClPC | 3,5-Dichlorophenyl β-cellobioside |
| 4-CNPC | 4-Cyanophenyl β-cellobioside |
| 4-BrPC | 4-Bromophenyl β-cellobioside |

### Xylosides

| | |
|---|---|
| 2,3-DNPX | 2,3-Dinitrophenyl β-D-xyloside |

| | |
|---|---|
| 2,5-DNPX | 2,5-Dinitrophenyl β-D-xyloside |
| 3,4-DNPX | 3,4-Dinitrophenyl β-D-xyloside |
| PNPX | 4-Nitrophenyl β-D-xyloside |
| 4-CNPX | 4-Cyanophenyl β-D-xyloside |

**Xylobiosides**

| | |
|---|---|
| 2,5-DNP$X_2$ | 2,5-Dinitrophenyl β-xylobioside |
| 3,4-DNP$X_2$ | 3,4-Dinitrophenyl β-xylobioside |
| P$NPX_2$ | 4-Nitrophenyl β-xylobioside |
| O$NPX_2$ | 2-Nitrophenyl β-xylobioside |

**Inactivators**

| | |
|---|---|
| 2F-DNPG | 2,4-Dinitrophenyl 2-deoxy-2-fluoro-β-D-glucoside |
| 2F-DNPGal | 2,4-Dinitrophenyl 2-deoxy-2-fluoro-β-D-galactoside |
| 2F-DNPC | 2,4-Dinitrophenyl 2-deoxy-2-fluoro-β-cellobioside |
| 2F-GMF | 2-Deoxy-2-fluoro 4-O-(β-glucosyl)-β-mannosyl fluoride |
| 2F-DNP$X_2$ | 2,4-Dinitrophenyl 2-deoxy-2-fluoro-β-xylobioside |
| 2FCb- | 2-Deoxy-2-fluoro-cellobiosyl- |
| 2FGM- | 2-Deoxy-2-fluoro 4-O-(β-glucosyl)-β-mannosyl- |
| 2dCb- | 2-Deoxy-cellobiosyl- |
| 2F$X_2$- | 2-Deoxy-2-fluoro-xylobiosyl- |

| | |
|---|---|
| N-BrAc-$CbNH_2$ | *N*-Bromoacetyl β-cellobiosylamine |
| BGTX | Benzyl 4-O-(β-glucosyl)-1-thio-β-D-xyloside |

**Amino acids**

| | |
|---|---|
| Ala | Alanine |
| Arg | Arginine |
| Asn | Asparagine |
| Asp | Aspartic Acid |
| Glu | Glutamic Acid |
| Ile | Isoleucine |
| Leu | Leucine |
| Thr | Threonine |
| Val | Valine |

**Enzymes**

| | |
|---|---|
| *C. fimi* | *Cellulomonas fimi* |
| *E. coli* | *Escherichia coli* |
| BSA | Bovine serum albumin |

**Kinetic and physical constants**

| | |
|---|---|
| $K_d$ | Dissociation constant for a substrate-enzyme complex |
| $K_m$ | Michaelis constant |
| $K_i$ | Dissociation constant for an inactivator-enzyme complex |
| $V_m$ | Maximal reaction velocity |
| $k_{cat}$ | Catalytic rate constant |
| $k_{obs}$ | Pseudo-first order rate constant |
| $k_2$ | Glycosylation rate constant |

| | |
|---|---|
| $k_3$ | Deglycosylation rate constant |
| $k_i$ | First-order rate constant for inactivation |
| $\beta_{1g}$ | Broensted constant |
| T | Temperature (K) |
| **k** | Boltzmann constant |
| h | Planck's constant |

**Others**

| | |
|---|---|
| m. p. | Melting point |
| TLC | Thin layer chromatography |
| NMR | Nuclear magnetic resonance |
| RP-HPLC | Reverse-phase high performance liquid chromatography |
| MS | Mass spectrometry |
| ESI-MS | Electrospray ionisation mass spectrometry |
| ESI-MS/MS | Electrospray ionisation tandem mass spectrometry |
| TIC | Total ion chromatogram |
| m/z | Mass to charge ratio |
| 311 PITC | 4-(3-Pyridinylmethyl-aminocarboxypropyl) Phenyl isothiocyanate |
| PTH | Phenylthiohydantoin |

## GLOSSARY

| | |
|---|---|
| Cellulases: | cellulolytic enzymes responsible for catalysing the conversion of cellulose to glucose. |
| Endoglucanases: | enzymes that catalyse the hydrolysis of cellulose to cello-oligosaccharides by cleaving relatively randomly along the cellulose chain. |
| Exoglucanases: | enzymes that catalyse the hydrolysis of cello-oligosaccharides and cellulose to cellobiose from either the non-reducing or reducing ends. |
| Exoglycanases: | enzymes that catalyse the hydrolysis of oligosaccharides and polysaccharides |
| Xylanases: | enzymes that catalyse the hydrolysis of xylan. |

## ACKNOWLEDGEMENTS

I wish to express my deepest appreciations to my supervisor, Dr. Stephen G. Withers, for his help and guidance throughout the time of this research. Thanks also to my coworkers for their helpfull discussions, allowing me to use the compounds they pains-takingly sythesised, and especially for their friendships. Special thanks to Ms. Karen Rupitz and Dr. Qingping Wang for technical assistance, to Dr. Shichang Miao, Dr. David Burgoyne and Mr. David Chow for performing the mass spectrometric analysis as well as to Dr. Lawrence McIntosh for performing $^{19}$F-NMR analysis of the protein samples. I would like to thank the NMR and elemental analysis staff of the Department of Chemistry for all their help and advise. Thanks to Drs. R. Aebersold (Department of Molecular Biotechnology, University of Washington), A. Warren, D. Kilburn and N. Gilkes (Department of Microbiology, University of British Columbia) as well as Dr. David Rose and Mr. Andre White (Department of Medical Biophysics, University of Toronto) for collaborating on this project.

Thanks to the University of British Columbia and Natural Sciences and Engineering Research Council of Canada for financial support. Special thanks to the Protein Engineering Network Centres of Excellence (PENCE) for funding such an exciting project and providing me with opportunities to attend several enlightening and informative conferences.

Thanks to my family and all my friends for their support and encouragement.

For VH, LT, HT, RT, NT, CT and AAM,
and for "Women Who (dare to) Run With
The Wolves" (C. P. Estés).

# CHAPTER I

# GENERAL INTRODUCTION

## 1-1 Glycosidases

Glycosidases are enzymes that catalyse the hydrolysis of the glycosidic linkage between two sugar residues (Figure 1-1). Interest in these enzymes has escalated in recent years due to their potential applications in many areas of industry, for example cellulases in biomass degradation and textiles, xylanases in the pulp and paper industry and of course amylases in the food and beverage industries.

Substrates for glycosidases are made up of two parts, a glycone portion and an aglycone portion (Figure 1-1). The aglycone portion in most natural substrates is another sugar residue, however since most of these enzymes are less specific for the aglycone than the glycone, this sugar can often be replaced by an alkyl or aryl group. This allows for the use of chromogenic substrates, making kinetic analysis of these enzymes more convenient.

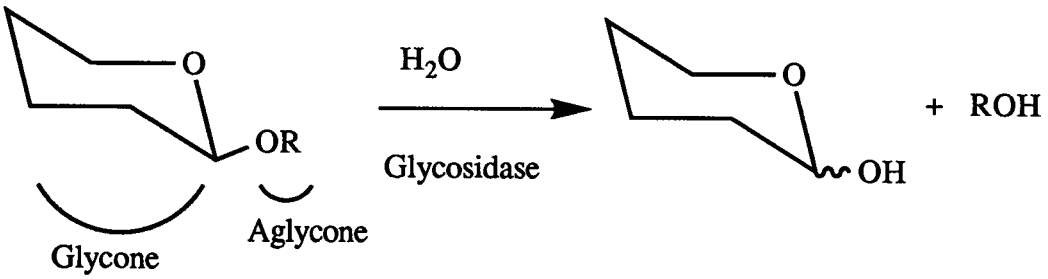


*Figure 1-1 Hydrolysis of glycosides by glycosidases.*

## 1-2 Classification of Glycosidases

Glycosidases constitute a large class of enzymes which is subdivided into smaller groups based on three features.

(1) The glycone to which it is reactive; for example a galactofuranosidase or a mannopyranosidase. However, it should be noted that although a glycosidase may be reactive against a variety of substrates, the enzyme is generally classified based on the sugar against which it is the most reactive.

(2) The anomeric configuration (α or β) of the glycosidic linkage that is to be cleaved. For example, a β-glucosidase will only catalyse the hydrolysis of β-glucosides and not α-glucosides (Figure 1-2).

(3) The relative anomeric configuration of the substrate *versus* the initial glycone product that is, if the anomeric configurations of the substrate and the initial product are the same then the enzyme is classified as a "retaining" glycosidase whereas if the anomeric configurations are different, then the enzyme is termed "inverting" (Figure 1-3).

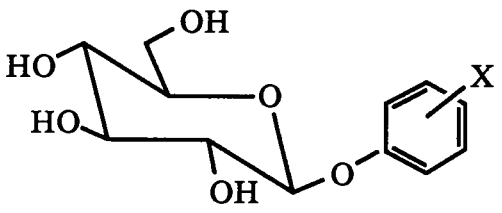


β-Glucoside

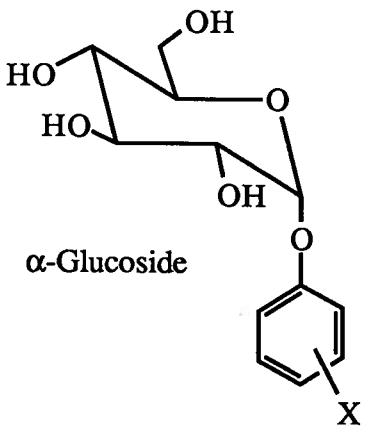


α-Glucoside

*Figure 1-2 Examples of α and β anomers of an aryl glucoside.*

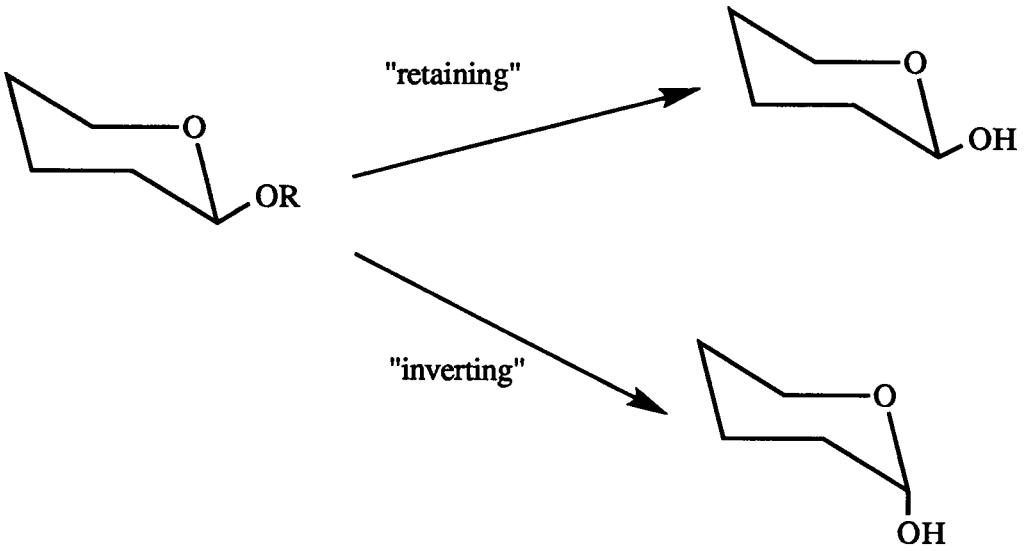


*Figure 1-3 Stereochemical classification of glycosidases.*

## 1-3 Cellulases

Cellulose, the most abundant material in nature, is a carbohydrate polymer made up of glucose units connected by β–(1-4) linkages. Conversion of cellulose to glucose is achieved by a cellulase complex which is composed of three types of glycosidases: endo-1,4-β-glucanases (endoglucanase, EC 3.2.1.4), exo-1,4-β-glucanases (cellobiohydrolase, EC 3.2.1.91) and β-glucosidases (cellobiase, EC 3.2.1.21). These enzymes are produced by a variety of organisms including microorganisms and plants. These enzymes can be individually secreted by the organism, as is the case for most fungal cellulases. In some cases the excreted cellulases can be organized into supramolecular structures called cellulosomes as is found in some bacterial cellulases. The cellulase complex is known to catalyse the hydrolysis of cellulose synergistically, although the detailed mechanism of this synergism is not well understood. The role of each individual glycosidase in the complex is the following. The endoglucanase catalyses the random cleavage of the cellulose into oligosaccharides, the exoglucanase then converts the oligosaccharides into cellobiose, generally cleaving from the non-reducing end and finally the β-glucosidase catalyses the

hydrolysis of cellobiose to glucose (Figure 1-4). Many cellulases have been isolated from a variety of organisms, cloned, sequenced and divided into families based on sequence similarity of their catalytic domains (Henrissat et al., 1989; Gilkes et al.; 1991; Henrissat & Bairoch, 1993). These families of glycanases also include a number of xylanases.

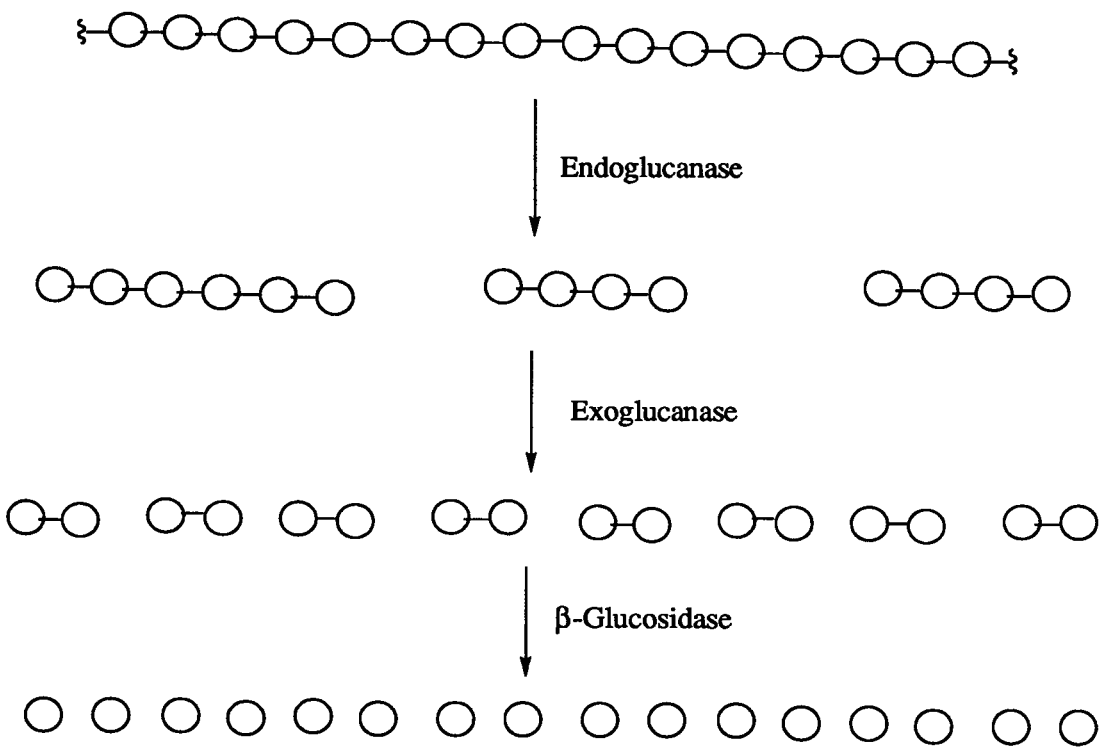


*Figure 1-4* *Schematic representation of the degradation of cellulose to glucose by the cellulase complex.*

Many cellulases are composed of at least two distinct domains; a catalytic domain and a cellulose-binding domain which are joined together by a linker region. The three-dimensional structures of the catalytic domains of a number of these cellulases have recently been determined by X-ray crystallography and these are shown in Table 1-1. Other structural information on these proteins includes the $^{1}$H-NMR structure of the cellulose-binding domain of *Trichoderma reesei* cellobiohydrolase II (Rouvinen et al., 1990) and that

of *Cellulomonas fimi* (Xu et al, 1995) as well as the tadpole-like structures of intact endoglucanase A and intact exoglycanase from *Cellulomonas fimi* as revealed by low angle X-ray studies (Pilz et al., 1990). Additional structural information has been derived from labeling studies of these enzymes with affinity labels and mechanism-based inactivators and thus has lead to the identification of catalytically important residues (discussed in Chapter IV).

Table 1-1: Cellulases for which the X-ray crystal structures have been solved.

| Cellulase | Organism | Reference |
|---|---|---|
| Cellobiohydrolase II | *Trichoderma reesei* | (Rouvinen et al, 1990) |
| Endoglucanase D | *Clostridium thermocellum* | (Juy et al., 1992) |
| Endocellulase $E_2$ | *Thermomonospora fusca* | (Spezio et al., 1993) |
| Endoglucanase V | *Humicola insolens* | (Davies et al., 1993) |
| 1,3-1,4-Glucanase | *Bacillus sp.* | (Keitel et al., 1993) |
| 1,3-Glucanase G II | *Barley* | (Varghese et al., 1994) |
| 1,3-1,4-Glucanase E II | *Barley* | (Varghese et al, 1994) |
| Exoglycanase | *Cellulomonas fimi* | (White et al., 1994) |
| Cellobiohydrolase I | *Trichoderma reesei* | (Divne et al., 1994) |

## 1-4 The Exoglycanase from *Cellulomonas fimi*

The enzyme used in this investigation is the exoglycanase from the soil bacterium, *Cellulomonas fimi*. The gene encoding the exoglycanase (Cex) has been cloned, expressed in *E. coli* and subsequently sequenced (O'Neill et al., 1986). The *C. fimi* exoglycanase is a 47 kDa protein comprising two domains which are separable by limited proteolysis into an active catalytic domain of 35 kDa and a cellulose-binding domain (~12 kDa) which binds cellulose and chitin (Ong et al., 1993) (Figure 1-5). These two domains are held together

by a linker region rich in proline and threonine residues. The 35 kDa catalytic domain is capable of catalysing the hydrolysis of small substrates (e.g. aryl β-cellobiosides), but cannot bind cellulose. *C. fimi* exoglycanase is a member of Family 10 (Henrissat & Bairoch, 1993) of β–glycanases, a group which also contains 8 xylanases. The three-dimensional structure of the catalytic domain of this enzyme has recently been solved by X-ray crystallography to 1.8 Å resolution (Figure 1-6) (White et al, 1994). The catalytic domain folds into an α/β–barrel containing eight parallel β-strands. There is an open cleft at the carboxyl terminal end and this is proposed to be the active site.

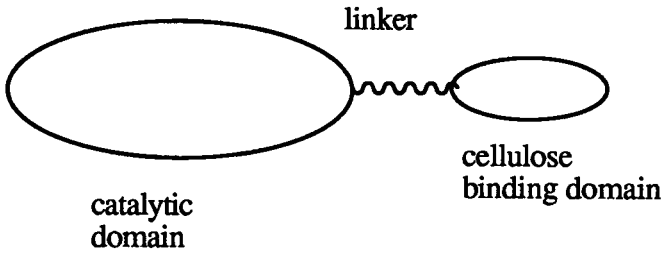


*Figure 1-5 Schematic representation of the structure of intact C. fimi exoglycanase.*

Previous investigations of the substrate specificity of *C. fimi* exoglycanase revealed it to be capable of hydrolysing cellulose (Figure 1-7, R = $CH_2OH$), xylan (Figure 1-7, R = H) (Gilkes et al., 1984) and small substrates such as aryl β-xylobiosides, aryl β-cellobiosides and aryl β-D-glucopyranosides (Tull et al., 1991). Analysis of the stereochemical outcome of the hydrolysis of glycosides by *C. fimi* exoglycanase using $^1H$-NMR revealed it to be a "retaining" glycosidase (Withers et al., 1986).

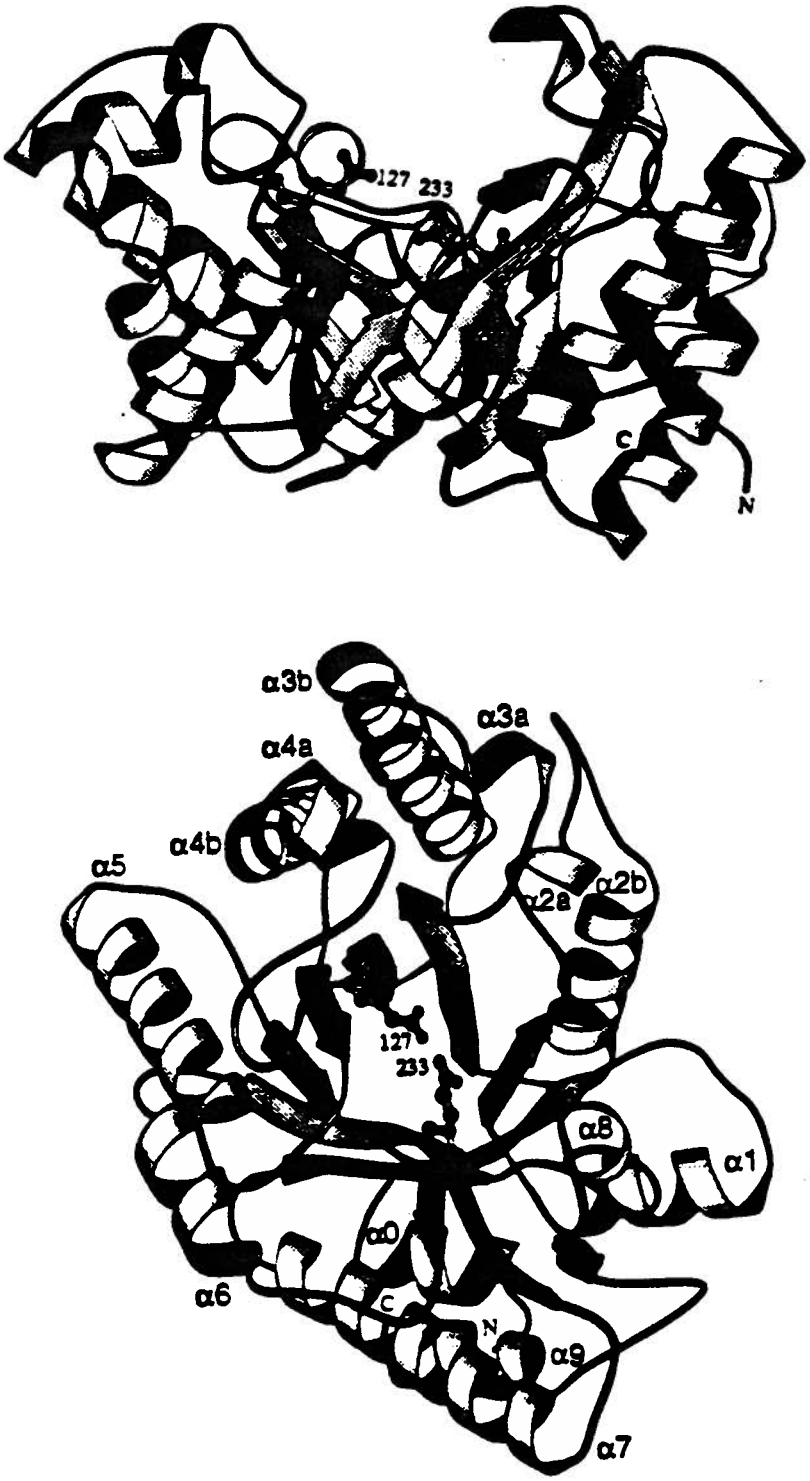


*Figure 1-6* *The X-ray crystal structure of the catalytic domain of C. fimi exoglycanase (White et al., 1994).*

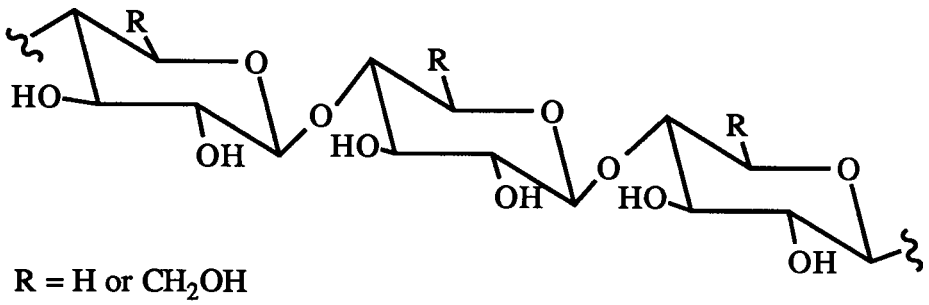


*Figure 1-7 Structure of xylan and cellulose.*

Two mechanisms put forth to describe the action of "retaining" glycosidases are a double displacement mechanism (Koshland, 1953) and a ring opening reaction (Capon, 1969; Post & Karplus, 1986). In recent years however, there has been an explosion of experimental evidence in support of the double displacement mechanism (see review by Sinnott, 1990) while the latter mechanism still lacks serious experimental support. This double displacement mechanism for *C. fimi* exoglycanase is illustrated in Figure 1-8. The first step involves displacement of the aglycone by an appropriately positioned carboxylate nucleophile in the active site to form an α-glycosyl-enzyme intermediate. In a second step, the intermediate is hydrolysed to yield β-cellobiose as the initial product and to regenerate the free enzyme. Both formation and hydrolysis of the glycosyl-enzyme intermediate occur via oxocarbonium ion-like transition states. Initial C-O bond cleavage is proposed to occur with acid assistance from an appropriately located carboxylic acid residue while hydrolysis of the intermediate occurs with general base catalysis from the same residue. It has also been suggested that most of the observed rate acceleration is expected to be derived from the non-covalent interactions between the enzyme and the substrate and its transition states.

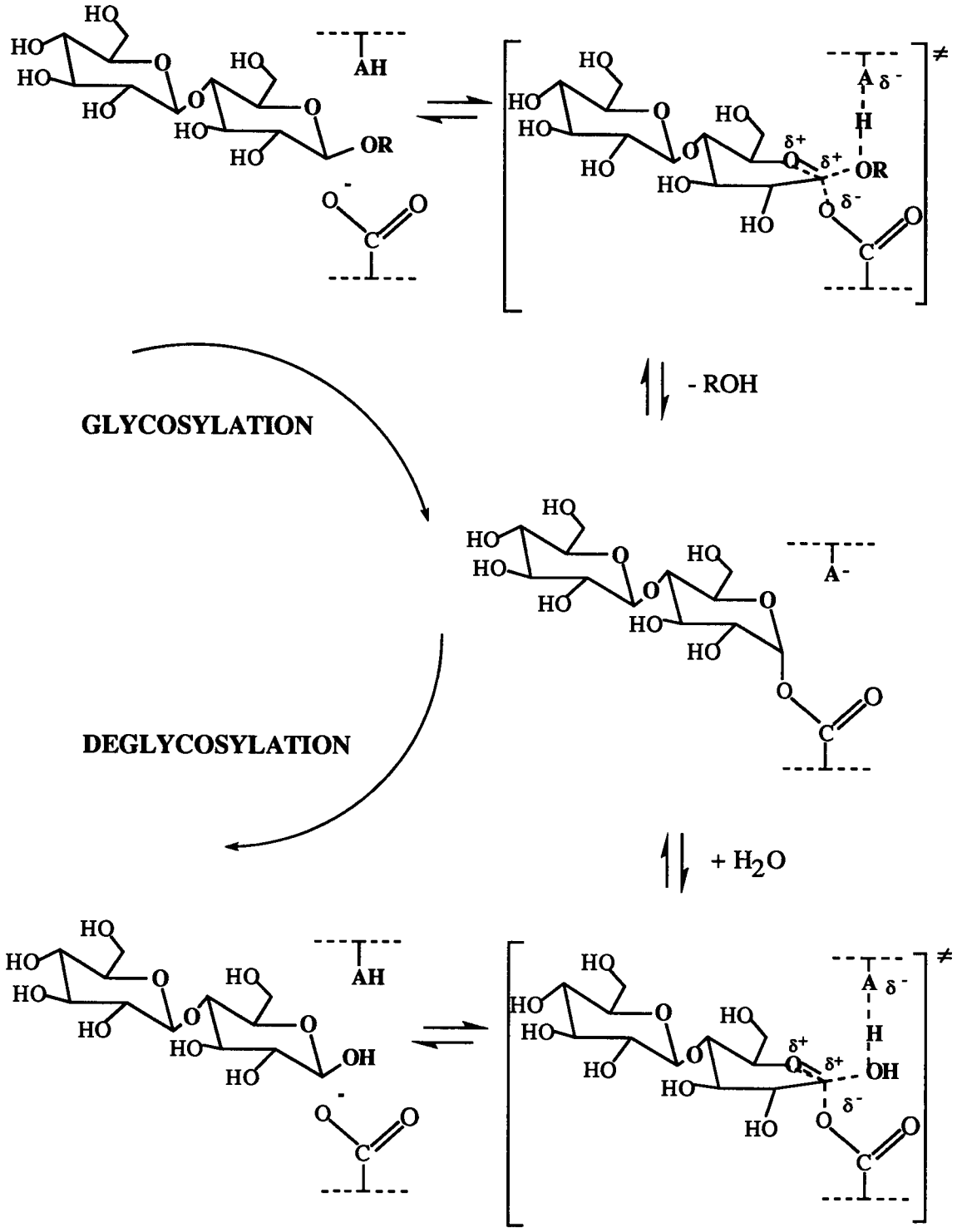


*Figure 1-8 Double displacement mechanism proposed for C. fimi exoglycanase.*

## 1-5 Mechanism Of "Retaining" Glycosidases: Evidence For A Double Displacement Mechanism

The large quantity of experimental evidence in support of several features of a double displacement mechanism for "retaining" glycosidases including *C. fimi* exoglycanase is discussed below.

### 1-5-1 Presence of a carboxylate nucleophile

Some of the most compelling evidence for the presence of an enzymic nucleophile is derived from X-ray crystallographic studies. The earliest evidence came from X-ray crystallographic studies of hen egg white lysozyme which is responsible for catalysing the hydrolysis of the peptidoglycan component of bacterial cell walls (Figure 1-9).

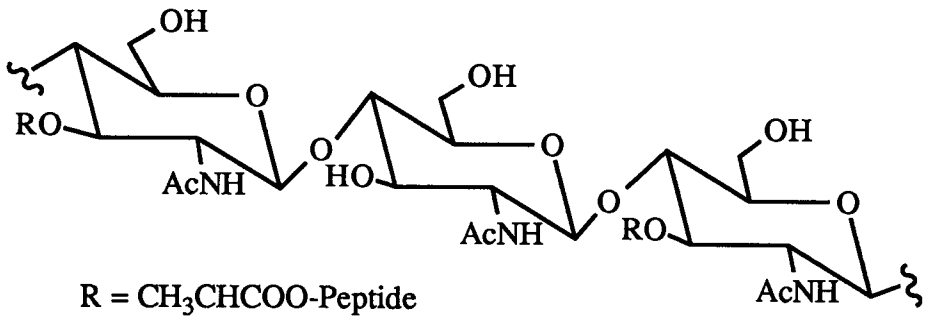


*Figure 1-9 The peptidoglycan substrate for lysozyme.*

The three-dimensional structure of hen egg white lysozyme (HEWL) identified carboxylate groups corresponding to Asp 52 and Glu 35 correctly positioned in the active site (Grutter et al., 1983). Recent X-ray crystallographic studies on other "retaining" glycosidases including *Trichoderma harzianum* xylanase (Campbell et al., 1993), *C. fimi* exoglycanase (White et al, 1994) and *E. coli* β-galactosidase (Jacobsen et al., 1994), have also identified carboxylate residues appropriately located to function as the catalytic nucleophile. Even more direct evidence for the existence of a catalytic carboxylate is

derived from glycosidases co-crystallized with either an inhibitor or a substrate in the active site. For example the X-ray crystal structure of *Bacillus circulans* E172C xylanase-xylotetraose complex revealed that Glu 78 is correctly oriented and within close enough proximity of the substrate to act as the catalytic nucleophile (Campbell et al., 1993) while the structure of *Trichoderma reesei* cellobiohydrolase I with 2-iodobenzyl-1-thio-β-D-cellobioside (Figure 1-10) at the active site indicates that Glu 212 is likely the catalytic nucleophile based on its position and environment within the active site (Divne et al, 1994).

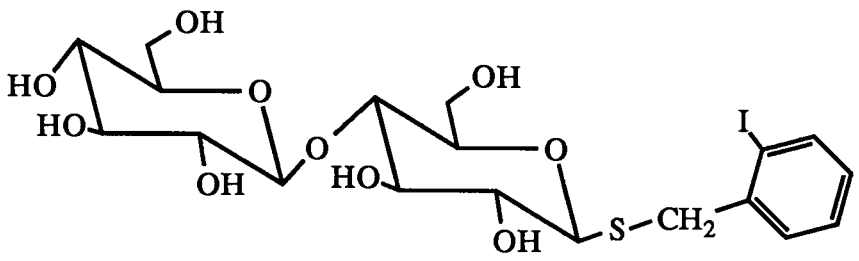


*Figure 1-10 Structure of 2-iodobenzyl-1-thio-β-D-cellobioside.*

In other cases the catalytic carboxylate groups have been identified by labeling experiments using group-specific labels. For example, the carboxylate-modifying reagent, 1-(4-azonia-4,4-dimethyl-pentyl)-3-ethylcarbodiimide iodide (EAC), has been used to identify Glu 87 as a substrate-protected carboxylate group in the active site of *Schizophyllum commune* xylanase A. This residue has been proposed to be the catalytic nucleophile in this enzyme (Bray & Clarke, 1994).

Labeling experiments using the mechanism-based inactivators, 2-deoxy-2-fluoro-glycosides, have been used successfully to identify the catalytic nucleophile. These compounds operate by trapping the glycosyl-enzyme intermediate, thus allowing identification of the nucleophile by subsequent isolation and sequencing of the labeled peptides. Indeed, the catalytic nucleophiles of several "retaining" glycosidases have been identified with these inactivators and these are listed in Table 1-2.

Table 1-2: List of catalytic nucleophiles identified by mechanism-based inactivators, 2-deoxy-2-fluoro-glycosides.

| Glycosidase | Nucleophile | Inactivator | Reference |
|---|---|---|---|
| *Agrobacterium* | | | |
| β-Glucosidase | Glu 358 | 2F-DNPG | (Withers et al.,1990) |
| *C. fimi* | | | |
| Exoglucanase | Glu 233 | 2F-DNPG | (Tull et al, 1991) |
| *C. thermocellum* | | | |
| Endoglucanase C | Glu 280 | 2F-DNPC | (Wang et al., 1993) |
| *E. coli* | | | |
| β-Galactosidase | Glu 537 | 2F-DNPGal | (Gebler et al., 1992) |
| Human | | | |
| Glucocerebrosidase | Glu 340 | 2F-DNPG | (Miao et al., 1994) |
| *B. subtilis* | | | |
| xylanase | Glu 78 | 2F-DNP$X_2$ | (Miao et al., 1994) |

Labeling studies of this sort with *C. fimi* exoglycanase and *E. coli* β-galactosidase have identified Glu 233 and Glu 537, respectively, as the catalytic nucleophiles in these enzymes and these findings were recently confirmed by the X-ray crystallographic structures which revealed these residues appropriately located within the active site to perform this role (White et al, 1994; Jacobsen et al, 1994).

### 1-5-2 Nature of the glycosyl-enzyme intermediate

The double displacement mechanism initially described by Koshland (1953) for "retaining" glycosidases proposed the formation of a covalent glycosyl-enzyme intermediate. However, based on the X-ray structure of the HEWL active site, Phillips has proposed that an ion-pair comprising Asp 52 and the oxocarbonium ion would be sufficiently long-lived for the leaving group to diffuse away from the active site and allow the glycosyl acceptor, water, to diffuse in and react (Blake et al., 1967). While additional evidence in support of an ion-pair intermediate comes from a recent X-ray crystallographic study of HEWL complexed with a product, N-acetyl muramyl-N-acetyl glucosaminyl-N-acetyl muramic acid (Strynadka & James, 1991), there has been considerably more evidence which strongly indicates formation of a covalent glycosyl-enzyme intermediate for many "retaining" glycosidases.

Substantial evidence for the covalent nature of a glycosyl-enzyme intermediate comes from secondary deuterium kinetic isotope effect measurements using substrates for which deglycosylation is rate determining. Values of $k_H/k_D$ = 1.20 - 1.25 have been measured for *E. coli* (lac Z) β-galactosidase (Sinnott, 1978), $k_H/k_D$ = 1.10 - 1.12 for *Agrobacterium* β-glucosidase (Kempton & Withers, 1992) and $k_H/k_D$ = 1.09 for *Botrydiplodia theobromae* β-glucosidase (Umezerika, 1988). These positive kinetic isotope effects reflect significant $sp^3$ to $sp^2$ rehybridisation at the anomeric centre (C-1) in going from the ground state glycosyl-enzyme intermediate to the deglycosylation transition state and this can only occur if the intermediate has more $sp^3$ character than the subsequent transition state.

Additional evidence for the covalency of the intermediate derives from inactivation studies of *Agrobacterium* β-glucosidase with 2-deoxy-2-fluoro-β-D-glycosides (Withers et al., 1987). These compounds inactivate β-glucosidase because the presence of the electronegative fluorine at C-2 destabilises both oxocarbonium ion-like transition states, thereby slowing down both the formation and the hydrolysis of the intermediate while the

presence of the good leaving group (fluoride or 2,4-dinitrophenolate) speeds up the glycosylation step thereby leading to the accumulation of the intermediate (discussed in Chapter II) (Figure 1-11). This glucosyl-enzyme intermediate is stable, with $t_{1/2} > 500$ hours at 37 °C in phosphate buffer, thus allowing the covalency and stereochemistry ($\alpha$) to be demonstrated by $^{19}$F-NMR (Withers & Street, 1988) as well as identification of the nucleophile as Glu 358 (Withers et al.1990). Trapping of this covalent species shows that such glycosyl-enzyme intermediates can exist and are stable.

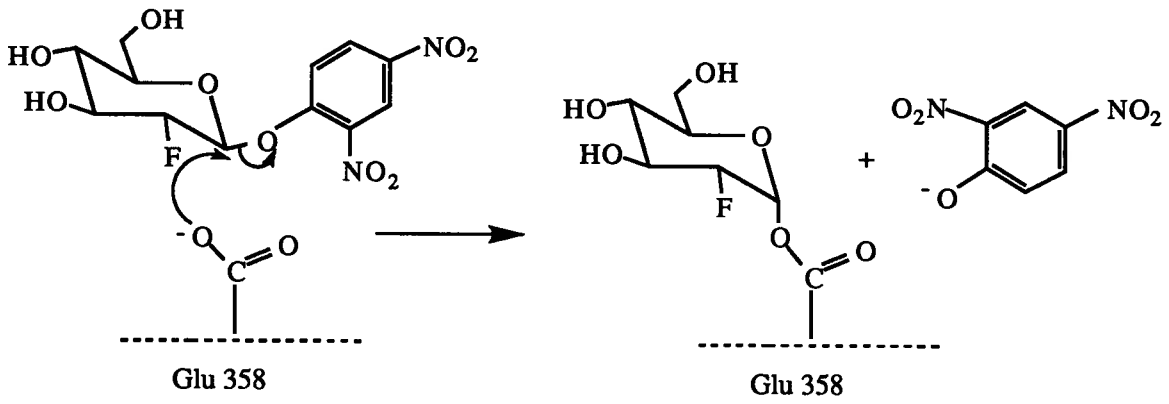


*Figure 1-11 Labeling the catalytic nucleophile (Glu 358) of Agrobacterium β-glucosidase with 2F-DNPG.*

Furthermore, the catalytic competence of the intermediate is demonstrated by the fact that in the presence of a suitable glycosyl acceptor such as 1-deoxy-β-D-glucosyl benzene, product is released and the free enzyme is reactivated. Analysis of this isolated reactivation product by mass spectrometry and both $^{1}$H and $^{19}$F-NMR was consistent with the structure of the disaccharide, 2'-deoxy-2'-fluoro 1-deoxy-β-cellobiosyl benzene. Presumably, this product is formed via a transglycosylation reaction involving attack on the anomeric carbon of the 2F-glucosyl-enzyme intermediate by the C-4 hydroxyl group of glucosyl benzene followed by subsequent displacement of the enzymic carboxylate group (Figure 1-12).

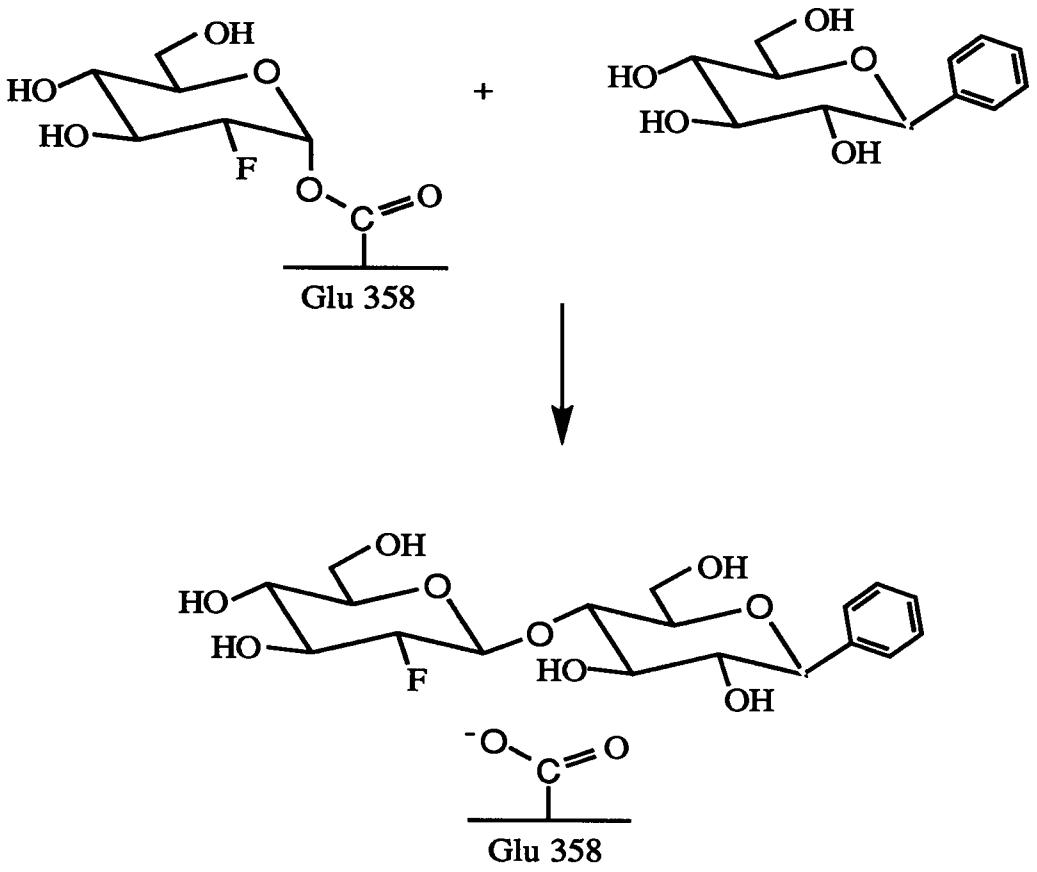


*Figure 1-12* *Reactivation of 2F-DNPG-inactivated Agrobacterium β-glucosidase in the presence of 1-deoxy-β-glucosyl benzene.*

Finally, studies of spontaneous (non-enzymatic) hydrolysis of glycosides have suggested that glycosyl cations are relatively unstable with estimated life times varying from $10^{-10}$ to $10^{-12}$ seconds in aqueous solutions (Amyes & Jencks, 1989; Bennet & Sinnott, 1986) compared to life times of 1 - 100 milliseconds for glycosyl-enzymes at ambient temperatures (Weber & Fink, 1980). It therefore seems unlikely that such an unstable species could exist, even within the stabilizing environment of an active site, without formation of a covalent bond (Sinnott & Souchard, 1973).

### 1-5-3 Oxocarbonium ion-like transition states

Evidence for oxocarbonium ion character at the transition states for formation and hydrolysis of the glycosyl-enzyme intermediate comes primarily from studies of transition state analogues, secondary deuterium kinetic isotope effects and linear free energy relationships using fluorinated and deoxygenated substrates. In addition, studies with 1,1-difluoro-substrates have provided a measure of the oxocarbonium ion character at the glycosylation transition state. The results from these studies are presented and discussed below.

Transition state analogues are glycoside derivatives that sufficiently mimic the oxocarbonium ion-like transition state in structure that they bind to the glycosidase significantly tighter than does the substrate. Features distinguishing the glycosyl cation from the parent glycoside are the following. Both the C-1 and O-5 atoms of the glycosyl cation share a full positive charge and the C-1, C-2, C-5 and O-5 atoms are coplanar (Figure 1-13) (Sinnott, 1987). Hence, a transition state analogue must have one or both of these features.

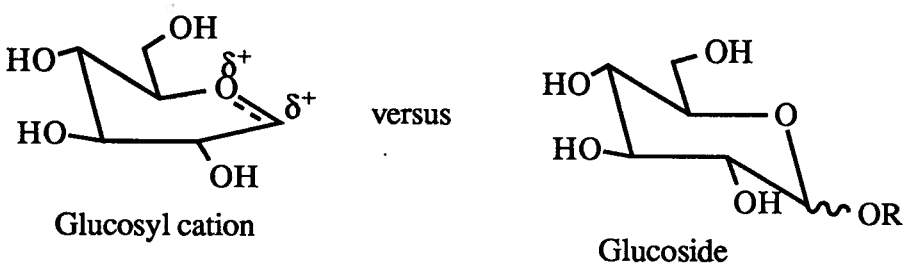


*Figure 1-13 Comparison of glycosyl cations with glycosides.*

Examples of classical transition state analogues include the aldonolactones and aldonolactams which resemble the glycosyl cation both in geometry and to some extent in charge (Figure 1-14). Generally, values of $K_i$ for these lactones are $10^2$ to $10^4$-fold lower

than $K_i$ values for the corresponding hexoses. For example, with *Aspergillus wentii* β-glucosidase $K_i$ (lactone) = 0.0095 mM *versus* $K_i$ (hexose) = 2.8 mM, with Jack bean α-mannosidase $K_i$ (lactone) = 0.12 mM *versus* $K_i$ (hexose) = 22 mM and finally with HEWL $K_i$ (lactone) = 0.000083 mM *versus* $K_i$ (hexose) = 0.01 mM (Legler, 1990). Comparable values of $K_i$ for aldonolactams with glycosidases have been reported (Legler, 1990).

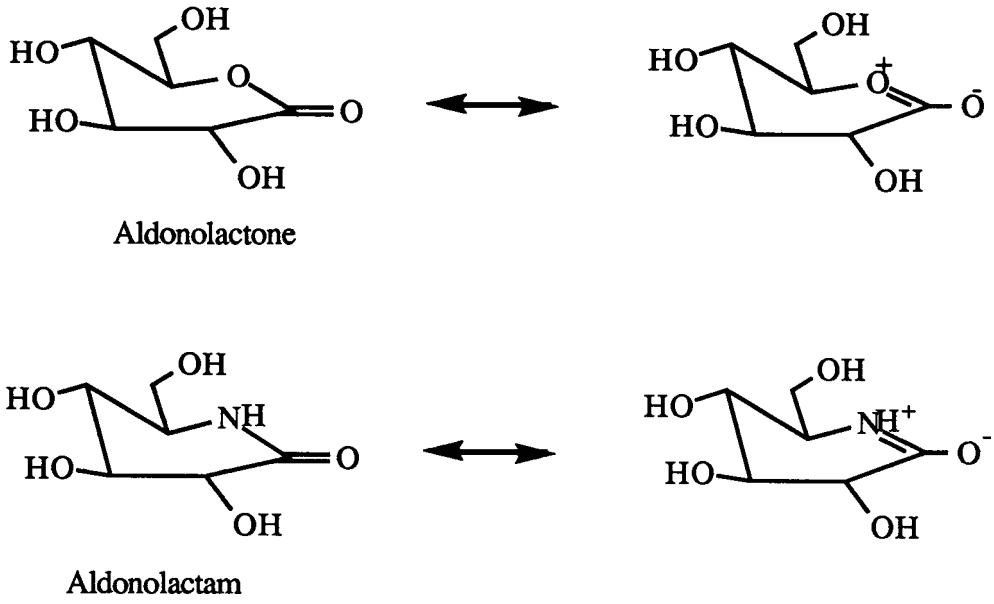


*Figure 1-14 Resonance structures for an aldonolactone and an aldonolactam.*

Some of the most potent inhibitors of glycosidases include the 5-amino-5-deoxy-aldose class of transition state analogues such as nojirimycin (Figure 1-15) and its analogues. Values of $K_i$ for these 5-amino-5-deoxy-aldose inhibitors with their corresponding glycosidase are found within the micromolar range, for example $K_i$ (nojirimycin) = 0.36 μM for *A. wentii* β-glucosidase, $K_i$ (galactonojirimycin) = 0.045 μM for *E. coli* β-galactosidase and $K_i$ (mannonojirimycin) = 1.2 μM for Jack bean α-mannosidase (Legler, 1990). These compounds are thought to mimic the glycosyl cation because in their protonated form they are isoelectronic with the glycosyl cation. It is likely

that the dehydrated forms of 5-amino-5-deoxy-aldose inhibitors are also excellent inhibitors of glycosidases, since in this form they are thought to mimic the glycosyl cation both in charge and in geometry.

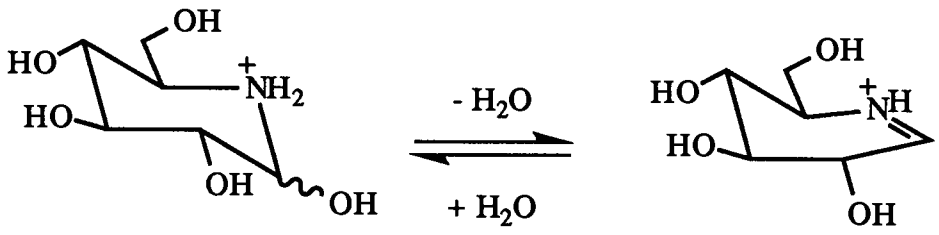


*Figure 1-15 Nojirimycin, a transition state analogue for glucosidases.*

Secondary deuterium kinetic isotope effect measurements on glycosidases using specific substrates for which the rate determining step is either glycosylation or deglycosylation have provided substantial evidence for oxocarbonium ion-like transition states during glycoside hydrolysis. For example, kinetic isotope effects measured on the glycosylation transition state include values of $k_H/k_D$ = 1.15 - 1.20 for *E. coli* (lac Z) β-galactosidase using β-D-galactopyranosyl pyridinium salts (Sinnott & Withers, 1974) and $k_H/k_D$ = 1.05 - 1.07 for *Agrobacterium* β-glucosidase using aryl β-D-glucopyranosides (Kempton & Withers, 1992). Similarly, kinetic isotope effects have also been reported on the deglycosylation transition state and these include values of $k_H/k_D$ = 1.2 - 1.25 for *E. coli* β-galactosidase (Sinnott, 1978) and $k_H/k_D$ = 1.09 for *Botrydiplodia theobromae* β-glucosidase (Umezerika, 1988).

The presence of a secondary deuterium kinetic isotope effect of $k_H/k_D > 1$ indicates that the isotopically-substituted carbon centre is converting from an $sp^3$ hybridized ground state to a transition state with significant $sp^2$ character in the rate determining step. If however, a value of $k_H/k_D = 1$ was measured, then that would indicate either an $S_N2$ mechanism as there would be no change in hybridization or that another step was rate

determining. Alternatively, values of $k_H/k_D < 1$ are indicative of a change in hybridization from $sp^2$ at the ground state to $sp^3$ at the transition state. Thus, the kinetic isotope effect measurements presented above, $k_H/k_D > 1$, are entirely consistent with oxocarbonium ion character at both transition states.

Additional evidence for oxocarbonium ion-like transition states during glycosidase-catalysed hydrolysis of glycosides derives from a linear free energy relationship study of *E. coli* β-galactosidase using deoxyfluoro-galactoside substrates substituted with fluorine at positions 2, 3, 4 and 6 around the galactosyl ring and deoxy-galactoside substrates with hydrogen substituted at positions 4 and 6 (McCarter et al., 1992). The correlation observed between $\log(k_{cat}/K_m)$ for the galactosidase-catalysed hydrolysis and $\log(k_{spont})$ for the spontaneous hydrolysis with these galactosides suggested that both the enzymic transition state and that for spontaneous hydrolysis are similarly affected by the substitutions at each position on the galactose ring. Since the major effect of substitution of a hydroxyl group by a fluorine or a hydrogen atom on the rate of spontaneous hydrolysis is electronic in nature (Withers et al., 1989; Withers et al., 1986), then the presence of this correlation with reaction constant of $\rho = 0.8$ provides direct evidence for the similar oxocarbonium ion character in the enzymic transition state. The scatter observed in the $\log(k_{cat}/K_m)$ *versus* $\log(k_{spont})$ plot (McCarter et al., 1992) is due to binding effects that are important in the enzyme-catalysed hydrolysis reaction (discussed in Chapter II) but are not a component of the spontaneous hydrolysis reaction. Similar correlations between enzymic and spontaneous hydrolysis of deoxy-and deoxyfluoro-substrates have been observed in linear free energy relationship studies of other related enzymes systems in which the transition state is believed to be oxocarbonium ion-like in nature. For example, with rabbit muscle glycogen phosphorylase *b*, an enzyme responsible for catalysing the reversible phosphorolysis of glycogen to produce glucose-1-phosphate, a reasonable correlation with a reaction constant of $\rho = 0.9$ was observed between $\log(V_m)$ for the phosphorylase-catalysed reaction and $\log(k_{hydrolysis})$ for the acid-catalysed hydrolysis reaction of deoxy-

and deoxyfluoro-α-D-glucopyranosyl phosphates (Street et al., 1989). These results, like those with *E. coli* β-galactosidase, are consistent with oxocarbonium ion character at the transition state for phosphorylase-catalysed hydrolysis of glucopyranosyl phosphates.

Recently, Sinnott and coworkers (Konstantinidis & Sinnott, 1991; Srinivasan et al., 1993) have attempted to quantitate the oxocarbonium ion character at the first transition state of "retaining" glycosidase-catalysed hydrolysis of glycosides using 1-fluoro-D-glycosyl fluorides and 1, 1-difluoro-D-glycosyl fluorides (Figure 1-16). Values of $k_{cat}/K_m$ for both the mono- and di-fluoride substrates were determined and used to calculate the differences in the free energies of activation ($\Delta\Delta G^{\ddagger}$) for the glycosylation step.


*Figure 1-16 Structure of 1-fluoro-D-glucosyl fluorides and 1,1-difluoro-D-glucosyl fluoride.*

Since introduction of an electronegative substituent such as fluorine at an already electron-deficient centre is expected to further destabilise that transition state then the values of $\Delta\Delta G^{\ddagger}$ are estimates of the degree of destabilisation caused by this second fluorine atom at the anomeric centre and thus provide some measure of the oxocarbonium ion character at the first transition state during glycoside hydrolysis. Rates of hydrolysis for the appropriate glucosyl fluoride anomer were 5000-fold ($\Delta\Delta G^{\ddagger}$ = 21.2 kJ mol$^{-1}$), 8000-fold ($\Delta\Delta G^{\ddagger}$ = 23.2 kJ mol$^{-1}$) and 200-fold ($\Delta\Delta G^{\ddagger}$ = 14.5 kJ mol$^{-1}$) greater than those for the 1-fluoro-D-glucosyl fluoride with yeast α-glucosidase, sweet almond β–glucosidase B and *Aspergillus wentii* β-glucosidase $A_3$, respectively (Konstantinidis & Sinnott, 1991).

Similarly, the rate of *E. coli* (lac Z) β-galactosidase-catalysed hydrolysis of β-D-galactosyl fluoride was 400-fold ($\Delta\Delta G^{\ddagger}$ = 15.2 kJ $mol^{-1}$) greater than that for the corresponding difluoride (Srinivasan et al, 1993). These results indicate that the presence of the second fluorine atom at C-1 destabilises the glycosylation transition state and thus is entirely consistent with the presence of oxocarbonium character at the glycosylation transition state.

### 1-5-4 General acid assistance

Koshland proposed that departure of the aglycone may proceed with acid assistance. Evidence which supports acid catalysis includes identification of suitably positioned carboxylic acid residues, Glu 35 and Glu 11, in the X-ray crystal structures of HEWL (Anderson et al., 1981) and GEWL (Grutter et al, 1983) respectively, which could function as acid catalysts. Similarly, the X-ray crystal structure of *E. coli* β-galactosidase revealed Glu 461 appropriately located within the active site to perform the role of acid catalyst in this enzyme (Jacobsen et al, 1994).

MacLeod and coworkers (1994) have developed a method to identify the acid catalyst in glycosidases. This new method was applied to *C. fimi* exoglycanase and it involves identification of highly conserved carboxylic acid residues by means of sequence alignment, site-directed mutagenesis of these residues to alanine and glycine followed by kinetic analysis of these mutants using substrates for which protonation of the leaving group is required (e.g. 4-bromophenyl β-cellobioside) and substrates requiring no acid assistance (e.g. 2,4-dinitrophenyl β-cellobioside). Glu 127 was identified as the acid catalyst in this enzyme by this means and this assignment has recently been confirmed by X-ray crystallographic analysis of the enzyme. Glu 127 was found to be appropriately located to perform the role (White et al, 1994) (discussed in Chapter III).

Additional supportive evidence for acid assistance in glycoside hydrolysis is derived from glycosidase-catalysed hydration of octenitol derivatives and glycals. *E. coli* β-galactosidase and coffee bean α-galactosidase catalyse the hydration of D-galacto-octenitol

to the galactooctulose derivatives (Figure 1-17) and these products were characterized by $^1$H-NMR (Weiser et al., 1992). This study showed that based on the stereochemistry of the hydrated products, protonation occurred from the α-face of the galactose ring with the α-galactosidase and the β-face with the β-galactosidase. These results are therefore consistent

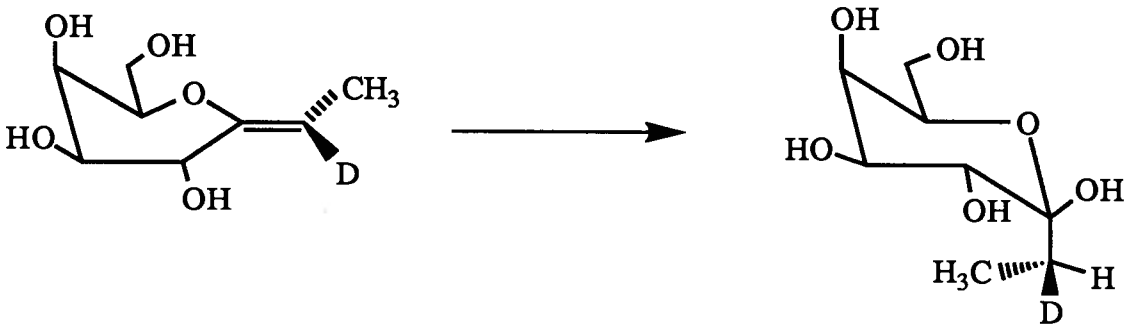


*Figure 1-17 Hydration of an octenitol derivative by E. coli β-galactosidase.*

with the presence of a residue in these enzymes that could function as an acid catalyst in the normal glycoside hydrolysis reaction.

Another $^1$H-NMR stereochemical investigation, in this case of coffee bean α-galactosidase with D-galactal in $D_2O$ revealed that deuteration (protonation) was from the α–face of the sugar ring and again this is consistent with the existence of an acid catalyst that could donate a proton in normal glycoside hydrolysis (Weiser et al, 1992). Similar results have also been obtained with three β-N-acetyl hexosaminidases from Jack bean, bovine kidney and human placenta using 2-acetamidoglucal. In all three cases, the hydration product identified by HPLC using authentic standards was N-acetyl-glucosamine while no observable amounts of N-acetyl-mannosamine were detected, indicating that the

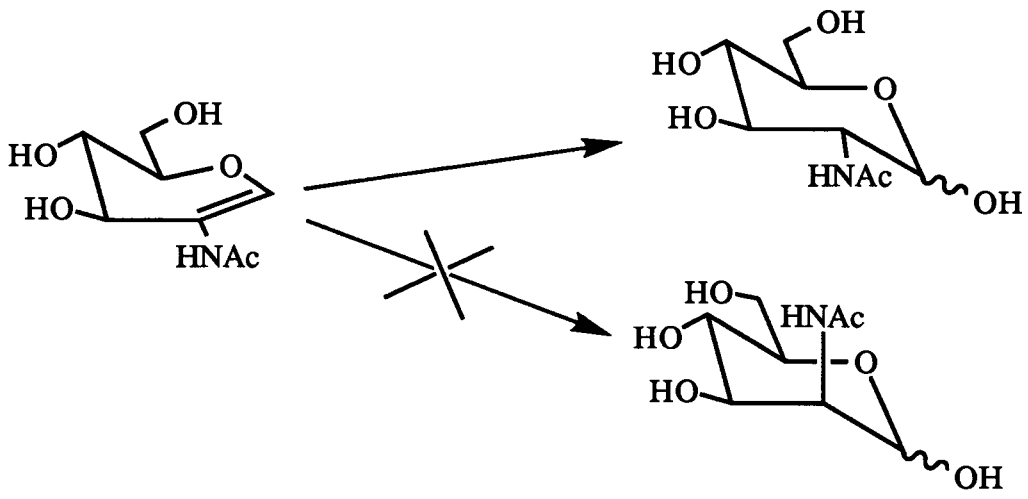


*Figure 1-18* *Hydration of 2-acetamidoglycal by β-N-acetyl hexosaminidases from Jack bean, bovine kidney and human placenta.*

proton was indeed delivered (Figure 1-18) from the β-face of the sugar ring (Lai & Withers, 1994). It should be noted however that in general, protonation of glycals occurs from the face of the sugar that is opposite to the acid catalyst (Sinnott, 1990). For example, $^1$H-NMR analysis of the hydration of cellobial with *Irpex lacteus* exo-β-(1,4)-cellulase and *Aspergillus niger* endo-β-(1,4)-cellulase in $D_2O$ revealed that deuteration (protonation) occurred from the α-face of the cellobiose ring (Kanda et al., 1986). In these cases it is believed that the proton is delivered by the catalytic nucleophile (Hehre et al., 1977; Kanda et al, 1986) and that reaction occurs via a concerted mechanism (Legler, 1990) (discussed in Chapter II).

Although there is evidence which clearly indicates the involvement of a general acid catalyst, there is also evidence suggesting that it is not essential for glycoside hydrolysis. For example, studies of *E. coli* β-galactosidase-catalysed hydrolysis of β-D-galactopyranosyl pyridinium salts (Figure 1-19) revealed $10^8$ to $10^{13}$-fold rate enhancements for the enzymatic hydrolysis compared to spontaneous hydrolysis (Jones et al., 1977). Since it is structurally impossible to protonate these compounds in a manner

which will assist aglycone departure, then none of this rate acceleration can be due to acid catalysis.

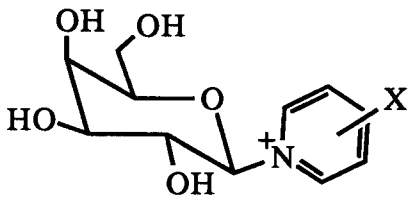


*Figure 1-19 Structure of β-D-galactosyl pyridinium cation.*

### 1-5-5 Non-covalent enzyme-substrate interactions

The large majority of the rate enhancement observed in catalysis by most enzymes is believed to be derived from non-covalent interactions between the enzyme and the substrate as the transition state is reached. With glycosidases and other carbohydrate binding proteins, these interactions are likely to be predominantly hydrogen bonds formed between the hydroxyl groups of the sugar and the enzyme. The binding energy derived from these interactions, when realized at the transition state, stabilizes that transition state and leads to a decrease in the activation energy of the reaction, hence a rate acceleration is observed.

Evidence for the existence of hydrogen bonds between hydroxyl groups of carbohydrates and proteins is derived from a number of sources including X-ray crystallographic studies. Examples in which this has been seen have included lectins, proteins that recognize and bind to complex carbohydrates, with oligosaccharides bound at the recognition sites. For example, the X-ray structure of *Erythrina corallodendron* lectin N-linked to a heptasaccharide and complexed with lactose revealed hydrogen bonds between the C-3 and C-4 hydroxyl groups of the galactose residue and Asp and Asn residues in the binding site (Shaanan et al., 1991). Similarly, the X-ray structure of rat

serum lectin complexed to an oligomannose asparaginyl-oligosaccharide revealed hydrogen bonds between the C-3 and C-4 hydroxyl groups of terminal mannose and Asn and Glu residues in the binding site (Weis et al., 1992). Indeed, hydrogen bonds have also been identified in glycosidases, for example hydrogen bonds between C-3 and C-6 hydroxyl groups of a β–(1,4)-N-acetyl-D-glucosamine trisaccharide and the active site Asp and Trp residues of lysozyme were identified in the X-ray crystal structure of the enzyme-sugar complex (Johnson et al, 1988).

Studies of glycosidases using deoxy-glycosides as substrates have given some indication of how much the interaction of each individual hydroxyl group can contribute to transition state stabilization and thus rate acceleration. For example, with *E. coli* β-galactosidase, values of $k_{cat}/K_m$ for the hydrolysis of 4-deoxy and 6-deoxy analogues of 2,4 dinitrophenyl β-D-galactoside were 500- and 1000-fold lower than that for the parent galactoside substrate (McCarter et al, 1992). Interactions at the C-2 hydroxyl group must be more important since the rate of hydrolysis of the 2-deoxy-galactosyl-enzyme intermediate is 5 x $10^5$-fold lower than that for the hydrolysis of the parent galactosyl-enzyme intermediate (Wentworth & Wolfenden, 1974). Thus, the C-2 hydroxyl group contributes at least 33.5 kJ/mole (8 kcal/mole) to the stabilization of the degalactosylation transition state (McCarter et al, 1992). Similarly, the C-5 hydroxymethyl group in lysozyme substrates must also provide important non-covalent interactions at the transition state since the rate of hydrolysis of the 6-deoxy trisaccharide shown in Figure 1-20 was 1300-fold lower than that for the corresponding C-5 hydroxymethyl substrate (Figure 1-20) (Ballardie et al., 1977).

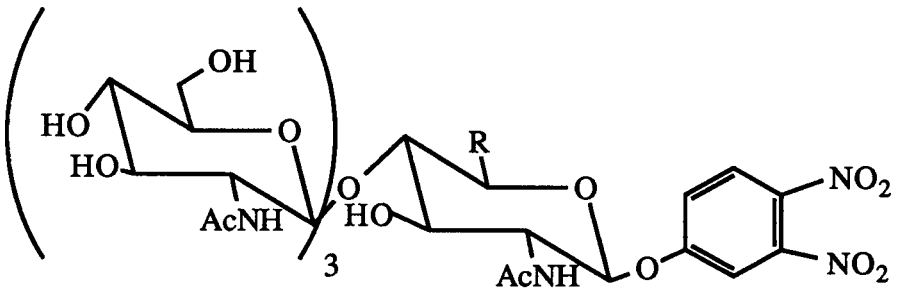


R = H or $CH_2OH$

*Figure 1-20 Substrate analogue for lysozyme.*

With *Aspergillus niger* glucoamylase, the $k_{cat}/K_m$ values for 4'- and 6'-deoxy maltose derivatives (Figure 1-21) are 1000- and 700-fold lower than those for the parent substrate, clearly indicating that these hydroxyl groups are involved in stabilizing the transition state (Sierks et al., 1992).

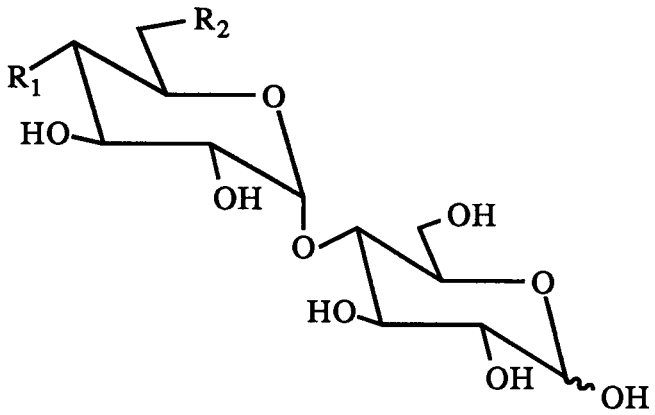


(a) $R_1$, $R_2$ = H, OH

(b) $R_1$, $R_2$ = OH, H

*Figure 1-21 Structure of deoxy-maltose derivatives.*

## 1-5 Aim of This Study

*C. fimi* exoglycanase has been classified as a retaining β-glycosidase and thus a double displacement mechanism is proposed. The aim of this study is to investigate the mechanism of this enzyme. This will be accomplished by first performing a detailed kinetic analysis on the native enzyme using pre-steady state analysis, linear free energy relationship studies, secondary deuterium kinetic isotope effect measurements, inactivation studies and pH-dependence studies. Pre-steady state analysis of the hydrolysis of aryl β-glycosides should provide evidence for a two step mechanism, identify the rate determining step and provide values for the rate constants for formation of the glycosyl-enzyme intermediate ($k_2$) and values for the dissociation constant for the enzyme-substrate complex ($K_d$). Linear free energy relationship studies should identify the rate determining and provide insights into the degree of negative charge accumulation on the phenolate oxygen at the glycosylation transition state. Secondary deuterium kinetic isotope effect measurements should provide a measure of the oxocarbonium ion character at each transition state. Inactivation studies with 2-deoxyfluoro-sugars coupled with $^{19}$F-NMR analysis should provide substantial evidence for the covalent nature and stereochemistry of the glycosyl-enzyme intermediate. Furthermore, inactivation studies with both 2-deoxy- and 2-deoxyfluoro- glycosides should provide evidence for the role of the C-2 hydroxyl group of the sugar during exoglycanase-catalysed hydrolysis of glycosides. The pH-dependence study of the exoglycanase activity may provide insight into the ionisation state of active site residues.

The mechanism of this exoglycanase will be further investigated by performing a detailed kinetic analysis similar to that performed on the native enzyme on point mutants generated individually at the catalytic nucleophile (Glu 233) and the acid-base catalyst (Glu 127). This is expected to provide further evidence in support of the proposed roles of these residues.

A second aim of this study is to use active site directed irreversible inactivators in combination with electrospray ionisation mass spectrometry to identify active site residues that are involved in either catalysis or binding.

More detailed aims, specific to each project, are provided at the end of the introduction of each chapter (Chapters II, III and IV).

# CHAPTER II

# DETAILED KINETIC ANALYSIS OF NATIVE *CELLULOMONAS FIMI* EXOGLYCANASE

## 2-1 Introduction to Different Kinetic Techniques

### 2-1-1 Kinetic scheme for a double displacement mechanism

"Retaining" glycosidases such as *C. fimi* exoglycanase are assumed to catalyse the hydrolysis of β-glycosides via a double displacement mechanism (Koshland, 1953). A kinetic scheme describing this reaction is

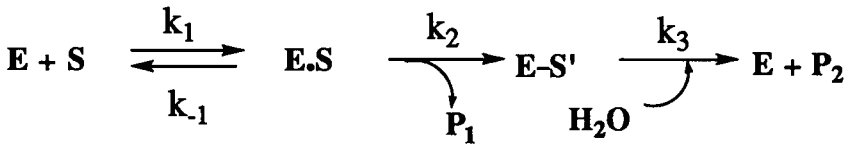


where $k_1$ and $k_{-1}$ are the rate constants for formation and dissociation of the Michaelis complex (E·S), respectively, while $k_2$ and $k_3$ are the rate constants for formation and hydrolysis of the glycosyl-enzyme intermediate (E-S'), respectively. The dissociation constant for the Michaelis-complex is expressed as

$$K_d = \frac{[E]\ [S]}{[ES]}$$

thus,

$$K_d = \frac{k_{-1}}{k_1}$$

The Michaelis-Menten parameters, $k_{cat}$, $K_m$ and $k_{cat}/K_m$ can be defined in terms of the rate constants as

$$k_{cat} = \frac{k_2 k_3}{k_2 + k_3}$$

$$K_m = \left(\frac{k_{-1} + k_2}{k_1}\right)\left(\frac{k_3}{k_2 + k_3}\right)$$

$$\frac{k_{cat}}{K_m} = \frac{k_1 k_2}{k_{-1} + k_2}$$

Values for $k_{cat}$, $K_m$ and $k_{cat}/K_m$ are obtained by performing steady state kinetic analysis.

### 2-1-2 Pre-steady state analysis of enzymatic reactions

Although steady state kinetic analysis of glycosidases can provide values for both $k_{cat}$ and $K_m$, such analysis provides very little information about the individual rate constants. Alternatively, pre-steady state kinetic analysis of enzymatic reactions can provide values for the rate constants of the individual steps in the mechanism as well as detect transient intermediates along the reaction pathway. When performing pre-steady state analysis on "retaining" glycosidases, only the initial conversion of the Michaelis-complex (**E.S**) to the glycosyl-enzyme intermediate (**E-S'**) is observed. Since only one mole of the aglycone is released per mole of enzyme, then these studies require large amounts of enzyme rather than catalytic quantities, as well as a large excess of substrate over enzyme in order to maintain pseudo-first order kinetics. Pre-steady state kinetic analysis of "retaining" glycosidases can be used to specifically characterise the formation of the glycosyl-enzyme intermediate provided the following criteria are satisfied. First, the rate of formation of the Michaelis-complex ($k_1$) must be greater than that for formation of the glycosyl-enzyme intermediate ($k_2$), otherwise the reaction may be at least partially diffusion-controlled. Second, the rate of dissociation of the Michaelis-complex to free enzyme and substrate ($k_{-1}$) must be greater than that for its conversion to the glycosyl-enzyme intermediate ($k_2$) in order to obtain a reliable estimate of the dissociation constant for the Michaelis-complex

($K_d$). Last, if the rate of the formation of the glycosyl-enzyme intermediate ($k_2$) is very much greater than that for its conversion to product and free enzyme ($k_3$), then the reaction scheme can be simplified to

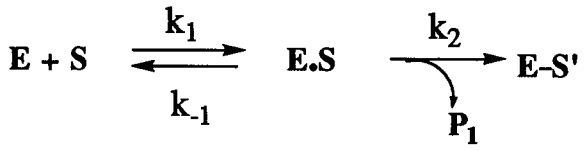


Ideally, if the rate of glycosylation ($k_2$) is much greater than that for deglycosylation ($k_3$) then formation of the glycosyl-enzyme intermediate would be expected to follow pseudo-first order kinetics over the entire observation period of the reaction. In general however, biphasic kinetics are observed for the release of the aglycone. During the pre-steady state phase of the reaction, initial aglycone release (the burst) follows pseudo-first order kinetics, but as the glycosyl-enzyme intermediate accumulates the rate of release of the aglycone becomes dependent on the rate of conversion of the intermediate to product and free enzyme. Eventually, a steady state is reached and the rate of aglycone release becomes constant. These biphasic kinetics are then fitted to an equation describing a first order process followed by a steady state phase to yield values for the pseudo-first order rate constants ($k_{obs}$) of the pre-steady state phase as well as values for the steady state rates. The pseudo-first order rate constants are fitted to the Michaelis-Menten equation,

$$k_{obs} = \frac{k_2\,[S]}{K_d + [S]}$$

thus yielding values for $k_2$ and $K_d$.

### 2-1-3 Linear free energy relationships as mechanistic probes of enzymatic reaction

*(a) The concept*: A series of modifications in the conditions of a reaction will nearly always result in a series of changes in either the rate and/or equilibrium of the reaction. If the same modifications affect either the rate or equilibrium of a reaction in the same way that they affect either the rate or equilibrium of a second reaction, then a linear free energy relationship must exist between the two sets of effects. This relationship is expressed mathematically as

$$\log \frac{k_{2,y}}{k_2} = \log \frac{k_{1,y}}{k_1} \times \text{constant}$$

where k represents either the rate or equilibrium constant of a reaction and $k_y$, that of the reaction in which there has been a modification in the reaction conditions (e.g. addition of a substituent). The term "free energy" in this relationship is appropriate as the rate is a reflection of the free energy of activation and the equilibrium constant reflects the standard free energy change of the reaction.

*(b) Linear free energy relationships in enzymology:* Linear free energy relationships are valuable tools for the elucidation of the mechanism of enzymatic reactions since they can provide valuable insights into the relationship between substrate structure and enzymatic activity. However, their applications are limited by two important aspects of enzymatic reactions, substrate binding and catalysis. Enzymes are rather specific for their substrates, thus modifications of the substrate could affect its binding to the enzyme active site. The resulting binding effects may then obscure the electronic effects of the substituents on the substrate. Furthermore, substrate modification could affect the orientation of the substrate reacting centre relative to the enzymatic catalytic residues and this in turn could

interfere with catalysis. Nevertheless, in favourable circumstances linear free energy relationships can be applied to enzymatic reactions. These have been applied extensively to the study of glycosidases (Dale et al., 1986), acyl transferases (Lowe & Yuthauong, 1971) and proteases (Riddle & Jencks, 1971). Since this work focuses on a glycosidase, an example from this group of enzymes has been selected in order to illustrate the type of results obtained and how they are interpreted to provide mechanistic insights.

*(c) Example of the application of linear free energy relationship*: The "retaining" glycosidase, *Agrobacterium faecalis* β-glucosidase catalyses the hydrolysis of aryl β-D-glucosides to glucose and the corresponding substituted phenol (Kempton & Withers, 1992). Values of log $k_{cat}$ for these substrates were plotted as functions of the phenol leaving group $pK_a$ in the form of a Broensted plot (Figure 2-1). The shape of the resulting plot is concave downward, providing evidence for a two step reaction mechanism and thus is consistent with the formation of a glucosyl-enzyme intermediate along the reaction pathway. The biphasic nature of this plot further indicates a change in the rate determining step as the phenol leaving group changes. The strong correlation observed between log $k_{cat}$ for substrates with poor leaving groups ($pK_a > 8$) and the phenol $pK_a$ suggests that the formation of the glucosyl-enzyme intermediate is the rate determining step for these substrates as this is the step involving cleavage of the phenolate-sugar bond. The value of the reaction constant, $\beta_{lg} = -0.7$, for this region of the plot is consistent with significant negative charge development on the oxygen of the departing phenolate at the glucosylation transition state. By contrast, the absence of any significant dependence of log $k_{cat}$ on the phenol $pK_a$ for the more reactive substrates ($pK_a < 8$) indicates that the initial C-O bond cleavage is not rate determining, but instead the rate determining step is most likely hydrolysis of the glucosyl-enzyme intermediate.

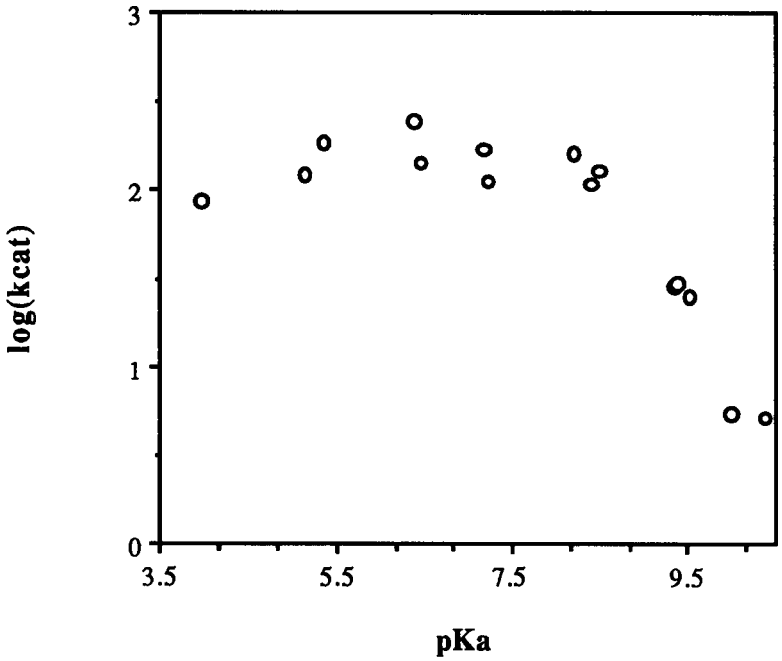


*Figure 2-1* *Broensted plot relating values of $k_{cat}$ for the hydrolysis of aryl β-glucosides by Agrobacterium β-glucosidase with the leaving group ability of the phenols. (Reproduced from Kempton & Withers, 1992).*

The above example demonstrates that application of linear free energy relationships in enzymology can provide useful mechanistic information about the identity of rate determining steps, the existence of intermediates along the reaction path, as well as valuable structural information about transition states.

### 2-1-4 Secondary deuterium kinetic isotope effects as transition state probes

*(a) The concept of kinetic isotope effects* : A kinetic isotope effect is the difference in the rate of a reaction resulting from an isotopic substitution in a reactant. It is given by the ratio of the rate constants for the isotopically unsubstituted and substituted reactants, for example $k_H/k_D$ for deuterium effects. If the bond to the isotopically substituted atom is

formed or broken in the rate determining step, then a primary isotope effect can be measured for the reaction. Alternatively, if a bond other than that to the isotopically substituted atom is formed or broken, then a secondary isotope effect can be measured for the reaction. These secondary isotope effects are the result of rehybridization occurring at the reacting centre in the rate determining step. Secondary isotope effects are classified as $\alpha$, $\beta$, $\gamma$ or $\delta$ (remote effects) based on the position of the isotopically substituted atom relative to the reacting centre. If the isotope is bonded directly to the atom undergoing rehybridization, then an $\alpha$-secondary isotope effect is measured whereas a $\beta$-secondary isotope effect is measured when the isotope is bonded to an atom adjacent to the reacting centre.

Although the isotopic substitution does not affect the electronic structure of a molecule, the mass difference between the isotopes will be reflected in the frequency of the vibrating atoms according to

$$\nu = \left(\frac{1}{2\pi}\right)\left(\frac{K}{\mu}\right)^{1/2}$$

where K, the force constant, of the bond does not change with isotopic substitution and $\mu$, the reduced mass of the vibrating system, is given by

$$\mu = \frac{m_1 m_2}{m_1 + m_2}$$

so that $m_1$ and $m_2$ are the masses of the two atoms forming the bond. If one mass is much larger than the other, for example a C-H bond, then $\mu$ is approximately equal to the smaller mass. Since all molecules have an intrinsic non-zero minimum energy called the zero-point energy expressed as

$$E_0 = \frac{1}{2} h\nu$$

then the zero-point energy can be related to the mass of the vibrating atoms by

$$E_0 = \frac{1}{4\pi} h\left(\frac{K}{\mu}\right)^{1/2}$$

For example, since deuterium has a greater mass than hydrogen, then the vibrations of the C-D bond contributes less to the zero-point energy of the molecule than those of the C-H bond. Thus, substitution of deuterium for hydrogen results in reduction of the molecule's zero-point energy.

*(b) α-Secondary deuterium kinetic isotope effects*: These effects arise from changes in the frequencies of the bending mode vibrations of the isotopic atoms upon reaching the transition state. The difference in the zero-point energy between the isotopically labeled reactants upon reaching the transition state depends on the changes in the force constants (K) of the bending mode vibration for the isotopic bond. If the reacting centre undergoes $sp^3$ to $sp^2$ rehybridization at the transition state of the rate determining step, then the frequency of the C-H(D) bending mode vibration is lowered, decreasing the force constant of the vibration. Since the difference in zero-point energies between the C-H and C-D bond vibrations is proportional to $(K/\mu)^{1/2}$, then the difference in zero-point energies at the transition state will be less than that at the ground state. Thus, the activation energy for the hydrogen-substituted reaction is lower than that for the deuterium-substituted reaction, resulting in a greater reaction rate for the hydrogen-substituted reaction. For these reaction types, "normal" kinetic isotope effects of $k_H/k_D > 1.0$ are measured. Alternatively, if the reacting centre undergoes $sp^2$ to $sp^3$ rehybridization at the transition state of the rate determining step, then the force constant for bond vibration increases, thus resulting in a

greater difference in zero-point energies at the transition state than that at the ground state. The activation energy for the hydrogen-substituted reaction is now greater than that for the deuterium-substituted reaction. For these types of reactions, "inverse" kinetic isotope effects of $k_H/k_D < 1.0$ are measured.

A "normal" α-secondary deuterium kinetic isotope effect can have a maximum value of $k_H/k_D = 1.40$. Generally however, values of $k_H/k_D = 1.10\text{-}1.25$ are considered indicative of a significant degree of $sp^3$ to $sp^2$ rehybridisation at the transition state of the rate determining step. An α-secondary deuterium kinetic isotope effect of $k_H/k_D = 1.0$ suggests little or no change in hybridisation at the transition state.

Enzymatic reactions are extremely sensitive to modifications in the electronic structure of the substrates. However, as isotopic substitutions do not alter the electronic nature of the isotopically-labeled compounds, α-secondary deuterium kinetic isotope effect measurements can be used as powerful probes for elucidating the mechanism of enzymatic reactions. Unlike other substrate modifications, isotopic substitutions have no effect on the binding of substrates at the active site of the enzyme. α-Secondary deuterium kinetic isotope effects are particularly useful since they provide valuable information pertaining to the structure of the transition state.

### 2-1-5 Fluorine and hydrogen substitutions as probes of enzymatic reactions

As previously discussed in Chapter I, non-covalent interactions between the substrate and the enzyme are proposed to account for most of the rate enhancement seen for enzymatic reactions. For glycosidases, these interactions are believed to be primarily hydrogen bonds formed between the hydroxyl groups of the sugar and the residues within the active site of the enzyme. Replacement of these hydroxyl groups can therefore provide insights into the enzymatic mechanism. Fluorine and hydrogen atoms are appropriate substitutions for the sugar hydroxyl groups since the bond lengths and van der Waals radii of both the C-H and C-F bonds are less than those for C-OH, thus the fluorine and

hydrogen atoms do not introduce repulsive interactions within the enzyme active site (Table 2-1) (Withers et al., 1988). However, two major effects, electronic and binding, must be considered when investigating the effect of fluorine or hydrogen substitution on an enzymatic reaction.

Table 2-1: Size comparison of C-H, C-F and C-OH groups (Withers et al., 1988).

| Group | Bond length (Å) | Van der Waals Radius (Å) | Total (Å) |
|---|---|---|---|
| C-H | 1.09 | 1.20 | 2.29 |
| C-F | 1.39 | 1.35 | 2.74 |
| C-OH | 1.43 | 2.10 | 3.53 |

*(a) Electronic effects*: These effects will be important since differences in the electronegativity of substituents will result in different responses of the oxocarbonium ion-like transition states. The relatively electronegative fluorine atom will destabilise the oxocarbonium ion-like transition state, thus slowing down the reaction. By contrast, the relatively electropositive hydrogen atom is expected to stabilise the oxocarbonium ion-like transition state, thus speeding up the reaction. Indeed, such effects have been reported previously for non-enzymatic, acid-catalysed hydrolysis of glycosides in which the reactions are known to proceed via oxocarbonium ion transition states (Capon, 1969; BeMiller, 1967; Withers et al., 1986; Withers et al., 1989). On the basis of electronic effects, the rate of glycoside hydrolysis is expected to change in the order deoxy > hydroxy > deoxyfluoro.

*(b) Binding effects*: These effects will be significant also since deletion of crucial hydrogen bonds will destabilise the transition state, thus slowing down the reaction. Binding effects upon the substitution of fluorine or hydrogen for a hydroxyl group will be

manifested in the following way. In a hydrogen bond, the functional group containing the interacting hydrogen atom is referred to as the "donor" and the atom carrying the lone pair electrons with which this hydrogen interacts is called the "acceptor" atom (for example, fluorine and oxygen). The hydroxyl group of the sugar can function both as a hydrogen-bond donor and acceptor while the fluorine atom of a deoxyfluoro-glycoside can only accept a hydrogen bond. This hydrogen bond to the fluorine atom is likely weaker than that to the oxygen of the hydroxyl group since the lone pair of electrons on the fluorine is more tightly held by the nucleus than those on the oxygen. The hydrogen of a deoxy-glycoside cannot participate in a significant hydrogen bond. Based on the hydrogen bonding potential of fluorine, hydrogen and the hydroxyl group, the rates of glycoside hydrolysis are expected to increase in the order hydroxy > deoxyfluoro > deoxy.

In reality, the binding and electronic effects are superimposed on each other in enzymatic reactions and thus difficult to quantitate individually. However, minimum estimates of the amount of transition state stabilisation contributed by individual hydroxyl groups can be obtained from the comparison of rates with deoxy substrates with those for the parent compound.

### 2-1-6 pH Dependence of enzymatic reactions

Although enzymes contain many ionising groups, the most important ionisations are those involved in substrate binding and catalysis, as well as those responsible for maintaining the enzyme in an active conformation. When interpreting pH profiles the following assumptions are made (Fersht, 1985). The ionising groups act as perfectly titrating acids and bases, only one active site ionisation state of the enzyme is capable of converting substrate to product, proton transfers of all ionising groups are faster than the catalytic steps in the reaction, and the rate determining step of the reaction does not change with pH. Plots of $k_{cat}/K_m$ *versus* pH will yield $pK_a$ values for ionising groups within the free enzyme and/or free substrate while plots of $k_{cat}$ *versus* pH will yield $pK_a$ values for the

ionising groups within the enzyme-substrate complex whose decomposition is rate determining.

### 2-1-7 Background on kinetic analysis of *C. fimi* exoglycanase

Previous studies of *C. fimi* exoglycanase (Tull, M. Sc. Thesis, 1991; Tull et al., 1991; Tull & Withers, 1994) revealed that it catalyses the hydrolysis of aryl β-cellobiosides to cellobiose and the corresponding substituted phenol (Figure 2-2).

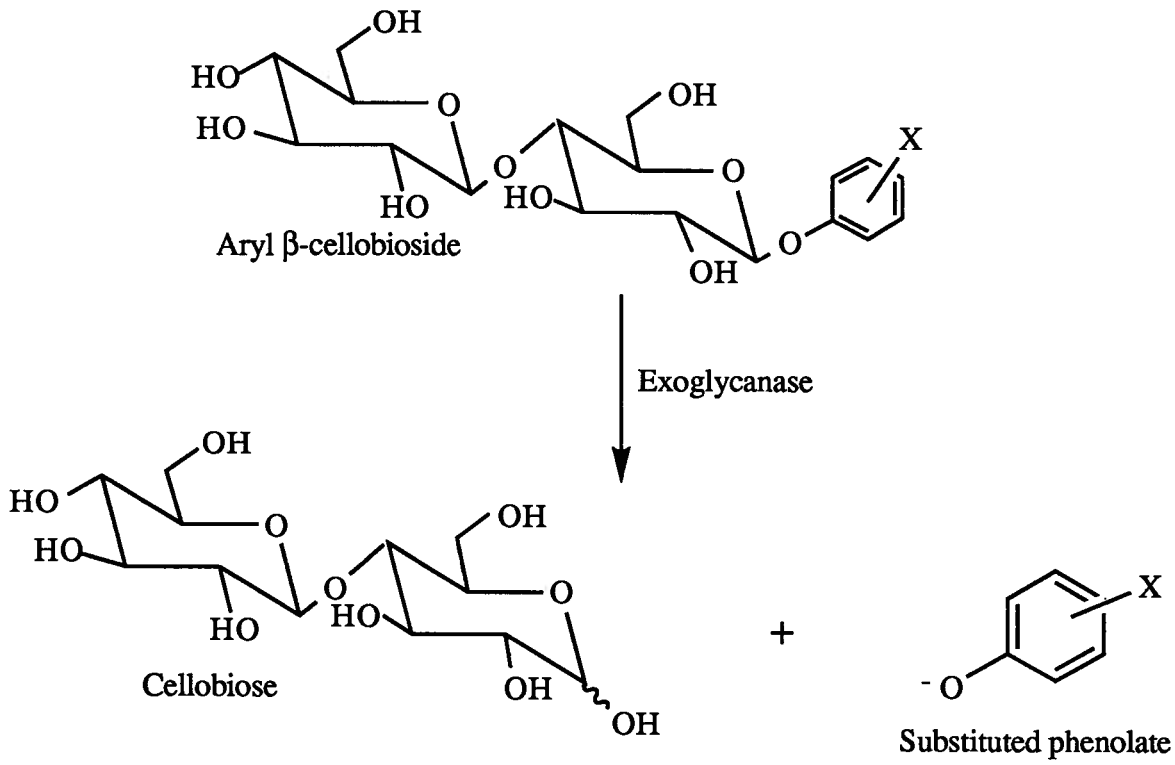


*Figure 2-2 C. fimi exoglycanase-catalysed hydrolysis of aryl β-cellobiosides.*

Similarly, this enzyme converts aryl β-D-glucosides to glucose and the corresponding substituted phenol. Values for $k_{cat}$, $K_m$ and $k_{cat}/K_m$ were determined for a series of aryl β-cellobiosides as well as for a series of aryl β-glucosides. Values of $k_{cat}/K_m$ for the hydrolysis of the cellobiosides were much higher than those for the corresponding

glucoside, as might be expected given that the normal mode of cello-oligosaccharide cleavage is one in which cellobiose is released. To probe the relationship between substrate structure and enzymatic activity a linear free energy relationship study was undertaken in which values of $\log(k_{cat})$ and $\log(k_{cat}/K_m)$ for these two substrate series were plotted as functions of the phenol leaving group $pK_a$ in the form of Broensted plots (Figure 2-3 and 2-4).

For the glucosides, both $\log(k_{cat})$ and $\log(k_{cat}/K_m)$ were linearly correlated with the phenol $pK_a$ indicating that both the rate determining step and first irreversible step (Appendix B-2) in the reaction are the formation of the glucosyl-enzyme intermediate as this is the step involving cleavage of the phenolate (Figure 2-3).

For the cellobiosides, the absence of any significant dependence of $\log(k_{cat})$ upon the phenol leaving group $pK_a$ across most of the range suggests that formation of the cellobiosyl-enzyme intermediate is not rate determining (Figure 2-4). Rather, hydrolysis of the cellobiosyl-enzyme intermediate is most probably rate limiting in this case. By contrast, the Broensted plot for $\log(k_{cat}/K_m)$ shows a modest linear dependence ($\beta_{lg} = -0.3$) across the entire $pK_a$ range (Figure 2-4). Since $k_{cat}/K_m$ reflects the first irreversible step in the reaction, likely initial C-O bond cleavage, then this dependence on leaving group ability is expected. Interestingly, a slight downward break at the higher $pK_a$ values seems to be present in the $\log(k_{cat})$ plot suggesting a change to rate determining glycosylation. However, this is somewhat obscured due to the relatively weak dependence of $\log(k_{cat})$ on the $pK_a$ in this region. Such biphasic Broensted plots are not uncommon with glycosidases since similar, though more pronounced, behaviour has been seen when probing substrate reactivity of β–glucosidases with aryl β-D-glucosides (Dale et al., 1986; Kempton & Withers, 1992). These results suggest that the rate determining step changes from deglycosylation to glycosylation with the poor leaving groups.

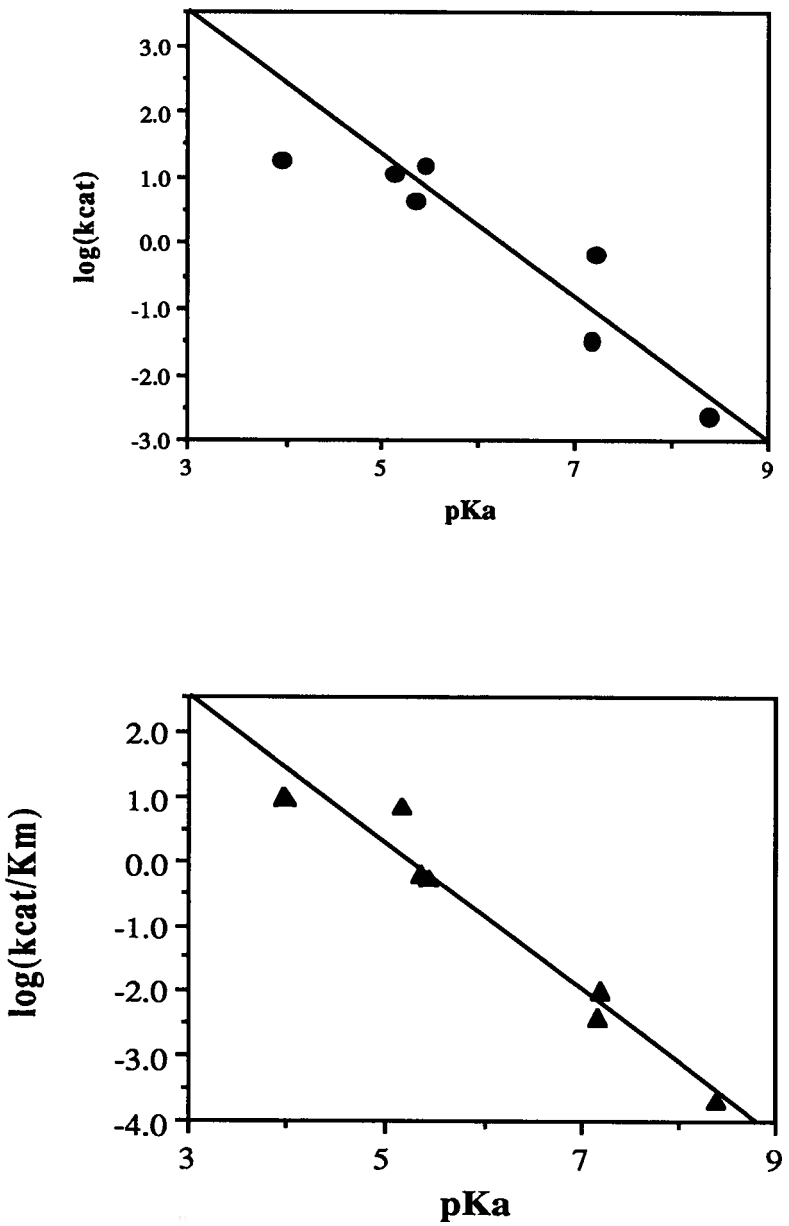


*Figure 2-3* *Broensted plots relating rates of C. fimi exoglycanase-catalysed hydrolysis of aryl β-glucosides with the leaving group ability of the phenols. (Upper) Plot of log($k_{cat}$) versus $pK_a$ of the aglycone phenols; (lower) plot of log($k_{cat}/K_m$) versus $pK_a$ of the aglycone phenols.*

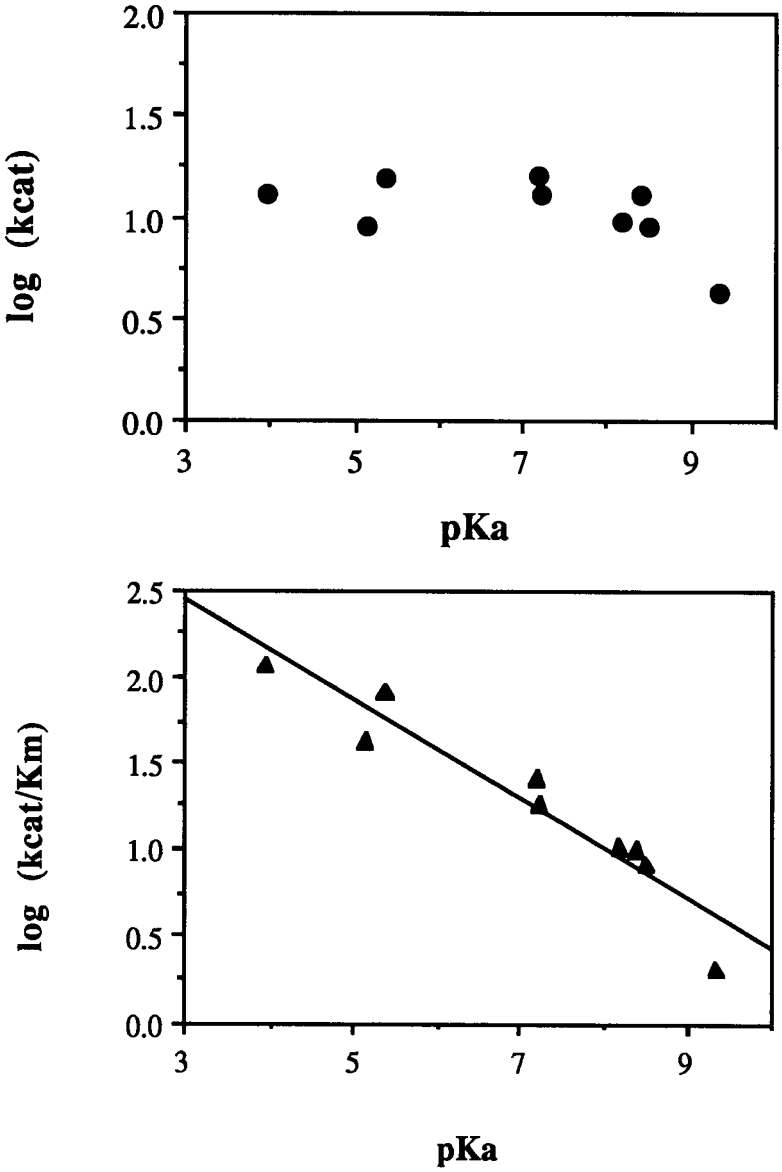


*Figure 2-4* *Broensted plots relating rates of C. fimi exoglycanase-catalysed hydrolysis of aryl β-cellobiosides with the leaving group ability of the phenols. (Upper) Plot of log($k_{cat}$) versus p$K_a$ of the aglycone phenols; (lower) plot of log($k_{cat}/K_m$) versus p$K_a$ of the aglycone phenols.*

These linear free energy relationship studies provide valuable insights into transition state structure. The large value of the Broensted constant ($\beta_{lg}$ = -1) for the glucosides, which is similar to those found for several β-glucosidases using similar glucosides (for example, $\beta_{lg}$ = -0.7 for *Agrobacterium* β-glucosidase (Kempton & Withers, 1992) and $\beta_{lg} \sim -1$ for sweet almond β-glucosidase (Dale et al., 1986)), reflects a large degree of negative charge accumulation on the phenolate oxygen at the glucosylation transition state. This indicates that there is almost complete C-O bond cleavage and relatively little proton donation to the departing phenolate at this transition state. By contrast, the Broensted constant for the cellobiosides ($\beta_{lg}$ = -0.3) is considerably less than that seen for the glucosides ($\beta_{lg}$ = -1), thus reflecting some degree of negative charge build up on the phenolate oxygen at the cellobiosylation transition state, but not as much as that seen at the glucosylation transition state. There are two likely causes for this difference. One could be that there is less C-O bond cleavage at the cellobiosylation transition state than at that for glucosylation. The other could be that general acid catalysis is more efficient in cellobioside hydrolysis, resulting in more proton donation than was seen for the glucosides. It is not easy to distinguish between these two possibilities.

The inactivators, 2F-DNPC and 2F-DNPG, are known to inactivate this exoglycanase by binding to the enzyme and forming covalent glycosyl-enzyme species (Tull et al., 1991; McCarter et al., 1993). The inactivated-enzymes are stable in buffer, but reactivate in the presence of a suitable glycosyl-acceptor (for example, cellobiose), presumably via a transglycosylation reaction. These results indicate that the covalent 2-deoxyfluoroglycosyl-enzymes are catalytically competent as they turn over to product, thus supplying further evidence for the proposed double displacement mechanism. Interestingly, inactivation of the enzyme by 2F-DNPC ($k_i/K_i$ = 6.12 x $10^{-1}$ $min^{-1}$ $mM^{-1}$) is $10^4$ times faster than by 2F-DNPG ($k_i/K_i$ = 5.56 x $10^{-5}$ $min^{-1}$ $mM^{-1}$) while both inactivated forms of the exoglycanase reactivate at comparable rates ($k_{hydrolysis}$ = 8.5 x $10^{-6}$ $min^{-1}$ and $k_{hydrolysis}$ = 1.3 x $10^{-5}$ $min^{-1}$ for the 2-deoxyfluorocellobiosyl- and 2-deoxyfluoroglucosyl-enzymes,

respectively). Interestingly, a somewhat similar situation is seen with the parent compounds, 2,4-DNPG and 2,4-DNPC. The $k_{cat}/K_m$ value for hydrolysis of 2,4-DNPC is ~10 times greater than that for hydrolysis of 2,4-DNPG, while the $k_{cat}$ values for hydrolysis of both substrates are comparable. This likely indicates that the glycosylation step is not rate determining for 2,4-DNPG, but rather another step, most likely deglycosylation. Indeed this would be consistent with the finding that the $\log(k_{cat})$ value for 2,4-DNPG falls slightly below the line defined by the other glucosides in the Broensted plot. These results suggest that the distal glucosyl unit of the cellobiosides increases the rate of glycosylation relative to that for the glucosides, but not the rate of deglycosylation.

## 2-2 Objectives of This Project

The aim of this project is the delineation of the detailed mechanism of *Cellulomonas fimi* exoglycanase by means of several different kinetic techniques. This will provide the first detailed kinetic characterisation of a cellulase and will lay the basis for understanding the consequences of mutations in other studies.

### 2-2-1 Pre-steady state analysis of aryl β-cellobiosides and aryl β-glucosides.

Stopped-flow kinetic analysis of the aryl β-cellobiosides may provide further evidence in support of the identity of the rate determining step previously deduced from the linear free energy relationship study. This analysis should also provide values for the rate constants for the formation of the cellobiosyl-enzyme intermediate ($k_2$) as well as values for the dissociation constant ($K_d$) of the E•S complex. Stopped-flow analysis of the aryl β–glucosides, 2,4-DNPG and PNPG, may provide evidence concerning the "true" identity of the rate-determining step for 2,4-DNPG.

## 2-2-2 Linear free energy relationships of aryl β-glycosides

*(a) Cellobiosides*: The presence of a linear free energy correlation between values of $k_2$ for the formation of the cellobiosyl-enzyme intermediate (derived from stopped-flow analysis) and the $pK_a$ of the phenol leaving group may provide insights into the degree of negative charge development at the glycosylation transition state for cellobioside hydrolysis.

*(b) Xylosides and xylobiosides:* Determination of the Michaelis-Menten kinetic parameters for *C. fimi* exoglycanase-catalysed hydrolysis of several aryl β-xylosides and aryl β-xylobiosides (Figure 2-5) may reveal further relationships between substrate structure and enzymatic activity. Furthermore, since gluco-sugars differ from xylo-sugars by the presence of the C-5 hydroxymethyl group then a comparison of the results for xyloside and xylobioside hydrolysis with those obtained previously for the hydrolysis of glucosides and cellobiosides may reveal any mechanistic function of the C-5 hydroxymethyl group.

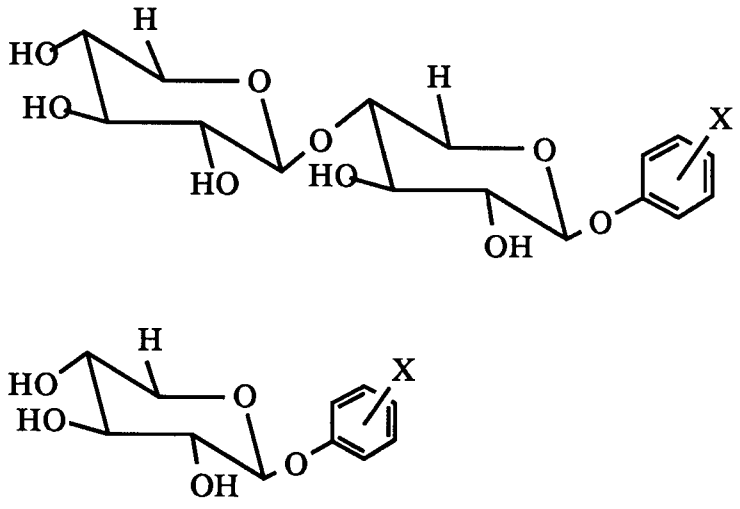


*Figure 2-5 Structures of aryl β-xylobiosides and aryl β-xylosides.*

### 2-2-3 α-Secondary deuterium kinetic isotope effects on aryl β-glycosides.

Values of $k_H/k_D$ for *C. fimi* exoglycanase-catalysed hydrolysis of aryl β-cellobiosides and aryl β-glucosides are expected to yield information on the degree of oxocarbonium ion character at the transition states, thus providing further insights into the identity of rate determining steps, the degree of bond cleavage at the transition states, as well as some indication of the extent of nucleophilic preassociation at the transition states.

### 2-2-4 Inactivation of *C. fimi* exoglycanase by 2-deoxy- and 2-deoxy-2-fluoro-sugars.

*(a) 2F-DNPX$_2$*: Inactivation-reactivation studies with 2,4-dinitrophenyl 2-deoxy-2-fluoro-β-xylobioside (Figure 2-6) can provide substantial evidence for the formation of a covalent glycosyl-enzyme intermediate during xylobioside hydrolysis by this enzyme.

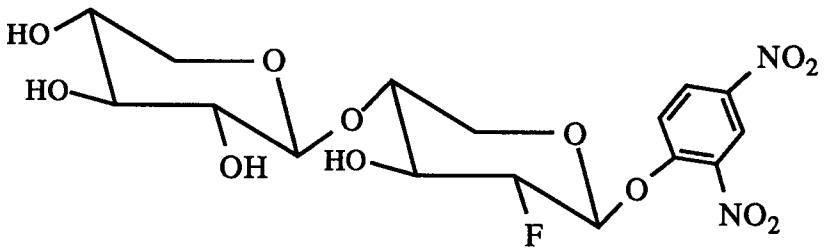


2F-DNPX$_2$

*Figure 2-6* *Structure of 2,4-dinitrophenyl 2-deoxy-2-fluoro-β-xylobioside (2F-DNPX$_2$).*

*(b) 2F-DNPC and 2F-GMF*: $^{19}$F-NMR analysis of *C. fimi* exoglycanase inactivated with 2,4-dinitrophenyl 2-deoxy-2-fluoro-β-cellobioside and 2-deoxy-2-fluoro 4-O-(β-glucosyl)-β-mannosyl fluoride (Figure 2-7) can yield information pertaining to the anomeric stereochemistry of the glycosyl-enzyme intermediate.

*(c) Cellobial*: As discussed in Chapter I, glycosidases are capable of catalysing the hydration of glycals to 2-deoxy-glycose products. Since glycals lack the hydroxyl group at the C-2 position then investigation of *C. fimi* exoglycanase using cellobial (Figure 2-8) in combination with results from previous studies with 2,4-dinitrophenyl 2-deoxy-2-fluoro-β-cellobioside and 2,4-dinitrophenyl β-cellobioside can provide information about the mechanistic role of the C-2 hydroxyl group during cellobioside hydrolysis.

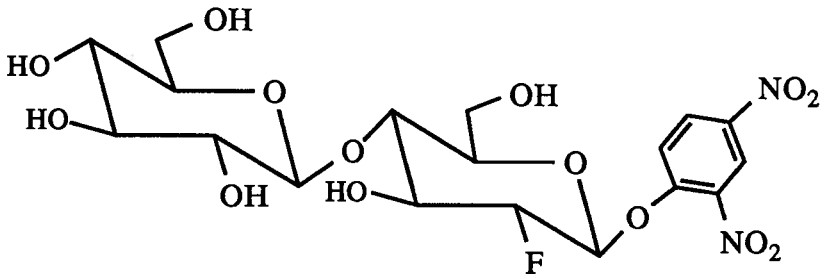


2F-DNPC

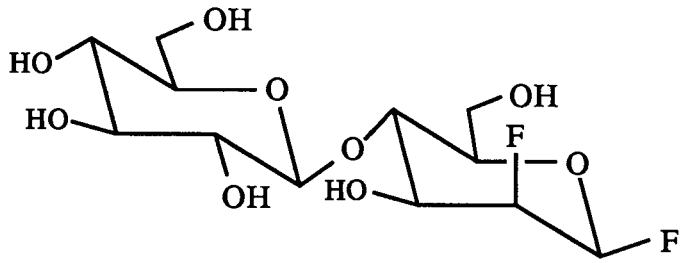


2F-GMF

*Figure 2-7* *Structures of 2,4-dinitrophenyl 2-deoxy-2-fluoro-cellobioside (2F-DNPC) and 2-deoxy-2-fluoro 4-O-(β-glucosyl)-β-mannosyl fluoride (2F-GMF).*

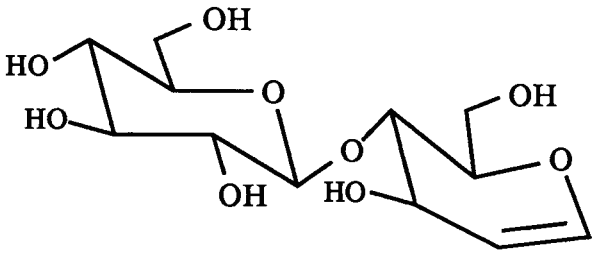


*Figure 2-8* *Structure of cellobial.*

### 2-2-5 pH Study

The pH dependence of the Michaelis-Menten parameters for cellobioside hydrolysis may provide insights into the ionisation state of active site residues involved in substrate binding and/or enzyme catalysis.

## 2-3 Results

### 2-3-1 Steady state kinetics for xylo-substrates

*C. fimi* exoglycanase catalyses the hydrolysis of aryl β-D-xylosides to the corresponding substituted phenol and xylose as well as catalysing the hydrolysis of aryl β-xylobiosides to the corresponding substituted phenol and xylobiose. Values for $V_m$ (maximum velocity) and $K_m$ were determined by fitting the initial rates of hydrolysis and the substrate concentrations to the Michaelis-Menten equation using the program GraFit (Leatherbarrow, 1990). These results are illustrated as Lineweaver-Burk plots (Appendix A-1 and A-2) for visual convenience. The Michaelis-Menten parameters for the xylosides (determined in collaboration with Ms. I. Setyawati) and xylobiosides, along with the $pK_a$ values for the phenol leaving groups, are listed in Tables 2-2 and 2-3. Values of $\log(k_{cat})$ and $\log(k_{cat}/K_m)$ for the xylosides are plotted as functions of the aglycone $pK_a$ in the form of Broensted plots (Figure 2-9) and in both cases a strong dependence upon the $pK_a$ is observed with Broensted constant, $\beta_{lg} = -0.8$ (correlation coefficient = 0.99) and -0.9 (correlation coefficient = 0.98) respectively. Equivalent plots of $\log(k_{cat})$ and $\log(k_{cat}/K_m)$ *versus* leaving group $pK_a$ for the xylobiosides are shown in Figure 2-10. Values of $\log(k_{cat})$ appear invariant with $pK_a$ over the narrow range of $pK_a$ of 5 - 7. The $\log(k_{cat}/K_m)$ Broensted plot appears scattered, however there are only four points thus interpretation is not truly warranted.

Table 2-2: Michaelis-Menten Parameters for the Hydrolysis of Aryl β-Xylosides by *C. fimi* Exoglycanase

| Phenol substituent | [a]$pK_a$ | $K_m$ (mM) | $k_{cat}$ ($s^{-1}$) | $k_{cat}/K_m$ ($mM^{-1}s^{-1}$) |
|---|---|---|---|---|
| 2,3-dinitro | 4.89 | 5.82 ± 0.62 | 70 ± 4 | 12 |
| 2,5-dinitro | 5.15 | 5.85 ± 0.89 | 108 ± 7 | 18 |
| 3,4-dinitro | 5.36 | 7.90 ± 2.32 | 22 ± 4 | 2.8 |
| 4-nitro | 7.18 | 20.0 ± 2.5 | 2.6 ± 0.2 | 0.13 |
| 4-cyano | 8.49 | 11.4 ± 1.0 | 0.098 ± 0.004 | 0.0089 |

[a]Phenol $pK_a$ values were taken from Barlin & Perrin (1966), Kortum et al. (1961), Robinson et al., (1960), and Ba-Saif & Williams (1988).

Table 2-3: Michaelis-Menten Parameters for the Hydrolysis of Aryl β-Xylobiosides by *C. fimi* Exoglycanase

| Phenol substituent | [a]$pK_a$ | $K_m$ (mM) | $k_{cat}$ ($s^{-1}$) | $k_{cat}/K_m$ ($mM^{-1}s^{-1}$) |
|---|---|---|---|---|
| 2,5-dinitro | 5.15 | 0.019 ± 0.004 | 27 ± 2 | 1443 |
| 3,4-dinitro | 5.36 | 0.012 ± 0.001 | 22 ± 1 | 1840 |
| 4-nitro | 7.18 | 0.015 ± 0.001 | 66 ± 2 | 4386 |
| 2-nitro | 7.22 | 0.078 ± 0.008 | 56 ± 2 | 714 |

[a]Phenol $pK_a$ values were taken from Barlin & Perrin (1966), Kortum et al. (1961), Robinson et al., (1960), and Ba-Saif & Williams (1988).

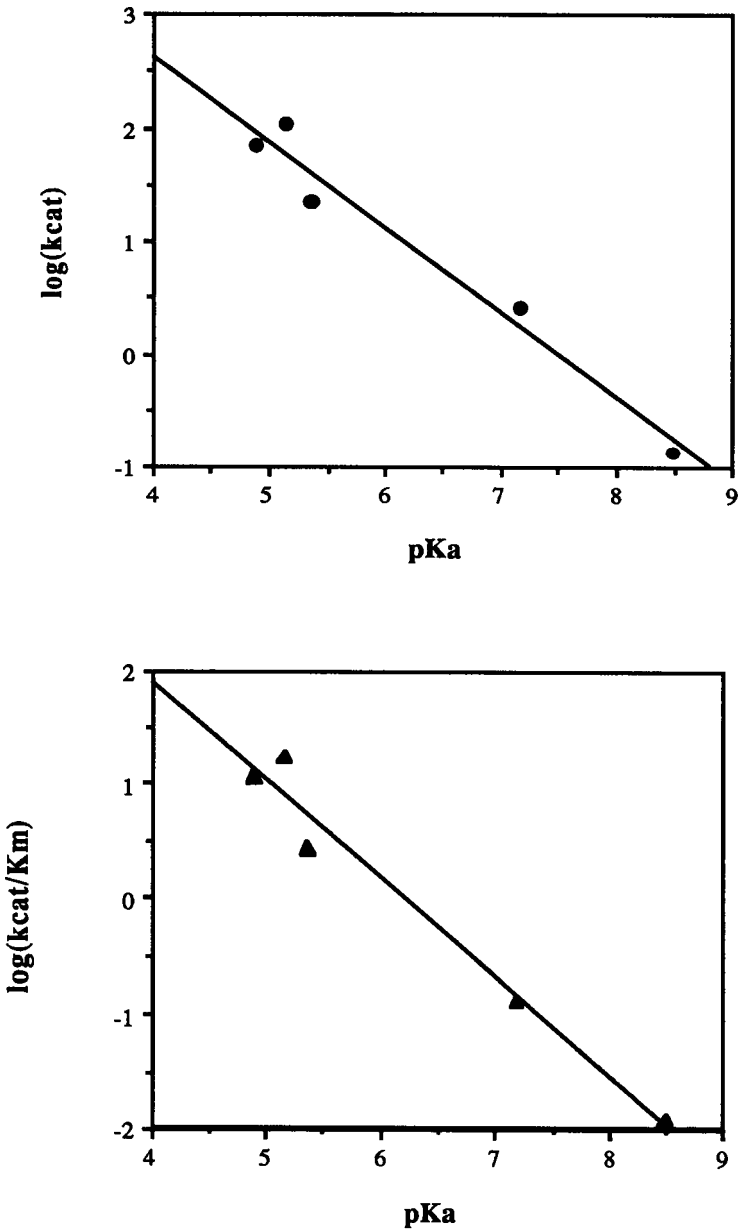


*Figure 2-9* *Broensted plots relating rates of C. fimi exoglycanase-catalysed hydrolysis of aryl β-xylosides with the leaving group ability of the phenols. (Upper) Plot of log($k_{cat}$) versus $pK_a$ of the aglycone phenols; (lower) plot of log($k_{cat}/K_m$) versus $pK_a$ of the aglycone phenols.*

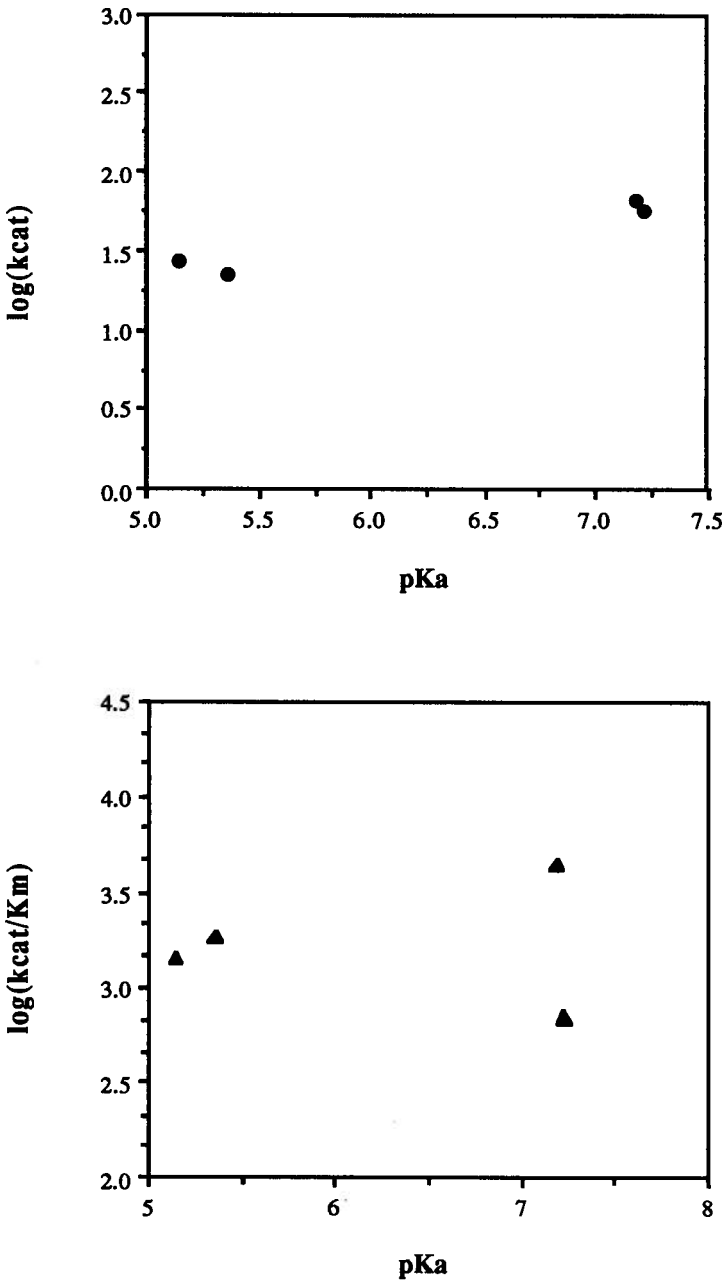


*Figure 2-10* *Broensted plots relating rates of C. fimi exoglycanase-catalysed hydrolysis of aryl β-xylobiosides with leaving group ability of the phenols. (Upper) Plot of log($k_{cat}$) versus p$K_a$ of the aglycone phenols; (lower) plot of log($k_{cat}/K_m$) versus p$K_a$ of the aglycone phenols.*

### 2-3-2 Pre-steady state kinetic analysis of the hydrolysis of gluco-substrates

Five aryl β-cellobiosides were subjected to pre-steady state analysis using a stopped-flow technique. Reaction rates were measured at five different substrate concentrations ranging from 0.2 x $K_d$ to $K_d$ and fitted to an equation describing a first order reaction followed by a steady state to yield values for the pseudo-first order rate constant ($k_{obs}$). Values for $k_2$ and $K_d$ were determined from these $k_{obs}$ values and substrate concentrations by direct fit to the Michaelis-Menten equation using the program GraFit (Leatherbarrow, 1990). These results are plotted as Lineweaver-Burk plots for visual convenience (Appendix A-3). The kinetic parameters for these five cellobiosides are presented in Table 2-4, along with the $pK_a$ values of the phenol leaving group as well as in the form of plots of $\log(k_2)$ and $\log(k_2/K_d)$ *versus* aglycone $pK_a$ (Figure 2-11). Good correlations are observed in both the $\log(k_2)$ (correlation coefficient = 0.93) and the $\log(k_2/K_d)$ (correlation coefficient = 0.91) plots, with slopes corresponding to Broensted constant, $\beta_{lg} = -0.3$.

Table 2-4: Pre-Steady State Parameters for Hydrolysis of Aryl β-Cellobiosides by *C. fimi* Exoglycanase.

| Phenol substituent | [a]$pK_a$ | $k_2$ ($s^{-1}$) | $K_d$ ($mM^{-1}$) | $k_2/K_d$ ($s^{-1}mM^{-1}$) |
|---|---|---|---|---|
| 2,4-dinitro | 3.96 | 1660 ± 236 | 10.0 ± 2.4 | 166 |
| 2,5-dinitro | 5.15 | 1160 ± 94 | 16.2 ± 2.0 | 72 |
| 3,4-dinitro | 5.36 | 626 ± 42 | 5.3 ± 0.7 | 118 |
| 4-nitro | 7.18 | 244 ± 67 | 12.4 ± 4.9 | 20 |
| 2-nitro | 7.22 | [b]ND | [b]ND | 13 |

[a]Phenol $pK_a$ values were taken from Barlin & Perrin (1966), Kortum et al. (1961), Robinson et al., (1960), and Ba-Saif & Williams (1988).
[b]ND = not determined

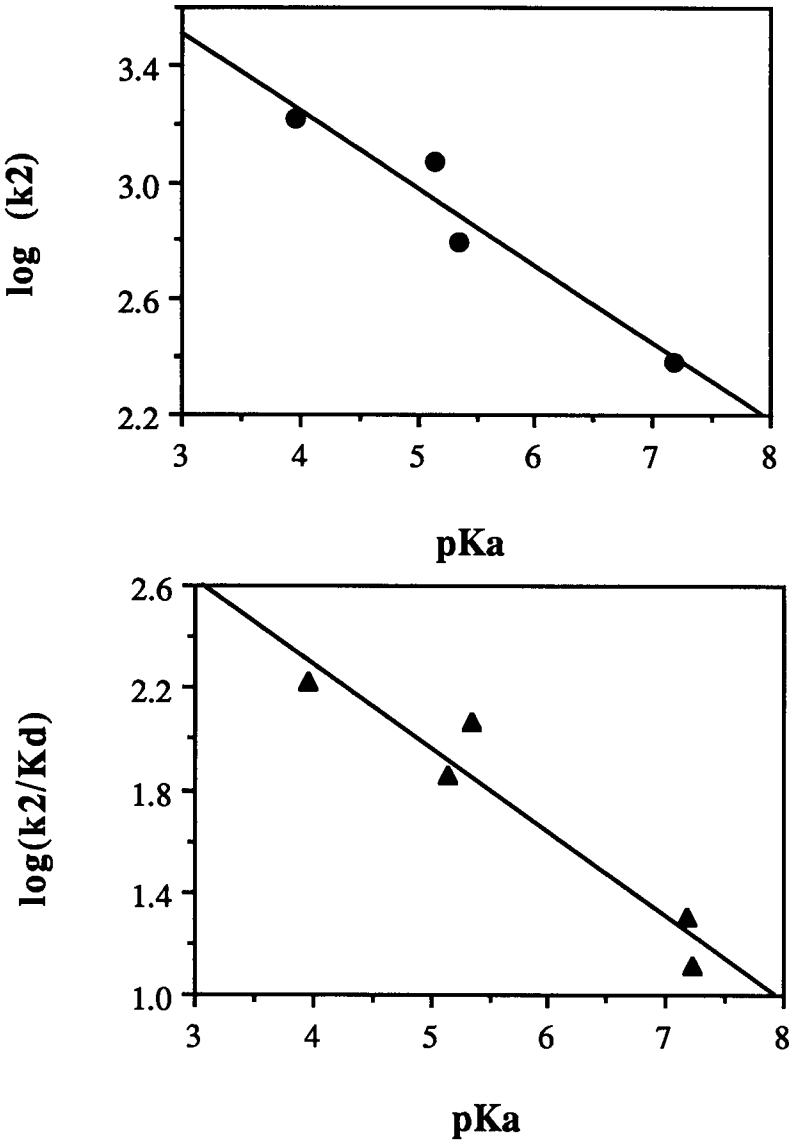


*Figure 2-11* *Broensted plots relating pre-steady state rates of C. fimi exoglycanase-catalysed hydrolysis of aryl β-cellobioside with leaving group ability of phenols. (Upper) Plot of log($k_2$) versus p$K_a$ of the aglycone phenols; (lower) plot of log($k_2/K_d$) versus p$K_a$ of the aglycone phenols.*

Two aryl β-D-glucosides, 2,4-DNPG and PNPG, were also subjected to pre-steady state analysis. Each glucoside was investigated at two different substrate concentrations. Like the cellobiosides, the exoglycanase concentration was selected to produce a burst of phenolate with a total absorbance change of 0.06 A. A burst of 2,4-dinitrophenolate of 0.05 A was observed for 2,4-DNPG while no burst could be detected for PNPG.

### 2-3-3 α-Secondary deuterium kinetic isotope effect measurements on gluco-substrates.

α-Secondary deuterium kinetic isotope effects were measured for three aryl β-cellobiosides and two aryl β-D-glucosides and are listed in Table 2-5 along with the rate determining step for each substrate.

Table 2-5: Secondary Deuterium Kinetic Isotope Effects Measured with *C. fimi* Exoglycanase

| Substrate | [a]RDS | $k_{cat}H/k_{cat}D$ |
|---|---|---|
| 2',4'-dinitrophenyl glucoside | DEGLY | 1.12 ± 0.02 |
| 4'-nitrophenyl glucoside | GLY | 1.12 ± 0.02 |
| 2",4"-dinitrophenyl cellobioside | DEGLY | 1.10 ± 0.02 |
| 4"-nitrophenyl cellobioside | DEGLY | 1.10 + 0.02 |
| 4"-bromophenyl cellobioside | GLY | 1.06 ± 0.02 |

[a]RDS, rate determining step.

### 2-3-4 Inactivation of *C. fimi* exoglycanase

Inactivation kinetic parameters for cellobial inactivation of *C. fimi* exoglycanase were determined by first calculating values of $k_{obs}$ by direct fit of the data to a first-order function using the program GraFit (Leatherbarrow, 1990) (Appendix A-8). Values of $K_i$ ~ 500 mM (binding constant) and $k_i$ ~ 2 $min^{-1}$ (inactivation rate constant) were determined by non-linear regression analysis using the program GraFit (Leatherbarrow, 1990). However, these values must be taken only as estimates since the insolubility of cellobial prevented study of *C. fimi* exoglycanase inactivation at cellobial concentrations greater than 60 mM. A more reliable value of $k_i/K_i = 2.9 \times 10^{-3} \pm 0.0001$ $min^{-1}$ $mM^{-1}$ was determined from the slope of the plot of $k_{obs}$ values *versus* cellobial concentration (Appendix A-8). Similar analysis of 2F-GMF inactivation of *C. fimi* exoglycanase yielded kinetic parameters of $K_i$ ~ 160 mM, $k_i$ ~ 0.069 $min^{-1}$ from the non-linear regression analysis while a more reliable value of $k_i/K_i = 4.4 \times 10^{-4} \pm 0.00004$ $mM^{-1}$ $min^{-1}$ was obtained from the slope of the $k_{obs}$ *versus* 2F-GMF concentration plot.

### 2-3-5 Reactivation of inactivated-*C. fimi* exoglycanase

Samples of cellobial-inactivated and 2F-$DNPX_2$-inactivated *C. fimi* exoglycanase were freed of excess inactivator by extensive dialysis, incubated in the presence a suitable glycosyl acceptor, and assayed for the return of enzymatic activity. Reactivation rates were then calculated from the slopes of plots of ln(full rate - observed rate) *versus* time or direct fit to a first order equation using the program GraFit (Leatherbarrow, 1990) (Appendix A-8 and A-9) and these are listed in Table 2-6.

Table 2-6: Rates of Reactivation of Inactivated *C. fimi* Exoglycanase in the Presence of a Glycosyl-Acceptor

| Glycosyl-enzyme species | $k_{react}$ (buffer) ($h^{-1}$) | $k_{react}$(cellobiose) ($h^{-1}$) |
|---|---|---|
| 2-deoxycellobiosyl- | $3.1 \times 10^{-2} \pm 0.003$ | $7.9 \times 10^{-2} \pm 0.008$ |
| 2-deoxyfluoroxylobiosyl- | $7.0 \times 10^{-4} \pm 0.0001$ | $1.8 \times 10^{-3} \pm 0.0002$ |

### 2-3-6 $^{19}$F-NMR analysis of inactivated-*C. fimi* exoglycanase

Samples of *C. fimi* exoglycanase were inactivated with either 2F-DNPC or 2F-GMF and subjected to $^{19}$F-NMR analysis. The $^{19}$F-NMR spectrum of the 2FCb-exoglycanase sample is shown in Figure 2-12, the broad peak at -195.5 ppm corresponding to 2FCb-exoglycanase. The signal at $\delta$ = -198.4 ppm corresponds to the C-2 fluorine of unreacted 2F-DNPC while that at $\delta$ = -198.1 ppm corresponds to the C-2 fluorine of either the hydrolysis product or a transglycosylation product. The $^{19}$F-NMR spectrum of the 2FGM-exoglycanase sample (Figure 2-13) reveals resonances at $\delta$ = -149.9 and -224.1 ppm corresponding to the C-1 and C-2 fluorines, respectively, of unreacted 2F-GMF while that at $\delta$ = -121.4 corresponds to released fluoride. The resonance at -205.4 ppm likely corresponds to the hydrolysis product, 2-deoxy-2-fluoro 4-O-(β-glucosyl)-α-mannose. The peak for the corresponding β-anomer would be expected to be very small since very little of the β-anomer is present at equilibrium and is likely buried under the peak at -224.1 ppm. The resonance at $\delta$ = -205.6 ppm in the dialysed sample corresponds to the C-2 fluorine of the 2FGM-exoglycanase. For the 2FGM-enzyme sample, since a high concentration of 2F-GMF (30 mM, $K_i$ ~ 160 mM) was required to inactivate the enzyme and since a low concentration of enzyme (9 mg/ml, 0.2 mM) was used, the signal for this 2FGM-exoglycanase is seen to be much smaller than those for the excess, unreacted 2F-GMF. For the 2FCb-enzyme sample, since the concentration of the

enzyme used was 0.2 mM and that of 2F-DNPC was ~1 mM, the signals for excess, unreacted 2F-DNPC and 2FCb-exoglycanase are seen to be comparable.

### 2-3-7 pH Study of *C. fimi* exoglycanase

The pH dependence of *C. fimi* exoglycanase was investigated using 2,4-DNPC as substrate over a pH range of 4.5 to 9.4. Values for $k_{cat}$ and $K_m$ were determined and are presented as plots of $k_{cat}$ *versus* pH in Figure 2-14. Values of $k_{cat}$ are seen to be independent of pH over this range, while $k_{cat}/K_m$ is seen to be dependent upon two ionisations of $pK_a = 4.1 \pm 0.1$ and $7.7 \pm 0.1$. The higher $pK_a$ value is a reliable value, but instability of the enzyme at low pH values precluded accurate determination of the lower ionisation constant. This value must therefore be taken simply as an estimate.

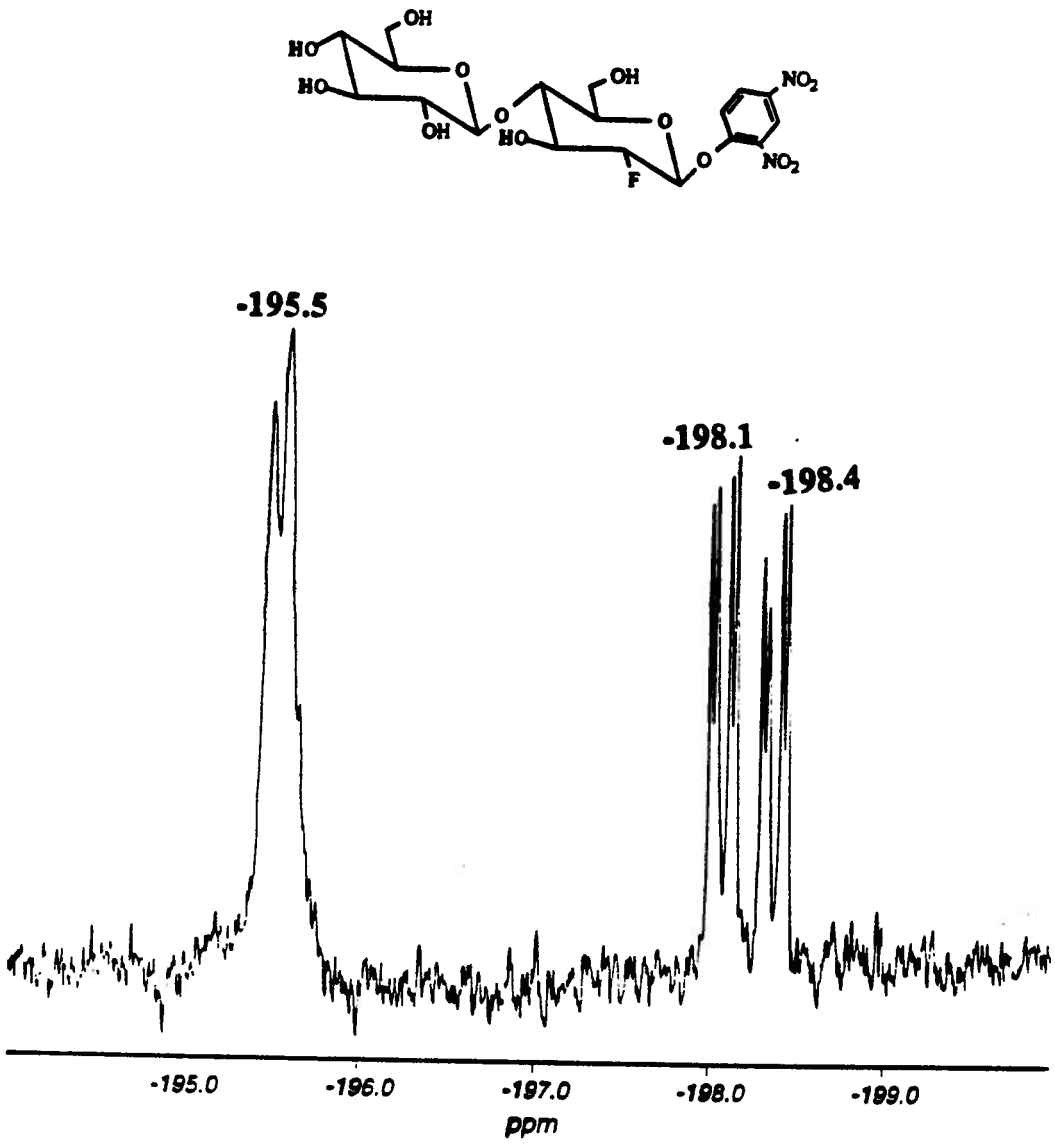


*Figure 2-12* *$^{19}$F-NMR spectrum of C. fimi exoglycanase inactivated by 2F-DNPC. [Enzyme] = 0.2 mM and [2F-DNPC] = 1.0 mM in 50 mM sodium phosphate buffer, 10% $D_2O$.*

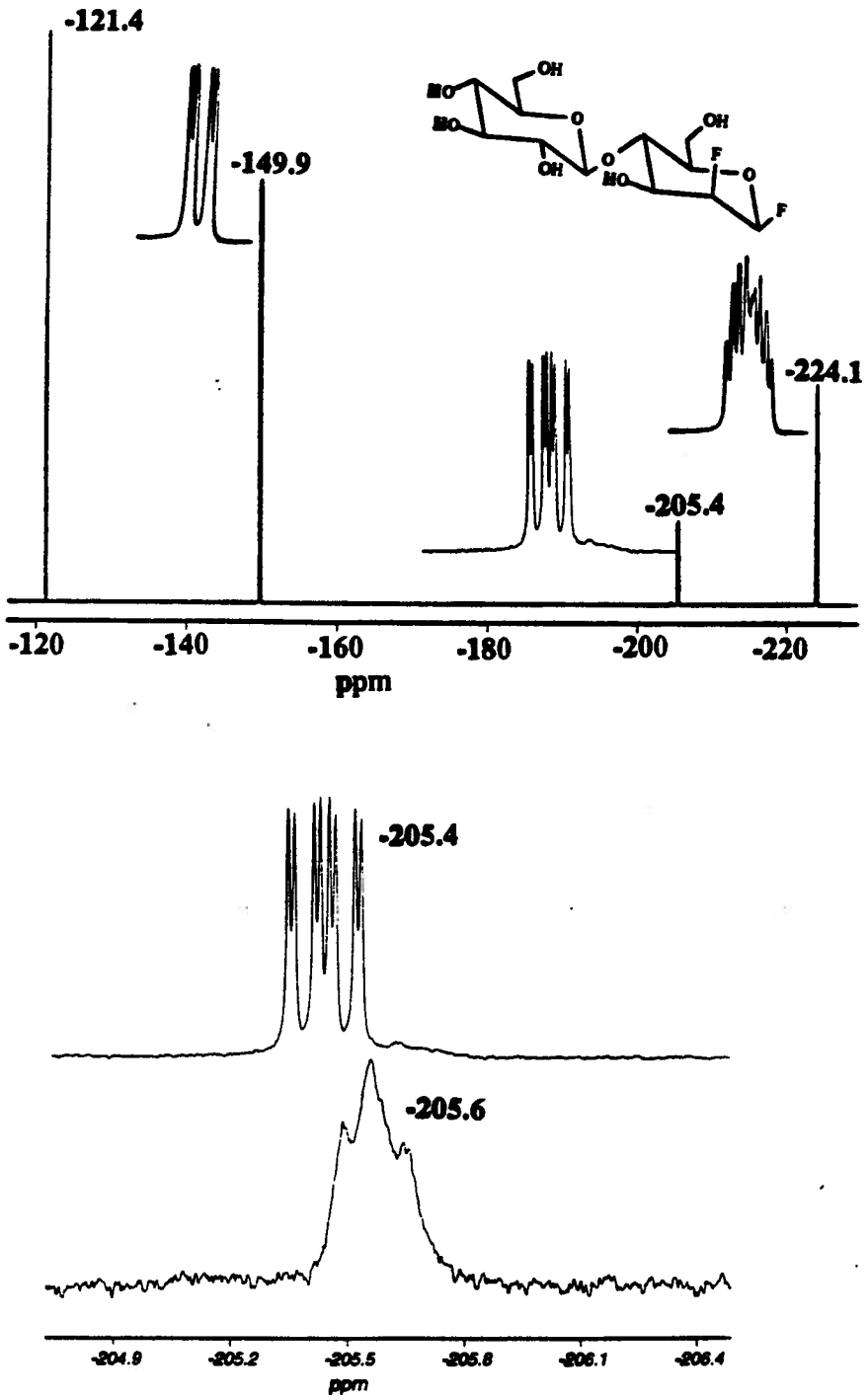


*Figure 2-13* *$^{19}$F-NMR spectra of C. fimi exoglycanase inactivated by 2F-GMF. [Enzyme] = 0.2 mM and [2F-GMF] = 30 mM in 50 mM sodium phosphate buffer, 10% $D_2O$. (Upper) $^{19}$F-NMR spectrum for the undialysed sample and (lower) $^{19}$F-NMR spectrum for the undialysed sample overlapped with that for the dialysed sample over the same ppm range.*

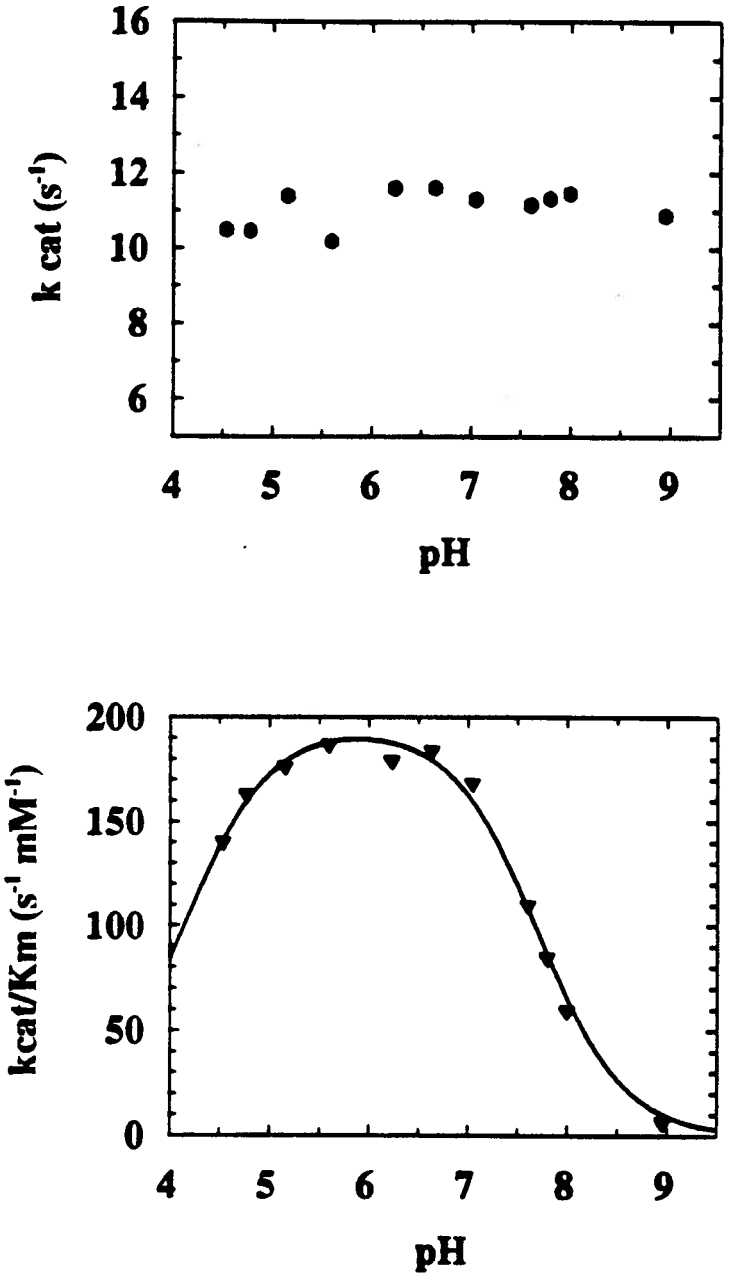


*Figure 2-14* *pH Dependence of the hydrolysis of 2,4-DNPC by native C. fimi exoglycanase.*

## 2-4 Discussion

### 2-4-1 pH Dependence of *C. fimi* exoglycanase

The substrate employed for these studies was 2,4-DNPC, for which the rate determining step is hydrolysis of the cellobiosyl-enzyme intermediate (*vide infra*). Values of $k_{cat}/K_m$ are seen to be dependent upon ionisations of approximate $pK_a = 4.1$ in the acidic limb of the pH profile and $pK_a = 7.7$ in the basic limb (Figure 2-14). This suggest that only one protonated state of the free enzyme is catalytically active. These $pK_a$ values are similar to those seen for free *Agrobacterium* β-glucosidase ($pK_a < 5$ and $pK_a = 7.0 - 7.2$) (Kempton & Withers, 1992). Interestingly, binding of the substrate to the exoglycanase shifts the $pK_a$ values of these groups considerably since no pH dependence is seen for the enzyme/substrate complex, as indicated by the pH independent $k_{cat}$ plot. Since the group in the free enzyme of $pK_a = 7.7$ must be protonated to be catalytically active then this ionisation likely reflects that of the general acid catalyst (Glu 127) which is required to protonate the departing aglycone in the glycosylation step. The group in the free enzyme of approximate $pK_a = 4.1$ which must be deprotonated to be catalytically active likely corresponds to the catalytic nucleophile (Glu 233). Alternatively, this ionisation could correspond to a group involved in accepting a proton from the catalytic nucleophile.

### 2-4-2 β-Glucanase activity of *C. fimi* exoglycanase

The large bursts of released, substituted phenolates observed in the stopped-flow analysis of the hydrolysis of the aryl β-cellobiosides indicate that for these substrates a step subsequent to aglycone release, most likely hydrolysis of the cellobiosyl-enzyme intermediate, is the rate determining step. These results are entirely consistent with those from a previous linear free energy relationship study of aryl β-cellobiosides (Tull & Withers, 1994) which revealed that values of $\log(k_{cat})$ were essentially invariant with the

$pK_a$ of the phenol leaving group over the $pK_a$ range 4-8, thus suggesting that deglycosylation was most probably the rate determining step.

Values of $\log(k_2)$ and $\log(k_2/K_d)$ are seen to be dependent on the $pK_a$ of the phenol leaving group with a Broensted constant of $\beta_{1g} = -0.3$ in both cases (Figure 2-11). These results suggest that both $k_2$ and $k_2/K_d$ reflect cleavage of the bond to the phenolate aglycone, thus formation of the cellobiosyl-enzyme. The slopes of plots of $\log(k_2)$ and $\log(k_{cat}/K_m)$ (Tull & Withers, 1994) *versus* $pK_a$ have exactly the same Broensted constant ($\beta_{1g} = -0.3$) as would be expected if both $k_2$ and $k_{cat}/K_m$ reflect the same step in the reaction. The stopped-flow results therefore provide further evidence in support of the proposal that the glycosylation step is the first irreversible step during cellobioside hydrolysis. In the previous linear free energy relationship study, the $\log(k_{cat})$ *versus* $pK_a$ plot (Figure 2-4) revealed an apparent slight downward break at the higher $pK_a$ values, possibly indicating a change in the rate determining step from deglycosylation to glycosylation (Tull & Withers, 1994). The stopped-flow analysis provides further insights into this phenomenon. Since the value of the Broensted constant for the $\log(k_2)$ plot is the same as the approximate value of the Broensted constant seen for this somewhat obscured $pK_a$-dependent region ($pK_a$ ~7 - 9) of the $\log(k_{cat})$ plot, this suggests that this region of the $\log(k_{cat})$ likely reflects formation of the cellobiosyl-enzyme. Thus the stopped-flow results, in combination with the $\log(k_{cat})$ *versus* $pK_a$ plot from the linear free energy relationship study, suggest that glycosylation is the rate determining step for aryl β-cellobiosides with poor leaving groups (phenol $pK_a > 7.5$) .

The value of the Broensted constant ($\beta_{1g} = -0.3$) seen for both the $\log(k_2)$ and $\log(k_2/K_d)$ plots (Figure 2-11) reflects relatively little negative charge accumulation on the departing phenolate oxygen at the glycosylation transition state for hydrolysis of these cellobiosides. As discussed in section 2-1-7, this Broensted constant ($\beta_{1g} = -0.3$) is considerably smaller than that previously seen for a series of aryl β-D-glucosides ($\beta_{1g} = -1$).

The identical α–secondary deuterium kinetic isotope effects ($k_H/k_D$ = 1.10) measured for the more reactive cellobiosides, 2,4-DNPC and PNPC, indicate substantial oxocarbonium ion character at the deglycosylation transition state (Table 2-5). This value is comparable to those reported for this step with other "retaining" β-glycosidases ($k_H/k_D$ = 1.11 for *Agrobacterium* β-glucosidase (Kempton & Withers, 1992) and $k_H/k_D$ = 1.2-1.25 for *E. coli* (lac z) β-galactosidase (Sinnott, 1978)) thus providing further evidence for the involvement of a covalent glycosyl-enzyme intermediate during glycoside hydrolysis since such secondary deuterium kinetic isotope effects could only be seen if the intermediate had more $sp^3$ character than the subsequent transition state. This value of the kinetic isotope effect suggests that there is relatively little preassociation of the nucleophile (water) at the deglycosylation transition state. By contrast, the smaller isotope effect ($k_H/k_D$ = 1.06) measured for the cellobiosylation step using 4-BrPC indicates a transition state for this substrate with lesser oxocarbonium ion character. This value falls well within the range ($k_H/k_D$ = 1.0 for *E. coli* (lac z) β-galactosidase (Sinnott, 1978) and $k_H/k_D$ = 1.10 for *Agrobacterium* β-glucosidase (Kempton & Withers, 1992)) of isotope effects measured on the glycosylation transition state with other "retaining" glycosidases. This small kinetic isotope effect, taken in combination with the small Broensted constant ($\beta_{lg}$ = -0.3) for cellobioside hydrolysis, is consistent with a relatively early cellobiosylation transition state with either little bond cleavage or considerable protonic assistance coupled with substantial nucleophilic pre-association.

### 2-4-3 β-Glucosidase activity of *C. fimi* exoglycanase

The absence of a pre-steady state burst of 4-nitrophenolate for PNPG, under conditions where a full burst of 4-nitrophenolate was observed for PNPC, indicates that hydrolysis of the glucosyl-enzyme intermediate is not rate determining for PNPG. Instead, it is likely that formation of the glucosyl-enzyme intermediate is the rate determining step for this substrate. These stopped-flow results are entirely consistent with those from a

previous linear free energy relationship study which revealed that values of $\log(k_{cat})$ were linearly dependent on the $pK_a$ of the phenol leaving group over the range $pK_a$ 4-8 and thus suggested that glucosylation is the rate determining step for these glucoside substrates. By contrast, a burst of 2,4 dinitrophenolate comparable in magnitude to that measured for 2,4-DNPC was observed for 2,4-DNPG. Like the cellobioside substrates, this result indicates that hydrolysis of the glucosyl-enzyme intermediate is most likely the rate determining step for 2,4-DNPG. This result is consistent with that from the linear free energy relationship study which revealed that the $\log(k_{cat})$ value for 2,4-DNPG falls below the line defined by the other substrates in the $\log(k_{cat})$ Broensted plot (Figure 2-3), as would be expected if the rate determining step for this glucoside was indeed deglycosylation. The deglycosylation rates for 2,4-DNPC and 2,4-DNPG are similar, indicating that, in strict contrast to the situation with the glycosylation step, the presence of the distal glucose moiety does *not* assist the deglycosylation process. In fact, exactly the same situation has been reported previously for the hydrolysis of 2FCb- and 2FGlu- (2-deoxyfluoroglucosyl) enzyme (discussed in Section 2-1-7, (Tull & Withers, 1994)).

A possible reaction coordinate diagram which describes this situation is shown in Figure 2-15, the energy levels are arbitrarily chosen. As a first approximation, it is assumed that the transition states for glycosylation and deglycosylation are similar in energy as expected for an evolved enzyme system and as shown by changes in the rate determining step with leaving group ability. A second assumption is that of uniform binding (Albery & Knowles, 1976), in that the distal glucosyl unit stabilises both transition states and the glycosyl-enzyme intermediate to a similar extent. As a consequence of this, the activation energy required for hydrolysis of the glucosyl-enzyme is seen to be comparable to that for hydrolysis of the cellobiosyl-enzyme, and thus is consistent with the similar rates of deglycosylation observed with glucoside and cellobioside substrates. Furthermore, since values of $K_m$ for the glucosides having glycosylation as the rate determining step, thus $K_m \sim K_d$, are comparable to $K_d$ values for the cellobiosides, obtained

from stopped-flow analysis ($K_m$ (PNPG) = 8.3 mM and $K_d$ (PNPC) = 12.4 mM), it is assumed that the ground state binding energy is similar for the glucosides and cellobiosides. As a result of this, the activation energy for formation of the glucosyl-enzyme is seen to be greater than that for formation of the cellobiosyl-enzyme, thus the glycosylation rates for the glucosides are lower than those for the cellobiosides.

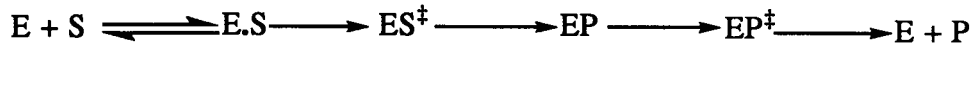


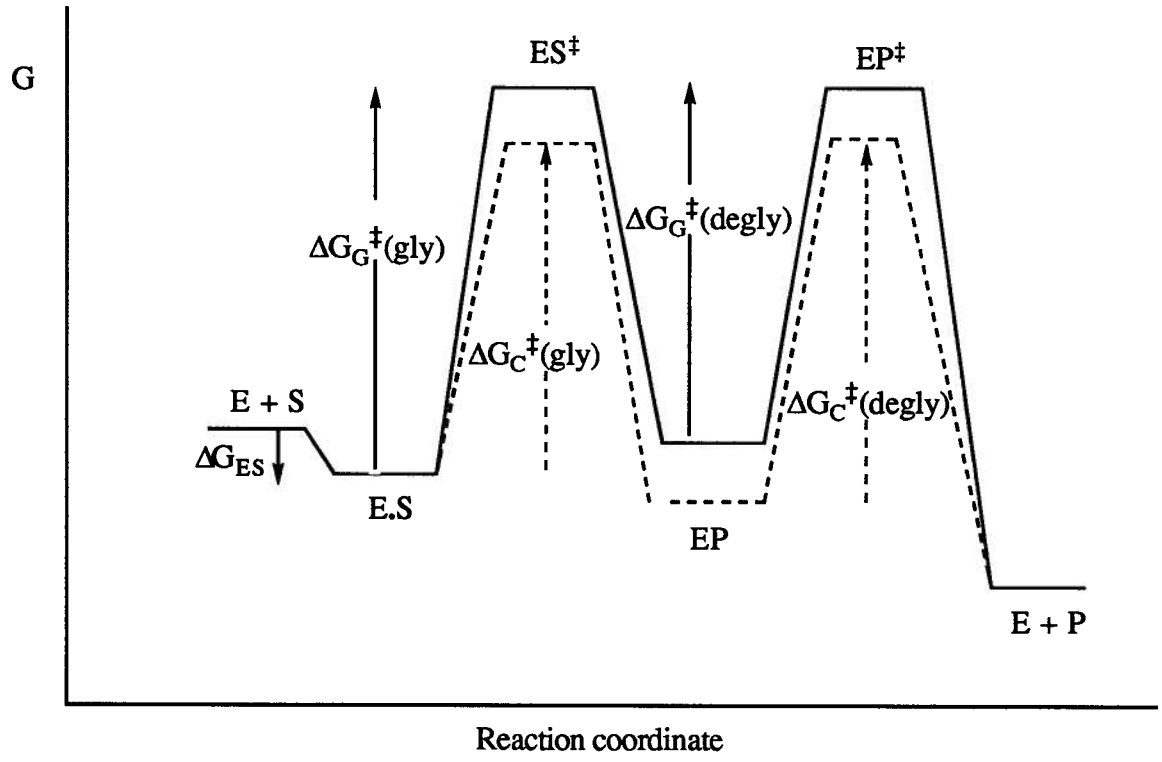


*Figure 2-15* *Reaction coordinate diagram illustrating the stabilisation produced by the distal glucosyl moiety of the cellobiosides (dashed line = glucosides, solid line = cellobiosides)*

The secondary deuterium kinetic isotope effect measured for PNPG ($k_H/k_D$ = 1.12) reflects substantial $sp^3$ to $sp^2$ rehybridization, thus a large degree of oxocarbonium ion

character at the glucosylation transition state. This necessarily implies considerable bond cleavage and little preassociation of the enzymatic carboxylate nucleophile. The value of this isotope effect is slightly larger than those reported for the glucosylation transition states in several other β-glucosidases, values tending to range from 1.0 for *E. coli* (lac z) β-galactosidase (Sinnott, 1978) to 1.10 for *Agrobacterium* β-glucosidase (Kempton & Withers, 1992). However it should be noted that interpretations are clouded somewhat by the known dependence of the kinetic isotope value on the nature of the leaving group involved in each case. For example, the kinetic isotope effect measured on the glucosylation transition state for *Agrobacterium* β-glucosidase was $k_H/k_D$ = 1.05 using MNPG while a value of $k_H/k_D$ = 1.10 was measured using PNPG (Kempton & Withers, 1992). This substantial degree of oxocarbonium ion character implied by the kinetic isotope effect measured for PNPG with *C. fimi* exoglycanase is however consistent with the relatively large Broensted constant ($\beta_{lg}$ = -1) obtained from the previous linear free energy relationship study of aryl β–glucosides which indicated a large amount of negative charge development on the phenolate oxygen at the glucosylation transition state. The kinetic isotope effect, taken in combination with the Broensted constant, reveals a glucosylation transition state for PNPG that is relatively late, with almost complete C-O bond cleavage, little protonic assistance, and relatively little pre-association of the carboxylate nucleophile. By contrast, the smaller kinetic isotope effect and lesser negative charge development at the transition state for formation of the cellobiosyl-enzyme suggest that this transition state is relatively early. This likely arises from the increased protonic assistance, possibly coupled with a greater degree of nucleophile preassociation by the catalytic nucleophile. The energy input required for formation of this more highly organised transition state is likely derived from the additional binding interactions with the distal glucosyl moiety.

The kinetic isotope effect for 2,4-DNPG ($k_H/k_D$ = 1.12) is also large, but falls well within the range measured for other glycosidases on the deglycosylation step ($k_H/k_D$ = 1.09 for *Botrydiplodia theobromae* β-glucosidase (Umezerika, 1988) to $k_H/k_D$ = 1.2-1.25

for *E. coli* (lac z) β-galactosidase (Sinnott, 1978)). Like the transition state for hydrolysis of the cellobiosyl-enzyme, the value of the isotope effect for 2,4-DNPG reflects a transition state for hydrolysis of the glucosyl-enzyme that involves substantial development of positive charge at the anomeric centre, extensive bond cleavage, and relatively little preassociation of the water.

### 2-4-4 Xylanase activity of *C. fimi* exoglycanase

Initial substrate specificity studies showed that *C. fimi* exoglycanase was capable of catalysing the hydrolysis not only of cellulose but also xylan, with comparable efficiency (Gilkes et al., 1984). A reinvestigation using aryl β-xylobiosides revealed that $k_{cat}/K_m$ values for xylobioside hydrolysis are in fact 30 -100 times higher than those for equivalent cellobiosides. This xylanase activity is not entirely surprising as *C. fimi* exoglycanase has been classified, on the basis of sequence similarities of catalytic domains, as a member of the F family of β-glycanases which is made up largely of xylanases (Gilkes et al., 1991; Henrissat & Bairoch, 1993). In addition, both *C. fimi* exoglycanase and xylanase Z from *Clostridium thermocellum* (whose cellulase activity is < 0.5% of the xylanase activity (Grepinet et al., 1988)) have been shown to be "retaining" glycosidases, thus implying that they share a common catalytic mechanism. Since cellobiosides differ from xylobiosides by the presence of the C-5 hydroxymethyl group, it is clear that this group cannot play an essential role in catalysis in the way shown for other glycosidases (Sinnott, 1987; Kempton & Withers, 1992). Instead the presence of this group rather seems to be slightly inhibitory. The X-ray crystal structure of the free exoglycanase and that of the enzyme crystallised with a 2FCb moiety covalently bond at the active site provide insights into this situation (White et al., 1995). Comparison of these structures reveals that upon binding the 2FCb moiety, Gln 87 is moved out of its original position and Trp 281 is rotated about its $C_\beta$-$C_\gamma$ bond to accommodate the C-5 hydroxymethyl groups of the distal and proximal glucosyl units, respectively. These results suggest that the presence of the C-5 hydroxymethyl

groups introduce steric interactions within the active site. This relief of steric strain is not achieved without a "cost", realised in less binding energy available for catalysis, thus lower rates of hydrolysis are observed for the cellobiosides relative to those for the xylobiosides. Presumably, any favourable interactions (hydrogen bonds) present at O-6 when cellobiosides are bound to the exoglycanase will be satisfied by bound water when xylobiosides are present, as seen for the L-arabinose/D-galactose binding protein (Quiocho et al., 1989). Other cellulases that have xylanase activity include endoglucanases E and H from *Clostridium thermocellum*, however, in those cases the cellulase activity is considerably greater than that of the xylanase (Hall et al., 1988; Yague et al., 1990).

Although only four xylobiosides were studied, the Broensted plots can still provide valuable insights into the rate limiting steps. Values of $\log(k_{cat})$ for hydrolysis of these aryl β-xylobiosides are seen to be independent of the phenol $pK_a$ over the narrow range of $pK_a$ 5-7 (Figure 2-10), indicating that hydrolysis of the xylobiosyl-enzyme is likely the rate determining step for these substrates. Since deglycosylation is also the rate determining step for the corresponding cellobiosides, these results suggest that the absence of the C-5 hydroxymethyl group does not affect the relative rates of glycosylation and deglycosylation. The $\log(k_{cat}/K_m)$ *versus* $pK_a$ plot is scattered and, as there are only four points, it is not possible to derive any meaningful information.

### 2-4-5 Xylosidase activity of *C. fimi* exoglycanase

Comparison of $k_{cat}/K_m$ values for hydrolysis of xylosides (Table 2-2) and xylobiosides (Table 2-3) reveals that the exoglycanase catalyses the hydrolysis of the xylosides $10^4$ times less efficiently than the corresponding xylobiosides. These results are consistent with previous findings that glucosides are hydrolysed less efficiently than corresponding cellobiosides and with the fact that hydrolysis of oligosaccharide substrates results in the formation of disaccharides, not monosaccharides. Values of $k_{cat}/K_m$ for xyloside hydrolysis are comparable to those for the corresponding glucosides (Tull &

Withers, 1994) while values of $k_{cat}/K_m$ for xylobiosides are 30 - 100 times higher than those for the corresponding cellobiosides, suggesting that it is the distal sugar whose C-5 hydroxymethyl group is inhibitory.

The strong correlations of both $\log(k_{cat})$ and $\log(k_{cat}/K_m)$ with the leaving group $pK_a$ for the xyloside substrates (Figure 2-9) indicate that both the rate determining step and the first irreversible step in catalysis are the formation of the xylosyl-enzyme. Comparison of these results with those for the glucosides, xylobiosides, and cellobiosides indicates that in general the rate determining step for *C. fimi* exoglycanase catalysed hydrolysis of the monosaccharide substrates is different from that for the corresponding disaccharide substrates. The large value of the Broensted constant ($\beta_{1g}$ = -0.8) for the $\log(k_{cat})$ plot reflects a large degree of negative charge build-up on the phenolate oxygen at the transition state for formation of the xylosyl-enzyme. This result is entirely consistent with the value of the Broensted constant ($\beta_{1g}$ = -0.9) for the $\log(k_{cat}/K_m)$ plot. The similarity of the Broensted constant for hydrolysis of both the xyloside and the glucosides ($\beta_{1g}$ = -1) (Tull & Withers, 1994) indicates that at the transition states for formation of the xylosyl-enzyme and the glucosyl-enzyme, C-O bond cleavage of the phenolate has proceeded to a similar extent and that the degree of proton donation is similar.

### 2-4-6 Inactivation-reactivation studies of *C. fimi* exoglycanase with 2F $DNPX_2$

As discussed in Chapter I, 2-deoxy-2-fluoro-β-D-glycosides have been used to inactivate several "retaining" glycosidases through trapping of covalent glycosyl-enzyme intermediates. The presence of the electronegative fluorine at C-2 destabilises the oxocarbonium ion-like transition states, thus slowing down both the glycosylation and deglycosylation steps while the good leaving group (for example 2,4-dinitrophenolate) accelerates glycosylation resulting in accumulation of the glycosyl-enzyme. Previous studies revealed that *C. fimi* exoglycanase is inactivated in the presence of 2F-$DNPX_2$

(Ziser et al., 1995 ). Formation of the 2-deoxyfluoroxylobiosyl-enzyme ($2FX_2$-enzyme) ($k_i/K_i$ = 16 $min^{-1}$ $mM^{-1}$) is 26-fold more efficient than formation of the 2FCb-enzyme ($k_i/K_i$ = 0.61 $min^{-1}$ $mM^{-1}$) (McCarter et al., 1993; Tull & Withers, 1994) as indicated by the relative $k_i/K_i$ values. This rate ratio is comparable to that seen for the relative $k_{cat}/K_m$ values for the hydrolysis of xylobiosides and the corresponding cellobiosides and thus is consistent with the view that the presence of the C-5 hydroxymethyl group is slightly inhibitory to catalysis.

Removal of excess 2F-$DNPX_2$ by extensive dialysis does not immediately restore enzymatic activity, consistent with the formation of a covalently bonded xylobiosyl-enzyme species. Conversion of the $2FX_2$-enzyme to free active enzyme, that is reactivation, can occur by two separate routes; either by a hydrolysis reaction or by transglycosylation of the xylobiosyl moiety to a suitable acceptor such as cellobiose. These two routes have been demonstrated previously for *Agrobacterium* β-glucosidase (Withers & Street, 1988). Transglycosylation in this case is presumed to involve nucleophilic attack by the C-4 hydroxyl group of cellobiose at the anomeric centre of the 2-fluoroxylobiosyl-enzyme. Reactivation of the inactivated-exoglycanase in this manner is consistent with the formation of a xylobiosyl-enzyme intermediate and its ability to be converted to product and free enzyme.

Reactivation of the 2-deoxyfluoroglycosyl-enzyme via the hydrolysis reaction provides values for the deglycosylation rates of these 2-deoxyfluoroglycosyl-enzyme species. Comparison of these deglycosylation rates with those for the parent glycosides can provide insights into the deglycosylation transition state for xylobioside hydrolysis. The deglycosylation rate for hydrolysis of the parent xylobiosides is 30 - 100 times higher than that for the equivalent cellobiosides while the deglycosylation rate for hydrolysis of the $2FX_2$-enzyme ($k_{react}$ = 7.0 x $10^{-4}$ $h^{-1}$) and the 2FCb-enzyme ($k_{react}$ = 5.1 x $10^{-4}$ $h^{-1}$) (Tull & Withers, 1994) are comparable. These results suggest that the presence of the fluorine atom at the C-2 position of the sugar has a greater destabilising effect on the transition state for

hydrolysis of the $2FX_2$-enzyme than on that for hydrolysis of the 2FCb-enzyme. These results likely reflect the fact that highly positively charged transition states will be more sensitive to fluorine substitution than ones with less positive charge (discussed in section 2-1-5). This suggests that the degree of oxocarbonium ion character at the transition state for hydrolysis of the xylobiosyl-enzyme is greater than that at the transition state for hydrolysis of the cellobiosyl-enzyme.

### 2-4-7 Characterisation of the glycosyl-*C. fimi* exoglycanase intermediate

*(a) Covalent nature*: The downward break in the $\log(k_{cat})$ *versus* $pK_a$ Broensted plot and the bursts of released phenolate seen in the stopped-flow study are consistent with the formation of a glycosyl-enzyme intermediate during *C. fimi* exoglycanase-catalysed hydrolysis of the aryl β-cellobiosides. Initial evidence for the covalent nature of this intermediate derives from studies of the inactivation of this exoglycanase by 2F-DNPC (McCarter et al., 1993; Withers et al., 1993). The catalytic competence of this 2FCb-enzyme intermediate has been demonstrated previously by its conversion to product and active enzyme via either a hydrolysis reaction or a transglycosylation reaction (McCarter et al., 1993; Tull & Withers, 1994). More recently, mass spectrometric analysis of this inactivated-*C. fimi* exoglycanase provided direct evidence for the formation of a 2FCb-enzyme as well as identified the modified active site amino acid as a glutamate residue, thus an ester linkage is formed between the anomeric carbon of the sugar and the active site residue of *C. fimi* exoglycanase (discussed in detail in Chapter IV).

*(b) Stereochemistry*: The stereochemistry of this ester linkage between the sugar and the exoglycanase was probed with the inactivators, 2F-DNPC and 2F-GMF, using $^{19}$F-NMR. The $^{19}$F-NMR spectrum of a sample of 2FCb-exoglycanase (Figure 2-12) reveals a resonance at $\delta$ = -198.4 ppm corresponding to the C-2 fluorine of unreacted 2F-DNPC (β- anomer). The broad signal resonating at $\delta$ = -195.5 ppm is consistent with a

fluorine attached to a macromolecule and thus presumably corresponds to the C-2 fluorine of the 2FCb-enzyme. Similarly for *Agrobacterium* β-glucosidase, the C-2 fluorine of the 2-deoxyfluoroglucosyl-enzyme is seen to resonate at $\delta$ = -197.3 ppm while the C-2 fluorine of the 2-deoxyfluoroglucosyl-β-fluoride inactivator resonated at $\delta$ = -203.4 ppm (Withers & Street, 1988). Although small differences ($\Delta\delta$ = 2.9 ppm) in $^{19}F$ chemical shifts between α– and β– anomers of 2-deoxyfluoroglycosyl esters are often seen (for example, the signal of the C-2 fluorine of the α-anomer of 1,3,4,6-tetra-O-acetyl-2-deoxy-2-fluoro-D-glucose is 1.5 ppm upfield of that of the β-anomer (Csuk & Glanzer, 1988)) the anomeric configuration of the ester linkage of the intermediate cannot be reliably deduced based only on this criteria.

2F-GMF is seen to inactivate *C. fimi* exoglycanase in a time-dependent manner (Appendix A-8, Figure A-8-2). Thus, $^{19}F$-NMR analysis of 2F-GMF-inactivated exoglycanase should provide further insights into the anomeric stereochemistry of the intermediate since the $^{19}F$ chemical shift for 2F-mannose and its derivatives is more sensitive to the anomeric configuration than that for 2F-glucose and its derivatives, a difference of approximately 20 ppm being seen between α- and β-anomers in all cases (Csuk & Glanzer, 1988). Samples of 2F-GMF-inactivated *C. fimi* exoglycanase and untreated enzyme were subjected to mass spectrometric analysis. The molecular weight of the unlabeled catalytic domain of *C. fimi* exoglycanase is 34 815 ± 7 Da while that for the catalytic domain treated with 2F-GMF is 35 155 ± 7 Da. The mass difference of 339 Da corresponds well with the mass increase of 327 Da expected if the exoglycanase was modified by a single 2-deoxyfluoro-4-O-β-glucosylmannosyl- (2FGM-) moiety. Thus, the mass spectrometric analysis is consistent with the formation of a covalent 2FGM-enzyme species. $^{19}F$-NMR analysis of this 2FGMF-inactivated exoglycanase sample (Figure 2-13) reveals signals at $\delta$ = -149.9 and -224.1 ppm corresponding to the C-1 and C-2 fluorines, respectively, of excess 2F-GMF inactivator. This inactivated enzyme sample was extensively dialysed against buffer to remove the sugars, and the dialysed sample

resubjected to $^{19}$F-NMR analysis. The single broad peak seen at $\delta$ = -205.6 ppm in the spectrum of the dialysed sample (Figure 2-13), some 18.5 ppm downfield from the C-2 fluorine of 2F-GMF, is consistent with the presence of 2FGM-enzyme. These $^{19}$F-NMR results are consistent with those reported for *Agrobacterium* β-glucosidase since the C-2 fluorine of the 2-deoxy-2-fluoro-D-β-mannosyl fluoride inactivator is observed to resonate at $\delta$ = -224.4 ppm while that of the 2-deoxyfluoromannosyl-enzyme resonates 23.4 ppm downfield at $\delta$ = -201.0 ppm (Withers & Street, 1988). Since α-anomers of 2-deoxy-2-fluoromannosyl esters are known to generally resonate 16-20 ppm downfield from β-anomers then the $^{19}$F signal at $\delta$ = -205.6 ppm for the 2FGM-enzyme is completely consistent with the α-anomeric configuration of the ester linkage. These results provide further evidence in support of the formation of a covalent α-glycosyl-enzyme intermediate during *C. fimi* exoglycanase-catalysed hydrolysis of glycosides.

### 2-4-8 *C. fimi* exoglycanase-catalysed hydration of cellobial

Hydration of glycals by "retaining" glycosidases involves initial protonation at C-2 of the glycal and attack at C-1 by the catalytic nucleophile to form a covalent 2-deoxyglycosyl-enzyme intermediate similar to that formed during glycoside hydrolysis. Generally, the proton is delivered by the catalytic nucleophile as revealed by deuterium labeling experiments. However, in a few cases it is believed that the proton is donated by the acid-base catalyst (discussed in detail in Chapter I). Subsequent hydrolysis of this 2-deoxyglycosyl-enzyme intermediate yields a 2-deoxy-glycose product and free enzyme. Legler (1990) has proposed a mechanism for the formation of the 2-deoxyglycosyl-enzyme intermediate involving the concerted syn addition of the carboxylic acid nucleophile across the double bond via a cyclic 6-membered transition state (Figure 2-16) while Matsui and coworkers (Matsui et al., 1993) have proposed an alternative mechanism involving an oxocarbonium ion. Hydrolysis of the 2-deoxyglycosyl-enzyme intermediate is believed to occur via an oxocarbonium ion-like transition state (Matsui, 1993).

*C. fimi* exoglycanase-catalysed hydration of glycals was probed using cellobial. Interestingly, rather than hydration occuring, *C. fimi* exoglycanase is seen to be inactivated in the presence of cellobial in a time-dependent manner (Appendix A-8). Mass spectrometric analysis of the inactivated-exoglycanase is consistent with the formation of a 2-deoxycellobiosyl- (2dCb-) enzyme (discussed in detail in Chapter IV), suggesting that the rate of formation of the intermediate is much greater than that of hydrolysis. This 2dCb-enzyme can be slowly converted to free enzyme and product via either a hydrolysis reaction or a transglycosylation reaction using a suitable glycosyl acceptor, such as cellobiose, in a manner similar to that seen for 2FGlu-, 2FCb- and $2FX_2$-exoglycanase, thus indicating that the 2dCb-enzyme intermediate is catalytically competent. These results are consistent with those reported for *E. coli* β-galactosidase since $^1H$ NMR experiments have revealed that this β-galactosidase is capable of converting D-galactal to glyceryl 2-deoxy β-D-galactoside in the presence of glycerol (Lehmann & Zieger, 1977). In contrast to *C. fimi* exoglycanase, studies with other glycosidases reveal that the corresponding 2-deoxyglycosyl-enzyme intermediates are not accumulated, but rather the glycals are readily converted to the 2-deoxy-glycose products (reviewed in Legler, 1990).

The large value of the dissociation constant ($K_i$ ~ 500 mM) for cellobial compared to the dissociation constants ($K_d$) for the aryl β-cellobiosides indicates that cellobial binds at least 30 times less efficiently than the cellobioside substrates. These results are consistent with those previously reported with other enzymes since glycals typically bind to glycosidases 10-100 times worse than do the corresponding glycosides (Legler, 1990). Given that glycals are somewhat similar to transition state analogues, in terms of their planar geometry

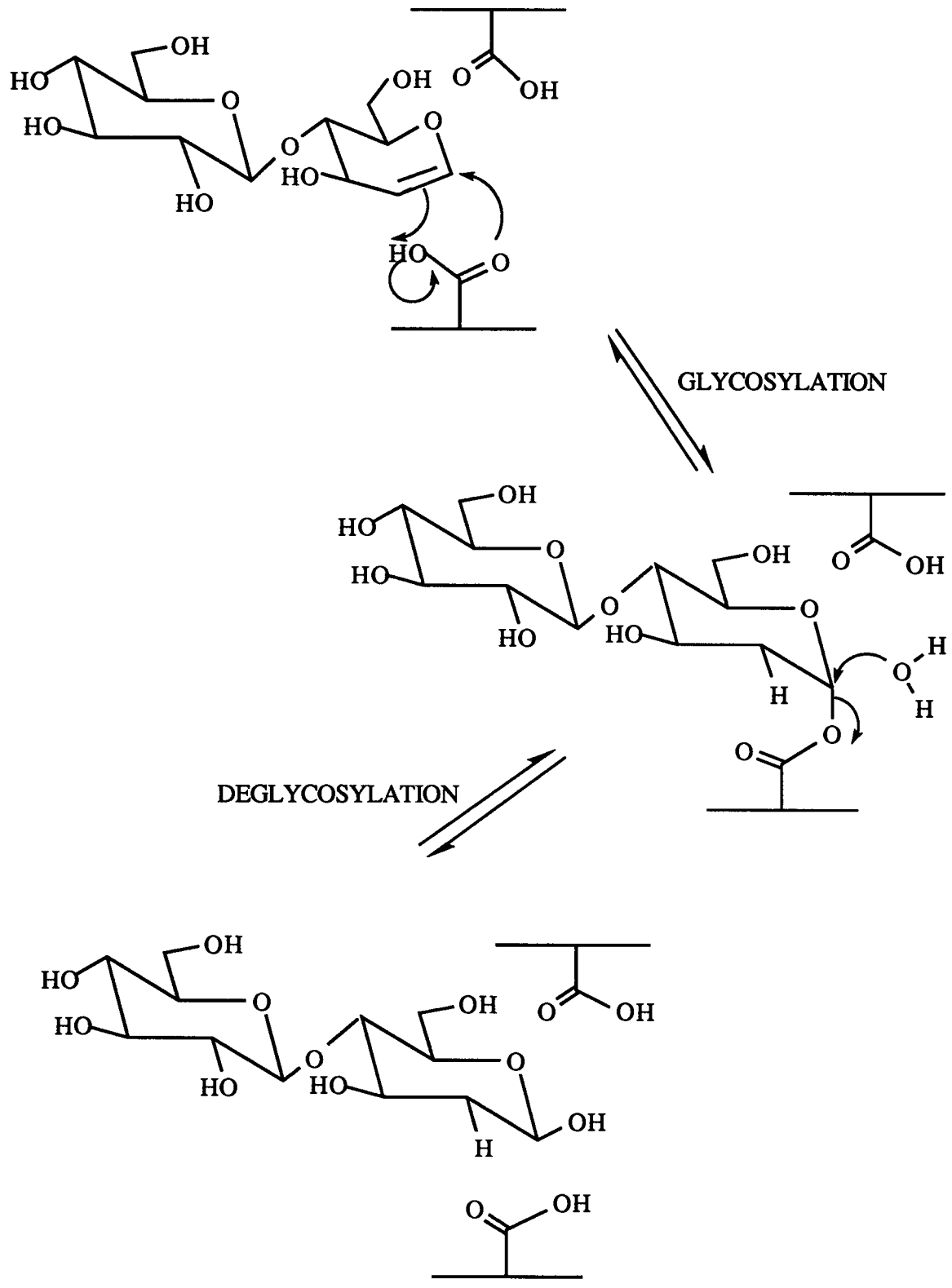


*Figure 2-16 Mechanism for glycosidase-catalysed hydration of a glycal.*

at C-1, this poor binding is likely a consequence of the absence of the C-2 hydroxyl group and thus the loss of important non-covalent interactions between the sugar and the enzyme. The X-ray crystal structure of the 2FCb-exoglycanase (White et al., 1995) provides some insights into this situation. The side chains of Asn 126 and Glu 233 are seen to be within hydrogen bonding distance of the fluorine atom at the C-2 position of the 2FCb moiety. This data suggest that the side chains of Asn 126 and Glu 233 are likely involved in hydrogen bonding interactions with the C-2 hydroxyl group of the parent cellobioside. Since the hydrogen atom at the C-2 position of cellobial cannot form hydrogen bonding interactions with Asn 126 and Glu 233, the absence of these interactions likely contributes to the poor binding ($K_i$ ~ 500 mM) seen for this sugar.

### 2-4-9 Effect of substitutions at C-2 on cellobioside hydrolysis rates

*(a) Fluorine substitution*: Formation of the 2FCb-exoglycanase ($k_i/K_i = 1.02 \times 10^{-2}$ $s^{-1}$ $mM^{-1}$) is $10^4$-fold less efficient than formation of the cellobiosyl-exoglycanase ($k_2/K_d$ = 166 $s^{-1}$ $mM^{-1}$) for a dinitrophenyl cellobioside. Similarly, rate reductions of $3 \times 10^2$ and $1 \times 10^5$ are seen on the glycosylation step for *Agrobacterium* β-glucosidase (Street et al., 1992) and *E. coli* β-galactosidase (McCarter et al., 1992) respectively, when the C-2 hydroxyl group is replaced by a fluorine atom. These results are consistent with destabilization of the oxocarbonium ion-like transition state for glycosylation due to the presence of the electronegative fluorine atom at C-2. As previously mentioned, the X-ray crystal structure for 2FCb-exoglycanase reveals that the amine group of Asn 126 and the carboxylate group of Glu 233 are seen to be within hydrogen-bonding distance of the C-2 position of the proximal glucosyl moiety of the 2FCb sugar, thus the fluorine atom can accept a hydrogen bond from the amine group. However, the hydroxyl group that is normally present at this C-2 position of the sugar could either donate or accept a hydrogen bond with the amine group of Asn 126, as well as form a hydrogen bond with Glu 233. Although these

hydrogen bonds are to the intermediate, presumably they will be present and stronger at the transition states. Thus, replacement of the C-2 hydroxyl group with a fluorine atom results in the loss of several important hydrogen bonds which serve to further destabilise the glycosylation transition state.

The rate of hydrolysis of the 2FCb-exoglycanase is $10^7$-fold lower than that of the cellobiosyl-enzyme. Similarly, rate reductions of $10^8$-fold have been reported on the deglycosylation step for both *Agrobacterium* β-glucosidase (Street et al., 1992) and *E. coli* β-galactosidase (McCarter et al., 1992) when a fluorine atom is substituted for the normal C-2 hydroxyl group. Comparison of the rate reductions seen on the glycosylation step ($10^4$-fold) with that seen on the deglycosylation step ($10^7$-fold) upon replacing the C-2 hydroxyl group with a fluorine atom indicates that the presence of the fluorine atom has a greater destabilising effect on the transition state for deglycosylation than on that for glycosylation. This interpretation is consistent with the previous suggestion of a greater degree of oxocarbonium ion character at the transition state for deglycosylation than at that for glycosylation, as suggested by the larger α-secondary deuterium kinetic isotope effect measured on the deglycosylation step using 2,4-DNPC and PNPC compared to that measured on the glycosylation step using 4-BrPC.

*(b) Hydrogen substitution*: Hydrolysis of the 2dCb-exoglycanase is $10^6$ times less efficient than that of the cellobiosyl-exoglycanase. Similarly, the rate of hydrolysis of the 2-deoxygalactosyl-β-galactosidase from *E. coli* is $10^5$ times lower than that for the galactosyl-enzyme (Wentworth & Wolfenden, 1974; Viratelle & Yon, 1980). Interestingly however, for *Aspergillus wentii* β-glucosidase, the rates of hydrolysis for both the 2-deoxyglucosyl- and glucosyl-enzymes were identical (Roeser & Legler, 1981). Substitution of a hydrogen atom for a hydroxyl group results in the loss of important hydrogen bonds normally present between the C-2 hydroxy group of the sugar and the enzyme, thus leading to destabilisation of the deglycosylation transition state. Comparison

of the rate of hydrolysis of the 2dCb-enzyme with that of the Cb-enzyme ($k_{cat}$ for 2,4-DNPC) indicates that the non-covalent interactions between C-2 of the sugar and the enzyme contribute at least ~9 kcal/mole[a]. This represents only a minimum estimate of the stabilisation energy contributed by the C-2 hydroxyl group since the electronic effects on the oxocarbonium ion-like transition state from the electropositive hydrogen at C-2 will partially compensate for the loss of these binding interactions.

## 2-5 Summary

*C. fimi* exoglycanase has been shown previously to hydrolyse its substrates with net retention of anomeric configuration, thus a double displacement reaction has been proposed to describe its mechanism of action.(Withers et al., 1986). This enzyme has been subjected to a detailed kinetic investigation with a range of aryl β-glycosides in order to provide additional evidence in support of the proposed mechanism.

Values of $k_{cat}$ are found to be invariant with pH whereas those of $k_{cat}/K_m$ are dependent upon two ionisations of $pK_a = 4.1$ in the acidic limb of the pH profile and $pK_a = 7.7$ in the basic limb, presumably corresponding to the catalytic nucleophile (Glu 233) and the acid catalyst (Glu 127), respectively. Secondary deuterium kinetic isotope effects on the glucosides revealed that the transition states for formation and hydrolysis of the glucosyl-enzyme are relatively late with almost complete bond cleavage and little preassociation of

---

[a]Determined using

$$\Delta\Delta G^{o\ddagger} = - RT \ln\left(\frac{k_{cat}\ (2,4\text{-DNPC})}{k_{hydrolysis}\ (2dCb\text{-enzyme})}\right)$$

the nucleophile. Further, the large negative charge accumulation seen on the phenolate oxygen as reflected by the value of the Broensted constant suggests that there is little protonic assistance at the transition state for formation of the glucosyl-enzyme.

Similar analyses on the cellobiosides in combination with previous inactivation studies with 2F-DNPC and 2F-DNPG reveal that the distal glucosyl moiety of the cellobiosides accelerates the rate of formation of the glycosyl-enzyme, but has no significant effect on its rate of hydrolysis. The smaller secondary deuterium kinetic isotope effect and lesser negative charge development on the phenolate oxygen for cellobiosyl-enzyme formation relative to that for glucosyl-enzyme formation suggest that the presence of the second glucosyl moiety results in an earlier transition state for cellobiosyl-enzyme formation. This likely arises from increased acid catalysis, possibly coupled with a greater degree of nucleophilic preassociation by the catalytic nucleophile. Presumably the energy input required for formation of this more highly organised cellobiosylation transition state relative to the glucosylation transition state is derived from the additional binding interactions with the distal glucosyl moiety of the cellobiosides. By contrast, the transition state for hydrolysis of the cellobiosyl-enzyme is seen to be similar to that for hydrolysis of the glucosyl-enzyme, occurring relatively late with significant C-O bond cleavage and oxocarbonium ion character.

Kinetic analysis with the xylo-substrates reveal that the substrate preference of this enzyme increases in the order glucosides < xylosides < cellobiosides < xylobiosides. These results, in combination with the X-ray crystal structure of 2FCb-exoglycanase (White et al., 1995), indicate that the distal C-5 hydroxylmethyl group is slightly inhibitory to catalysis. The comparable Broensted constants for xyloside and glucoside hydrolysis reveals that the transition states for formation of the xylosyl-enzyme and the glucosyl-enzyme are similar.

Inactivation studies with 2F-DNPC and cellobial reveal that the C-2 hydroxyl group of the sugar is necessary for catalysis. Inspection of the X-ray crystal structure of the 2FCb-exoglycanase revealed that the C-2 hydroxyl group, normally present at this position, likely forms strong hydrogen bonds with the enzyme at the transition state, most likely with Asn 126 and Glu 233. Removal of this hydroxyl group is seen to decrease the binding energy available for stabilisation of the deglycosylation transition state by at least 9 kcal/mole.

Mass spectrometric analysis of 2FCb-exoglycanase provided further evidence in support of the covalent nature of the glycosyl-enzyme intermediate formed during *C. fimi* exoglycanase catalysed hydrolysis of glycosides. Additional evidence was derived from the values of the secondary deuterium kinetic isotope effects measured for glycosides having deglycosylation as the rate determining step ($k_H/k_D$ = 1.12 for the glucoside and $k_H/k_D$ = 1.10 - 1.12 for the cellobiosides), since such effects could only be seen if the intermediate has more $sp^3$ character than the subsequent deglycosylation transition state. $^{19}$F-NMR analysis of the 2FCb- and 2FGM-enzymes provided evidence for the α-stereochemistry of the anomeric linkage between the sugar and the enzyme.

All the data presented are consistent with the proposed double displacement mechanism for this exoglycanase.

# CHAPTER III

# DETAILED KINETIC ANALYSIS OF MUTANTS OF *C. FIMI* EXOGLYCANASE

## 3-1 Introduction

Site directed mutagenesis can be used to systematically replace individual residues within a protein one at a time and thus provides a way of probing the role of specific residues in binding and catalysis. These studies have been performed extensively on several glycosidases in order to identify possible candidates for the role of acid-base catalyst (Sierks et al., 1990; Chauvaux et al., 1992; Svensson & Sogaard, 1993; MacLeod et al., 1994; Juncosa et al., 1994; Wang et al., 1995; Damude et al., 1995) as well as for the role of catalytic nucleophile (Malcolm et al., 1989; Holm et al., 1990; Grace et al., 1990; Py et al., 1991; Svensson & Sogaard, 1993; Juncosa, 1994). For example, several conserved carboxylate residues within *Clostridium thermocellum* endoglucanase D were individually replaced with alanine residues and the mutants characterised kinetically (Chauvaux et al., 1992). The $k_{cat}$ value for the hydrolysis of PNPC by the Glu555Ala mutant was reduced 4 $x10^3$-fold relative to the native enzyme while other properties (e.g., $K_m$ and affinity for $Ca^{2+}$) remained basically unchanged. Based on the behaviour of this Glu555Ala mutant relative to that for the other mutants, Glu 555 was proposed to be the acid-base catalyst in this enzyme. This assignment has been confirmed by the X-ray crystal structure of the enzyme co-crystallised with the inhibitor, o-iodobenzyl-β-D-thiocellobioside at the active site. This revealed that Glu 555 was appropriately positioned within the active site of the enzyme to perform this role (Juy et al., 1992). Indeed a similar strategy but with much more extensive kinetic analysis, has been used successfully to identify the acid-base catalyst in *C. fimi* exoglycanase (MacLeod et al., 1994) and *Agrobacterium* β-glucosidase (Wang et al., 1995) as Glu 127 and Glu 170 respectively. In the case of the exoglycanase, this assignment has been confirmed by X-ray crystallographic analysis (White et al., 1994).

Site directed mutagenesis of glycosidases can also be used to further investigate the role of putative catalytic nucleophiles and acid-base catalysts identified previously from

independent studies such as labeling experiments. For example, the catalytic nucleophile of *Agrobacterium* β-glucosidase has been identified as Glu 358 by trapping of the enzyme as a 2-deoxyfluoro-α-D-glucosyl-enzyme intermediate using the mechanism-based inactivator 2,4-dinitrophenyl 2-deoxy-2-fluoro-β-D-glucoside (2F-DNPG) (Withers et al., 1990). Replacement of Glu 358 by asparagine and glutamine residues using site directed mutagenesis generated mutant enzymes which were essentially completely inactivated (Withers et al., 1992). Since the catalytic nucleophile must stabilise the oxocarbonium ion-like transition states, form a covalent linkage with the substrate and in addition serve as a good leaving group, then the loss of enzymatic activity upon conversion of the carboxylate group (Glu 358) to an amide group (Asn and Gln) is certainly consistent with the role of Glu 358 as the catalytic nucleophile. By contrast, shortening the carboxylate side chain by replacing Glu 358 by an aspartate residue resulted in a mutant for which the $k_{cat}$ value was reduced 2.5 x $10^3$-fold, corresponding to an increase in activation energy of ~4.5 kcal/mole. Thus withdrawing the negatively charged carboxylate group ~1 Å away from the reacting centre of the sugar destabilises the glycosylation transition state by at least 4.5 kcal/mole. These results are completely consistent with the role of Glu 358 as the catalytic nucleophile. Furthermore, this kinetic analysis of Glu358Asp provided new insights into the mechanistic consequences of mispositioning catalytic nucleophiles within glycosidases.

## 3-2 Objectives Of This Project

The objective of this project is to probe the roles of the catalytic nucleophile and the acid-base catalyst of *C. fimi* exoglycanase through detailed kinetic analysis of mutants generated at these positions in this enzyme by site directed mutagenesis.

*Catalytic nucleophile*: Previously, Glu 233 was identified as the catalytic nucleophile in *C. fimi* exoglycanase from labeling studies using the mechanism-based inactivator, 2F-DNPG (Tull et al., 1991). This assignment has been confirmed recently by X-ray crystallographic analysis of this enzyme (White et al., 1994). A mutant in which Glu

233 has been replaced with an aspartate residue has been prepared by Dr. Alasdair MacLeod, Department of Microbiology, University of British Columbia, allowing for further investigation of its role. A kinetic analysis of this mutant, similar to that previously performed on the native enzyme, should provide insights into the mechanistic consequences of pulling the catalytic nucleophile of *C. fimi* exoglycanase away from the reacting centre of the substrate (Figure 3-1).

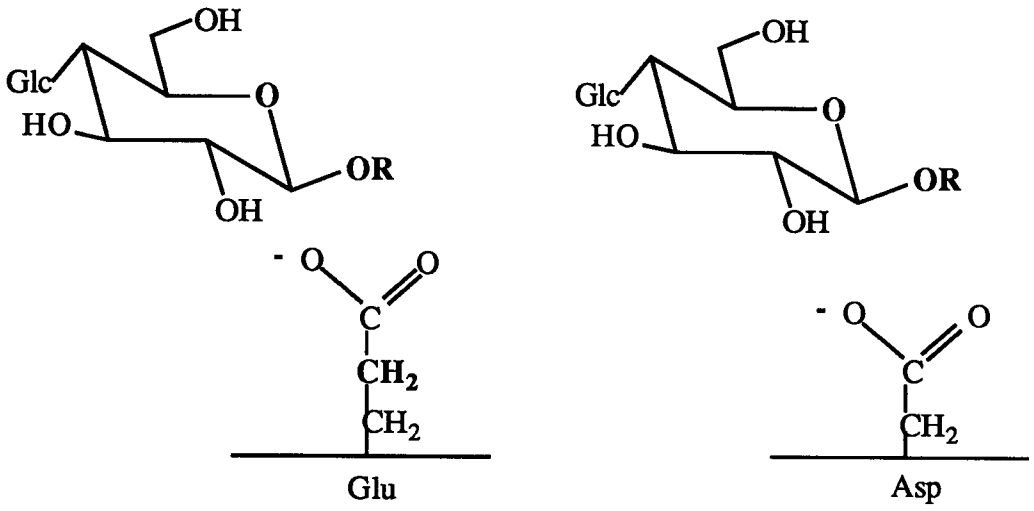


*Figure 3-1* *Replacement of the catalytic nucleophile of C. fimi exoglycanase (Glu 233) by an aspartate.*

*Acid-base catalyst*: Glu 127 has been identified previously as the acid-base catalyst in *C. fimi* exoglycanase through a combination of site directed mutagenesis of conserved carboxylate residues to alanine residues and kinetic analysis of the resulting mutants (MacLeod et al., 1994). In this investigation, the mechanistic consequences of removal of the acid-base catalyst of *C. fimi*, Glu 127, (Figure 3-2) are explored further through detailed kinetic analysis of the Glu127Ala mutant.

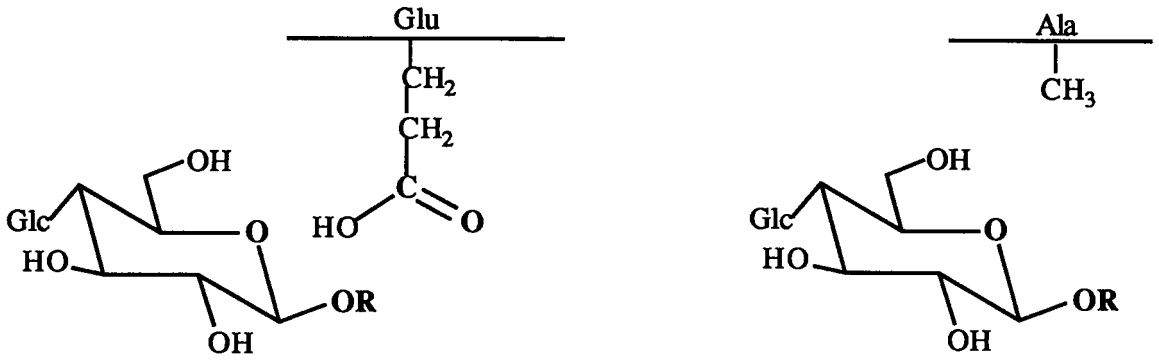


*Figure 3-2* *Replacement of the acid-base catalyst of C. fimi exoglycanase, Glu 127, by an alanine residue.*

## 3-3 Results For The Glu233Asp *C. fimi* Exoglycanase (Nucleophile) Mutant

### 3-3-1 Substrate reactivity

Aryl β-cellobiosides, aryl β-D-glucosides and $PNPX_2$ were reacted with the Glu233Asp *C. fimi* exoglycanase mutant and the kinetic parameters determined. The kinetic parameters for $PNPX_2$ are $k_{cat} = 0.011 \pm 0.001\ s^{-1}$, $K_m = 0.018 \pm 0.001$ mM and $k_{cat}/K_m = 0.61\ s^{-1}\ mM^{-1}$. Values for $k_{cat}$, $K_m$ and $k_{cat}/K_m$ for the cellobiosides and glucosides are listed in Table 3-1 and 3-2 along with the $pK_a$ values of the phenol leaving group. The Michaelis-Menten kinetic parameters for the cellobiosides are plotted as functions of the phenol $pK_a$ in the form of Broensted plots and these are shown in Figure 3-3 along with those for the native enzyme. Values of $\log(k_{cat})$ are independent of the $pK_a$ values over the range $pK_a = 4 - 9$. In contrast, the $\log(k_{cat}/K_m)$ plot reveals a relatively weak dependence ($\beta_{lg} = -0.3$, correlation coefficient = 0.94) of $\log(k_{cat}/K_m)$ upon the $pK_a$ values across the full range of substrates studied.

Table 3-1: Michaelis-Menten Parameters for the Hydrolysis of Aryl β-D-cellobiosides by the Glu233Asp Mutant.

| Phenol substituent | [a]$pK_a$ | $K_m$ (mM) | $k_{cat}$ ($s^{-1}$) | $k_{cat}/K_m$ ($s^{-1}mM^{-1}$) |
|---|---|---|---|---|
| 2,4 -dinitro | 3.96 | 0.086 ± 0.006 | 0.0031 ± 0.0001 | 0.036 |
| 3,4-dinitro | 5.36 | 0.10 ± 0.004 | 0.0027 ± 0.0001 | 0.027 |
| 4-nitro | 7.18 | 0.66 ± 0.03 | 0.0038 ± 0.0001 | 0.0058 |
| 2-nitro | 7.22 | 0.62 ± 0.02 | 0.0030 ± 0.0001 | 0.0048 |
| 4-cyano | 8.49 | 1.6 ± 0.4 | 0.0028 ± 0.0005 | 0.0018 |
| 4-bromo | 9.34 | 1.2 ± 0.3 | 0.0025 ± 0.0002 | 0.0021 |

[a]Phenol $pK_a$ values were taken from Barlin & Perrin (1966), Kortum et al. (1961), Robinson et al., (1960), and Ba-Saif & Williams (1988).

Table 3-2: Michaelis-Menten Parameters for the Hydrolysis of Aryl β-D-Glucosides by the Glu233Asp Mutant.

| Phenol substituent | [a]$pK_a$ | $K_m$ (mM) | $k_{cat}$ ($s^{-1}$) | $k_{cat}/K_m$ ($s^{-1}mM^{-1}$) |
|---|---|---|---|---|
| 2,4-dinitro | 3.96 | 1.4 ± 0.1 | 0.0035 ± 0.0001 | 0.0026 |
| 2,5-dinitro | 5.15 | 2.0 ± 0.1 | 0.0039 ± 0.0001 | 0.0020 |
| 3,4-dinitro | 5.36 | 5.5 ± 2.0 | 0.0010 ± 0.0004 | 0.00018 |
| 2-chloro-4-nitro | 5.45 | 20 ± 2 | 0.0018 ± 0.0001 | 0.000089 |

[a]Phenol $pK_a$ values were taken from Barlin & Perrin (1966); Kortum et al. (1961); Robinson et al (1960); and Ba-Saif & Williams (1988).

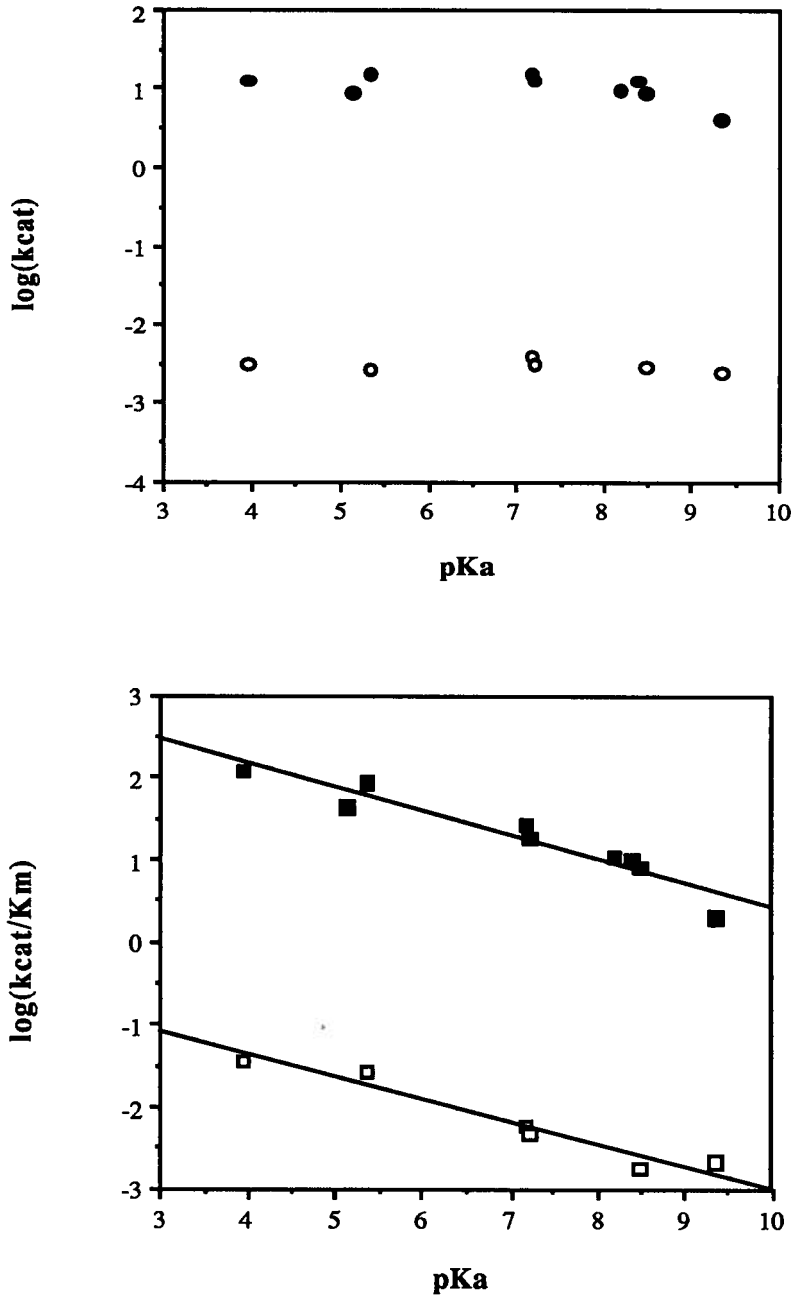


*Figure 3-3* *Broensted plots relating rates of native enzyme- (solid points) and Glu233Asp mutant- (open points) catalysed hydrolysis of aryl β-cellobiosides with the leaving group ability of the phenols.*

### 3-3-2 α-Secondary deuterium kinetic isotope effect

A secondary deuterium kinetic isotope effect on $k_{cat}$ of $k_H/k_D = 1.09 \pm 0.02$ was measured for the Glu233Asp mutant using 2,4-DNPC, exactly as with the native enzyme.

### 3-3-3 pH Study

The pH dependence of Glu233Asp mutant was investigated using 2,4-DNPC as the substrate over the pH range 4.6 - 8.4. Values for $k_{cat}$ and $K_m$ were determined at the different pH values exactly as with the native enzyme and these are presented as plots of $k_{cat}$ and $k_{cat}/K_m$ *versus* pH in Figure 3-4. Interestingly values of both $k_{cat}$ and $k_{cat}/K_m$ are seen to be independent of pH.

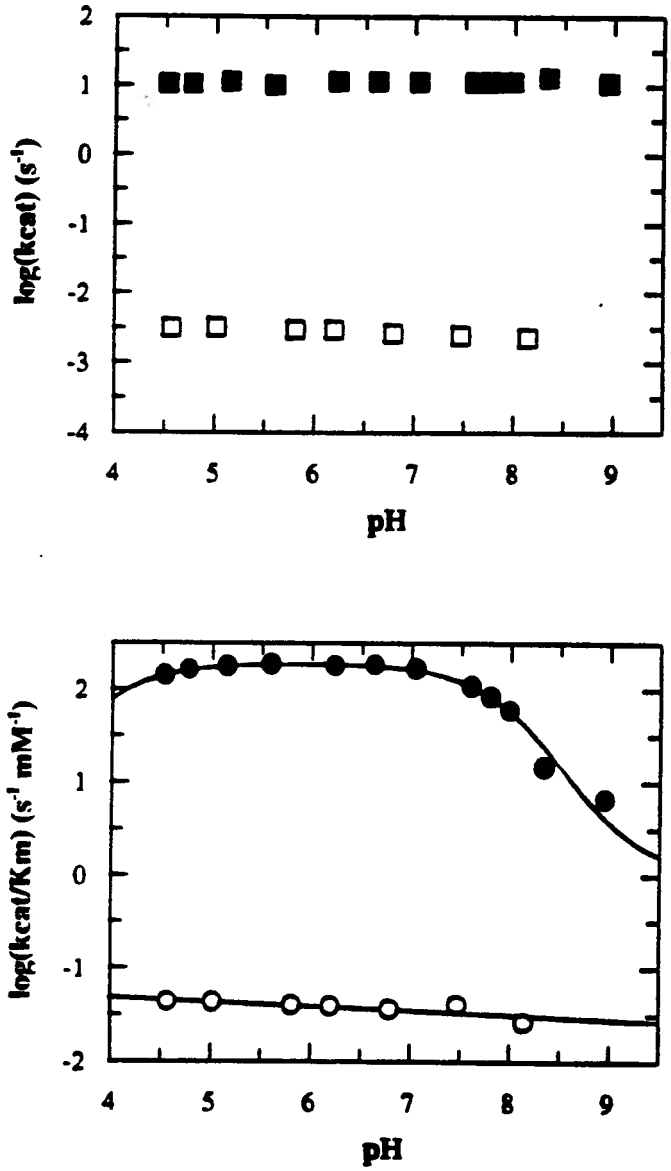


*Figure 3-4* *pH Dependence of the hydrolysis of 2,4-DNPC by the Glu233Asp mutant (open points) and native enzyme (solid points)*

## 3-4 Results For Glu127Ala *C. Fimi* Exoglycanase (Acid-Base Catalyst) Mutant

### 3-4-1 Substrate reactivity

Michaelis-Menten kinetic parameters were determined for five aryl β-cellobiosides with the Glu127Ala mutant and these are listed, in addition to the two values determined previously (MacLeod et al., 1994) in Table 3-3 along with the $pK_a$ values for the corresponding phenolate leaving groups. Values of $\log(k_{cat})$ and $\log(k_{cat}/K_m)$ are plotted as functions of the $pK_a$ of the phenolate leaving group in the form of Broensted plots and these are shown in Figure 3-5 along with those for the native enzyme. Values of $\log(k_{cat})$

Table 3-3: Michaelis-Menten Parameters for the Hydrolysis of Aryl β-Cellobiosides by the Glu127Ala Mutant

| Phenol substituent | [b]$pK_a$ | $K_m$ (mM) | $k_{cat}$ ($s^{-1}$) | $k_{cat}/K_m$ ($s^{-1}mM^{-1}$) |
|---|---|---|---|---|
| 2,4-dinitro[a] | 3.96 | 0.0003 | 0.040 | 133 |
| 3,4-dinitro | 5.36 | 0.0008 ± 0.0002 | 0.072 ± 0.007 | 90 |
| 4-nitro | 7.18 | 0.020 ± 0.002 | 0.033 ± 0.001 | 1.65 |
| 2-nitro | 7.22 | 0.021 ± 0.003 | 0.021 ± 0.001 | 1.0 |
| 3,5-dichloro | 8.19 | 0.15 ± 0.03 | 0.0027 ± 0.0005 | 0.018 |
| 4-cyano | 8.49 | 0.43 ± 0.01 | 0.015 ± 0.0001 | 0.035 |
| 4-bromo[a] | 9.36 | 1.9 | $1.4 \times 10^{-5}$ | $7.4 \times 10^{-6}$ |

[a](MacLeod et al., 1994)

[b]Phenol $pK_a$ values were taken from Barlin & Perrin (1966), Kortum et al. (1961), Robinson et al., (1960), and Ba-Saif & Williams (1988).

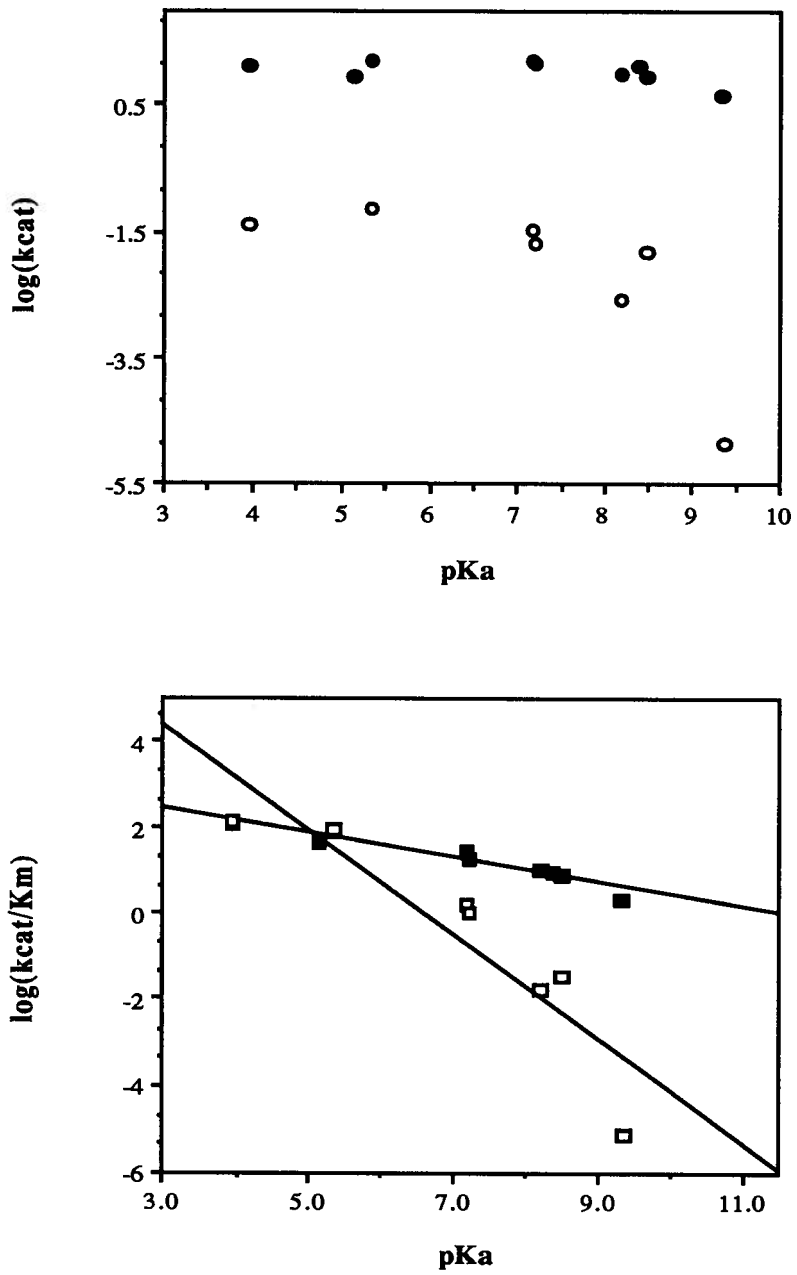


*Figure 3-5.* *Broensted plots relating rates of native enzyme- (solid points) and Glu127Ala mutant- (open points) catalysed hydrolysis of aryl β-cellobiosides with the leaving group ability of the phenols.*

are invariant with $pK_a$ over the range $pK_a$ 4 - 7 but become dependent on $pK_a$ at the higher $pK_a$ values as reflected by the downward break in the plot. The approximate Broensted constant for this $pK_a$ dependent region of the plot corresponds to $\beta_{lg} \sim -1.2$ (correlation coefficient = 0.73). A similar trend is apparent in the $\log(k_{cat}/K_m)$ *versus* $pK_a$ Broensted plot though the data are more scattered. The points fit reasonably well to a line of slope $\beta_{lg} \sim -1.2$ (correlation coefficient = 0.82) but with the more reactive substrates falling beneath this line, as has been seen previously (Kempton & Withers, 1992).

### 3-4-2 Stopped-flow analysis

Pre-steady state kinetic analyses of the Glu127Ala mutant were carried out for three cellobioside substrates, exactly as with the native enzyme. The results are presented in Table 3-4 and in the form of plots of $\log(k_2)$ and $\log(k_2/K_d)$ *versus* $pK_a$ (Figure 3-6) with slopes corresponding to Broensted constants of $\beta_{lg} \sim -0.8$ (correlation coefficient = 0.95) and -0.7 (correlation coefficient = 0.87), respectively.

Table 3-4: Pre-Steady State Parameters for Hydrolysis of Aryl β-Cellobiosides by the Glu127Ala Mutant

| Phenol substituent | [a]$pK_a$ | $k_2$ ($s^{-1}$) | $K_d$ (mM) | $k_2/K_d$ ($s^{-1}mM^{-1}$) |
|---|---|---|---|---|
| 2,4-dinitro | 3.96 | 192 ± 7 | 0.68 ± 0.06 | 282 |
| 3,4-dinitro | 5.36 | 3.31 ± 0.07 | 0.019 ± 0.002 | 179 |
| 4-nitro | 7.18 | 0.30 ± 0.01 | 0.17 ± 0.02 | 1.79 |

[a]Phenol $pK_a$ values were taken from Barlin & Perrin (1966); Kortum et al. (1961); Robinson et al., (1960); and Ba-Saif & Williams (1988).

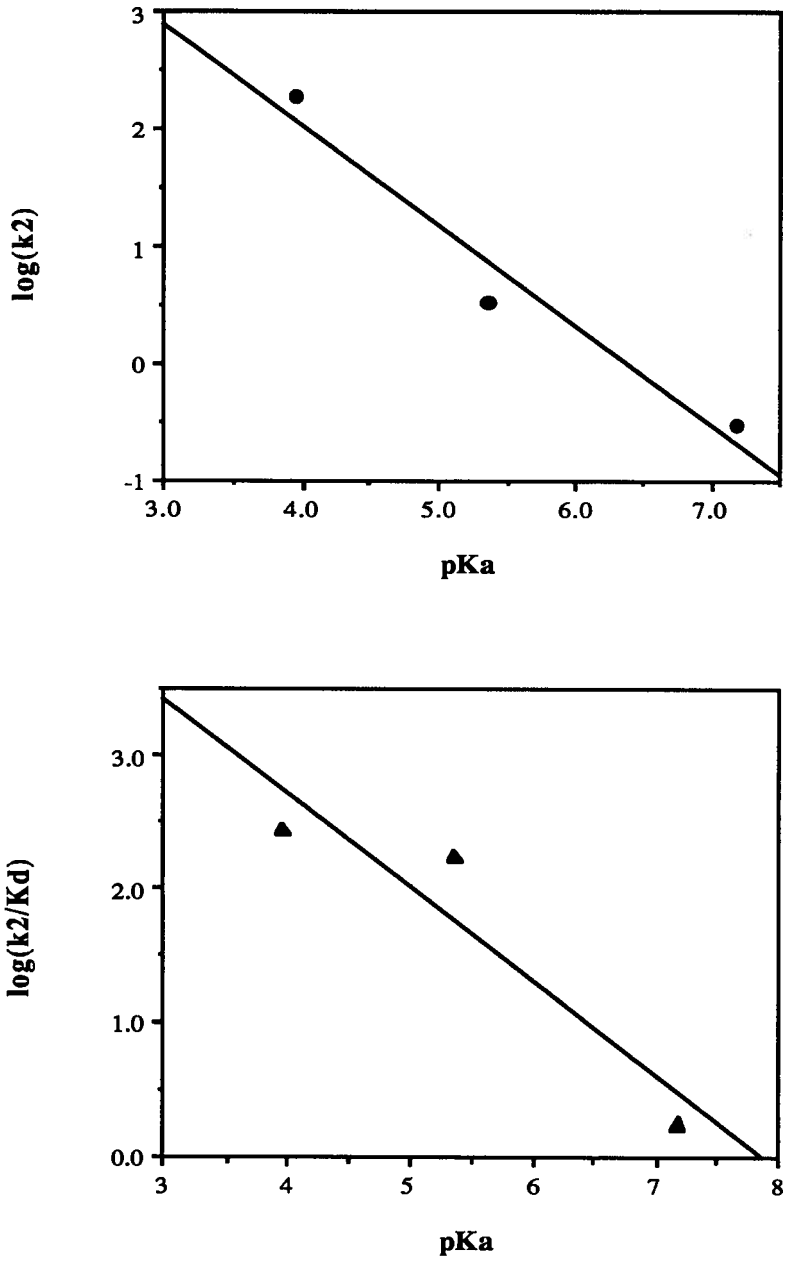


*Figure 3-6* *Broensted plots relating pre-steady state rate of Glu127Ala mutant catalysed hydrolysis of aryl β-cellobiosides with the leaving group ability of the phenols.*

### 3–4–3 α-Secondary deuterium kinetic isotope effect

A secondary deuterium kinetic isotope effect on $k_{cat}$ of $k_H/k_D = 1.08 \pm 0.2$ was measured for the Glu127Ala mutant using 2,4-DNPC, exactly as with the native enzyme.

### 3-4-4 pH Study

Two cellobioside substrates, 2,4-DNPC and PNPC, were used to investigate the pH dependence of Glu127Ala mutant catalysis over the pH range 4.6 - 9.5. Values for $k_{cat}$ were determined by measuring rates of hydrolysis at saturating concentrations of 2,4-DNPC (75 x $K_m$). Values for $k_{cat}/K_m$ were determined by following the time courses for the hydrolysis of PNPC at concentrations much lower than $K_m$ (0.2 x $K_m$), since at [S] << $K_m$, rates of hydrolysis are first order in substrate and the observed rate constants ($k_{obs}$) correspond to $k_{cat}/K_m$ (discussed in Appendix B-1). These results are presented as plots of $k_{cat}$ and $k_{cat}/K_m$ *versus* pH in Figure 3-7. Values of $k_{cat}/K_m$ are seen to be dependent upon only one ionisation of $pK_a = 5.9 \pm 0.1$ in its acidic limb. Interestingly, values of $k_{cat}$ appear to be dependent upon an ionisation of $pK_a \sim 5.0 \pm 0.1$ in the basic limb of the pH-profile. Although such pH-profiles are uncommon, this log($k_{cat}$) pH-profile is reproducible. This ionisation of $pK_a \sim 5.0$ is only an estimate since instability of Glu127Ala mutant at low pH values precludes a more accurate determination.

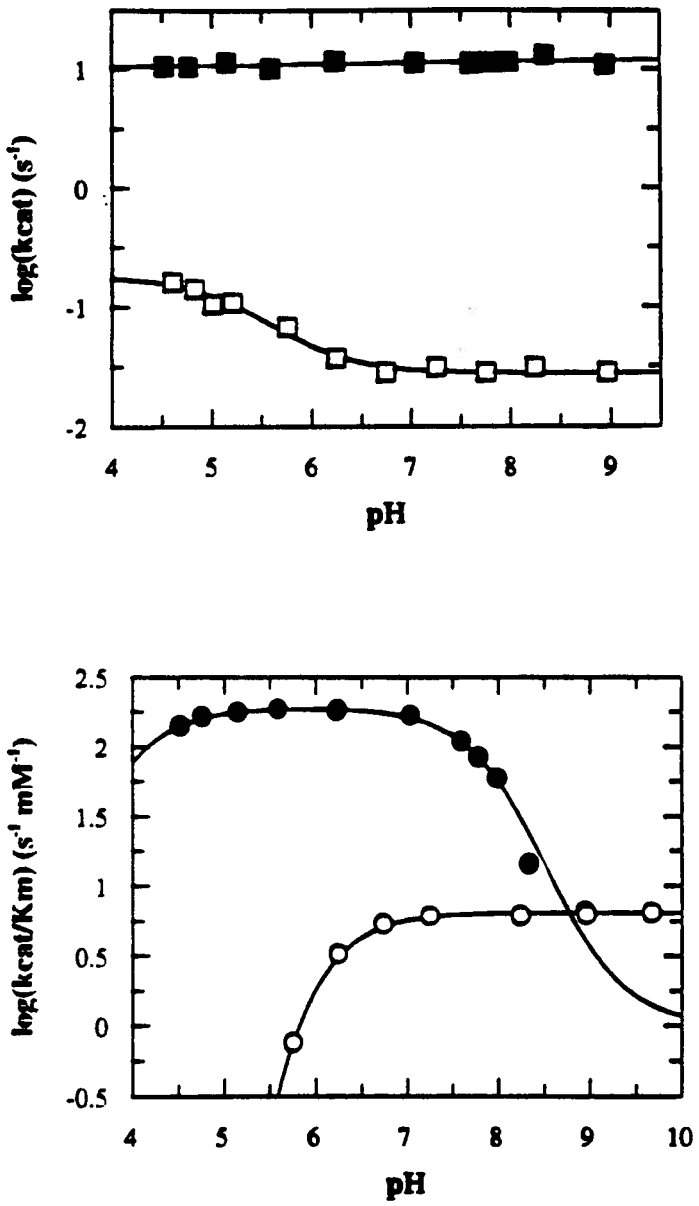


*Figure 3-7* *pH Dependence of the hydrolysis of cellobiosides by the Glu127Ala mutant (open points) and native enzyme (solid points).*

## 3-5 Discussion Of The Glu233Asp *C.Fimi* Exoglycanase (Nucleophile) Mutant

### 3-5-1 Proposed role of the catalytic nucleophile in *C. fimi* exoglycanase catalysis

Based on the double displacement mechanism proposed for *C. fimi* exoglycanase-catalysed hydrolysis of glycosides (Withers et al., 1986) the role of the catalytic nucleophile involves the formation of a covalent linkage with the sugar in the glycosyl-enzyme intermediate in the first step of catalysis. In the second step, the catalytic nucleophile must serve as a good leaving group. Furthermore, the catalytic nucleophile must also assist in the stabilisation of the oxocarbonium ion-like transition states through electrostatic interactions. The catalytic nucleophile presumably plays a minimal role in ground state binding since interactions between the sugar and the catalytic nucleophile at the ground state would likely be disrupted as the reaction proceeds to the transition state and would therefore be inhibitory. This is consistent with the view that interactions realised at the transition state rather than at the ground state, stabilise the transition state, thus lowering the activation energy of the reaction (Fersht, 1985).

### 3-5-2 pH Dependence of the Glu233Asp *C. fimi* exoglycanase mutant

The pH dependence of Glu233Asp was investigated using 2,4-DNPC, a substrate for which deglycosylation is the rate determining step. The similar pH profiles observed for $k_{cat}$ and $k_{cat}/K_m$ indicate that binding of the substrate does not perturb the ionisations in the free Glu233Asp mutant enzyme. Like that for the native enzyme, values of $k_{cat}$ for the Glu233Asp mutant are seen to be independent of pH over the range studied. By contrast, the pH profile of $k_{cat}/K_m$ for the native enzyme is quite different from that of the Glu233Asp mutant. Values of $k_{cat}/K_m$ for the Glu233Asp mutant are seen to be independent of pH while the $k_{cat}/K_m$ pH profile for the native enzyme reveals two

ionisations of $pK_a$ = 4.1 and 7.7 likely corresponding to the catalytic nucleophile (Glu 233) and the acid catalyst (Glu 127), respectively. These results suggest that the ionisations seen in the free native enzyme are perturbed to values outside the pH range studied. The X-ray structure of this exoglycanase provides some insights into this situation. For the native enzyme, Glu 233 is seen to be within hydrogen bonding distance of both His 205 and Asn 169; and His 205 within hydrogen bonding distance of Asp 235 (White et al., 1994). This hydrogen bonding net work is shown schematically in Figure 3-8. Since Asp 235, His 205 and Glu 233 are highly conserved residues within this family of β-glucanases, it has been suggested that the hydrogen bonding network of Asp235-His205-Glu233 likely plays an important role in maintaining the ionisation state of the nucleophile (Glu 233) (White et al., 1994). Modeling studies with the native enzyme X-ray crystal structure (without further structural refinement) can provide some preliminary indication of the hydrogen bonding interactions that are likely lost or altered by converting Glu 233 to an aspartate residue. This study reveals that both His 205 and Asn 169 are no longer within hydrogen bonding distance of the catalytic nucleophile when Glu 233 is shortened by 1 Å. The absence of these hydrogen bonding interactions in the Glu233Asp mutant would therefore be expected to modify the environment of the active site, thus altering the ionisation states of both the catalytic nucleophile and acid-base catalyst, as suggested by the pH-profiles.

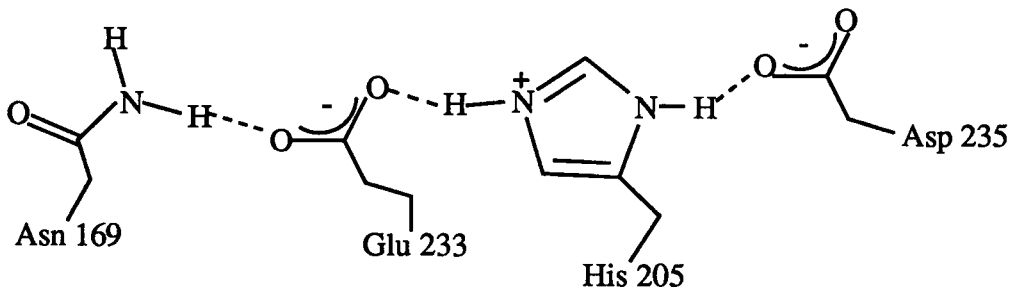


*Figure 3-8* *Schematic diagram illustrating the hydrogen bonding net work around Glu 233.*

### 3-5-3 Substrate specificity of the Glu233Asp mutant

Comparison of the $k_{cat}/K_m$ values for hydrolysis of the cellobiosides (Table 3-1) with those for the corresponding glucosides (Table 3-2) reveals that, like the native exoglycanase, the Glu233Asp mutant catalyses the hydrolysis of cellobiosides more efficiently than glucosides. Likewise, the Glu233Asp mutant catalyses the hydrolysis of $PNPX_2$ more efficiently than PNPC as was seen for the native enzyme. These results indicate that truncation of the catalytic nucleophile likely affects the mechanism for hydrolysis of the cellobiosides, the glucosides and the xylobiosides in a similar manner.

### 3-5-4 Rate determining steps for Glu233Asp mutant catalysis

The Broensted plot of $\log(k_{cat}/K_m)$ *versus* $pK_a$ (Figure 3-3) for the Glu233Asp mutant-catalysed hydrolysis of aryl β-cellobiosides reveals a strong dependence of the rate on the leaving group ability of the phenolate aglycone across the $pK_a$ range studied, as was seen with the native enzyme. This indicates that the first irreversible step in the reaction is still the formation of the cellobiosyl-enzyme intermediate. The value of the Broensted constant, $\beta_{lg} = -0.3$, for hydrolysis of the cellobiosides with the Glu233Asp mutant is the same as that found previously for hydrolysis of these substrates with the native enzyme. Similarly for *Agrobacterium* β-glucosidase, the Broensted constants for hydrolysis of aryl β-D-glucosides with the native enzyme ($\beta_{lg} = -0.7$) and with the Glu358Asp catalytic nucleophile mutant ($\beta_{lg} = -0.7$) were found to be the same indicating that mispositioning of the carboxylate group does not affect the degree of negative charge development on the departing phenolate at the glycosylation transition state, thus the degree of C-O bond cleavage or proton donation (Withers et al., 1992). By contrast, the absence of a correlation between values of $\log(k_{cat})$ and leaving group $pK_a$ over the entire $pK_a$ range studied ($pK_a$ = 4 - 9) for the Glu233Asp mutant suggests that the rate determining step is not C-O bond cleavage of the phenolate but most likely hydrolysis of the cellobiosyl-enzyme intermediate. For the native enzyme, deglycosylation was seen to be the rate determining step only for

the cellobiosides with good leaving groups ($pK_a < \sim 7.5$) while glycosylation became the rate determining step for those cellobiosides with poorer leaving groups ($pK_a > \sim 7.5$). Thus shortening the catalytic nucleophile side chain has changed the rate determining step for the poorer substrates from glycosylation to deglycosylation. Interestingly, exactly the opposite situation is found for *Agrobacterium* β-glucosidase (Withers et al., 1992). Conversion of the glutamate catalytic nucleophile (Glu 358) of this β-glucosidase to an aspartate residue resulted in a change in the rate determining step from deglycosylation to glycosylation for hydrolysis of all the aryl β-D-glucosides studied.

### 3-5-5 Effect of mispositioning the carboxylate group on the individual steps of the reaction.

*Glycosylation step*: Values of $k_{cat}/K_m$ reflect the first irreversible step ( Appendix B-2) in the reaction which is the glycosylation step for the cellobiosides and presumably also for the glucosides and the xylobioside studied. Estimates of the effect on the glycosylation step of mispositioning of the carboxylate group can therefore be obtained from the relative $k_{cat}/K_m$ values for the Glu233Asp mutant and the native enzyme. Values of $k_{cat}/K_m$ for hydrolysis of the cellobiosides (except 4-BrPC) by the Glu233Asp mutant are 3-4 x $10^3$-fold lower than those for the native enzyme. These rate reductions are similar to those seen for *Agrobacterium* β-glucosidase (Withers et al., 1992) and *E. coli* β-galactosidase (Yuan et al., 1994) (2.5 x $10^3$-fold and 2 - 9 x $10^3$-fold, respectively) upon replacement of the glutamate catalytic nucleophiles with aspartate residues. Presuming that the majority of this effect is due to changes in the transition state and not ground state interactions (*vide supra*) then this rate reduction corresponds to an increase in the glycosylation transition state energy of ~5 kcal/mole. Interestingly, the $k_{cat}/K_m$ value for hydrolysis of 4-BrPC is reduced to a lesser extent (~9 x $10^2$-fold, $\Delta\Delta G^{o\ddagger} \sim 4$ kcal/mole) than those for hydrolysis of the more reactive cellobiosides. This suggest that the moving the carboxylate 1 Å away from the reacting centre has a lesser destabilising effect on the

glycosylation transition state for hydrolysis of 4-BrPC than on those for hydrolysis of the more reactive cellobiosides. Presumably, this is because the glycosylation transition state for hydrolysis of 4-BrPC is already more destabilised than those for hydrolysis of the more reactive cellobiosides with the native enzyme.

Values of $k_{cat}/K_m$ for hydrolysis of 2,4-DNPG and 3,4-DNPG are seen to be reduced (~3 x $10^3$-fold) a similar amount to that seen for the equivalent cellobiosides. Similarly, both the $k_{cat}/K_m$ values for PNPC and $PNPX_2$ hydrolysis are reduced ~3 x $10^3$-fold. These results indicate that mispositioning the carboxylate group destabilises the glycosylation transition states for hydrolysis of cellobiosides, glucosides and xylobiosides to a similar extent.

*Deglycosylation step*: The deglycosylation rate constant for cellobioside hydrolysis, obtained from $k_{cat}$ values for 2,4-DNPC, 3,4-DNPC, PNPC and ONPC, is also reduced 4 x $10^3$-fold, corresponding to an increase in activation energy of $\Delta\Delta G^{o\ddagger}$ = ~5 kcal/mole, upon replacing the glutamate residue with an aspartate. Since shortening the side chain of the catalytic nucleophile would almost certainly result in a strained covalent cellobiosyl-enzyme intermediate, then the above value of $\Delta\Delta G^{\ddagger}$ represents a <u>minimum</u> estimate of the actual increase in the deglycosylation transition state energy. Since the increase in energy of the glycosylation transition state is ~5 kcal/mole while that of the deglycosylation transition state is likely greater than 5 kcal/mole, this indicates that mispositioning the negatively charged carboxylate group probably has a greater destabilising effect on the transition state for deglycosylation than on that for glycosylation (Figure 3-9). This situation is most clearly seen for 4-BrPC. The glycosylation rate for this substrate is reduced only ~9 x $10^2$-fold while the deglycosylation rate is reduced at least 4 x $10^3$-fold upon pulling the carboxylate group ~1 Å away from the reacting anomeric carbon. This interpretation is certainly consistent with the findings that for Glu233Asp mutant, deglycosylation is the rate determining step for <u>all</u> the cellobiosides studied while for the native enzyme,

deglycosylation is only rate determining for the more reactive cellobiosides (e.g. 2,4-DNPC) and glycosylation is rate determining for less reactive cellobiosides (e.g. 4-BrPC).

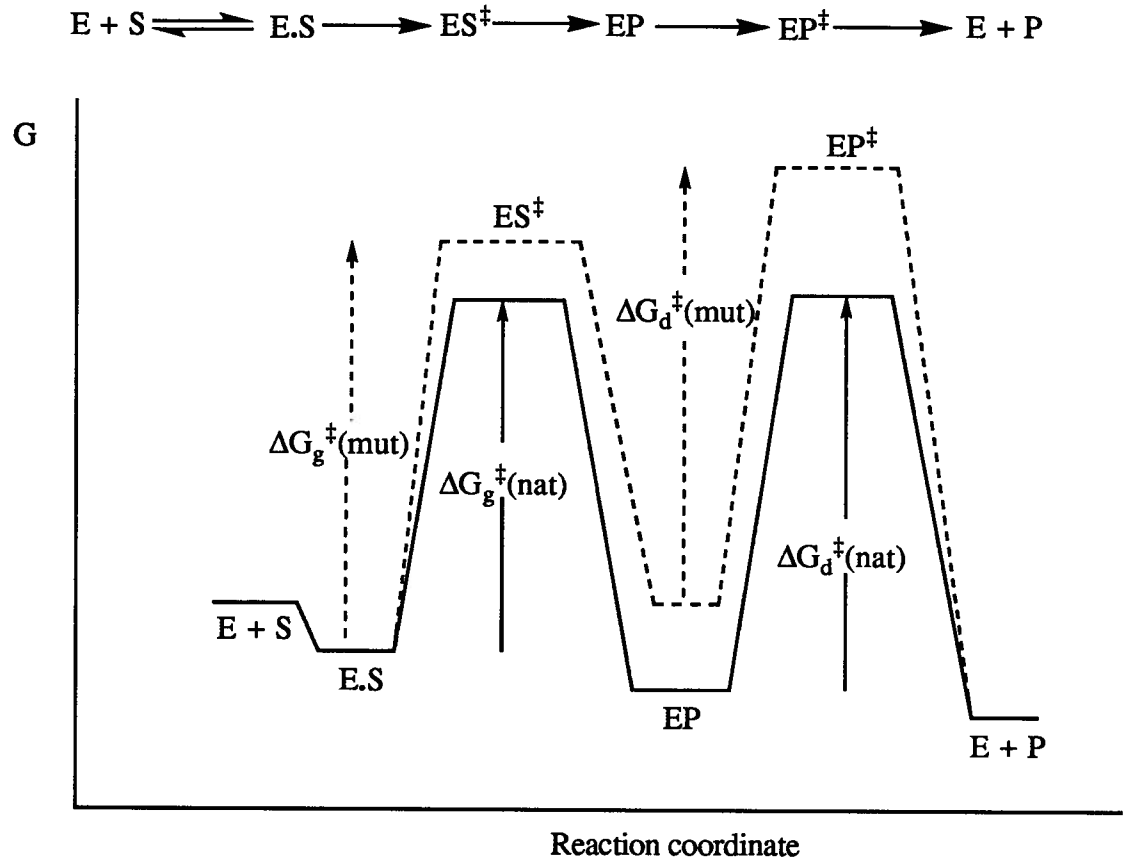


*Figure 3-9* *Reaction coordinate diagram illustrating the effect of shortening the catalytic nucleophile on the glycosylation and deglycosylation transition states.*

The α-secondary deuterium kinetic isotope effects measured for the native enzyme and the Glu233Asp mutant provide further insights into this situation. The similar kinetic isotope effects measured for 2,4-DNPC with the native enzyme ($k_H/k_D$ = 1.10) and the Glu233Asp mutant ($k_H/k_D$ = 1.09) indicate that there is a similar extent of oxocarbonium ion development at the transition states for hydrolysis of the cellobiosyl-enzyme

intermediate in both cases, thus the extent of C-O bond cleavage of the carboxylate in the deglycosylation step is not significantly affected by truncation of the catalytic nucleophile.

## 3-6 Discussion Of Glu127Ala *C. Fimi* Exoglycanase (Acid-Base Catalyst) Mutant

### 3-6-1 Proposed role of the acid-base catalyst in *C. fimi* exoglycanase catalysis

The role of the acid-base catalyst, based on the proposed mechanism of action of *C. fimi* exoglycanase, involves donation of a proton (general acid catalysis) to the oxygen of the leaving aglycone to assist with C-O bond cleavage through stabilisation of the leaving group in the first step of the reaction. In the second step of catalysis, this same residue is proposed to abstract a proton (general base catalysis) from the attacking water, thus assisting with nucleophilic attack on the glycosyl-enzyme intermediate. Removal of this residue would therefore be expected to affect both steps in catalysis.

### 3-6-2 pH Dependence of Glu127Ala *C. fimi* exoglycanase mutant

The pH dependence of $k_{cat}/K_m$ was investigated using PNPC as the substrate, while that of $k_{cat}$ was investigated with 2,4-DNPC, a substrate for which the deglycosylation step is rate determining. Recall that values of $k_{cat}/K_m$ for native enzyme catalysis are dependent upon two ionisations of $pK_a = 4.1$ and 7.7. In contrast, the $k_{cat}/K_m$ *versus* pH profile (Figure 3-7) of Glu127Ala catalysis reveals a single ionisation of $pK_a = 5.9$ in the acidic limb but no ionisations at the higher pH values. These results suggest that the group responsible for the ionisation of $pK_a = 7.7$ in the native enzyme, which must be in its deprotonated state to be catalytically active, has been removed. Indeed similar results have been reported for TEM-1 β-lactamase (Delaire et al., 1991), recombinant protein tyrosine phosphatase from *Yersinia enterocolitica* (Zhang et al., 1994) and *Agrobacterium* β-glucosidase (Wang et al., 1995) upon mutation of the acid-base catalysts. Insights into

this shift in $pK_a$ from 4.1 to 5.9 may be obtained from the X-ray crystal structure of *C. fimi* exoglycanase (White et al., 1994). Glu 127 is seen to interact with Asn 126, Gln 203, Trp 84 and a water molecule, which presumably are involved in maintaining the ionisation state of Glu 127 in the free enzyme. Conversion of Glu 127 to an alanine residue would therefore be expected to result in the loss of these hydrogen bonding interactions, as well as to alter the local charge density within the active site. Thus, the shift in $pK_a$ from 4.1 to 5.9 is likely due to these changes occurring in the active site upon removal of the negatively charged carboxylate group of Glu 127. Assignment of this ionisation of $pK_a = 5.9$ to a specific group is not a trivial matter. Since this ionisation reflects a group that must be deprotonated to be catalytically active, then it most likely corresponds to the catalytic nucleophile.

Differences between the native enzyme and the Glu127Ala mutant are also seen in the pH dependence of $\log(k_{cat})$. While no ionisations in the enzyme/substrate complex are seen for the native enzyme, an increase in $k_{cat}$ with decreasing pH, below pH ~ 6, is seen for the mutant, corresponding to an ionisation of $pK_a \sim 5$. Although such pH-profiles are uncommon, this $\log(k_{cat})$ pH-profile is reproducible. Since the rate determining step for this substrate is deglycosylation, this ionisation is likely due to a group which interacts with the catalytic nucleophile (Glu 233), increasing its leaving group ability.

### 3-6-3 Effect of removal of the acid-base catalyst on β-glucanase activity

The biphasic $\log(k_{cat})$ *versus* $pK_a$ Broensted plot (Figure 3-5) seen for Glu127Ala catalysis indicates that deglycosylation is likely the rate determining step for the more reactive cellobiosides (phenol leaving group pKa < 7) whereas glycosylation is rate determining for the less reactive cellobiosides (phenol leaving group pKa > 7) as seen with the native enzyme. The results from the stopped-flow analysis are consistent with these findings. For the three most reactive cellobiosides (2,4-DNPC, 3,4-DNPC and PNPC)

studied, the observed bursts of released, substituted phenolates indicate that a step following aglycone departure, likely deglycosylation, is rate determining for these substrates.

By contrast, the $\log(k_{cat}/K_m)$ *versus* $pK_a$ Broensted plot (Figure 3-5) appears scattered, thus it is difficult to interpret. Similarly for *Agrobacterium* β-glucosidase, the $\log(k_{cat}/K_m)$ *versus* $pK_a$ Broensted plot for hydrolysis of β-glucosides by the acid-base catalyst mutant, Glu170Gly, is also seen to be scattered (Wang et al., 1995). Presumably this scattering is due to the superimposition of binding effects onto the electronic factors (discussed in section 2-1-5). However values of $\log(k_{cat}/K_m)$ for the Glu127Ala mutant may still be used to provide insights into transition state structure for hydrolysis of these cellobiosides. If the scatter observed is truly due to binding effects and if these same binding effects are present in the data on the native enzyme, then a plot of $\log(k_{cat}/K_m)$ for the Glu127Ala mutant versus $\log(k_{cat}/K_m)$ for the native enzyme should be reasonably linear as these binding effects will be subtracted. The slope of such a plot will provide a measure of the relative charge development on the phenolate oxygen in the two cases. Indeed the $\log(k_{cat}/K_m)_{Glu127Ala}$ *versus* $\log(k_{cat}/K_m)_{native}$ plot (Figure 3-10) is linear with a correlation coefficient of 0.9 and a slope of 4.0, indicating much greater charge development on the phenolate oxygen at the glycosylation transition state with the mutant enzyme. Since the Broensted constant for the $\log(k_{cat}/K_m)$ *versus* $pK_a$ plot with the native enzyme corresponds to $\beta_{1g} = -0.3$ (Tull et al., 1994) then this slope of 4.0 would indicate that the Glu127Ala mutant has a $\beta_{1g} = -1.2$. This value of the Broensted constant ($\beta_{1g} = -1.2$) is comparable to that for the $pK_a$ dependent region of the $\log(k_{cat})$ *versus* $pK_a$ plot ,as expected if they reflect the same step (glycosylation) in catalysis.

Although only three substrates were subjected to pre-steady state kinetic analysis, the larger values of the Broensted constant seen for the $\log(k_2)$ and $\log(k_2/K_d)$ *versus* $pK_a$ plots (Figure 3-6) ($\beta_{1g} = -0.8$ and -0.7, respectively) with the mutant enzyme relative to that seen with the native enzyme ($\beta_{1g} = -0.3$) are consistent with the larger Broensted

constant seen on $\log(k_{cat}/K_m)$ with the mutant enzyme. Since $k_{cat}/K_m$ provides information about the first irreversible step in the enzymatic reaction (Appendix B-2), then these results suggest that glycosylation is still the first irreversible step with the Glu127Ala mutant as is the case with the native enzyme. The larger value of the Broensted constant with Glu127Ala ($\beta_{lg} = -1.2$) relative to that for native exoglycanase ($\beta_{lg} = -0.3$) reflects a much greater degree of negative charge accumulation on the oxygen of the departing phenolate at the glycosylation transition state for Glu127Ala catalysis. These results suggest that there is less proton donation to the phenolate oxygen at the glycosylation transition state in the Glu127Ala mutant than in the native enzyme, exactly as would be predicted when the acid catalyst has been removed. These results are therefore completely consistent with the role of Glu 127 as the acid catalyst.

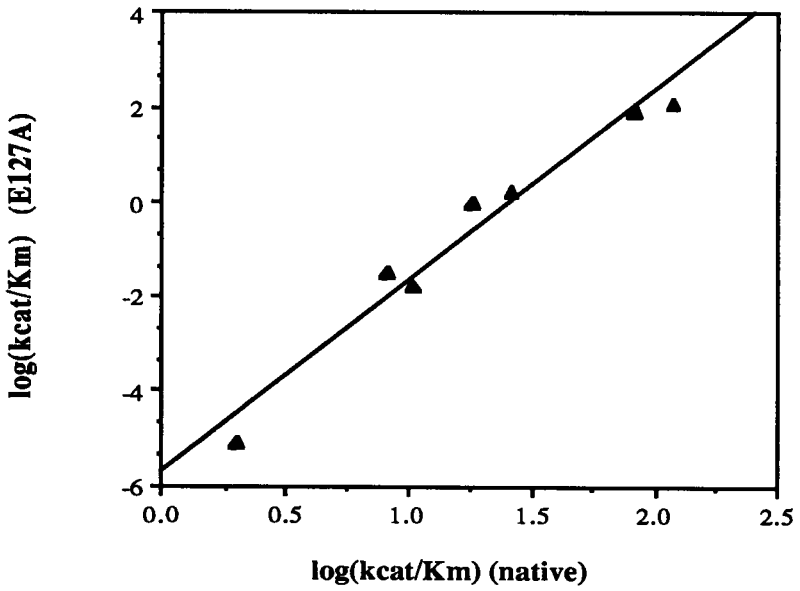


*Figure 3-10* *Linear free energy relationship correlating the glycosylation steps for the native and the Glu127Ala mutant.*

### 3-6-4 Effect of removal of the acid-base catalyst on the individual steps in the reaction

*Glycosylation step*: The glycosylation rate constants ($k_2$) (Table 3-4) from the stopped flow analysis for 2,4-DNPC and 3,4-DNPC hydrolysis are reduced 9- and 189-fold, respectively while that for PNPC hydrolysis is reduced 800-fold respectively, upon replacement of the glutamate residue with an alanine residue. The glycosylation rate constants for 3,5-DClPC and 4-CNPC, obtained from $k_{cat}$ values, are reduced 3560- and 600-fold, respectively with the Glu127Ala mutant. These results clearly indicate that the effect of removal of the carboxylate group of Glu 127 on the glycosylation step is dependent on the leaving group ability of the aglycone. Thus, substrates with good leaving groups such as 2,4-DNPC which require little acid catalytic assistance for departure are not greatly affected while those substrates with poorer leaving groups such as 3,5-DClPC are more severely affected by removal of the carboxylate group. These results are in complete agreement with those previously reported on the glycosylation step of Glu127Ala catalysis since the value of $k_{cat}/K_m$ for 2,4-DNPC was seen to be essentially unaffected by removal of the carboxylate group while that for 4-BrPC was reduced ~3 x $10^5$-fold relative to native enzyme catalysis. This behaviour of Glu127Ala is entirely consistent with the proposed role of Glu 127 as the acid catalyst in *C. fimi* exoglycanase. Similar results have been reported for *Agrobacterium* β-glucosidase when Glu 170, the proposed acid-based catalyst, was replaced with a glycine residue (Wang et al., 1995).

*Deglycosylation step*: The deglycosylation rate constant ($k_3$) for the cellobiosyl-enzyme, obtained from $k_{cat}$ values (Table 3-3), is seen to be reduced ~200 to 600-fold with the Glu127Ala mutant. Therefore removal of the general base catalyst increases the deglycosylation transition state energy by 3-4 kcal/mole. Interestingly however, the secondary deuterium kinetic isotope effect measured for 2,4-DNPC with the Glu127Ala mutant ($k_H/k_D$ = 1.08) and with the native enzyme ($k_H/k_D$ = 1.10) are comparable,

indicating that there is a similar degree of oxocarbonium ion character at the two deglycosylation transition states and thus likely a similar degree of C-O bond cleavage.

## 3-7 Summary

All the data presented on the Glu233Asp and Glu127Ala mutants are consistent with the roles of Glu 233 and Glu 127 as the catalytic nucleophile and acid-base catalyst, respectively.

Pulling the carboxylate group of the catalytic nucleophile 1 Å away from the reacting anomeric centre of the sugar by conversion of Glu 233 to an aspartate residue is seen to reduce the rate of the glycosylation step 3-4 x $10^3$-fold and that of the deglycosylation step 4 x $10^3$-fold relative to native enzyme catalysis. Interestingly, moving the carboxylate group 1 Å away is seen to have a greater destabilising effect on the transition state for deglycosylation than on that for glycosylation. Presumably this is because the transition state for deglycosylation has greater oxocarbonium ion character than that for glycosylation.

Removal of the carboxylate group of the acid-base catalyst is seen to reduce the deglycosylation rate 200-300-fold while the pre-steady-state kinetic analysis reveals that the effect on the glycosylation step is dependent upon the leaving group ability of the aglycone.

# CHAPTER IV

# LABELING STUDIES OF *C. FIMI* EXOGLYCANASE USING ACTIVE SITE-DIRECTED IRREVERSIBLE INACTIVATORS

## 4-1 Introduction

Active site-directed irreversible inactivators are structural analogues of the normal substrates, thus are capable of taking advantage of the binding specificity of the enzyme for its substrates. These inactivators bind within the active site forming a non-covalent enzyme-inactivator complex and are attacked by a nearby nucleophilic residue, resulting in the formation of a covalent bond between the enzyme and the inactivator, thus inactivation.

Active site-directed inactivators have been extensively used in enzymology. For example, in the absence of X-ray crystallographic data, irreversible inactivators can provide structural information, as the derivatised active site residue can be identified by using a radiolabeled analogue of the inactivator to identify a labeled, proteolytically derived peptide, which is then sequenced. The function of the labeled residue can be further probed by mutagenic studies.

### 4-1-1 Criteria for active site-directed irreversible inactivators

In order to be characterised as an irreversible inactivator specifically targetted to the enzyme active site and capable of being used to identify active site residues, candidate compounds must satisfy the following list of requirements (Silverman, 1988; Legler, 1990; Wold, 1978).

(1) Inactivation should be time-dependent and follow pseudo-first order kinetics.

(2) Saturation kinetics should be observed. That is, the rate of inactivation should be proportional to the concentration of the inactivator at low concentrations relative to the dissociation constant, but independent at high concentrations when there is no free enzyme in solution.

(3) Protection against inactivation using a substrate or competitive inhibitor should be observed. That is, the rate of inactivation should be lower in the presence of a substrate or competitive inhibitor than in its absence, thus providing evidence for the inactivator binding at the active site.

(4) Inactivation should be irreversible. Thus the inactivated enzyme should remain inactive after it is subjected to techniques such as dialysis or gel filtration which remove excess and loosely bound inactivators.

(5) The stoichiometry of the inactivation reaction should be one mole of inactivator bound per one mole of active site since inactivation of the enzyme specifically requires blockage of the active site.

(6) The inactivator should be reasonably stable against spontaneous decomposition under the reaction conditions.

(7) The inactivator must have a high non-covalent affinity for the active site, thus ensuring that the active site is specifically labeled at low inactivator concentrations.

(8) The enzyme-inactivator bond must be stable against denaturation, proteolysis and conditions used for isolation and sequencing of the labeled peptide, thus allowing identification of the labeled amino acid residue.

Two classes of active site-directed irreversible inactivators that satisfy these criteria are affinity labels and mechanism-based inactivators.

### 4-1-2 Affinity labels

This class of active site-directed irreversible inactivators constitutes substrate analogues containing a highly reactive functional group such as isocyanate, epoxide or bromoacetyl groups. However due to their high intrinsic reactivity, affinity labels can react with several different residues both within and outside the active site, resulting in non-specific labeling of the enzyme. This problem can generally be circumvented by inactivating the enzyme at low concentrations of the inactivator, thereby taking advantage of the high specificity of the active site for the inactivator. Alternatively, labeling experiments can be performed in the absence and in the presence of a competitive inhibitor which protects the active site from derivatisation by the affinity label. Labeled active site residues can then be

identified by eliminating from consideration residues labeled in the presence of the competitive inhibitor.

*(a) Glycosyl epoxides:* Affinity labels have been extensively used to map the active site of several glycosidases. Examples include the use of *N*-bromoacetyl glycosylamines (Figure 4-1) to inactivate *E. coli* β-galactosidase (Naider et al., 1972), *Aspergillus wentii* β-glucosidase (Legler, 1977) and *Agrobacterium* β-glucosidase (Black et al., 1993) as well as β-D-glucosyl isothiocyanate (Figure 4-1) which inactivates sweet almond β-glucosidase (Shulman et al., 1976). However by far the most extensively used group of affinity labels for studying glycosidases are the glycosyl epoxide derivatives (Figure 4-2).

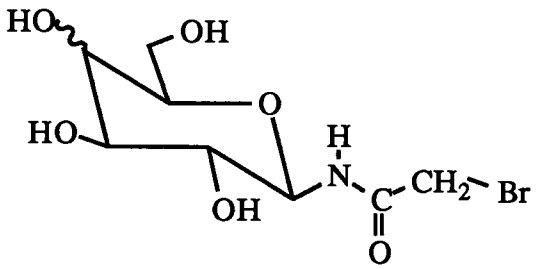


N-Bromoacetyl β-D-glycosylamine

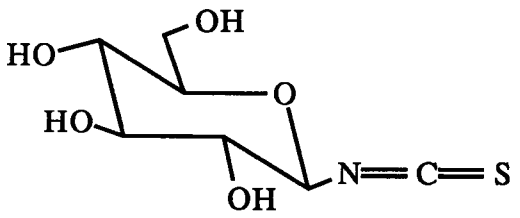


β-D-Glucosyl isothiocyanate

*Figure 4-1 Examples of affinity labels.*

Glycosyl epoxides inactivate glycosidases because when protonated either by the acid catalyst or another residue within close proximity, they are converted to reactive species which are susceptible to nucleophilic attack by neighbouring amino acid residues (Figure 4-2). Indeed these compounds have been successfully used to label and identify active site residues, the earliest study involving inactivation of hen egg white lysozyme with {$^{14}$C}-2,3-epoxy propyl chitobioside. Sequencing of the purified, radiolabeled, proteolytically derived peptide revealed Asp 52 as the modified residue (Eshdat et al.,

1974) while X-ray crystallographic analysis of the inactivated enzyme complex was consistent

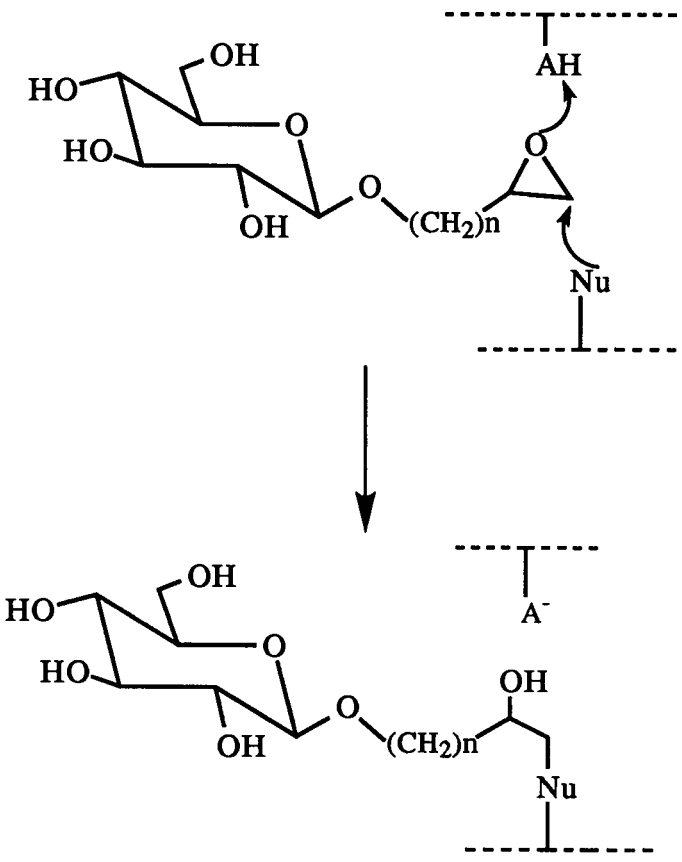


*Figure 4-2 Mechanism for inactivation of glycosidases by glycosyl epoxides.*

with the role of this residue as the catalytic nucleophile (Moult et al., 1973). Other studies involving the use of glycosyl epoxide inactivators have included those with several cellulases. For example, both the *Bacillus amyloliquefaciens* 1,3-1,4-β-D-glucan 4-glucanohydrolase and *Bacillus macerans* 1,3-1,4-β-glucanase are inactivated with 3,4-epoxy butyl β-cellobioside (Hoj et al., 1992; Keitel et al., 1993) while *Trichoderma reesei* endoglucanase III is inactivated with 4',5'-epoxy pentyl β-cellobioside (Macarron et al., 1993). The labeled residues in the *Bacillus amyloliquefaciens* and *Trichoderma reesei*

enzymes were identified as Glu 105 and Glu 329, respectively and proposed to be the catalytic nucleophiles in these enzymes. In the *Bacillus macerans* enzyme, the labeled residue was identified as Glu 105 by X-ray crystallographic analysis of the inactivated enzyme complex and proposed to be a catalytically important residue based on mutagenesis studies (Keitel et al., 1993).

### 4-1-3 Mechanism-based inactivators

Another group of irreversible inactivators designed to specifically bind at the active site of target enzymes is that of mechanism-based inactivators. These inactivators do not contain highly reactive functional groups and thus are relatively unreactive structural analogues of the substrates. However, they are transformed into the inactivating species via an enzyme-catalysed process. For an inactivator to be classified as mechanism-based, it must comply with the following two additional requirements. First, a catalytic step must be shown to be involved in the inactivation process and second, inactivation of the enzyme should occur prior to release of the activated species. This ensures the identity of the structure of the inactivated-enzyme complex as well as ensures that the inactivation process occurs at the active site (Silverman, 1988). As a consequence, mechanism-based inactivators tend to be more specific for the enzyme active site than affinity labels due to their inherently lower reactivity and requirement for catalytic activation.

*(a) Conduritol epoxides*: One class of mechanism-based inactivators of glycosidases that has been widely used is that of the conduritol epoxides. These epoxides are tetrahydroxycyclohexanes containing an endocyclic epoxide, thus are structural analogues of the glycone portion of glycosides (Figure 4-3). The electron-withdrawing effects of the neighbouring hydroxyl groups result in greatly reduced reactivity of the epoxide group against acid catalysis and nucleophilic addition, thus rendering conduritol epoxides relatively inert to spontaneous hydration. These compounds are therefore good candidates

as mechanism-based inactivators since they will only react with proteins if bound in a position that permits proton donation by an acidic group to the epoxide oxygen followed by nucleophilic attack at C-1 and subsequent formation of a covalent bond (Figure 4-3). In glycosidases, the residues appropriately located to perform these roles are the acid-catalyst and the catalytic nucleophile, the residues normally involved in glycoside hydrolysis.

Conduritol epoxide derivatives have been synthesized and shown to be inactivators of several glycosidases including *Aspergillus wentii* β-glucosidase and *E. coli* β-galactosidase (Legler, 1990). In all cases studied, the modified residues were identified as carboxylate groups and further confirmation of this was obtained by treating the inactivated enzyme with hydroxylamine (Figure 4-3). The reaction product in all cases was identified as inositol produced by *trans*-opening of the epoxide which is consistent with the existence of an ester linkage between a carboxylate group of the enzyme and the conduritol epoxide inactivator. The modified carboxylate residue was proposed to be the catalytic nucleophile based upon the mechanism of enzyme inactivation by conduritol epoxides. For example, with *Aspergillus wentii* β-glucosidase, an aspartate residue was labeled using $^{3}H$-conduritol cis-B epoxide (Bause & Legler, 1974), treatment of the inactivated enzyme with hydroxylamine produced (+)-chiro-inositol (Legler, 1968) and thus this aspartate residue was assigned the role of the catalytic nucleophile (Bause & Legler, 1974). This assignment was later confirmed when the residue involved in the formation of the 2-deoxy-glucosyl-enzyme intermediate during p-nitrophenyl-2-deoxy-β-D-glucopyranoside hydrolysis was identified as the same asparate residue labeled by conduritol cis-B epoxide (Roeser & Legler, 1981). However it should be noted that in other cases, the enzymic residue modified by conduritol epoxide derivatives is not always the catalytic nucleophile. For example, the residue labeled in *E. coli* β-galactosidase by conduritol C epoxide was identified as Glu 461, and thus proposed to be the catalytic nucleophile (Herrchen & Legler, 1984). Kinetic analysis of the mutants generated at position 461 of this β-galactosidase revealed that the $k_{cat}$ values for hydrolysis of 2-nitrophenyl-β-D-galactoside

were reduced 7500-, 1056-, 2083-, 18- and 3700-fold upon replacement of the glutamate with aspartate, glycine, glutamine, histidine and lysine, respectively (Cupples et al., 1990).

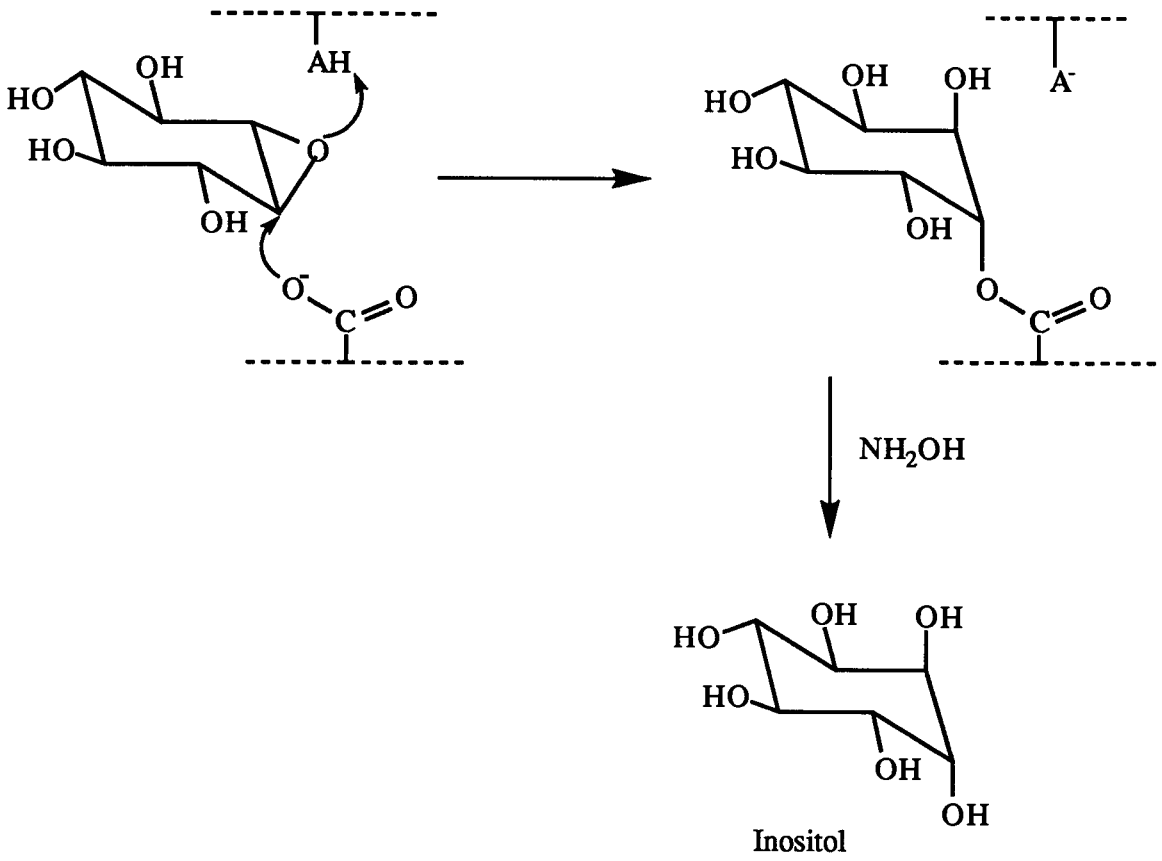


*Figure 4-3* *Inactivation of a glycosidase by a conduritol epoxide and release of inositol upon hydroxylamine treatment.*

Surprisingly, the most conservative change, replacement of the glutamate with aspartate, resulted in the greatest rate reduction while less conservative changes such as the replacement of the glutamate with histidine resulted in a mutant with significant enzymatic activity. These results are inconsistent with those obtained from kinetic studies performed on mutants generated at the catalytic nucleophile (Glu 358) of *Agrobacterium* β-glucosidase (Withers et al., 1992). In the case of the β-glucosidase, values of $k_{cat}$ were seen to be

reduced 2500-fold with the aspartate mutant and greater than $10^5$-fold with the glutamine mutant and thus are consistent with the role of Glu 358 as the catalytic nucleophile. These results prompted a reinvestigation of the identity of the catalytic nucleophile by Gebler and coworkers using the more specific mechanism-based inactivator, 2,4-dinitrophenyl-2-deoxy-2-fluoro-β-D-galactopyranoside, which functions via formation of a stabilised 2-deoxyfluoroglycosyl-enzyme intermediate (*vide infra*) (discussed in Chapter I). This study identified Glu 537 as the catalytic nucleophile (Gebler et al., 1992). Subsequent kinetic studies of the mutants made at position 537 were entirely consistent with this assignment (Yuan et al., 1994). It has been suggested by Gebler and coworkers (1992) that Glu 461 is likely the acid catalyst, an assignment more consistent with the mutagenesis results. Conduritol C epoxide is thought to have labeled Glu 461 instead of the catalytic nucleophile in *E. coli* β-galactosidase (Glu 537) because the absence of the C-5 hydroxymethyl group which is present in normal galactoside substrates presumably allows alternative binding modes within the active site and thus allows the inactivator to react with other active site residues (Withers & Aebersold, 1995).

## 4-2 Background And Objectives Of This Project

The aim of this project is to identify active site residues in *C. fimi* exoglycanase that are important in either catalysis or substrate binding by using active site directed irreversible inactivators and a combination of mass spectrometric techniques. This project has been a collaborative effort between our laboratory and that of Dr. Ruedi Aebersold where the mass spectrometric analysis was performed.

Previously, 2,4-dinitrophenyl 2-deoxy-2-fluoro-β-D-glycosides have been shown to be good mechanism-based inactivators of several "retaining" glycosidases, specifically derivatising the catalytic nucleophile (discussed in Chapter I). They have therefore been used to label and identify this key residue. Both 2,4-dinitrophenyl 2-deoxy-2-fluoro-β-D-glucoside and its cellobioside analogue are inactivators of *C. fimi* exoglycanase,

inactivating in a time dependent manner according to pseudo-first order kinetics (Tull & Withers, 1994; McCarter et al., 1993; Tull et al., 1991). The 2-deoxyfluoroglucosyl-inactivated exoglycanase is stable, with $t_{1/2}$ ~ 800 hours, thereby allowing identification of the catalytic nucleophile involved in glucoside hydrolysis as Glu 233 (Tull et al., 1991). Similarly, the 2-deoxyfluorocellobiosyl-exoglycanase intermediate is seen to be stable ($t_{1/2}$ ~ 1300 hours) and thus should allow for the identification of the catalytic nucleophile involved in cellobioside hydrolysis.

Hydration of glycals by glycosidases involves the same catalytic residues as those participating in normal glycoside hydrolysis (discussed in Chapters I & II). Recall that the reaction involves protonation of the glycal by either the acid catalyst or the catalytic nucleophile, attack at the C-1 position of the glycal by the catalytic nucleophile, and formation of a 2-deoxyglycosyl-enzyme intermediate. In a second step the intermediate is hydrolysed, releasing a 2-deoxy-glycose product and free enzyme. If the rate of hydrolysis of the intermediate is lower than that of its formation, then the enzyme accumulates as the intermediate. Further, if hydrolysis is sufficiently slow, this may provide a means of trapping the catalytic nucleophile. Identification of this 2dCb-amino acid residue can therefore confirm the identity of the catalytic nucleophile in *C. fimi* exoglycanase.

Previously, the affinity label, *N*-bromoacetyl cellobiosylamine, was shown to inactivate *C. fimi* exoglycanase in a time-dependent manner according to pseudo-first order kinetics with inactivation kinetic parameters $K_i$ = 9.1 mM, $k_i$ = 0.083 $min^{-1}$ and $k_i/K_i$ = 9.1 x $10^{-3}$ $min^{-1}mM^{-1}$ (Appendix A-8, Figure A-8-3, Black et al., 1993). Since *N*-bromoacetyl glycosylamines can react with any suitable nucleophile within range due to their high intrinsic reactivity, then the cellobiosyl analogue of this inactivator has the potential to identify residues important in either catalysis or substrate binding which have not been identified by other methods.

Therefore, the objectives of this project are to use the mechanism-based inactivators, 2,4-dinitrophenyl 2-deoxy-2-fluoro-β-cellobioside (2F-DNPC) and cellobial

to identify the catalytic nucleophile involved in *C. fimi* exoglycanase-catalysed hydrolysis of cellobiosides as well as to use the affinity label, *N*-bromoacetyl cellobiosylamine, to identify other active site residues.

## 4-3 Results And Discussion

### 4-3-1 Labeling studies of *C. fimi* exoglycanase using 2,4-dinitrophenyl 2-deoxy-2-fluoro-β-D-cellobioside

#### (a) Stoichiometry of inactivation

A sample of *C. fimi* exoglycanase were inactivated with 2,4-dinitrophenyl 2-deoxy-2-fluoro-β-D-cellobioside and then subjected to electrospray ionisation mass spectrometric analysis, along with a sample of unlabeled exoglycanase. Masses of 47,114 +/- 7 and 47,441 +/- 7 Da were recorded and correspond to the molecular weights of unlabeled exoglycanase and 2-fluoro-cellobiosyl-exoglycanase, respectively (Figure 4-4). The mass difference between the 2-fluoro-cellobiosyl-exoglycanase sample and the unlabeled enzyme corresponds to 327 Da. Since the mass of the 2-deoxyfluoro-cellobiosyl moiety is 327 Da, then this result suggests that one mole of 2,4-dinitrophenyl 2-deoxy-2-fluoro-β-D-cellobioside inactivates one mole of exoglycanase.

#### (b) Strategy for identification of the 2-deoxyfluorocellobiosyl-labeled residue.

The approach that will be used to identify the 2-deoxyfluoro-cellobiosyl-modified residue is shown schematically in Figure 4-5. It involves labeling the exoglycanase with the inactivator, proteolytic digestion of the labeled enzyme, identification and purification of the labeled peptides by high-performance liquid chromatography-electrospray ionisation tandem mass spectrometry (HPLC-ESI-MS/MS) and subsequent sequencing to identify the labeled peptide.

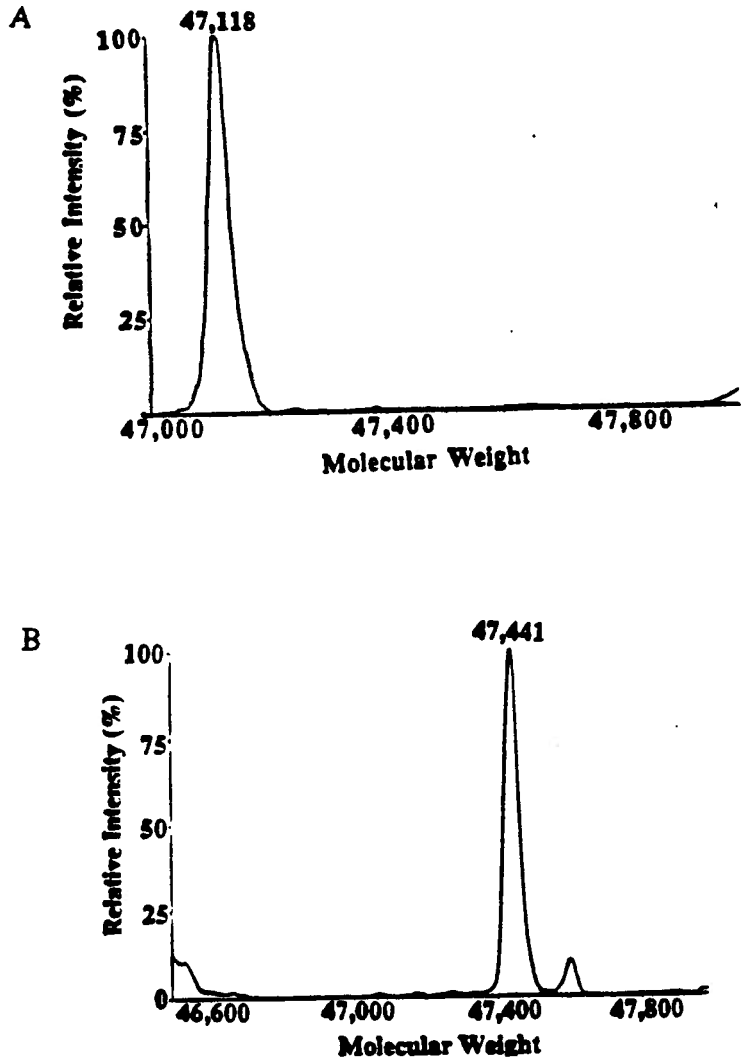


*Figure 4-4* *Electrospray ionisation mass spectra showing stoichiometry of inactivation of C. fimi exoglycanase by 2F-DNPC. Reconstructed mass spectra of unlabeled enzyme (upper) and labeled enzyme (lower).*

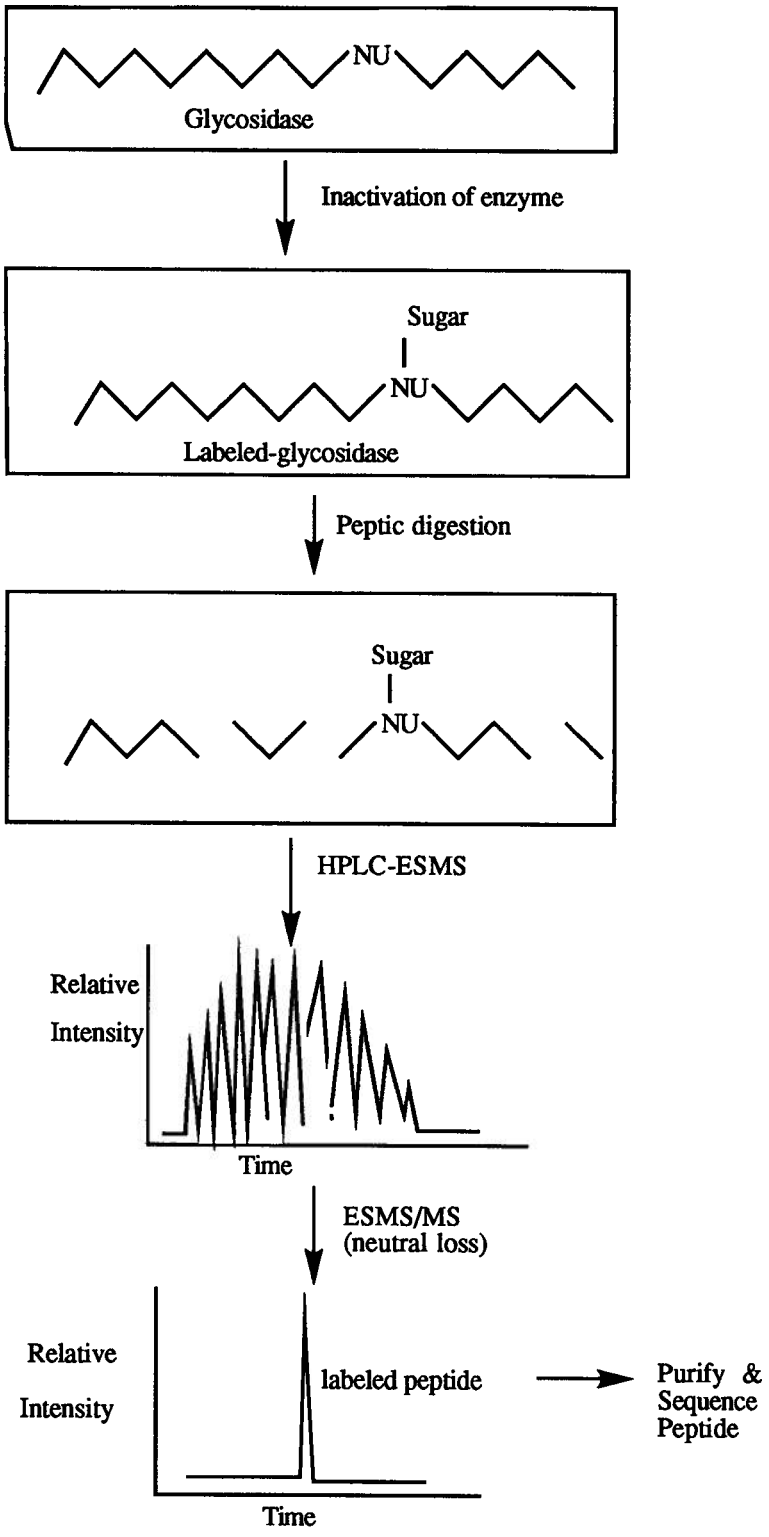


*Figure 4-5* *Scheme of the method used to identify the residue in C. fimi exoglycanase labeled by 2F-DNPC and cellobial.*

### (c) Identification of the residue modified by 2,4-dinitrophenyl 2-deoxy-2-fluoro-β-cellobioside

A sample of *C. fimi* exoglycanase was completely inactivated with 2F-DNPC and subjected to peptic proteolysis, along with a sample of unlabeled enzyme. The resulting peptide mixtures were individually separated by RP-HPLC using the electrospray ionisation mass spectrometer as a detector, scanning in the normal MS mode as described in Chapter V by Dr. Shichang Miao in Dr. Ruedi Aebersold's laboratory. A large number of peaks is observed in the total ion chromatogram (TIC), consistent with the presence of many peptides in the mixture (Figure 4-6, upper spectrum). The 2FCb-labeled peptide in the mixture was then identified in a second run using the tandem mass spectrometer scanned in the neutral loss mode (Figure 4-6, middle spectrum). In this mode the peptide ions are subjected to limited fragmentation by collision with argon-nitrogen mixture in a collision cell. This results in the loss of a neutral sugar species from the peptide, leaving the peptide with its original charge, but a decreased mass. In the case of the 2FCb-labeled sample the neutral species is expected to be the 2FCb-moiety since the ester linkage between the 2FCb-moiety and the peptide is one of the more labile linkages present and thus readily undergoes homolytic cleavage. Indeed, the collision conditions used were sufficient to break the ester bond but not generally the amide bonds of the peptide backbone. This resulting peptide is identified when the two quadrupoles are scanned in a linked manner such that only the peptide ions differing in $m/z$ by the mass of the neutral species can pass through both quadrupoles and be detected. In some cases it may be necessary to scan for $m/z$ differences of one half or one third the mass of the neutral species as the peptide may be doubly or triply charged. When the tandem mass spectrometer was scanned in the neutral loss mode, searching for a mass loss corresponding to the 2FCb-moiety of $m/z$ = 327 Da, no signal was detected. However, when scanned for a mass loss

of *m/z* = 163.5 Da corresponding to the elimination of the 2FCb-moiety from the doubly charged peptide species, a single peak of *m/z* = 529 Da was observed in the TIC (Figure 4-6, lower spectrum). Similar tandem mass spectrometric analysis of a peptic digest of unlabeled exoglycanase revealed no peaks in the TIC, suggesting that the signal at *m/z* = 529 Da in the TIC of the labeled sample corresponded to the derivatised peptide.

The identity of this peptide can be easily probed by calculation of its mass. The peptide observed of *m/z*= 529 Da for the doubly charged species (Figure 4-6, lower spectrum) has molecular weight 1056 Da [(529 x 2) - 2H]. Since the mass of the label is 327 Da the molecular weight of the unlabeled peptide must be 730 Da (1056 - 327 + 1H). Clues to the identity of this peptide were then obtained by searching the amino acid sequence of this exoglycanase (O,Neill et al., 1986) for all possible peptides of mass 730 Da. Nine peptides of mass 730.4 ± 0.1 Da could be identified, one of which contains the active site peptide (Val-Arg-Ile-Thr-Glu-Leu) previously identified by the standard method using tritiated 2F-DNPG (Tull et al., 1991).

The 2FCb-modified peptide was isolated from the peptic mixture by RP-HPLC using a post column flow splitter to divert 85% of the eluent to a fraction collector while the remaining 15% was introduced into the mass spectrometer, scanning in the neutral loss mode. The purified 2FCb-peptide was sequenced using the Edman degradation. The peptide was identified as Val-Arg-Ile-Thr-Glu-Leu and the labeled residue as a glutamate residue. Sequence alignment of this peptide with the known amino acid sequence of *C. fimi* exoglycanase revealed Glu 233 as the labeled residue. Thus, the catalytic nucleophile involved in cellobioside hydrolysis, Glu 233, is exactly the same as that involved in glucoside hydrolysis.

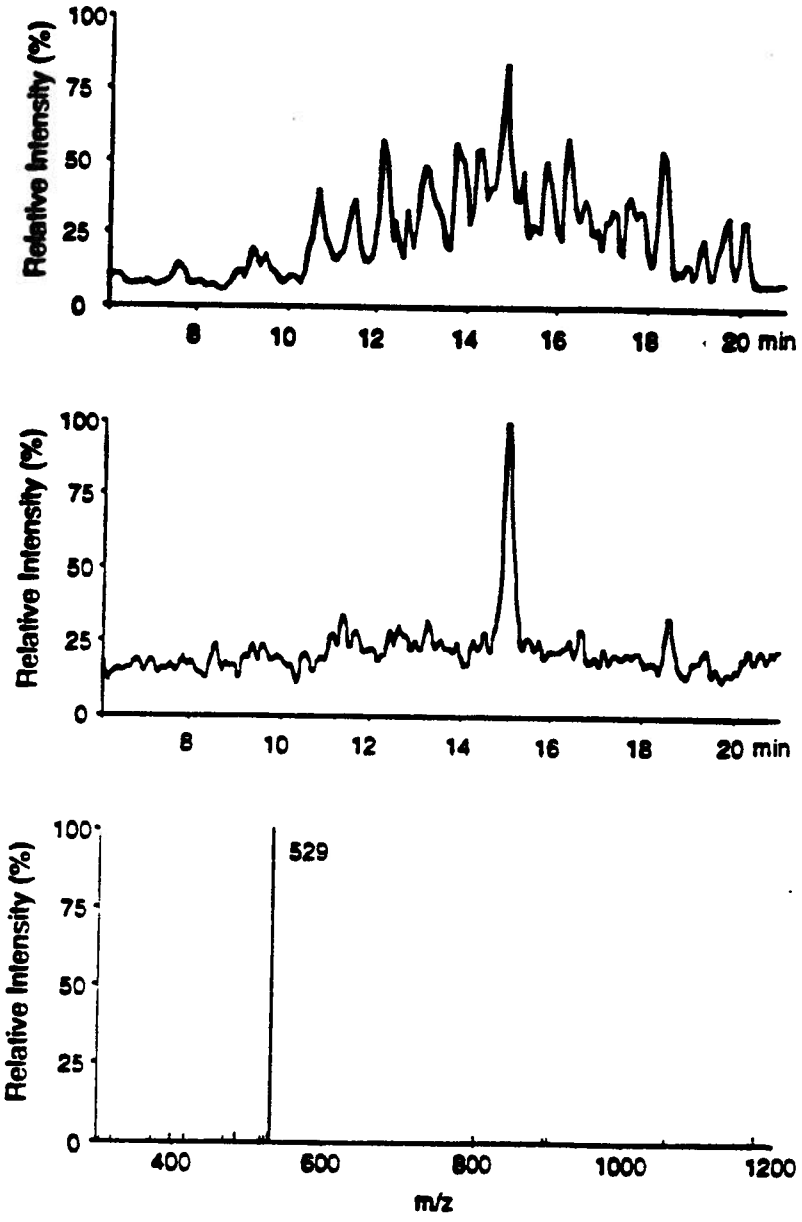


*Figure 4-6* *Electrospray ionisation mass spectra of a peptic digest of C. fimi exoglycanase inactivated by 2F-DNPC. (Upper) TIC of digest in normal MS mode, (middle) TIC of digest in neutral loss mode and (lower) mass spectrum of peptide in the middle panel.*

### 4-3-2 Labeling studies of *C. fimi* exoglycanase using cellobial

#### (a) Stoichiometry of inactivation

Samples of cellobial-inactivated and untreated *C. fimi* exoglycanase were subjected to electrospray ionisation mass spectrometric analysis. Molecular weights of 47,118 +/- 7 Da and 47,423 +/- 7 Da corresponding to the unlabeled and labeled enzyme species respectively, were recorded (Figure 4-7). This mass difference of 305 Da between the 2dCb-exoglycanase sample and the unlabeled enzyme corresponds well with the mass of a single 2dCb moiety (308 Da) and thus is consistent with a stoichiometry of inactivation of one mole of 2dCb moiety per mole of enzyme.

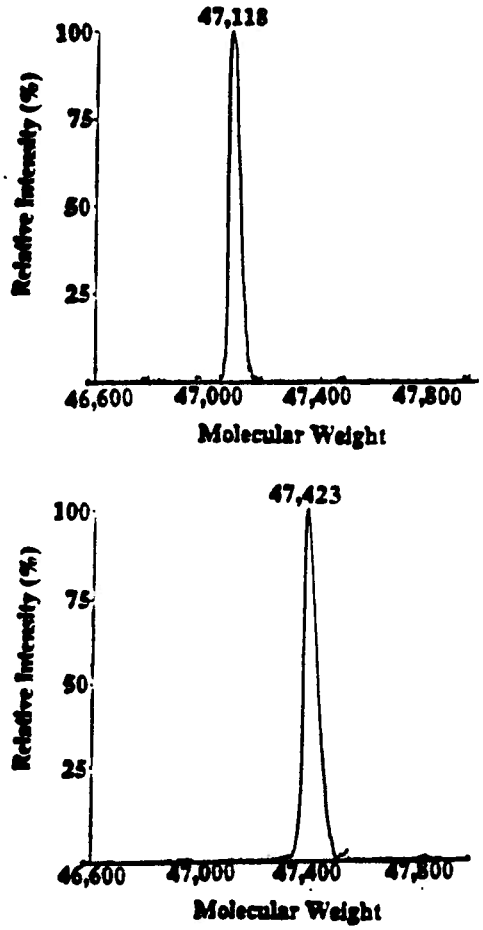


*Figure 4-7* *Electrospray ionisation mass spectra showing the stoichiometry of inactivation of C. fimi exoglycanase by cellobial. Reconstructed mass spectra of unlabeled enzyme (upper) and labeled enzyme (lower).*

**(b) Identification of the residue modified by cellobial**

Further confirmation of Glu 233 as the catalytic nucleophile involved in cellobioside hydrolysis could be obtained using cellobial since it is also expected to derivatise the catalytic nucleophile and since the 2dCb-enzyme intermediate is stable with $t_{1/2} \sim 23$ hours. This approach has been used previously to identify the catalytic nucleophile in *Aspergillus wentii* β-glucosidase. D-$^{14}$C-glucal was seen to label the same aspartate residue in *Aspergillus wentii* β-glucosidase as that previously labeled by conduritol B epoxide and thus this aspartate residue has been assigned the role of the catalytic nucleophile (Legler et al., 1979). A sample of *C. fimi* exoglycanase was inactivated with cellobial, the labeled exoglycanase digested with pepsin and the digest subjected to neutral loss tandem mass spectrometric analysis searching for a mass loss of 308 Da corresponding to the mass of a 2dCb-moiety. The single peak observed in the neutral loss TIC at $m/z$ = 1039 Da corresponded to the singly charged labeled peptide (Figure 4-8), hence the labeled peptide has molecular weight 1038 Da and the unlabeled peptide has molecular weight 730 Da (1038 - 308 + 1H), likely corresponding to the Val-Arg-Ile-Thr-Glu-Leu peptide. This suggests that Glu 233 is the catalytic nucleophile involved in cellobial hydration and in cellobioside hydrolysis.

Indeed, the catalytic nucleophiles in other glycosidases have been identified using this new neutral loss tandem mass spectrometric method. For example, the labeled peptides identified in 2F-DPNC-inactivated *Clostridium thermocellum* endoglucanase C and 2F-DNPG-inactivated *Agrobacterium* β-glucosidase by this mass spectrometric technique were exactly the same as those identified by the standard radiolabeling technique (Tull et al., 1995). These results therefore further confirmed Glu 280 (Wang et al., 1993) and Glu 358 (Withers et al., 1990) as the catalytic nucleophiles in the endoglucanase and the β-glucosidase, respectively. In addition, this mass spectrometric approach was used to identify, for the first time, Glu 340 and Glu 78 as the catalytic nucleophiles in human

glucocerebrosidase and *Bacillus subtilis* xylanase respectively, using the appropriate 2-deoxy-2-fluoro-glycosides (Miao et al 1994a; Miao et al., 1994b).

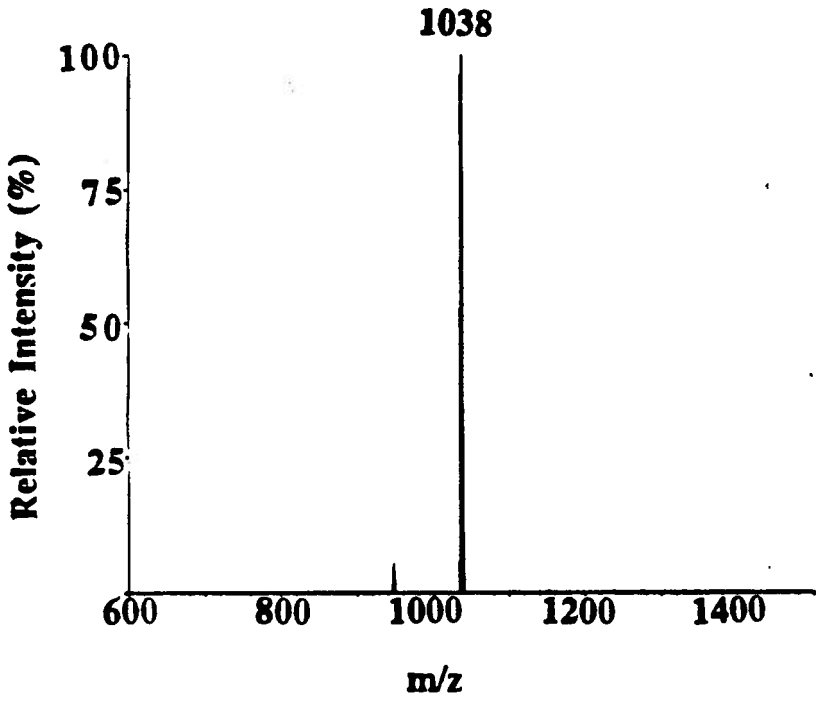


*Figure 4-8* *Neutral loss tandem electrospray ionisation mass spectrum of a peptic digest of C. fimi exoglycanase inactivated by cellobial.*

### 4-3-3 Labeling studies of *C. fimi* exoglycanase with *N*-bromoacetyl cellobiosylamine

#### (a) Protection against inactivation

Samples of *C. fimi* exoglycanase were incubated in the presence of *N*-bromoacetyl cellobiosylamine and either 0 or 9.7 mM of the competitive inhibitor, benzyl 4-O-(β-D-

glucopyranosyl)-1-thio-β-D-xylopyranoside (Figure 4-9) (BGTX, $K_i$ = 3.0 mM). Aliquots were removed at different time intervals and assayed for exoglycanase activity using saturating concentrations of 2,4-DNPC (Appendix A-8, Figure A-8-3). Values of $k_{obs}$ in the absence and presence of BGTX were 6.0 x $10^{-2}$ and 1.2 x $10^{-2}$ $min^{-1}$, respectively as expected if BGTX and *N*-bromoacetyl cellobiosylamine are competing for the same site. These results suggest that inactivation of *C. fimi* exoglycanase by *N*-bromoacetyl cellobiosylamine involves blockage of the active site and therefore likely involves derivatisation of a residue present at the active site.

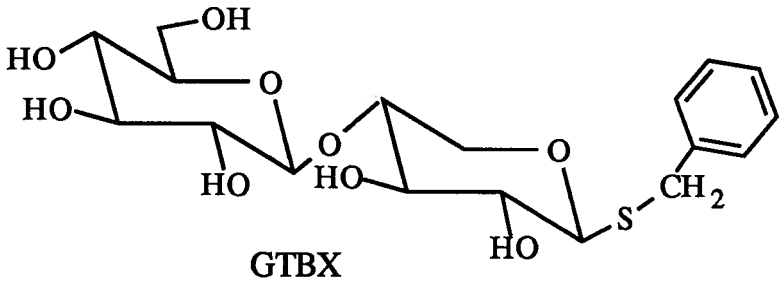


*Figure 4-9 Structure of benzyl 4-O-(β-D-glucopyranosyl)-1-thio-β-D-xylopyranoside.*

### (b) Stoichiometry of inactivation

As affinity labels, *N*-bromoacetyl glycosylamines are relatively reactive compounds capable of modifying glycosidases (Figure 4-10) at more than one site and indeed such results have been reported. For example, electrospray ionisation mass spectrometric analysis of *Agrobacterium* β-glucosidase inactivated with *N*-bromoacetyl glucosylamine revealed incorporation of up to three *N*-acetyl glucosylamine moieties into the enzyme while radiolabeling studies of *N*-bromoacetyl galactosylamine inactivation of *E. coli* β-galactosidase revealed incorporation of two moles of *N*-acetyl galactosylamine per active site (Yariv et al., 1971). However, in both cases the inactivation kinetics suggested a simple pseudo-first order process (Black et al., 1993).

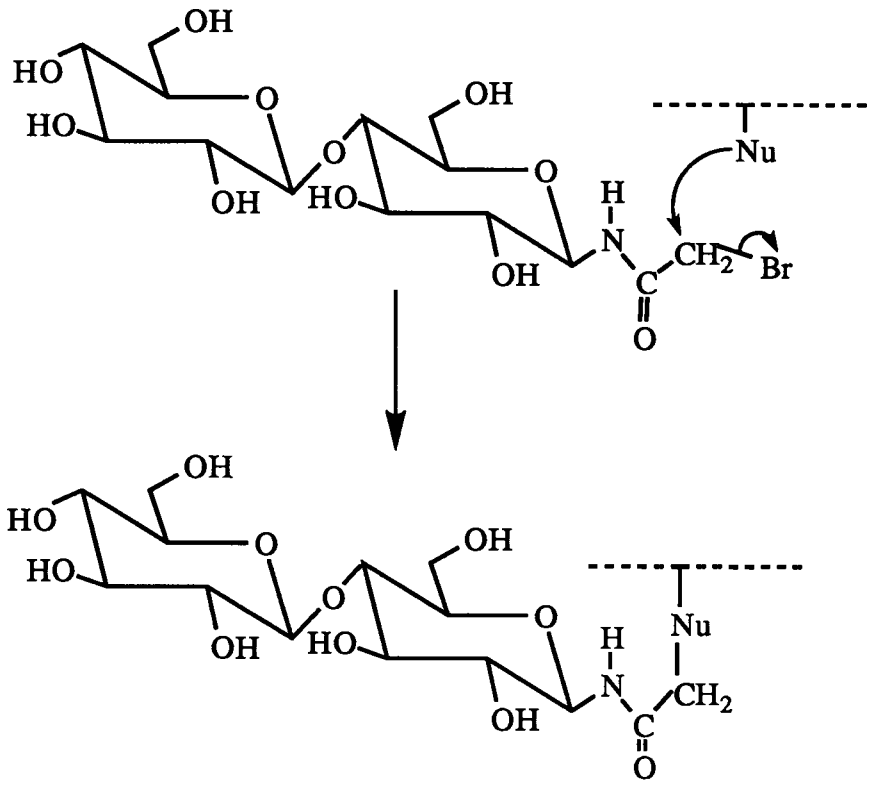


*Figure 4-10* *Mechanism of inactivation of C. fimi exoglycanase by N-bromoacetyl cellobiosylamine.*

The stoichiometry of inactivation of *C. fimi* exoglycanase by *N*-bromoacetyl cellobiosylamine was investigated as described for 2F-DNPC inactivation. The molecular weight of the unlabeled exoglycanase sample was 47,118 +/- 7 Da while that for the labeled sample was 47,496 +/- 5 Da (Figure 4-11). This mass difference of 378 Da corresponds well with the mass increase of 382 Da expected if the exoglycanase was derivatised by a single N-acetyl cellobiosylamine moiety. The very small peak observed at 47,873 corresponds to an enzyme species in which two *N*-acetyl cellobiosylamine moieties have bound, however this could be suppressed by shortening the incubation time. This inactivation stoichiometry of one mole of *N*-acetyl cellobiosylamine incorporated per mole

of exoglycanase, together with the results from the protection study suggest that *N*-bromoacetyl cellobiosylamine is a good candidate affinity label to be used to identify important active site residues of *C. fimi* exoglycanase.

### (c) Strategy for identification of *N*-acetyl cellobiosylamine-labeled residue

Identification of the residue modified by *N*-bromoacetyl cellobiosylamine, as shown schematically in Figure 4-12, involved comparative LC-MS analysis of proteolytic digests derived from labeled and unlabeled exoglycanase. The labeled peptide will be identified by search the chromatogram of the labeled sample looking for a peptide ion that is absent in the unlabeled sample and that differs from a specific peptide in the unlabeled sample by the mass of the inactivator.The labeled residue in the isolated peptide will then identified by first sequencing the peptide using a novel 311 PITC (phenyl isothiocyanate derivative) sequencing chemistry (Hess et al., 1995; Bures et al., 1995) and then by using tandem mass spectrometry to structurally characterise the released 311 PTH (phenylthiohydantoin) amino acid derivative. Sequence alignment of the peptide with the known amino acid sequence of this exoglycanase will be used to determine the exact residue labeled in the enzyme.

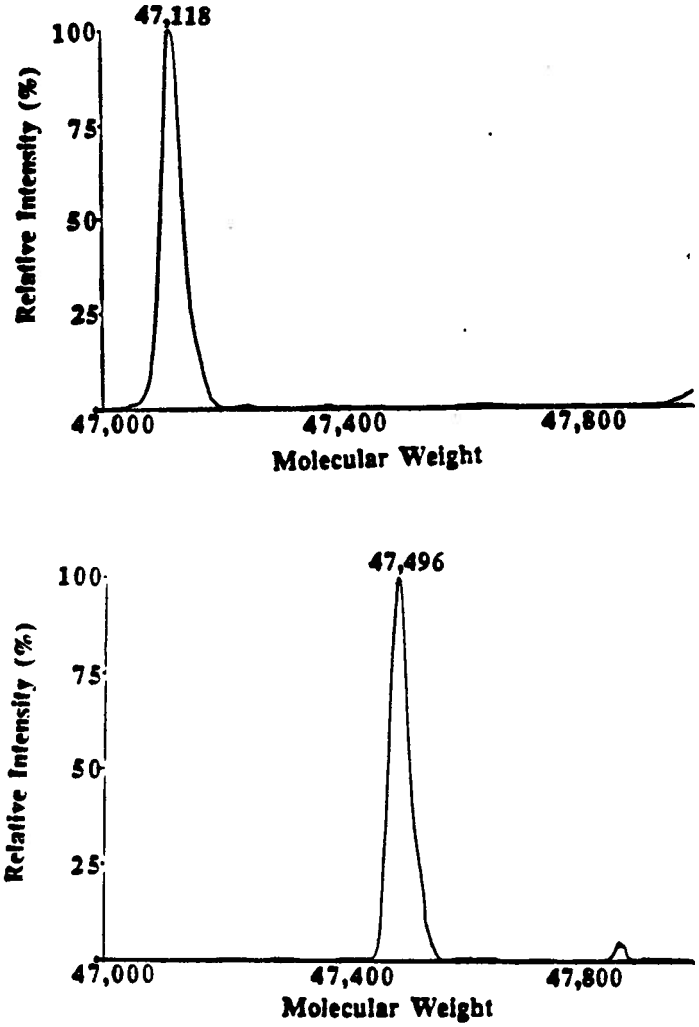


*Figure 4-11* *Electrospray ionisation mass spectra showing the stoichiometry of inactivation of C. fimi exoglycanase by N-bromoacetyl cellobiosylamine. Reconstructed mass spectra of unlabeled enzyme (upper) and labeled enzyme (lower).*

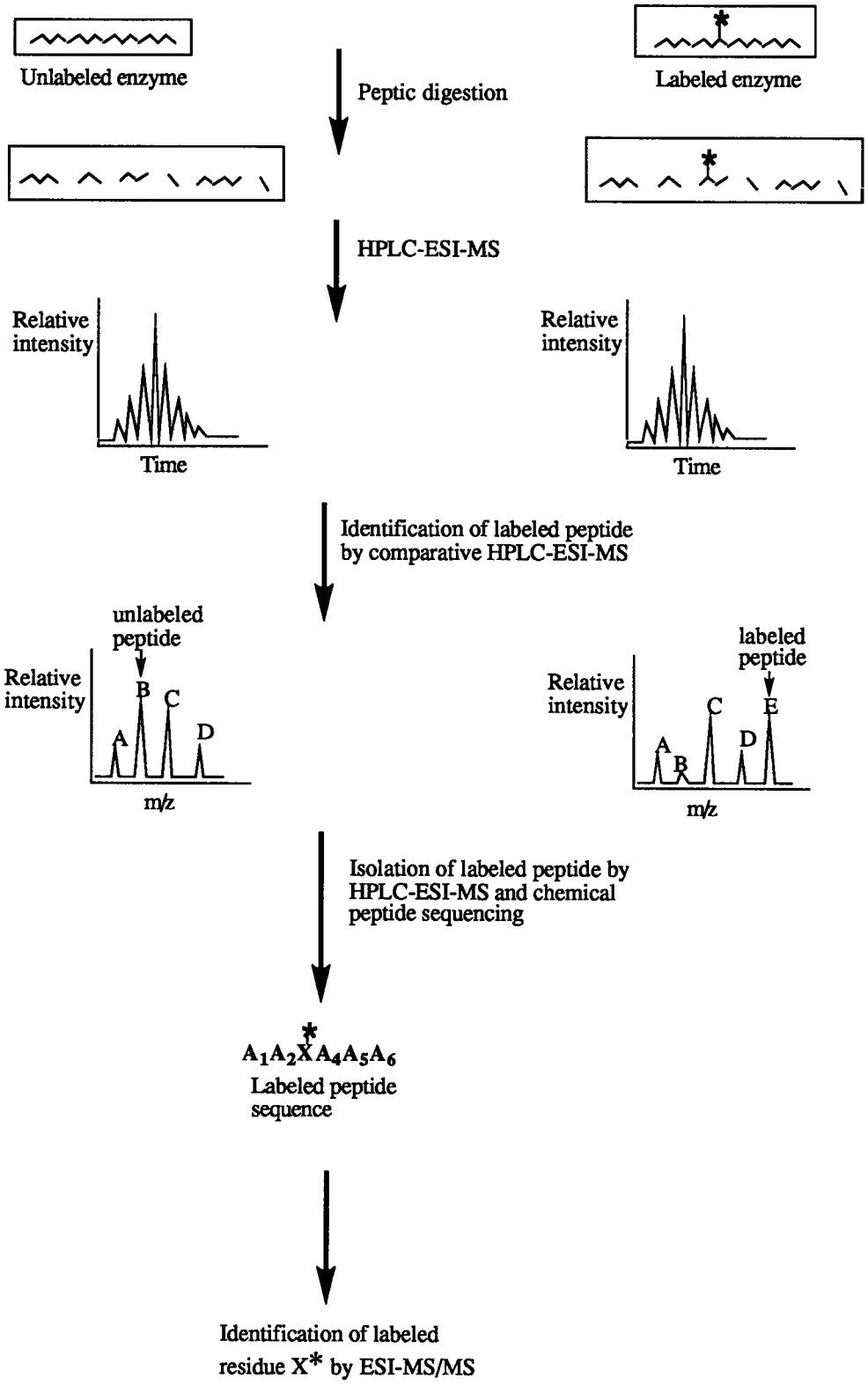


*Figure 4-12* *Scheme of the method used to identify the residue in C. fimi exoglycanase labeled by N-bromoacetyl cellobiosylamine.*

### (d) Identification of peptide modified by *N*-bromoacetyl cellobiosylamine

A sample of the exoglycanase from *C. fimi* was inactivated with *N*-bromoacetyl cellobiosylamine and subjected to proteolytic digestion with pepsin, yielding a mixture of peptides. A sample of unlabeled exoglycanase was also subjected to peptic digestion using similar conditions. The mixtures of peptides from the labeled and unlabeled samples were individually separated by RP-HPLC using the electrospray ionisation mass spectrometer as a detector. When the spectrometer is scanned in the normal MS mode, the total ion chromatogram (TIC) of the labeled and unlabeled exoglycanase peptic digests displayed a large number of peaks which arise from every peptide in the mixture (Figure 4-13, upper spectrum). No significant, reproducible differences could be detected between the chromatograms of the two digests. The labeled peptide was identified by using this mass information. It was expected that the masses of the relevant active site peptide in the labeled and unlabeled enzyme digests must differ by the mass of the *N*-acetyl cellobiosylamine moiety (382 Da). Therefore, the masses of the peptides under each peak in the labeled sample were compared with the masses of the peptides from the corresponding region in the TIC of the unlabeled exoglycanase sample. All the peptides present in the labeled sample were present in the unlabeled sample at comparable retention times, with the exception of a single peptide of mass 1028 Da (Figure 4-13, lower spectrum) which was only detected in the digest from the inhibited enzyme. The TIC of the unlabeled sample was then searched for a possible counterpart unlabeled peptide of mass 646 Da (Figure 4-13, middle spectrum) corresponding to the mass difference between this peptide of mass 1028 Da and the *N*-acetyl cellobiosylamine label of mass 382 Da. Indeed such a peptide was observed in the unlabeled sample. This peptide of mass 646 Da was also present in the TIC of the labeled sample (Figure 4-13, lower spectrum) at a retention time similar to that of the 646 Da peptide in the unlabeled sample although its intensity was reduced compared to that

of the corresponding peptide in the unlabeled sample. These results suggested that the peptide of mass 1028 Da was likely the modified peptide and that the appearance of the peptide of mass 646 Da in the labeled sample was due to incomplete inactivation of the exoglycanase and/or cleavage of the *N*-acetyl cellobiosylamine from the labeled peptide during proteolysis or chromatography. The labeled peptide was purified to homogeneity by RP-HPLC, monitored by ESI-MS. Candidate peptides were then identified by inspection of the amino acid sequence of the exoglycanase and searching for all possible peptides with this mass. Nine possible peptides of mass 646 +/- 1 were identified within the *C. fimi* exoglucanase sequence (O'Neill et al., 1986).

### (e) Identification of the labeled residue

To unambiguously assign the labeled peptide within the exoglycanase amino acid sequence and to characterise the labeled residue, the isolated peptide was sequenced using the novel 311 PITC (4-(3-pyridinylmethyl-aminocarboxypropyl) phenyl isothiocyanate, 311 = molecular weight of reagent) sequencing reagent (Hess et al., 1995) by Mr. David Chow in Dr. Reudi Aebersold's laboratory. This automated sequencing involved attaching the isolated peptide to a solid support and stepwise derivatisation of the N-terminal amino acid by the 311 PITC reagent. The 311 PTH- (phenylthiohydantoin-) derivatised residues are sequentially separated by RP-HPLC and analysed by on-line electrospray ionisation mass spectrometry. Thus, the 311 PTH-residues are identified both by their mass and by the chromatographic retention time.

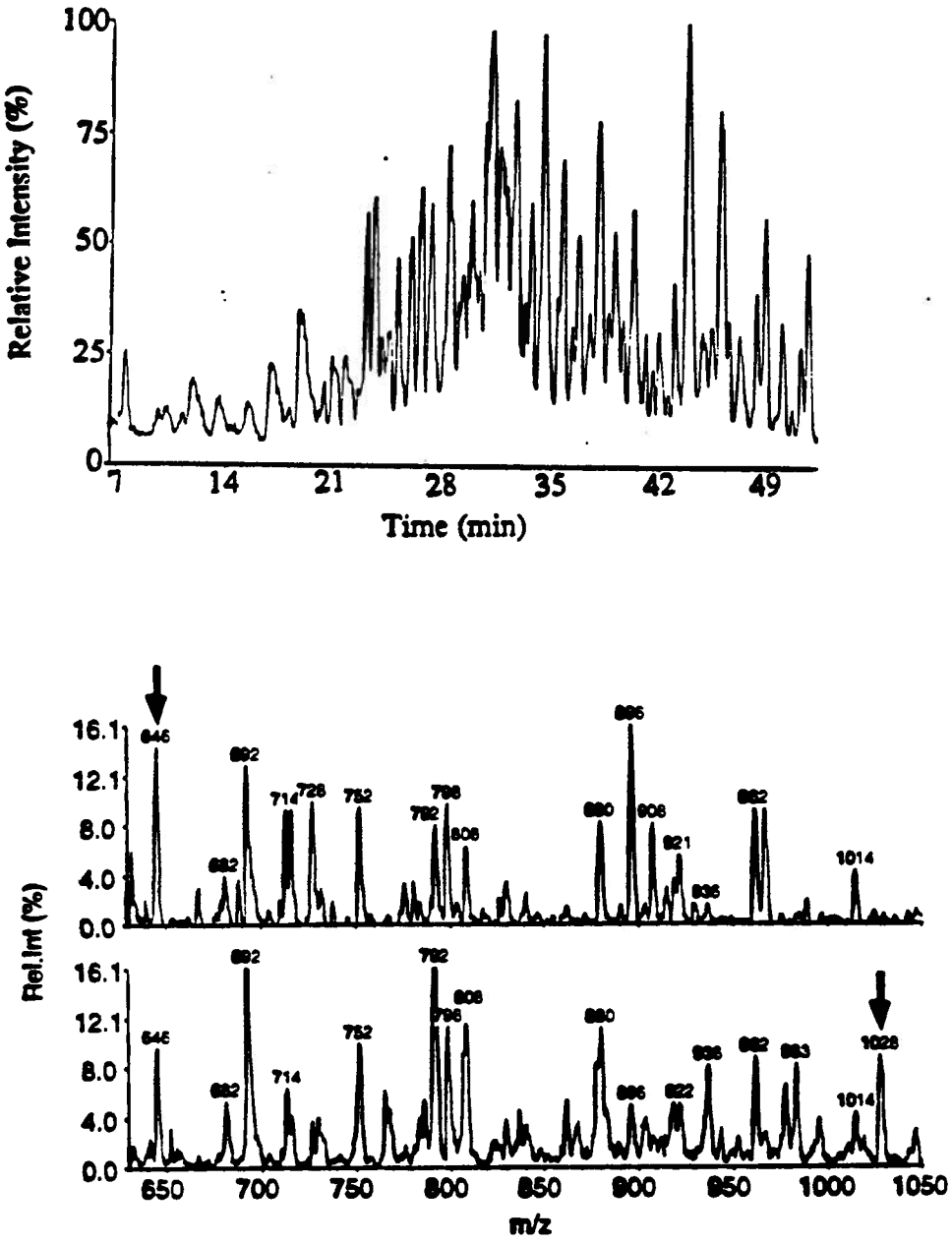


*Figure 4-13* *Electrospray ionisation mass spectrum of a peptic digest of C. fimi exoglycanase inactivated by N-bromoacetyl cellobiosylamine, TIC in the normal MS mode (upper). Comparative ESI-MS of a section (retention time = 24 - 25 min) of the TIC of the unlabeled (middle) and labeled (lower) C. fimi exoglycanase peptic digest.*

In a first sequencing experiment, the amino acid derivatives in each step were detected by ESI-MS, scanned over a range of 300 - 850 Da. The peptide sequence was identified as Asp-Val-Val-Asn-X-Ala. The residue X observed in cycle 5 denotes an ion of $m/z$ = 822 Da (Figure 4-14) which does not correspond to the modified 311 PTH derivative of a known amino acid. However, this mass corresponded exactly with the expected mass for the 311 PTH of the N-acetyl cellobiosylamine ester of a glutamic acid residue shown in Figure 4-15. The other signals in the chromatogram represented background levels of contaminating amino acid derivatives or other impurities which coeluted with the $m/z$ = 822 Da species. To further characterise the derivative released in cycle 5, another aliquot of the isolated, labeled peptide was sequenced and the released residue with mass 822 Da was subjected to collision-induced fragmentation in the mass spectrometer. Figure 4-15 shows the generated daughter ions and an interpretation of the mass spectrum. Since some of the daughter ions are known to be derived from the sequencing reagent and the structure of the inactivator was known, it was relatively simple to interpret the tandem mass spectrum.

Sequence alignment of the identified peptide with the known amino acid sequence of the exoglycanase indicates that the modified residue corresponds to Glu 127. This residue has previously been identified as the acid-base catalyst in this exoglycanase through mutation of conserved glutamate and aspartate residues and kinetic analysis of these mutants (MacLeod et al., 1994). These results clearly illustrate the usefulness of N-bromoacetyl glycosylamine affinity labels in identifying important catalytic residues in glycosidases.

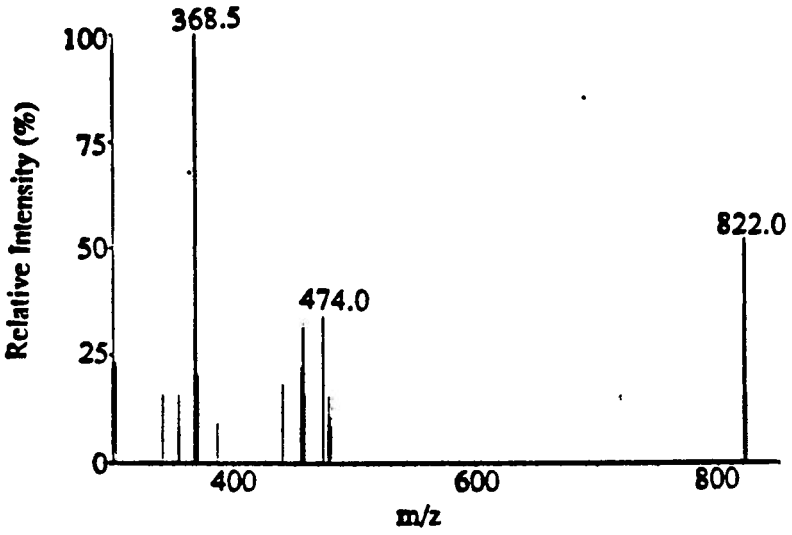


*Figure 4-14* *Electrospray ionisation mass spectrum of the 311 PTH derivative released in cycle 5 during sequencing of the labeled peptide.*

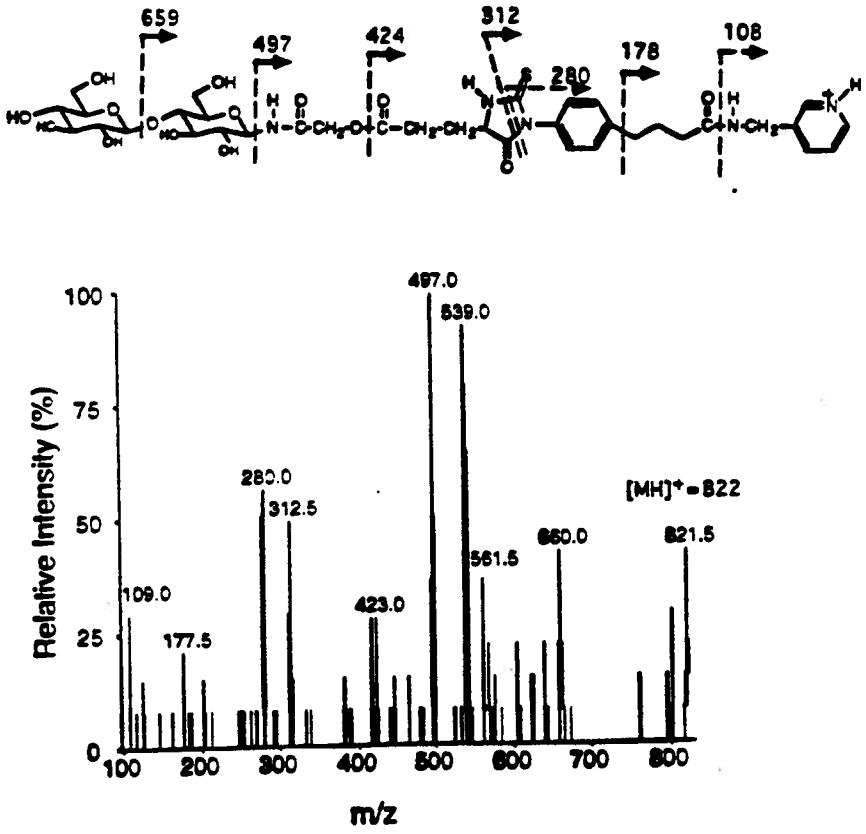


*Figure 4-15* *Tandem electrospray ionisation mass spectrum of the 311 PTH derivative released in cycle 5 during sequencing of the labeled peptide.*

### 4-3-4 Comparison of the radiolabeled and the mass spectrometric approaches used to identify labeled residues in glycosidases

Traditionally, identification of the labeled residues in enzymes using irreversible active site-directed inactivators involves synthesis of a radiolabeled analogue of the inactivator which is then used to covalently derivatise the target enzyme. The radiolabeled, inactivated enzyme is then proteolysed, generating a mixture of peptides. The radiolabeled peptide is isolated by HPLC and the purified peptide sequenced by the Edman degradation, thus revealing the identity of the modified peptide. Although this method has been used successfully, its application is limited by the complex syntheses frequently required for the introduction of a radioisotope into the inactivator. In addition this method is time consuming, technically demanding and requires micromole amounts of the labeled enzyme.

The mass spectrometric approach presented and discussed in the previous sections circumvents the limitations and difficulties associated with this standard radioactive approach. This new approach involves modification of the enzyme with a non-radioactive active site-directed inactivator, proteolytic digestion of the labeled enzyme, identification and isolation of the purified labeled peptide by RP-HPLC electrospray ionisation mass spectrometry and sequencing the purified peptide either by the standard Edman degradation, by tandem mass spectrometry or by a novel sequencing approach which couples peptide sequencing chemistry to electrospray ionisation mass spectrometry. The labeled peptide in the mixture is identified based on any one or a combination of the following criteria. First, the presence of the label on the peptide can result in the peptide having a different retention time on the RP-HPLC column compared to the corresponding unlabeled peptide. The labeled peptide can then be identified by screening the HPLC-MS data from the unlabeled and labeled samples looking for the disappearance of a specific peptide ion within a selected time window upon inactivation of the enzyme (Withers & Aebersold, 1995). Second, labeling results in a mass increase of the peptide compared to

the unlabeled counterpart. This mass shift is then used, as in the case of N-bromoacetyl cellobiosylamine-inactivated *C. fimi* exoglycanase, to identify the labeled peptide by searching the HPLC-MS datasets looking for a new peptide ion in the labeled sample but absent in the unlabeled sample that differs from a specific peptide ion in the unlabeled sample by the mass of the label. Finally, if a linkage within the labeled peptide, other than the amide bonds, is susceptible to collision-induced fragmentation (e.g. ester bond) and results in the elimination of a neutral species of reproducible and predictable mass upon limited fragmentation as was observed with the 2FCb- and 2dCb-*C. fimi* exoglycanase samples, then the labeled peptide can be identified using the tandem mass spectrometer with the second quadrupole offset from the first by the mass of the neutral species.

A potential problem associated with the neutral loss tandem mass spectrometric approach is cleavage of the amide bonds, releasing amino acids of the same *m/z* value as that of the label which results in significant background signal. However, this problem may be circumvented by performing a similar mass spectrometric analysis on a control sample of unlabeled enzyme. For example, neutral loss tandem mass spectrometric analysis of a 2-deoxy-2-fluoroglucosyl *Agrobacterium* β-glucosidase digest, searching for a mass loss of *m/z* = 165 Da, revealed several peaks in the chromatogram (Tull et al., 1995). Similar analysis of an unlabeled enzyme sample yielded an identical chromatogram with the exception of the absence of two strong signals. These two signals correspond to two 2-deoxy-2-fluoro-glucosyl-peptides that have lost the label while the other signals correspond to unlabeled peptides that underwent fragmentations resulting in loss of a neutral species of *m/z* = 165 Da. In this case the most likely candidate for the neutral species lost in the control was a phenylalanyl residue which has this identical *m/z* value.

In contrast to the standard, radioactive approach, the mass spectrometric approach is rapid, non-radioisotopic, sensitive and only requires picomole amounts of labeled enzyme. The generality of the neutral loss approach has been demonstrated with different types of glycosidase using mechanism-based inactivators (Tull et al., 1995; Miao et al.,

1994a; Miao et al., 1994b). These mass spectrometric approaches offer an alternative to the standard radioactive method.

## 4-4 Summary

The mechanism-based inactivators, 2F-DNPC and cellobial were used to identify the catalytic nucleophile involved in *C. fimi* exoglycanase-catalysed hydrolysis of cellobiosides as Glu 233. This residue has been identified previously as the catalytic nucleophile involved in glucoside hydrolysis. Identification of the labeled residue involved inactivation of the enzyme with non-radioactive inactivator and proteolytic digestion of the labeled enzyme. The 2FCb- and 2dCb-peptide were selectively identified by collision-induced loss of a neutral fragment of known mass (2FCb or 2dCb) from the labeled peptide.The modified residue was identified by sequencing the isolated 2FCb-peptide by standard Edman degradation.

The N-acetyl cellobiosylamine-labeled residue was identified as Glu 127, the acid-base catalyst. This involved labeling the enzyme with the non-radioactive inactivator, peptic digestion of the labeled and unlabeled enzyme and ESI-MS analysis of the digests. The N-acetyl cellobiosylamine peptide was identified by comparative peptide mapping of the digests. The labeled residue was identified using a new protein sequencing chemistry coupled to ESI-MS and structurally characterised by tandem mass spectrometry.

These results illustrate the usefulness of active site directed irreversible inactivators in identifying important catalytic residues in glycosidases. Further, these results show that these new mass spectrometric approaches present an alternative to the standard radioactive approach used to identify labeled residues within enzymes.

# CHAPTER V

# MATERIALS AND METHODS

## 5-1 Synthesis

### 5-1-1 General procedures and materials

Melting points (m.p.) were determined using a Laboratory Devices Mel-Temp II melting point apparatus and are uncorrected.

$^1H$ Nuclear magnetic resonance (NMR) spectroscopy was performed on either a Varian XL-300 spectrometer at 300 MHz or a Bruker WH-400 operating at 400 MHz. Chemical shifts given are on the $\delta$ scale, using tetramethylsilane (TMS) as external reference ($\delta = 0.00$ ppm) for samples in $CDCl_3$ or 2,2-dimethyl-2-silapentane-5-sulphonate ($\delta = 0.00$ ppm) as an external reference for samples in $D_2O$.

$^{19}F$ NMR spectra were recorded on a Bruker AC-200 spectrometer at a field strength of 188 MHz. Chemical shifts are reported relative to $CFCl_3$ ($\delta = 0.00$ ppm) and were referenced against external trifluoroacetic acid ($\delta = -76.53$ ppm). Signals upfield of $CFCl_3$ are assigned negative values.

Micro-analyses were performed by Mr. Peter Borda in the Micro-analytical Laboratory, Department of Chemistry, University of British Columbia, Vancouver.

Solvents and reagents used were either reagent, certified or spectral grade. Dry solvents were prepared as follows. Methanol was distilled from magnesium turnings in the presence of iodine, acetyl chloride was refluxed over phosphorus pentachloride and then distilled.

Thin layer chromatography (TLC) was performed using aluminium-backed Merck Kieselgel 60F-254 analytical plates. Generally, acetylated compounds were run in ethyl acetate-hexanes mixtures (1:1) while deacetylated compounds were run in ethyl acetate-methanol-water (7:2:1). Compounds were visualized by employing UV light and/or charring with 10% sulphuric acid in methanol. Preparative TLC was performed on a Model 7924T chromatotron using 1 mm and 4 mm silica gel plates prepared from either silica Type H (10-40 microns) and calcium sulphate (1/2-hydrate) or silica gel 60 $PF_{254}$

containing gypsun. Flash column chromatography was performed according to Clark-Still and coworkers (1977) using Kieselgel 60 (230-400 mesh) silica gel.

The following compounds were prepared and generously provided by co-workers in this laboratory. 2,4-Dinitrophenyl β-D-glucopyranoside was prepared by Dr. Mark Namchuk while 2,4-dinitrophenyl-{1-$^2$H}-β-D- and 4-nitrophenyl-{1-$^2$H}-β-D-glucopyranosides were synthesized by Ms. Julie Kempton. 3,4-Dinitrophenyl-, 2,5-dinitrophenyl-, 2-nitrophenyl- and 4-nitrophenyl-β-xylobiosides as well as 2,4-dinitrophenyl-2-deoxy-2-fluoro-β-xylobioside were synthesized by Dr. Lothar Ziser. Similarly, 3,4-dinitrophenyl-, 2,5-dinitrophenyl-, 2-nitrophenyl- and 4-nitrophenyl- β-D-xylopyranosides were synthesized by Dr. Lothar Ziser. 4-Cyanophenyl β-D-xylopyranoside was prepared in collaboration with Ms. Ika Setyawati. Benzyl 4-O-(β-D-glucopyranosyl)-1-thio-β-D-xylopyranoside was prepared by Mr. Rajpal Chandi. 2,4-Dinitrophenyl-, 3,4-dinitrophenyl-, 3,5-dichlorophenyl-, 3-nitrophenyl-, and 4-cyanophenyl-β-cellobioside as well as 2,4-dinitrophenyl-2-deoxy-2-fluoro β-cellobioside were prepared for my M. Sc. thesis and their syntheses have been described (Tull & Withers, 1994).

### 5-1-2 General compounds

*2, 3, 6, 2', 3', 4', 6'-Hepta-O-acetyl-α-cellobiosyl bromide (1)*

Compound **1** was synthesized by the method of (Fischer & Zemplen, 1910). Cellobiose octa-O-acetate (10 g, 14.75 mmol) was dissolved in $CHCl_3$ (50 mL), glacial acetic acid (350 mL) and 45% HBr-glacial acetic acid (15 mL) were added and the mixture stirred at 15 °C overnight. The reaction mixture was poured over ice-water and the product extracted with $CHCl_3$. The $CHCl_3$ layer was washed (3 times) with water, washed (2 times) with saturated aqueous sodium bicarbonate, dried over $MgSO_4$ and evapourated *in vacuo* to leave an orange oil. The product (**1**) was crystallised from $CHCl_3$-diethyl ether

yielding white needle-like crystals (8.10 g, 11.59 mmol, 79%). M. p. 169-170 °C (lit. m. p. 180 °C) (Fischer & Zemplen, 1910).

*2, 3, 6, 2', 3', 4', 6'-Hepta-O-acetyl-α-{1-$^2$H}-cellobiosyl bromide (2)*

2, 3, 6, 2', 3', 4', 6'-Hepta-O-acetyl-D-cellobiose (4.8 g, 7.55 mmol) dissolved in DMSO (16 mL) and acetic anhydride (10 mL) was stirred at room temperature overnight. The mixture was poured over water, centrifuged and the solvent decanted leaving a colourless syrup. The syrup was washed in this way 10 times and then dried overnight. The syrup was dissolved in THF (10 mL), sodium borodeuteride (190 mg) in $D_2O$ (1 mL) was added and the reaction allowed to proceed at room temperature for 2 hours. The solvent was evapourated *in vacuo* leaving a colourless syrup. 2, 3, 6, 2', 3', 4', 6'-Hepta-O-acetyl-[1-$^2$H]-cellobiose was purified from the contaminating protio-cellobiose octaacetate which arose from incomplete oxidation, by flash column chromatography using ethyl acetate-hexanes (2:1). The purified deuterio-hemiacetal was dissolved in THF (5 mL), sodium borodeuteride (30 mg) in $D_2O$ (0.2 mL) and acetic anhydride added and the reaction mixture stirred at room temperature overnight. After concentration, the remaining syrup was dissolved in $CHCl_3$, washed with water (2 x 50 mL), dried over $MgSO_4$ and the solvent evapourated *in vacuo*. 1, 2, 3, 6, 2', 3', 4', 6'-Octa-O-acetyl β-[1-$^2$H]-cellobiose was crystallised from ethanol to yield a white solid (900 mg, 1.33 mmol, 18 %). M. p. 197-199 °C. $^1$H NMR ($CDCl_3$): δ 5.45 (dd, 1 H, $J_{2,3}$ 10 Hz, $J_{3,4}$ 9 Hz, H-3), 5.15 (t, 1 H, $J_{2',3'}$ 9 Hz, $J_{3',4'}$ 9 Hz, H-3'), 5.10 (t, 1 H, $J_{3',4'}$ 9 Hz, $J_{4',5'}$ 9 Hz, H-4'), 5.00 (d, 1 H, $J_{2,3}$ 10 Hz, H-2), 4.95 (dd, 1 H, $J_{1',2'}$ 8 Hz, $J_{2',3'}$ 9 Hz, H-2'), 4.55 (d, 1 H, $J_{1',2'}$ 8 Hz H-1'), 4.50 (dd, 1 H, $J_{5,6b}$ 2 Hz, $J_{6a,6b}$ 12 Hz, H-6b), 4.40 (dd, 1 H, $J_{5',6b'}$ 4 Hz, $J_{6a',6b'}$ 12 Hz, H-6b'), 4.15 (dd, 1 H, $J_{5,6a}$ 4 Hz, $J_{6a,6b}$ 12 Hz, H-6a), 4.05 (dd, 1 H, $J_{5',6a'}$ 2 Hz, $J_{6a',6b'}$ 12 Hz, H-6a'), 4.00 (ddd, 1 H, $J_{4,5}$ 9 Hz, $J_{5,6a}$ 4 Hz, $J_{5,6b}$ 2 Hz, H-5), 3.80 (t, 1 H, $J_{3,4}$ 9 Hz, $J_{4,5}$ 9 Hz, H-4), 3.65 (ddd, 1 H, $J_{4',5'}$ 9 Hz, $J_{5',6a'}$ 2 Hz, $J_{5',6b'}$ 4 Hz, H-5'), 1.95-2.15 (8 s, 24 H, 8 (OAc)).

Deuterio-acetobromocellobiose (**2**) was then synthesised from deuterio-cellobiose octaacetate by exactly the same method as the protio-compound (660 mg, 0.95 mmol, 71%). M. p. 169-171 °C.

### 5-1-3 {$^1$H}-aryl β-cellobiosides

*4"-Bromophenyl β-cellobioside (4-BrPC)(3)*

Hepta-O-acetyl-α-cellobiosyl bromide (**1**) (1.5 g, 2.21 mmol) dissolved in acetone (20 mL) was added to the 4-bromophenol dissolved in 1M NaOH (5 mL ) and stirred at room temperature for 48 hours. The solvent was then evapourated *in vacuo* and the remaining syrup diluted with water and extracted with $CHCl_3$. The organic phase was washed (3 x 50 mL) with saturated sodium bicarbonate, dried over $MgSO_4$, gravity filtered and evapourated *in vacuo*. The acetylated product was crystallised from ethyl acetate-ethanol as a white crystal (535 mg, 0.68 mmol, 31%). M. p. 231-233 °C $^1$H NMR ($CDCl_3$): δ 7.40 (d, 2 H, J 9 Hz, H-3", H-5"), 6.85 (d, 2 H, J 9 Hz, H-2", H-6"), 5.25 (t, 1 H, $J_{2,3}$ 9 Hz, $J_{3,4}$ 9 Hz, H-3), 5.15-5.20 (m, 2 H, H-2 & H-3'), 5.05 (t, 1 H, $J_{3',4'}$ 9 Hz, $J_{4'5'}$ 9 Hz, H-4'), 5.00 (d, 1 H, $J_{1,2}$ 8 Hz, H-1), 4.95 (dd, 1 H, $J_{1',2'}$ 8 Hz, $J_{2',3'}$ 9 Hz, H-2'), 4.50-4.55 (m, 2 H, H-1' & H-6b), 4.35 (dd, 1 H, $J_{5',6b'}$ 4 Hz, $J_{6a',6b'}$ 12 Hz, H-6b'), 4.15 (dd, 1 H, $J_{5,6a}$ 5 Hz, $J_{6a,6b}$ 12 Hz, H-6a), 4.05 (dd, 1 H, $J_{5',6a'}$ 2 Hz, $J_{6a',6b'}$ 12 Hz, H-6a'), 3.85 (t, 1 H, $J_{3,4}$ 9 Hz, $J_{4,5}$ 10 Hz, H-4), 3.75 (ddd, 1 H, $J_{4,5}$ 10 Hz, $J_{5,6a}$ 5 Hz, $J_{5,6b}$ 2 Hz, H-5), 3.65 (ddd, 1 H, $J_{4',5'}$ 9 Hz, $J_{5',6a'}$ 2 Hz, $J_{5',6b'}$ 4 Hz, H-5'), 1.95-2.15 (7 s, 21 H, 7(OAc)).

Compound **3** was prepared from the acetylated compound (170 mg, 0.32 mmol) using the method of Sinnott & Souchard. The protected compound was dissolved in methanol (15 ml), 1 M sodium methoxide (0.15 ml) was added and the reaction stirred at room temperature for 2 hours. The excess base was neutralised with Amberlite IR-120 (H+) cation exchange resin. The resin was removed by gravity filtration and washed several times with methanol, and the solvent evapourated *in vacuo*. Compound **3** was

recrystallised from methanol-diethyl ether as a white powder (13 mg, 0.026 mmol, 12%). M. p. 223-224 °C. $^1$H NMR ($CD_3OD$): δ 7.40 (d, J 8 Hz, H-3", H-5"), 7.00 (d, J 8 Hz, H-2", H-6"), 4.95 (d, $J_{1,2}$ 8 Hz, H-1), 3.20-4.90 (m, H(2-6)and H(1'-6')). Anal. Calcd. for $C_{18}H_{25}O_{11}Br$: C, 43.46; H, 5.23. Found: C,43.06; H, 5.09.

*2",5"-Dinitrophenyl β-cellobioside (2,5-DNPC) (4)*

2,5-Dinitrophenyl 2, 3, 6, 2', 3', 4', 6'-hepta-O-acetyl-β-cellobioside was prepared from hepta-O-acetyl-α-cellobiosyl bromide (760 mg, 0.95 mmol), silver oxide (760 mg) and 2,5-dinitrophenol (769 mg, 4.13 mmol) in $CH_3CN$ (10 mL) stirred over Drierite at room temperature for 24 hours. The Drierite was removed by gravity filtration, wash several times with $CHCl_3$ and the solvent evapourated *in vacuo* .The remaining yellow syrup was dissolved in $CHCl_3$, washed with saturated sodium bicarbonate, dried over $MgSO_4$ and evapourated *in vacuo*, resulting in an pale yellow syrup. The acetylated product was purified by flash column chromagraphy using ethyl acetate-hexanes (3 : 2) and was crystallised from ethyl acetate-ethanol as a white solid (490 mg, 0.61 mmol, 64%). M. p. 208 - 209 °C. $^1$H NMR ($CDCl_3$): δ 8.23 (d, 1 H, $J_{4",6"}$ 2 Hz, H-6"), 8.05 (dd, 1 H, $J_{3",4"}$ 9 Hz, $J_{4",6"}$ 2 Hz, H-4"), 7.90 (d, 1 H, $J_{3",4"}$ 9 Hz, H-3"), 5.23-5.33 (m, 3 H, H-1, H-2 & H-3), 5.18 (t, 1 H, $J_{2',3'}$ 9 Hz, $J_{3',4'}$ 9 Hz, H-3'), 5.08 (t, 1 H, $J_{3',4'}$ 9 Hz, $J_{4',5'}$ 9 Hz, H-4'), 4.95 (dd, 1 H, $J_{1',2'}$ 8 Hz, $J_{2',3'}$ 9 Hz, H-2'), 4.62 (dd, 1 H, $J_{5,6b}$ 2 Hz, $J_{6a,6b}$ 12 Hz, H-6b), 4.55 (d, 1 H, $J_{1',2'}$ 8 Hz, H-1'), 4.38 (dd, 1 H, $J_{5',6b'}$ 4 Hz, $J_{6a',6b'}$ 12 Hz, H-6b'), 4.05-4.15 (m, 2 H, H-6a & H-6a'), 3.85-3.95 (m, 2 H, H-4 & H-5), 3.70 (ddd, 1 H, $J_{4',5'}$ 9 Hz, $J_{5',6a'}$ 2 Hz, $J_{5',6b'}$ 4, H-5'), 2.00-2.20 (7 s, 21 H, 7(OAc)).

Compound **4** was prepared from this acetylated cellobioside using the method of Ballardie and coworkers. The protected compound (480 mg, 0.60 mmol) was suspended in methanol (50 ml), cooled to 0 °C, acetyl chloride (0.5 ml) was added and the reaction stirred at 4 °C overnight. The solvent was evapourated *in vacuo* and the resulting white sold washed with anhydrous diethyl ether (10 x 5 ml). Compund 4 was crystallised from

ethanol as a white solid (77 mg, 0.15 mmol, 25%). M. p. 169-171 °C. $^1$H NMR ($CD_3OD$): δ 8.25 (d, J 2 Hz, H-6"), 8.10 (m, H-3" & H-4"), 5.40 (d, $J_{1,2}$ 8 Hz, H-1), 3.25-3.95 (m, H(2-6) and H(1'-6')). Anal. Calcd for $C_{18}H_{24}O_{15}N_2.0.5H_2O$: C, 41.78; H, 4.84; N, 5.42. Found: C, 41.94; H, 5.14; N, 5.17.

### 5-1-4 {$^2$H}-aryl β-cellobiosides

*2, 4-Dinitrophenyl β-{1-$^2$H}-cellobioside (D-2,4-DNPC) (5)*

2, 3, 6, 2', 3', 4', 6'-Hepta-O-acetyl-D-{1-$^2$H}-cellobiose (300 mg, 0.51 mmol) and 1,4-diazabicyclo(2.2.2)octane (190 mg, 1.70 mmol) were stirred over molecular sieves (4 Å) in DMF (20 mL) for three hours. Fluorodinitrobenzene (120 mg, 0.64 mmol) was added and the reaction was allowed to proceed at room temperature for 24 hours. The sieves were removed by gravity filtration, washed with $CHCl_3$ and the combined extracts evapourated *in vacuo*. The remaining yellow solid was dissolved in $CHCl_3$ (20 mL), washed (3 x 20 mL) with saturated sodium bicarbonate and dried over anhydrous $MgSO_4$. The solvent was evapourated *in vacuo* yielding 2",4"-dinitrophenyl 2, 3, 6, 2', 3', 4', 6' hepta-O-acetyl β-{1-$^2$H}-cellobioside which was crystallised from ethyl acetate-hexanes as a white solid (140 mg, 0.17 mmol, 33%). M. p. 214-215 °C. $^1$H NMR ($CDCl_3$) δ: 8.70 (d, 1 H, $J_{3",5"}$ 3 Hz, H-3"), 8.43 (dd, 1 H, $J_{3",5"}$ 3 Hz, $J_{5",6"}$ 9 Hz, H-5"), 7.43 (d, 1 H, $J_{5",6"}$ 9 Hz, H-6"), 5.28 (t, 1 H, $J_{2,3}$ 8 Hz, $J_{3,4}$ 8 Hz, H-3), 5.15-5.23 (m, 2 H, H-2 & H-3'), 5.08 (t, 1 H, $J_{3',4'}$ 9 Hz, $J_{4',5'}$ 9 Hz, H-4'), 4.95 (dd, 1 H, $J_{1',2'}$ 8 Hz, $J_{2',3'}$ 9 Hz, H-2'), 4.55-4.65 (m, 2 H, H-1' & H-6b), 4.38 (dd, 1 H, $J_{5',6b'}$ 4 Hz, $J_{6a',6b'}$ 12 Hz, H-6b'), 4.05-4.13 (m, 2 H, H-6a & H-6a'), 4.00 (dd, 1 H, $J_{3,4}$ 8 Hz, $J_{4,5}$ 10 Hz, H-4), 3.90 (ddd, 1 H, $J_{4,5}$ 10 Hz, $J_{5,6a}$ 5 Hz, $J_{5,6b}$ 2 Hz, H-5), 3.70 (ddd, 1 H, $J_{4',5'}$ 9 Hz, $J_{5',6a'}$ 2 Hz, $J_{5',6b'}$ 4 Hz, H-5'), 2.00-2.15 (7 s, 21 H, 7(OAc)).

Compound **5** was prepared from the acetylated cellobioside using the method of Ballardie and coworkers. The protected compound (130 mg, 0.16 mmol) was suspended in methanol (15 ml), cooled to 0 °C, acetyl chloride (0.15 ml) was added and the reaction

stirred at 4 °C overnight. The solvent was evapourated *in vacuo* and the resulting white sold washed with anhydrous diethyl ether (10 x 5 ml). Compound **5** was crystallised from methanol-diethyl ether as a white solid (22 mg, 0.027 mmol, 17%). M. p. 180 °C dec. $^1$H NMR (CD3OD) δ: 8.73 (d, 1 H, J3",5" 3 Hz, H-3"), 8.45 (dd, 1 H, J3",5" 3 Hz, J5",6" 9 Hz, H-5"), 7.63 (d, 1 H, J5",6" 9 Hz, H-6"), 4.45 (d, 1 H, J1',2' 8 Hz, H-1'), 3.20-3.95 (m, H(2-6) & H(2'-6'). Anal. Calcd for $C_{18}H_{23}DO_{15}N_2$.: C, 42.44; H, 4.72; N, 5.50. Found: C, 42.03; H, 4.82; N, 5.44.

*4-Nitrophenyl β-{1-$^2$H}-cellobioside (D-PNPC) (6)*

The acetylated compound, 4-nitrophenyl 2, 3, 6, 2', 3', 4', 6'-hepta-O-acetyl-β-{1-$^2$H}-cellobioside was prepared from hepta-O-acetyl-α-{1-$^2$H}-cellobiosyl bromide (290 mg, 0.42 mmol), silver oxide (290 mg) and 4-nitrophenol (290 mg, 2.09 mmol) in $CH_3CN$ (5 mL) stirred over drierite at room temperature for 24 hours. The Drierite was removed by gravity filtration, wash several times with $CHCl_3$ and the solvent evapourated *in vacuo* .The remaining yellow syrup was dissolved in $CHCl_3$, washed with saturated sodium bicarbonate, dried over $MgSO_4$ and evapourated *in vacuo*, resulting in an pale yellow syrup. This acetylated product was crystallised from ethyl acetate-ethanol as a white solid (150 mg, 0.20 mmol, 48%). M. p. 237-239 °C.$^1$H NMR ($CDCl_3$) δ: 8.18 (d, 2 H, J 9 Hz, H-3" & 5"), 7.05 (d, 2 H, J 9 Hz, H-2" & 6"), 5.28 (t, 1 H, $J_{2,3}$ 9 Hz, $J_{3,4}$ 9 Hz, H-3), 5.12-5.20 (m, 2 H, H-2 & H-3'), 5.05 (t, 1 H, $J_{3',4'}$ 9 Hz, $J_{4',5'}$ 9 Hz, H-4"), 4.93 (dd, 1 H, $J_{1',2'}$ 8 Hz, $J_{2',3'}$ 9 Hz, H-2'), 4.50-4.55 (m, 2 H, H-1' & H-6b), 4.35 (dd, 1 H, $J_{5',6b'}$ 4 Hz, $J_{6a',6b'}$ 12 Hz, H-6b'), 4.13 (dd, 1 H, $J_{5,6a}$ 5 Hz, $J_{6a,6b}$ 12 Hz, H-6a), 4.05 (dd, 1 H, $J_{5',6a'}$ 2 Hz, $J_{6a',6b'}$ 12 Hz, H-6a'), 3.78-3.90 (m, 2 H, H-4 & H-5), 3.68 (ddd, 1 H, $J_{4',5'}$ 9 Hz, $J_{5',6a'}$ 2 Hz, $J_{5',6b'}$ 4 Hz, H-5'), 2.00-2.10 (7 s, 21 H, 7(OAc)).

Compound **6** was prepared from the acetylated cellobioside using method of Ballardie and coworkers. The protected compound (143 mg, 0.19 mmol) ) was suspended in methanol (15 ml), cooled to 0 °C, acetyl chloride (0.15 ml) was added and the reaction

stirred at 4 °C overnight. The solvent was evapourated *in vacuo* and the resulting white sold washed with anhydrous diethyl ether (10 x 5 ml). Compound **6** was purified by flash column chromatography (12 : 2 : 1 ethyl acetate-MeOH-$H_2O$) and crystallised from water-diethyl ether as a white solid (15 mg, 0.032 mmol, 17%). M.p. 254-255 °C. $^1H$ NMR ($CD_3OD$) δ: 8.23 (d, J 9 Hz, H-3" & H-5"), 7.23 (d, J 9 Hz, H-2" & H-6"), 4.45 (d, $J_{1',2'}$ 8 Hz, H-1'), 3.20-3.95 (m, H(2-6) & H(2'-6')). Anal. Calcd for $C_{18}H_{24}DO_{13}N_2$ $1.5H_2O$.: C, 43.99; H, 5.70; N, 2.85. Found: C, 44.24; H, 5.65; N, 2.75.

*4-Bromophenyl β-{1-$^2H$}-cellobioside (D-4-BrPC) (7)*

4-Bromophenyl 2, 3, 6, 2', 3', 4', 6'-hepta-O-acetyl-β-{1-$^2H$}-cellobioside was prepared from hepta-O-acetyl-α-cellobiosyl bromide (400 mg, 0.63 mmol), silver oxide (400 mg) and 4-bromophenol (400 mg, 2.32 mmol) in $CH_3CN$ (10 mL) stirred over Drierite at room temperature for 24 hours. The Drierite was removed by gravity filtration, wash several times with $CHCl_3$ and the solvent evapourated *in vacuo* .The remaining syrup was dissolved in $CHCl_3$, washed with saturated sodium bicarbonate, dried over $MgSO_4$ and evapourated *in vacuo*. The acetylated product was crystallised from ethyl acetate-ethanol as a white solid (260 mg, 0.33 mmol, 52%). M. p. 231-232 °C. $^1H$ NMR ($CDCl_3$): δ 7.40 (d, 2 H, J 9 Hz, H-3", H-5"), 6.85 (d, 2 H, J 9 Hz, H-2", H-6"), 5.25 (t, 1 H, $J_{2,3}$ 9 Hz, $J_{3,4}$ 9 Hz, H-3), 5.15-5.20 (m, 2 H, H-2 & H-3'), 5.05 (t, 1 H, $J_{3',4'}$ 9 Hz, $J_{4'5'}$ 10 Hz, H-4'), 4.95 (dd, 1 H, $J_{1',2'}$ 8 Hz, $J_{2',3'}$ 9 Hz, H-2'), 4.50-4.55 (m, 2 H, H-1' & H-6b), 4.35 (dd, 1 H, $J_{5',6b'}$ 4 Hz, $J_{6a',6b'}$ 12 Hz, H-6b'), 4.15 (dd, 1 H, $J_{5,6a}$ 5 Hz, $J_{6a,6b}$ 12 Hz, H-6a), 4.05 (dd, 1 H, $J_{5',6a'}$ 2 Hz, $J_{6a',6b'}$ 12 Hz, H-6a'), 3.85 (t, 1 H, $J_{3,4}$ 9 Hz, $J_{4,5}$ 10 Hz, H-4), 3.75 (ddd, 1 H, $J_{4,5}$ 10 Hz, $J_{5,6a}$ 5 Hz, $J_{5,6b}$ 2 Hz, H-5), 3.65 (ddd, 1 H, $J_{4',5'}$ 10 Hz, $J_{5',6a'}$ 2 Hz, $J_{5',6b'}$ 4 Hz, H-5'), 1.95-2.15 (7 s, 21 H, 7(OAc)).

Compound **7** was prepared from the acetylated compound (200 mg, 0.25 mmol) using the method of Sinnott & Souchard. The protected compound was dissolved in

methanol (20 ml), 1 M sodium methoxide (0.20 ml) was added and the reaction stirred at room temperature for 2 hours. The excess base was neutralised with Amberlite IR-120 (H+) cation exchange resin. The resin was removed by gravity filtration and washed several times with methanol, and the solvent evapourated *in vacuo*. Compound (**7**) was purified by flash column chromatography (11 : 2 : 1 ethyl acetate-MeOH-$H_2O$) and crystallised from water-diethyl ether as a white solid (22 mg, 0.055 mmol, 18%) M.p. 222-223 °C. $^1$H NMR ($CD_3OD$) δ: 7.40 (d, J 9 Hz, H-3" & H-5"), 7.02 (d, J 9 Hz, H-2" & H-6"), 4.43 (d, $J_{1',2'}$ 8 Hz, H-1'), 3.20-3.95 (m, H(2-6) & H(2'-6')). Anal. Calcd for $C_{18}H_{24}DO_{18}Br$: C, 43.37; H, 5.22. Found: C, 42.96; H, 5.28.

### 5-1-5 Inactivators

*Cellobial* (**8**)

3, 6, 2', 3', 4', 6'-Hexa-O-acetyl cellobial was synthesised from acetobromocellobiose (4 g, 5.73 mmol) dissolved in 90% glacial acetic acid (50 mL) was cooled to 12-15 °C. Chloroplatinic acid (one drop of ~0.5% chloroplatinic acid in 50% acetic acid) and zinc (20 g) was added to the mixture and stirred at 12-15 °C for 2 hours. The reaction mixture was diluted with water (125 mL), the zinc filtered and washed and the product extracted with $CHCl_3$ (2 x 50 mL). The organic layer was washed with saturated sodium bicarbonate, dried over $MgSO_4$ and evapourated *in vacuo* resulting in an orange syrup. The product crystallised from $CHCl_3$-hexanes (1:4) as clear crystals (1.8 g, 3.21 mmol, 56%). M. p. 134-135 °C (Lit. m. p. 134-135°C, (Kanda et al., 1986))

Compound **8** was prepared from the acetylated compound (350 mg, 0.62 mmol) using the method of Sinnott & Souchard. The protected compound was dissolved in methanol (30 ml), 1 M sodium methoxide (0.30 ml) was added and the reaction stirred at room temperature for 1 hours. The excess base was neutralised with Amberlite IR-120 (H+) cation exchange resin. The resin was removed by gravity filtration and washed several times with methanol, and the solvent evapourated *in vacuo*. Compound **8** was

crystallised from hot ethanol as a white solid (130 mg, 0.42 mmol, 68%): M. p. 174-175 °C. (lit. mp 175 -176 °C (Kanda et al., 1986)) $^1$H NMR.($CD_3OD$) δ: 6.35 (dd, 1 H, $J_{1,3}$ 2 Hz, $J_{1,2}$ 6 Hz, H-1), 4.70 (dd, 1 H, $J_{1,2}$ 6 Hz, $J_{2,3}$ 2 Hz, H-2), 4.48 (d, 1 H, $J_{1',2'}$ 8 Hz, H-1'), 4.30 (dt, 1 H, $J_{4,5}$ 7 Hz, $J_{5,6a}$ 2 Hz, $J_{5,6b}$ 2 Hz, H-5), 3.80-4.00 (m, 4 H, H-3, H-3', H-4', H-5' & H-6b), 3.73 (dd, 1 H, $J_{4,5}$ 7 Hz, $J_{3,4}$ 10 Hz, H-4), 3.20-3.63 (m, 4 H, H-2', H-6a' & H-6b'). Anal. Calcd for $C_{12}H_{20}O_9$: C, 46.75; H, 6.49. Found: C, 46.64; H, 6.38.

*2-Deoxy-2-fluoro-4-O-{β-D-glucopyranosyl}-β-D-mannosyl fluoride (2F-GMF) (9)*

Acetylated cellobial (4 g, 7.14 mmol) was dissolved in acetonitrile (40 mL) and 2% $F_2$ gas in neon bubbled into the reaction mixture for 10 minutes at room temperature. The solvent was evapourated *in vacuo* leaving an orange oil behind. The acetylated compound, 2-deoxy-2-fluoro-3,6-di-O-acetyl-4-O-{2', 3', 4', 6'-tetra-O-acetyl-β–D-glucopyranosyl} β-mannosyl fluoride, was partially purified by flash column chromatography using diethyl ether-$CHCl_3$ (1 : 1) and on the chromatotron using diethyl ether-$CHCl_3$ (3 : 1). The product was further purified from the 2-fluoro-cellobioside analogue on the chromatotron using ethyl acetate-hexanes (45 : 55) and crystallised from hot ethanol as clear crystals (460 mg, 0.78 mmol, 11%). M. p. 147-149 °C. $^1$H NMR ($CDCl_3$) δ: 5.48 (dd, 1 H, $J_{1,F1}$ 51 Hz, $J_{1,F2}$ 11 Hz, H-1), 5.20 (ddd, 1 H, $J_{2,3}$ 3 Hz, $J_{3,4}$ 8 Hz, $J_{3,F2}$ 20 Hz, H-3), 5.15 (t, 1 H, $J_{2',3'}$ 9 Hz, $J_{3',4'}$ 9 Hz, H-3'), 5.03 (t, 1 H, $J_{3',4'}$ 9 Hz, $J_{4',5'}$ 9 Hz, H-4'), 4.90 (dd, 1 H, $J_{1',2'}$ 8 Hz, $J_{2',3'}$ 9 Hz, H-2'), 4.83 (dd, 1 H, $J_{2,F1}$ 12 Hz, $J_{2,F2}$ 48 Hz, H-2), 4.55 (d, 1 H, $J_{1',2'}$ 8 Hz, H-1'), 4.50 (dd, 1 H, $J_{5',6b'}$ 5 Hz, $J_{6a',6b'}$ 12 Hz, H-6b'), 4.30 (dd, 1 H, $J_{5,6b}$ 6 Hz, $J_{6a.6b}$ 12 Hz, H-6b), 4.18 (dd, 1 H, $J_{5,6a}$ 6 Hz, $J_{6a,6b}$ 12 Hz, H-6a), 3.95-4.05 (m, 2 H, H-4 & H-6a'), 3.78 (q, 1 H, $J_{4,5}$ 5 Hz, $J_{5,6a}$ 6 Hz, $J_{5,6b}$ 6 Hz, H-5), 3.68 (ddd, 1 H, $J_{4',5'}$ 9 Hz, $J_{5',6a'}$ 2 Hz, $J_{5',6b'}$ 5 Hz, H-5'). $^{19}$F NMR ($CDCl_3$) δ: -145.5 (dt, $J_{1,F1}$ 51 Hz, $J_{2,F1}$ 12 Hz, $J_{F1,F2}$ 13 Hz, F-1), -218.7 (m, F-2).

Compound **9** was prepared from the acetylated compound (110 mg, 0.18 mmol) using the method of Sinnott & Souchard. The protected compound was dissolved in methanol (15 ml), 1 M sodium methoxide (0.15 ml) was added and the reaction stirred at room temperature for 2 hours. The excess base was neutralised with Amberlite IR-120 (H+) cation exchange resin. The resin was removed by gravity filtration and washed several times with methanol, and the solvent evapourated *in vacuo*.. Compound **9** was purified by high performance liquid chromatography using a Waters 712 WISP HPLC equipped with a Waters 410 differential refractometer. The crude reaction mixture was loaded onto a Dextropak (25 x 10 cm) column, eluted with water at a flow rate of 7 mL/min and the fractions collected manually. Fractions containing pure compound **9** were pooled and lyophilised to yield a white solid (25 mg, 0.072 mmol, 40%): M. p. 170-172 °C. $^{1}$H NMR ($CD_3OD$) δ: 5.58 (dd, 1 H, $J_{1,F1}$ 48 Hz, $J_{1,F2}$ 14 Hz, H-1), 4.98 (d, 1 H, $J_{2,F2}$ 50 Hz, H-2), 4.45 (d, 1 H, $J_{1',2'}$ 7 Hz, H-1'), 3.20-3.40 (m, H(3-6) & H(2'-6')). $^{19}$F NMR ($D_2O$) δ: -148.7 (dd, $J_{1,F1}$ 48 Hz, $J_{1,F2}$ 14 Hz, F-1), -222.8 (m, F-2). Anal. Calcd for $C_{12}H_{20}O_9F_2$: C, 41.62; H, 5.78. Found: C, 41.90; H, 5.86.

*Bromoacetic anhydride* (**10**)

Compound **10** was prepared from dicyclohexylcarbodiimide (1.2 g, 5.8 mmol) in cold $CCl_4$ (6 mL) was added slowly to bromoacetic acid (1 g, 7.2 mmol) dissolved in cold $CCl_4$ (4 mL) and allowed to stir for 5 minutes at 0 °C. The reaction mixture was allowed to warm up to room temperature and the dicyclohexylurea biproduct was filtered leaving product **10** in solution. Bromoacetic anhydride was crystallised from $CCl_4$ at -20 °C as white crystals (955 mg, 3.67 mmol, 63%). M. p. 39 - 41 °C (lit. m. p. 41-42 °C (Thomas, 1977))

*N-Bromoacetyl-β-cellobiosylamine (N-BrAcCb-$NH_2$)(11)*

Cellobiose (1.0 g, 2.79 mmol) was dissolved in water (10 mL), ammonium bicarbonate added until the solution was saturated and stirred for 10 days with occasional ammonium bicarbonate resaturations. Evapouration of the solvent *in vacuo* yielded a white gum. Partial purification by flash chromatography (2:2:1 ethyl acetate-methanol-water) gave a mixture of β-D-cellobiosylamine and cellobiose. Bromoacetic anhydride (900 mg, 3.46 mmol) was then added to a solution of this mixture in DMF (10 mL) and stirred at room temperature for 3 hour. The solution was poured over ice-cold anhydrous ether and stirred for an hour. Purification by flash chromatography (5:2:1 ethyl acetate-methanol-water) and crystallization from methanol-diethyl ether yielded compound **11** as a white solid (582 mg, 45 %). M.p. 143-145 °; $^1$H NMR ($CD_3OD$): δ 4.80 (d, 1 H, $J_{1,2}$ 8 Hz, H-1), 4.41 (d, 1 H, $J_{1',2'}$ 8 Hz, H-1'), 3.87 (s, 2 H, $C\underline{H}_2BrCO$), 3.25-3.90 (m, 11 H, H-2,3,4,5,6a,6b,3',4',5',6a',6b'), 3.22 (t, 1 H, $J_{2',1'}$ 8, $J_{2',3'}$ 8 Hz, H-2'). Anal Calcd. for $C_{14}H_{24}NO_{11}Br$: C, 36.36; H, 5.19; N, 3.03. Found: C, 36.35; H, 5.40; N, 2.95.

## 5-2 Enzymology

### 5-2-1 General materials and procedures

All chemicals were of analytical reagent grade. 4-Nitrophenyl- and 2-nitrophenyl-β-cellobiosides, buffer materials and all other chemicals were obtained from either Sigma or Aldrich Chemical Companies. Intact (molecular weight = 47 kDa) and truncated (molecular weight = 35 kDa) native *Cellulomonas fimi* exoglycanase as well as the Glu233Asp and Glu127Ala mutants were provided by Drs. R. A. J. Warren, N. Gilkes, D. Kilburn, and Dr. A. MacLeod, Department of Microbiology, University of British Columbia.

All absorbance measurements were recorded on a Pye-Unicam 8700 UV/Vis spectrometer equipped with a circulating water bath. All protein and peptide mass spectra were recorded by either Dr. David Burgoyne or Dr. Shichang Miao in Dr. Ruedi Aebersold's laboratory, Biomedical Research Centre, University of British Columbia using

a PE-Sciex API III triple quadrupole mass spectrometer (PE-Sciex, Thornhill, Ontario) equipped with an ionspray ion source. Protein and peptide samples were separated by reverse phase high performance liquid chromatography (RP-HPLC) on an Ultrafast Microprotein Analyser (Michrom BioResources Inc., Auburn, CA) directly interfaced with the mass spectrometer using solvent A: 0.05% trifluoroacetic acid, 2% acetonitrile in water and solvent B: 0.045% trifluoroacetic acid, 80% acetonitrile in water. The system was equipped with a post-column flow splitter to introduce 15% of the HPLC eluate into the mass spectrometer while 85% was collected for further analysis (Hess et al., 1993).

### 5-2-2 Determination of steady state kinetic parameters

All steady state kinetic studies were performed by recording changes in UV/Vis absorbance using a Pye-Unicam 8700 spectrophotometer equipped with a circulating water bath. Reactions were monitored at wavelengths where there was a convenient absorbance difference between the initial glycoside and the phenol product as previously reported (Kempton & Withers, 1992) using the same extinction coefficients. Initial rates of exoglycanase-catalysed hydrolysis of aryl β-D-glycosides were determined by incubating solutions of the appropriate substrate concentrations in 50 mM sodium phosphate buffer, pH 7.0 and 1 mg/mL BSA at 37 °C in 1-cm cuvettes within the spectrophotometer until thermally equilibrated. Reactions were initiated by the addition of enzyme, and release of the phenol product was monitored at the appropriate wavelength. In order to ensure linear kinetics and to obtain a sufficient absorbance change for accurate calulation of the rates, the concentration of the enzyme added and the length of time that the reaction was monitored was selected such that less than 10% of the total substrate was converted to product.

Initially, approximate values of $K_m$ and $V_{max}$ were calculated from three point Lineweaver-Burk plots where the initial rates of hydrolysis for three widely varied substrate concentrations were measured. More accurate values for $K_m$ and $V_{max}$ were then determined by measuring the initial rates of hydrolysis for 5-8 different substrate

concentrations which generally ranged from 0.2 to 5 times $K_m$ except when limited by substrate insolubility. These results are illustrated as Lineweaver-Burk double reciprocal plots for visual convenience in Appendix A where the enzyme concentrations, the wavelengths and the molar extinction coefficients used are indicated in the legends. However, due to the inaccuracy introduced by the nonlinear error span of the double reciprocal analysis, the values of $K_m$ and $V_{max}$ were determined actually by nonlinear regression analysis using the program GraFit (Leatherbarrow, 1990). Standard errors for these constants were calculated by the same fitting program.

### 5-2-3 Determination of pre-steady state kinetic parameters

Pre-steady state kinetic measurements were performed on an Applied Photophysics MV 17 microvolume stopped flow spectrophotometer equipped with a Grant constant temperature bath. Reactions were monitored at the same wavelengths as in the steady state kinetic studies. The concentration of enzyme used in each case was chosen to yield a burst with a total absorbance change of 0.06 A. Rates were determined by equilibrating solutions of enzyme and of the appropriate concentrations of substrate in 50 mM sodium phosphate buffer, pH 7.0 to 37 °C. The reactions were monitored by following the release of the phenol product at the appropriate wavelength. Reaction rates were measured at five different substrate concentrations ranging from 0.2 x $K_d$ to ~$K_d$ whenever possible. The measurement at each substrate concentration was repeated 3-4 times, the traces averaged and fitted to an equation describing a first order reaction followed by a steady state. This yielded values of the pseudo-first order rate constant ($k_{obs}$) and the steady state rate at each substrate concentration. Values of $K_d$ and $k_2$ were determined from these $k_{obs}$ values by direct fit to the equation

$$k_{obs} = \frac{k_2[S]}{K_d + [S]}$$

using the program GraFit (Leatherbarrow, 1990). Standard errors for these constants were calculated by the same fitting program. For visual convenience, these results are presented as Lineweaver-Burk plots in Appendix A along with the enzyme concentrations, wavelength and molar extinction coefficients used.

### 5-2-4 Secondary deuterium kinetic isotope effect measurements

Isotope effects were determined by comparison of the initial rates of hydrolysis of high (4 - 7 times the $K_m$ value) concentrations of protio and deuterio substrates determined spectrophotometrically. In most cases, quartz cells were filled with the appropriate concentration of diluted enzyme and incubated at 37 °C, reaction being initiated by the addition of a small volume (50 - 100 µl) of (thermally equilibrated) substrate. When substrate solubilities precluded this approach it was necessary to add the enzyme to the pre-equilibrated substrate. Rates of protio and deuterio substrate hydrolysis were determined in alternation until a total of 8 or 9 rates for each (protio and deuterio) substrate had been measured. Average rates for the protio and deuterio substrates were then calculated and the rate taken to give the isotope effect. Errors provided are the standard deviation of the average kinetic isotope effect.

### 5-2-5 pH Study

*(a) Extinction coefficients of 2,4 dinitrophenol*

2,4-Dinitrophenol was dried *in vacuo* overnight, weighed and dissolved in a known volume of water. Aliquots of stock 2,4-dinitrophenol were added to the appropriate buffers, equilibrated to 37 °C and the absorbance recorded at 400 nm. The extinction coefficients of 2,4-dinitrophenol at the different pH values were determined from these measurements using Beer's law:

$$\varepsilon = \frac{A}{bc}$$

where A corresponds to the absorbance, b to the cell pathlength (1 cm) and c to the concentration of 2,4-dinitrophenol. In order to determine if the pH had changed due to the addition of 2,4-dinitrophenol, the pH of the solution was measured after recording the absorbance. The buffers used were 50 mM citrate (pH 4-6), 50 mM phosphate (pH 6-8), 50 mM Tris (pH 8-9) and 50 mM carbonate-bicarbonate (pH 9-10). The extinction coefficients determined are 9.0, 9.2, 9.6, 9.9, 10.2, 10.6, 10.7 and 10.9 $mM^{-1}$ $cm^{-1}$ at pH 4.53, 4.61, 4.78, 5.01, 5.16, 5.60, 6.25, and 6.8 respectively.

*(b) pH dependence of enzyme kinetic parameters*: The dependence of $k_{cat}$ and $k_{cat}/K_m$ on pH for the native enzyme and the Glu233Asp mutant was determined as follows. Rates of exoglycanase-catalysed hydrolysis at different pH values were determined by incubating 6 different concentrations of 2,4-DNPC in the appropriate buffer containing 1 mg/mL BSA and 145 mM NaCl at 37 °C until thermally equilibrated. The reaction was initiated by addition of enzyme, dinitrophenolate release was monitored at 400 nm and values for $k_{cat}$ and $K_m$ determined as previously described. The dependence of $k_{cat}$ on pH for Glu127Asp was determined by thermally equilibrating saturating concentrations of 2,4-DNPC (75 x $K_m$) in the appropriate buffer containing 1 mg/mL BSA and 145 mM NaCl at 37 °C and the reaction initiated by enzyme addition. Values of $k_{cat}$ were then calculated from the initial rates of hydrolysis using the appropriate extinction coefficient for 2,4-dinitrophenol. The pH dependence of $k_{cat}/K_m$ for the Glu127Ala mutant was determined by incubating PNPC at a final concentration of 0.2 x $K_m$ in the appropriate buffer and 1 mg/mL BSA and 145 mM NaCl at 37 °C until thermally equilibrated. The reactions were initiated by the addition of enzyme and the release of 4-nitrophenolate was monitored by following the absorbance at 400 nm until the substrate was depleted. The change in absorbance with time was fitted to a first order rate equation using the program GraFit (Leatherbarrow, 1990) which

yielded values for the pseudo-first order rate constant at each pH value. Since at low substrate concentrations (S<<Km) the reaction rates are given by the equation

$$v = \frac{k_{cat}[E][S]}{K_m}$$

then $k_{obs}$ values correspond to $k_{cat}/K_m$. In order to ensure that the pH had not changed during the reaction, the pH of each reaction mixture was measured after recording the rates of hydrolysis.

### 5-2-6 Inactivation kinetics

The kinetic parameters for the inactivation of *C. fimi* exoglycanase by cellobial and 2F-GMF were determined as follows. *C. fimi* exoglycanase was incubated in 50 mM sodium phosphate buffer, pH 7.0 containing 1 mg/ml BSA at 37 °C in the presence of varying concentrations of the inactivator. Concentrations of cellobial used were 1.0, 7.1, 10.0, 29.9, and 54.2 mM while concentrations of 2F-GMF used were 4.1, 8.2, 14.4, 24.6, and 30.8 mM. Aliquots of these inactivation mixtures were removed at different time intervals and diluted into reaction cells containing a large volume of substrate (2,4-DNPC) at saturating concentration (1 mM, 10 x $K_m$). This stopped the inactivation both by dilution of the inactivator and by competition for the excess substrate. The residual enzymatic activity was determined from the rate of hydrolysis of the substrate, which is directly proportional to the amount of active enzyme. The inactivation was monitored until 80-90% of the enzymatic activity was lost. Pseudo-first order rate constants ($k_{obs}$) for inactivation were calculated for each inactivator concentration by direct fit of each curve to a first-order function, and then values of $k_i$ and $K_i$ were determined from these $k_{obs}$ values by direct fit to the equation

$$k_{obs} = \frac{k_i[I]}{K_i + [I]}$$

using the program GraFit (Leatherbarrow, 1990) (Appendix A-8). However, due to the very large values of $K_i$ for both cellobial and 2F-GMF and the limited solubility of these inactivators, these values must be taken as only estimates of $K_i$ and $k_i$. Nevertheless, since at very low inactivator concentrations ([I] << $K_i$), values of $k_{obs}$ are given by the equation

$$k_{obs} = \frac{k_i[I]}{K_i}$$

then accurate values of $k_i/K_i$ for cellobial and 2FGMF inactivation can be calculated from the slopes of plots of $k_{obs}$ *versus* inactivator concentrations (Appendix A-8).

### 5-2-7 Protection against inactivation

Protection against exoglycanase inactivation by cellobial was investigated as follows. Samples of exoglycanase (0.015 mg, 0.073 mg/ml) were incubated in 50 mM sodium phosphate buffer, pH 7.0 at 37 ℃ containing the cellobial (11.09 mM) and the competitive inhibitor, BGTX ($K_d$ = 3.0 mM), at concentrations of 0 or ~2.0 mM. Aliquots were removed at different time intervals, diluted into reaction cells containing saturating concentrations of 2,4-DNPC (0.66mM ~ 7 x Km) in 50 mM sodium phosphate buffer, pH 7.0 at 37 °C, and the residual enzyme activity monitored by following the release of the dinitrophenolate at 400 nm as described above. Pseudo-first order rate constants for inactivation at each BGTX concentration were calculated and compared to determine the degree of protection afforded by BGTX against inactivation.

Protection against *C. fimi* exoglycanase inactivation by N-bromoacetyl cellobiosylamine was investigated similarly using an inactivator concentration of 3.5 mM and BGTX concentration of 9.7 mM. Protection against 2F-GMF inactivation was investigated using an inactivator concentration of 30.8 mM and BGTX concentration of 2 mM.

### 5-2-8 Reactivation kinetics

Reactivation of cellobial-inactivated exoglycanase was investigated as follows. A sample of inactivated exoglycanase (0.25 mg, 5 mg/ml) were extensively dialysed at 4 °C against several changes of 50 mM sodium phosphate buffer pH 7.0 in order to remove the excess inactivator. Aliquots of the dialysed inactivated enzyme (0.018 mg)were added to buffer solutions containing BSA (1 mg/mL) and either buffer alone or 50 mM cellobiose. These solutions were incubated at 37 °C and monitored for return of enzymatic activity by periodic removal of samples and assayed using 2,4-DNPC as described above. Reactivation rates were calculated by fitting these data to first-order curves by nonlinear regression analysis (Leatherbarrow, 1990) andthese are illustrated in Appendix 8.

### 5-2-9 $^{19}$F-NMR analysis of 2-deoxy-2-fluoro-glycosyl-*C.fimi* exoglycanase

Samples of *C. fimi* exoglycanase (5 mg, 9 mg/ml) were individually inactivated with either 2F-DNPC (1.0 mM) or 2FGMF (30 mM) in 50 mM sodium phosphate buffer (500 µl) pH 7.0 containing 10% $D_2O$ at 37°C. The inactivated enzyme samples were analysed on a 470 MHz VARIAN for $^{19}$F NMR by Dr. Lawrence McIntosh in the Department of Chemistry, University of British Columbia, Vancouver. The 2F-GMF-inactivated exoglycanase sample was dialysed extensively against 50 mM sodium phosphate buffer, pH 7.0 at 4 °C, reconcentrated to ~9 mg/ml using a Millipore UFC-10 polysulfone membrane concentrator and resubmitted for $^{19}$F-NMR analysis. The spectrum for the 2F-DNPC-inactivated *C. fimi* exoglycanase sample was recorded using sweepwidth of 23460.4 Hz and repetition time of 2.2 seconds at a pulse angle of 90 °C. The signals are averaged over 6198 transient and referenced to external fluoride at $\delta$ = -121.39 ppm. The spectrum for the 2F-GMF-inactivated enzyme sample was recorded using sweepwidth of 53619.3 Hz and repetition time of 3.2 seconds at a pulse angle of 90 °C. The signals are

averaged over 14936 transients and referenced to internal fluoride at $\delta$ = -121.39 ppm. The spectra were processed with a 2 - 4 Hz linebroadening and baseline flattening.

### 5-2-10 Stoichiometry of inactivation

The stoichiometry of *C. fimi* exoglycanase inactivation by the disaccharides 2F-DNPC, 2F-DNPX$_2$, 2FGMF, cellobial and N-bromoacetyl cellobiosylamine was determined by subjecting samples of inactivated exoglycanase (10 μg, 1 mg/ml) and untreated enzyme (10 μg, 1 mg/ml) to mass spectrometric analysis on a PE-Sciex API III triple quadrupole mass spectrometer. This involved introduction of the protein sample into the mass spectrometer through a microbore PLRP column (1 x 50 mm) on the Michrom HPLC system using a gradient of 20-100% solvent B (solvent A: 0.05% trifluoroacetic acid, 2% acetonitrile in water and solvent B: 0.045% trifluoroacetic acid, 80% acetonitrile in water) over 10 minutes followed by 100% solvent B over 2 minutes. The mass spectrometer, in the single quadrupole mode, was scanned over a m/z range of 300-2400 Da. Protein molecular weights were determined from this data using the deconvolution software supplied by Sciex.

### 5-2-11 Identification of the residue labeled by 2F-DNPC and cellobial

The exoglycanase (100 μg, 9.8 mg/ml) was completely inactivated with either 2F-DNPC (1.0 mM) or cellobial (60 mM) in 50 mM sodium phosphate buffer, pH 7.0 at 37 °C. Samples of labeled and unlabeled enzyme were digested using 1:100 pepsin (w/w, pepsin : exoglycanase) in 50 mM sodium phosphate buffer, pH 2.0 at room temperature. and the resulting digests subjected to mass spectrometric analysis by Dr. Shichang Miao. This involved individually loading the digest (~0.05 μg) onto a C18 Reliasil column (1 x 150 mm) and eluting the separaed peptides directly into the mass spectrometer using a gradient of 0-60% solvent B over 20 minutes followed by 100% solvent B for 2 minutes at a flow rate of 50 μl/minute. In this mass spectrometric experiment, the mass analyser in the

single quadrupole mode was scanned over *m/z* range of 300-2400 Da. The labeled peptide was identified in a second mass spectrometric experiment in which the peptide ions were subjected to collision-induced fragmentation in the second quadrupole. In this experiment the mass spectrometer was scanned in the neutral loss mode searching for a mass loss corresponding to the loss of the label from a peptide ion in the singly or doubly charged state. The triple quadrupole mass analyser was scanned over a *m/z* range of 300-1200 Da with collision gas (10% $N_2$ diluted with Ar) thickness of 3.2-3.6 x $10^{14}$ molecules/$cm^2$ in the second quadrupole.

The 2-deoxyfluoro-cellobiosyl peptide was purified by RP-HPLC using the mass spectrometer scanned in the neutral loss mode as the detector. This involved loading aliquots of the labeled digest on to the C18 Reliasil column and eluting with the gradient described above. A post-column flow splitter was used to introduce 15% of the eluent into the mass spectrometer while the remaining 85% was fractionated (Hess et al., 1993). The fraction containing the labeled peptide was concentrated *in vacuo* and rechromatographed on the same column using a gradient of 0-20% solvent B over 50 minutes followed by 100% solvent B over 2 minutes at a flow rate of 50 µl/min. The resultant labeled peptide was sufficiently pure to be sequenced. This peptide was sequenced by solid phase Edman degradation on a Milligen/BioSearch Model 6600 protein sequencer in the laboratory of Dr. Ruedi Aebersold at the Biomedical Research Centre, University of British Columbia, Vancouver. This involved the sequential derivatisation of the N-terminal amino acid to phenylthiohydantoins (PTH) followed by the separation and identification of the PTH-residues by HPLC.

### 5-2-12 Identification of the residue labeled by N-bromoacetyl cellobiosylamine

An aliquot of *C. fimi* exoglycanase (1.0 mg, 8 mg/ml) was inactivated with N-bromoacetyl cellobiosylamine (30 mM) in 50 mM sodium phosphate buffer, pH 7.0 at 37

°C. Samples of labeled and unlabeled exoglycanase were completely digested using 1:100 pepsin (w/w, pepsin: exoglycanase) in 50 mM sodium phosphate buffer pH 2.0 at room temperature. Mass spectrometric analysis of these digests was performed by Dr. David Burgoyne in the laboratory of Dr. Ruedi Aebersold. This involved individually loading the digest (10 µg) onto a C18 column (Reliasil, 1 x 150 mm) and then eluting the peptides directly into the mass spectrometer with a gradient of 0-20 % solvent B over 50 minutes followed by 100% solvent B for 2 minutes at a flow rate of 50 µl/min. The quadrupole mass analyser, in the single quadrupole mode, was scanned over a *m/z* range of 300 - 2400 Da. The fraction containing the labeled peptide was identified from this mass information.

The N-acetyl cellobiosylamine labeled peptide was purified by RP-HPLC on a C18 Reliasil (1 x 150 mm) column using the mass spectrometer scanned in the single quadrupole mode as a detector. The peptides were eluted with a gradient of 0-60% solvent B over 20 minutes followed by 100% solvent B over 2 minutes at a flow rate of 50 µl/min. The post-column flow splitter was utilised to introduce 15% of the eluent into the mass spectrometer while the remaining 85% was fractionated. The fraction containing the labeled peptide was concentrated *in vacuo* and the labeled peptide further purified by reloading onto the C18 Reliasil column and eluting with a gradient of 0-20% solvent B over 50 minutes followed by 100% solvent B over 2 minutes at a flow rate of 50 µl/min.

The isolated, labeled peptide was sequenced in Dr. Ruedi Aebersold's laboratory by Mr. David Chow using a novel Edman sequencing reagent. This automated sequencing involved derivatising the N-terminal amino acid residues using 4-(3-pyridinylmethyl-aminocarboxypropyl) phenyl isothiocyanate (311 PITC, Hess et al., 1995), loading the PTH derivatives onto a Reliasil BDS C18 column (1 x 50 mm) and eluting the PTH derivatives directly into the mass spectrometer with a gradient of 0-100% solvent B in 8 minutes at a flow rate of 50 µl/min. In this experiment the mass analyser was scanned over m/z of 300 - 850 Da. This experiment identified the mass of the covalently modified residue. The structure of the modified residue was further characterised in a second

sequencing experiment in which the ion corresponding to the modified amino acid was subjected to collision-induced fragmentation. In this second experiment the mass spectrometer was scanned over a mass range of 100-850 Da with collision gas thickness of $6.0 \times 10^{14}$ molecules/cm$^2$ in the second quadrupole.

## REFERENCES


Albery, W. J., & Knowles, J. R. (1976) *Biochemistry 15*, 5631.

Amyes, T. L., & Jencks, W. P. (1989) *J. Am. Chem. Soc. 111*, 7888.

Anderson, W. F., Grutter, M. G., Remington, S. J., Weaver, L. H., & Matthews, B. W. (1981) *J. Mol. Biol. 147*, 523.

Ballardie, F., Capon, B., Derek, J., & Sutherland, G. (1973) *J. Chem. Soc., Perkin. Trans. I*, 2418.

Ballardie, F. W., Capon, B., Cuthbert, M. W., & Dearie, W. M. (1977) *Bioorg. Chem. 6*, 483.

Barlin, G. S., & Perrin, D. D. (1966) *Q. Rev. Chem. Soc. 20*, 75.

Ba-Saif, S. A., & Williams, S. (1988) *J. Org. Chem. 53*, 2204.

Bause, E., & Legler, G. (1974) *Hoppe-Seyler's Z. Physiol. Chem. 355*, 438.

BeMiller, J. N. (1967) *Adv. Carb. Chem. Biochem. 22*, 25

Bennet, A., & Sinnott, M. L. (1986) *J. Am. Chem. Soc. 108*, 7287.

Black, T., Kiss, L., Tull, D., & Withers, S. G. (1993) *Carbohydr. Res. 250*, 195.

Blake, C. C. F., Johnson, L. N., Mair, G. A., North, A. C. T., Phillips, D. C., & Sarma, V. R. (1967) *Proc. R. Soc. Lond. B 167*, 365.

Bray, M. R., & Clarke, A. J. (1994) *Eur. J. Biochem. 219*, 821.

Bures, E. J., Nika, H., Chow, D. T., Morrison, H., Hess, D., & Aebersold, R. (1995) *Anal. Biochem. 224*, 364.

Campbell, R., Rose, D., Wakarchuk, W., To, R., Sung, W., & Yaguchi, M., (1993) *A comparison of the structures of of the 20 kD xylanases from Trichoderma harzianum and Bacillus circulans,* in *Proceedings of the 2nd TRICEL symposium on Trichoderma reesei cellulases and other hydrolases,* (Suominen, P., & Reinikainen, T., Ed.) p 63. Foundation for Biotechnical and Industrial Fermentation Research, Helsinki, Finland.

Capon, B. (1969) *Chem. Rev. 69*, 407.

Chauvaux, S., Beguin, P., & Aubert, J.-P. (1992) *J. Biol. Chem. 267*, 4472.

Csuk, R., & Glanzer, B. I. (1988) *Adv.Carbohydr. Chem. Biochem 46*, 73.

Cupples, C. G., Miller, J. H., & Huber, R. E. (1990) *J. Biol. Chem. 265*, 5512.

Dale, M. P., Kopfler, W. P., Chait, I., & Byers, L. D. (1986) *Biochemistry 25*, 2522.

Damude, H. G., Withers, S. G., Kilburn, D. G., Miller, R. C. Jr., & Warren, R. A. J. (1995) *Biochemistry 34*, 2220.

Davies, G. J., Dodson, G. G., Hubbard, R. E., Tolley, S. P., Dauter, Z., Wilson, K. S., Hjort, C., Mikkelsen, J. M., Rasmussen, G., & Schulein, M. (1993) *Nature, 365* 362.

Delaire, M., Lenfant, F., Labia, R., & Masson, K. (1991) *Protein Eng., 4*, 805.

Divne, C., Stahlberg, J., Reinikainen, T., Ruohonen, L., Petterson, G., Knowles, J. K. C., Teeri, T., & Jones, T. A. (1994) *Science 265*, 524.

Eshdat, Y., Dunn, A., & Sharon, N. (1974) *Proc. Natl. Acad. Sci. U. S. A. 71*, 1658.

Fersht, A., (1985) *Enzyme Structure and Mechanism.* 2nd ed., Freeman, W. H. & Co., New York.

Fischer, E., & Zemplen, G. (1910) *Ber. Dtsch. Chem. 43*, 2536.

Gebler, J. C., Aebersold, R., & Withers, S. G. (1992) *J. Biol. Chem. 267*, 11126.

Gilkes, N. R., Henrissat, B., Kilburn, D. G., Miller, R. C. Jr., & Warren, R. A. J. (1991) *Microbiol. Rev. 55*, 303.

Gilkes, N. R., Langford, M., Kilburn, D. G., Miller, R. C. Jr., & Warren, R. A. J. (1984) *J. Biol. Chem 259*, 10455.

Gilkes, N. R., Warren, R. A. J., Miller, R. C. Jr., & Kilburn, D. G. (1988) *J. Biol. Chem. 263*, 10401.

Grace, M. E., Graves, P. N., Smith, F. I., & Grabowski, G. A. (1990) *J. Biol. Chem. 265*, 6827.

Grepinet, O., Chebrou, M.-C., & Beguin, P. (1988) *J. Bacteriol. 170*, 4576.

Grutter, M. G., Weaver, L. H., & Matthews, B. W. (1983) *Nature 303*, 828.

Hall, J., Hazlewood, G. P., Barker, P. J., & Gilbert, H. J. (1988) *Gene 69*, 29.

Hehre, E. J., Genghof, D. S., Sternlicht, H., & Brewer, C. F. (1977) *Biochemistry 16*, 1780.

Henrissat, B., & Bairoch, A. (1993) *Biochem. J. 293*, 781.

Henrissat, B., Claeyssens, M., Tomme, P., Lemsle, L., & Mornon, J.-P. (1989) *Gene 81*, 83.

Herrchen, M., & Legler, G. (1984) *Eur. J. Biochem. 138*, 527.

Hess, D., Covey, T. C., Winz, R., Brownsey, R., & Aebersold, R. (1993) *Protein Sci. 2*, 1342.

Hess, D., Nika, H., Chow, D. T., Bures, E. J., Morrison, H., & Aebersold, R. (1995) *Anal. Biochem. 224*, 373.

Hoj, P. B., Condron, R., Traeger, J. C., McAuliffe, J. C., & Stone, B. A. (1992) *J. Biol. Chem. 267*, 25059.

Holm, L., Koivula, A., Lehtovaara, P. M., Hemminki, A., & Knowles, K. C. (1990) *Protein Eng. 3*, 181.

Huber, E. R., & Chivers, P. T. (1993) *Carbohydr. Res. 250*, 9.

Jacobsen, R. H., Zhang, X.-J., DuBose, R. F., & Matthews, B. W. (1994) *Nature 369*, 761.

Johnson, L. N., Cheetham, J., McLaughlin, P. J., Acharya, K. R., Barford, D., & Phillips, D. C. (1988) *Curr. Top. Microbiol. Immuno. 139*, 81

Jones, C. C., Sinnott, M. L., & Souchard, I. J. L. (1977) *J. Chem. Soc. Perkin Trans II*, 1191.

Juncosa, M., Pons, J., Dot, T., Querol, E., & Planas, A. (1994) *J. Biol. Chem., 269*, 14530.

Juy, M., Amit, A. G., Alzari, P. M., Poljak, R. J., Claeyssens, M., Beguin, P., & Aubert, J.-P. (1992) *Nature 357*, 89.

Kanda, T., Brewer, C. F., Okada, G., & Hehre, E. J. (1986) *Biochemistry 25*, 1159.

Keitel, T., Simon, O., Borriss, R., & Heinemann, U. (1993) *Proc. Natl. Acad. Sci. U.S.A. 90*, 5287.

Kempton, J. B., & Withers, S. G. (1992) *Biochemistry 31*, 9961.

Konstantinidis, A., & Sinnott, M. L. (1991) *Biochem. J. 279*, 587.

Kortum, G., Vogel, W., & Andrussow, K. (1961) *Pure Appl. Chem. I*, 450.

Koshland, D. E. (1953) *Biol. Rev. 28*, 416.

Lai, E. C. K., & Withers, S. G. (1994) *Biochemistry 33*, 14743.

Leatherbarrow, R. J. (1990) *GraFit Version 2.0,* Erithacus Software Ltd., Staines, U. K.

Lehmann, J., & Zieger, B. (1977) *Carbohydr. Res.* 58, 73.

Legler, G. (1968) *Hoppe-Seyler's Z. Physiol. Chem. 349*, 767.

Legler, G. (1977) *Methods Enzymol. 46*, 368.

Legler, G. (1990) *Adv. Carb. Chem. Biochem. 48*, 319.

Legler, G., Roeser, K.-R., & Illig, H.-K. (1979) *Eur. J. Biochem. 101*, 85.

Lowe, G., & Yuthauong, Y. (1971) *Biochem. J. 124*, 117.

Macarron, R., van Beeumen, J., Henrissat, B., de la Mata, I., & Claeyssens, M. (1993) *FEBS Lett. 316*, 137.

MacLeod, A. M., Lindhorst, T., Withers, S. G., & Warren, R. A. J. (1994) *Biochemistry 33*, 6571.

Malcolm, B. A., Rosenberg, S., Corey, M. J., Allen, J. S., DeBaetselier, A., & Kirsch, J. F. (1989) *Proc. Natl. Acad. Sci. U. S. A. 86*, 133.

Matsui, H., Tanaka, Y., Brewer, C. F., Blanchard, J. S., & Hehre, E. J. (1993) *Carbohydr. Res. 250*, 45.

McCarter, J., Adam, M., Braun, C., Namchuk, M., Tull, D., & Withers, S. G. (1993) *Carbohydr. Res. 249*, 77.

McCarter, J., Adam, M., & Withers, S. G. (1992) *Biochem. J. 286*, 721.

Miao, S., McCarter, J. D., Grace, M., Grabowski, G., Aebersold, R., & Withers, S. G. (1994) *J. Biol. Chem., 269*, 10975.

Miao, S., Ziser, L., Aebersold, R., & Withers, S. G. (1994) *Biochemistry 33*, 7027.

Moult, J., Eshdat, Y., & Sharon, N. (1973) *J. Mol. Biol. 75*, 1.

Naider, F., Bohak, Z., & Yariv, J. (1972) *Biochemistry 11*, 3202.

O'Neill, G., Goh, S. H., Warren, R. A. J., Kilburn, D. G., & Miller, R. C. Jr. (1986) *Gene 44*, 325.

Ong, E., Gilkes, N. R., Miller, R. C. Jr., Warren, R. A. J., & Kilburn, D. G. (1993) *Biotechnology and Bioengineering 42*, 401.

Pilz, I., Schwarz, E., Kilburn, D. G., Miller, R. C. Jr., Warren, R. A. J., & Gilkes, N. R. (1990) *Biochem. J. 271*, 277.

Post, C., & Karplus, M. (1986) *J. Am Chem. Soc. 108*, 1317.

Py, B., Bortoli-German, I., Haiech, J., Chippaux, M., & Barras, F. (1991) *Protein Eng. 4*, 325.

Quiocho, F. A., Wilson, D. K., & Vyas, N. K. (1989) *Nature 340*, 404.

Riddle, B., & Jencks, W. P. (1971) *J. Biol. Chem. 246*, 3250.

Ritchie, C. D. (1972) *Acc. Chem. Res. 5*, 348.

Robinson, R. A., Davis, M. M., Paabo, M., & Bower, V. E. (1960) *J. Res. Natl. Bur. Stand. Sect. A64*, 347.

Roeser, K.-R., & Legler, G. (1981) *Biochim. Biophys. Acta 657*, 321.

Rouvinen, J., Bergfors, T., Teeri, T., Knowles, J. K. C., & Jones, T. A. (1990) *Science 249*, 380.

Schowen, R. L. (1978) in *Transition States of Biochemical Processes* (Gandour, R., & Schowen, R.L., Eds.) p 77, Plenum Press, New York.

Shaanan, B., Lis, H., & Sharon, N. (1991) *Science 254*, 862.

Shulman, M. L., Shiyan, S. D., & Khorlin, A. Y. (1976) *Biochim. Biophys. Acta 445*, 169.

Sierks, M., Ford, C., Reilly, P., & Svensson, B. (1990) *Protein Eng. 3*, 193.

Sierks, M. R., Bock, K., Refn, S., & Svensson, B. (1992) *Biochemistry 31*, 8972.

Silverman, R. B. (1988) *Chemistry and Enzymology 1*, 3.

Sinnott, M. L. (1978) *FEBS Lett. 94*, 1.

Sinnott, M. L. (1987) in *Enzyme Mechanism* (Page, M. I., Williams, A., Eds.) p 259, Royal Society of Chemistry, London.

Sinnott, M. L. (1990) *Chem. Rev. 90* 1171.

Sinnott, M. L., & Souchard, I. J. L. (1973) *Biochem. J. 133*, 89.

Sinnott, M. L., & Withers, S. G. (1974) *Biochem. J. 143*, 751.

Spezio, M., Wilson, D. B., & Karplus, P. A. (1993) *Biochemistry 32*, 9906.

Srinivasan, K., Konstantinidis, A., Sinnott, M. L., & Hall, G. (1993) *Biochem. J. 291*, 15.

Street, I. P., Kempton, J. B., & Withers, S. G. (1992) *Biochemistry 31*, 9970.

Street, I. P., Rupitz, K., & Withers, S. G. (1989) *Biochemistry 28*, 1581.

Strynadka, N. C. J., & James, M. N. G. (1991) *J. Molec. Biol. 220*, 401.

Svensson, B., & Sogaard, M. (1993) *J. Biotechnol. 29*, 1.

Thomas, E. W. (1977) *Methods Enzymol. 46*, 362.

Tull, D., Miao, S., Withers, S. G., & Aebersold, R. (1995) *Anal. Biochem. 224*, 509.

Tull, D., & Withers, S. G. (1994) *Biochemistry 33*, 6363.

Tull, D., Withers, S. G., Gilkes, N. R., Kilburn, D. G., Warren, R. A. J., & Aebersold, R. (1991) *J. Biol. Chem. 266*, 15621.

Tull, D. (1991) M. Sc. Thesis. University of British Columbia.

Umezerika, G. M. (1988) *Biochem. J. 254*, 73.

Varghese, J. N., Garrett, T. P. J., Colman, P. M., Chen, L., Hoj, P. B., & Fincher, G. B. (1994) *Proc. Natl. Acad. Sci. USA 91*, 2785.

Viratelle, O. M., & Yon, J. M. (1980) *Biochemistry 19*, 4143.

Wang, Q., Trimbur, D., Graham, R., Warren, R. A. J., & Withers, S. G. (1995) *Biochemistry*. In press.

Wang, Q., Tull, D., Meinke, A., Gilkes, N. R., Warren, R. A. J., Aebersold, R., & Withers, S. G. (1993) *J. Biol. Chem. 268*, 14096.

Weber, J. P., & Fink, A. L. (1980) *J. Biol. Chem. 255*, 9030.

Weis, W. I., Drickamer, K., & Hendrickson, W. A. (1992) *Nature 360*, 127.

Weiser, W., Lehmann, J., Matsui, H., Brewer, C. F., & Hehre, E. J. (1992) *Arch. Biochem. Biophys. 292*, 493.

Wentworth, D. F., & Wolfenden, R. (1974) *Biochemistry 13*, 4715.

White, A., Tull, D., Withers, S. G., & Rose, D. R. (1995) In preparation.

White, A., Withers, S. G., Gilkes, N. R., & Rose, D. R. (1994) *Biochemistry 33,* 12546

Withers, S. G., & Aebersold, R. (1995) *Protein Sci 4,* 361.

Withers, S. G., Dombroski, D., Berven, L. A., Kilburn, D. G., Miller, R. C. Jr., Warren, R. A. J., & Gilkes, N. R. (1986) *Biochem. Biophys. Res. Commun. 139*, 487.

Withers, S. G., MacLennan, D. J., & Street, I. P. (1986) *Carbohydr. Res. 154*, 127.

Withers, S. G., Percival, M. D., & Street, I. P. (1989) *Carbohydr. Res. 187*, 43.

Withers, S. G., Rupitz, K., Trimbur, D., & Warren, R. A. J. (1992) *Biochemistry 31*, 9979.

Withers, S. G., & Street, I. P. (1988) *J. Am. Chem. Soc. 110*, 8551.

Withers, S. G., Street, I. P., Bird, P., & Dolphin, D. H. (1987) *J. Am. Chem. Soc. 109*, 7530.

Withers, S. G., Street, I. P., & Percival, M. D.(1988) *in Fluorinated carbohydrates: Chemical and Biochemical Aspects* (Taylor, N. F., Ed.) p 59, American Chemical Society, Washington, D. C.

Withers, S. G., Tull, D., Gebler, J., Braun, C., Aebersold, R., Wang, Q., Warren, R. A. J., Kilburn, D. G., & Gilkes, N. R. (1993) in*Mechanistic Studies on Cellulases. Trichodermareesei Cellulases and other Hydrolases* (Suominen, P., & Reinikainen, T., Eds.) p 117. Foundation for Biotechnical and Industrial Fermentation Research, Helsinki, Finland.

Withers, S. G., Warren, R. A. J., Street, I. P., Rupitz, K., Kempton, J. B., & Aebersold, R. (1990) *J. Am. Chem. Soc. 112*, 5887.

Wold, F. (1978) *Methods Enzymol. XLVI*, 3.

Xu, G.-Y., Ong, E., Gilkes, N. R., Kilburn, D. G., Muhandiram, D. R., Harris-Brandts, M., Carver, J. P., Kay, L. E, & Harvey, T. S. (1995) *Biochemistry 34,* 6993.

Yague, E., Beguin, P., & Aubert, J.-P. (1990) *Gene 89* 61.

Yariv, J., Wilson, K. J., Hildersheim, J., & Blumberg, H. (1971) *FEBS Lett. 15*, 24.

Yuan, J., Martinez-Bilbao, M., & Huber, R. E. (1994) *Biochem. J. 299*, 527.

Zhang, Z.-Y., Wang, Y., & Dixon, J. E. (1994) *Proc. Natl. Acad. Sci. U. S. A. 91*, 1624.

Ziser, L., Setyawati, I., & Withers, S. G. (1995) *Carbohydr. Res.*, In press.

# APPENDIX A

# GRAPHICAL REPRESENTATION OF KINETIC DATA

**A-1 Absorbance *versus* Time Plots for Hydrolysis of ONPC with the Glu233Asp Mutant.**

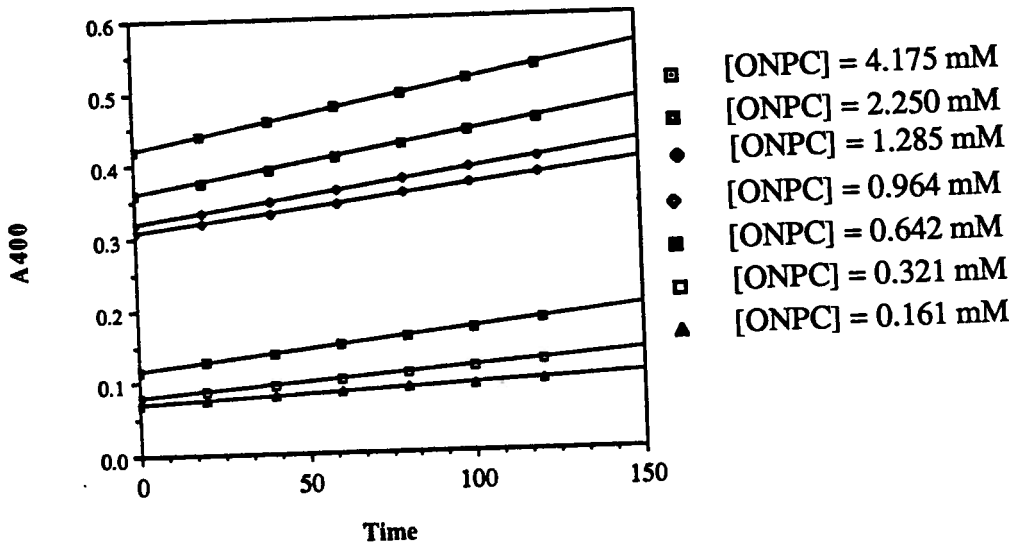


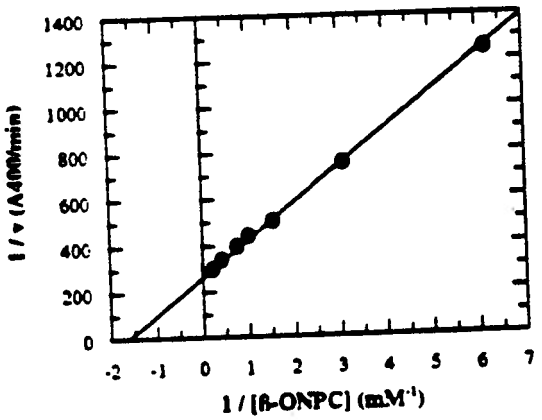

## A-2 Lineweaver-Burk Plots for the Hydrolysis of Aryl β-Xylosides by Native *C. fimi* Exoglycanase.

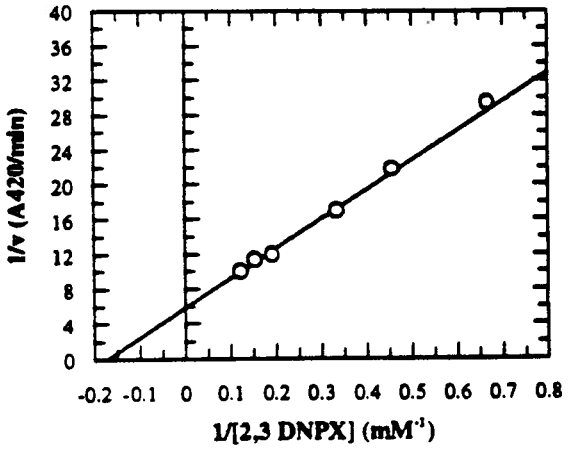


[E] = 0.00035mg/ml
λ = 420 nm; Δε = 5.44 $mM^{-1}$ $cm^{-1}$

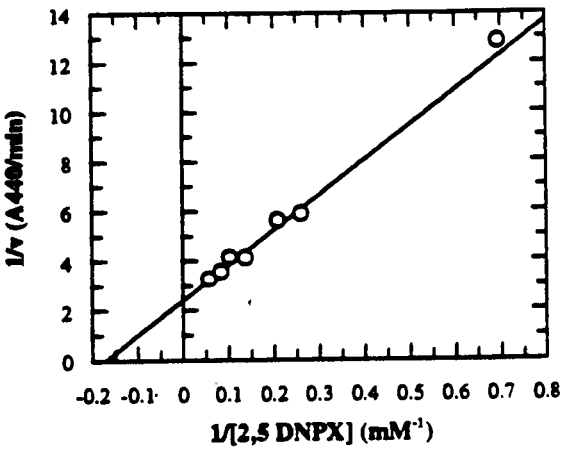


[E] = 0.00070mg/ml
λ = 440 nm; Δε = 5.44 $mM^{-1}$ $cm^{-1}$

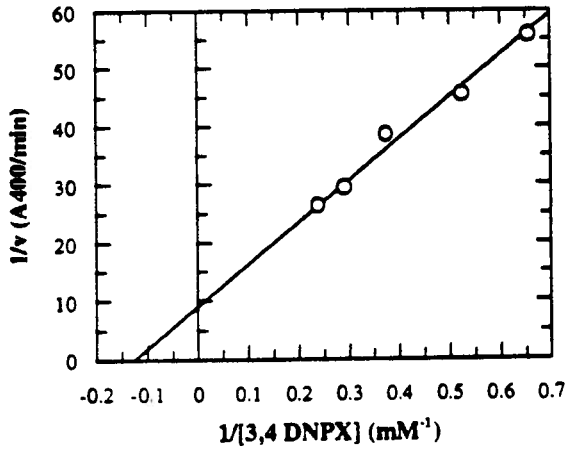


[E] = 0.00035mg/ml
λ = 400 nm; Δε = 11.05 $mM^{-1}$ $cm^{-1}$

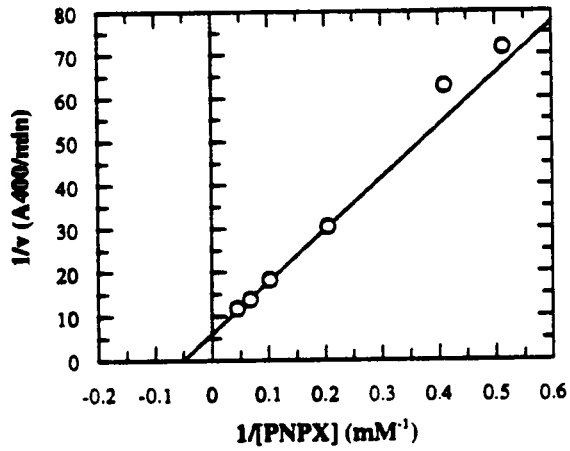


[E] = 0.0069mg/ml
λ = 400 nm; Δε = 7.28 $mM^{-1}$ $cm^{-1}$

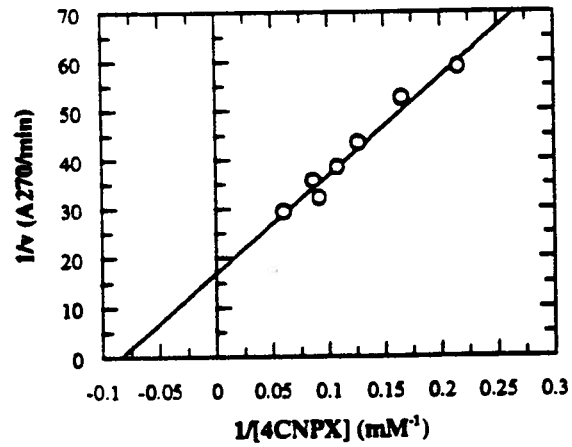


[E] = 0.11mg/ml
λ = 270 nm; Δε = 3.10 $mM^{-1}$ $cm^{-1}$

## A-3 Lineweaver-Burk Plots for the Hydrolysis of Aryl β-Xylobiosides by Native *C. fimi* Exoglycanase.

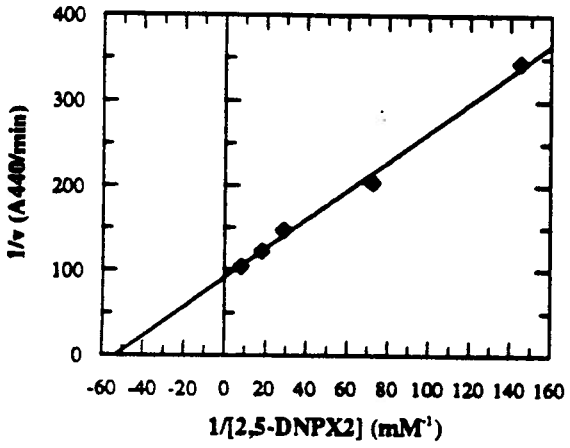


[E] = 7.36 x $10^{-5}$ mg/ml
λ = 440 nm; Δε = 4.29 $mM^{-1}$ $cm^{-1}$

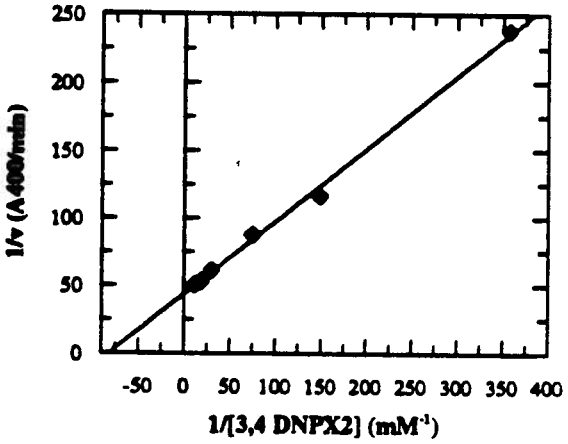


[E] = 7.36 x $10^{-5}$ mg/ml
λ = 400 nm; Δε = 11.09 $mM^{-1}$ $cm^{-1}$

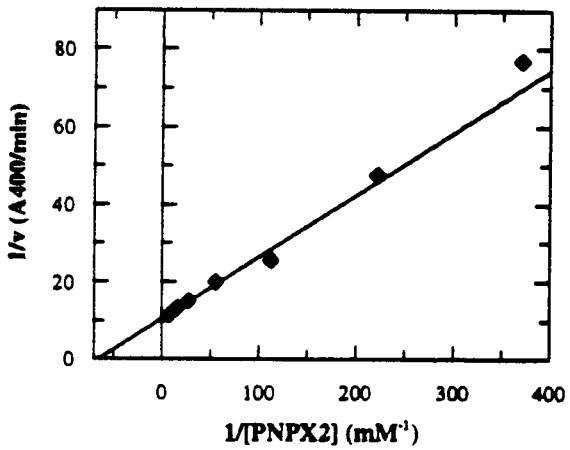


[E] = 1.56 x $10^{-4}$ mg/ml
λ = 400 nm; Δε = 7.28 $mM^{-1}$ $cm^{-1}$

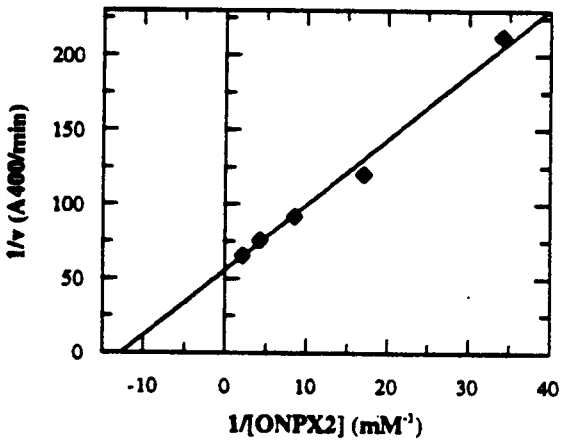


[E] = 1.16 x $10^{-4}$ mg/ml
λ = 400 nm; Δε = 2.17 $mM^{-1}$ $cm^{-1}$

## A-4 Absorbance *versus* Time Plots for Pre-Steady State Analysis of PNPC with the Native Enzyme.

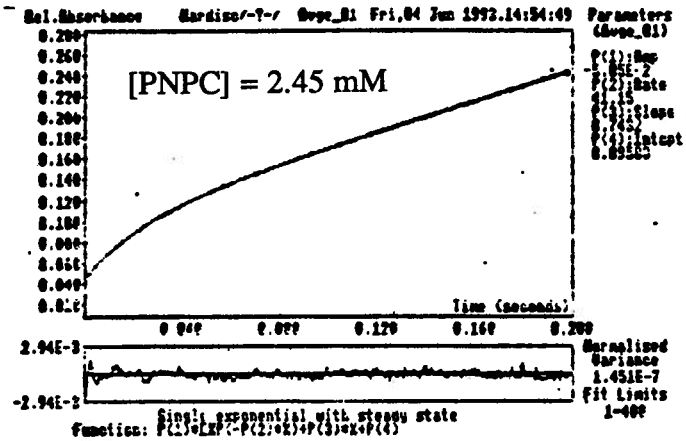


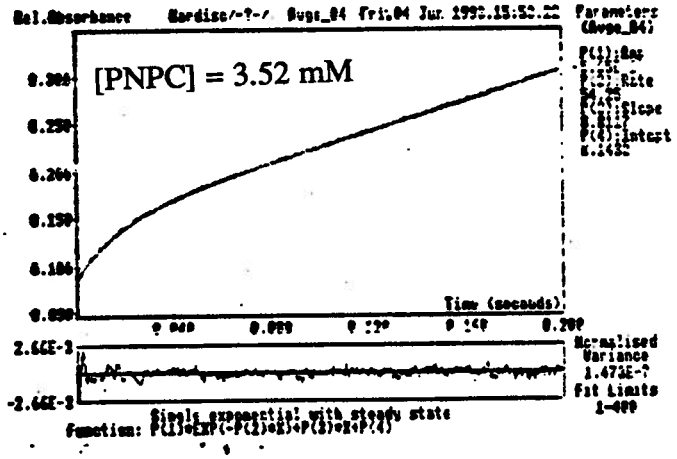


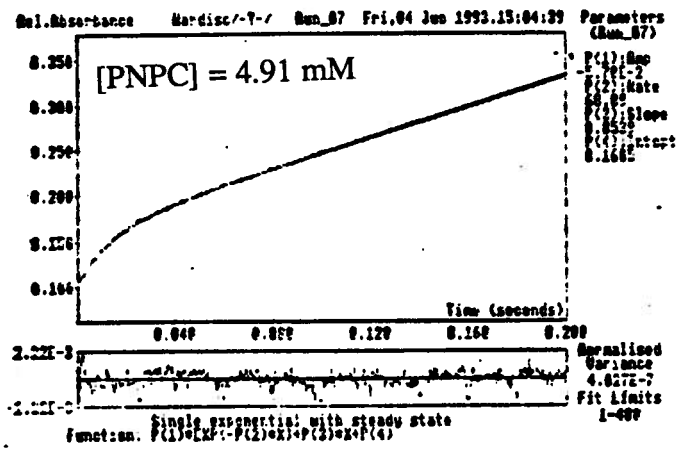


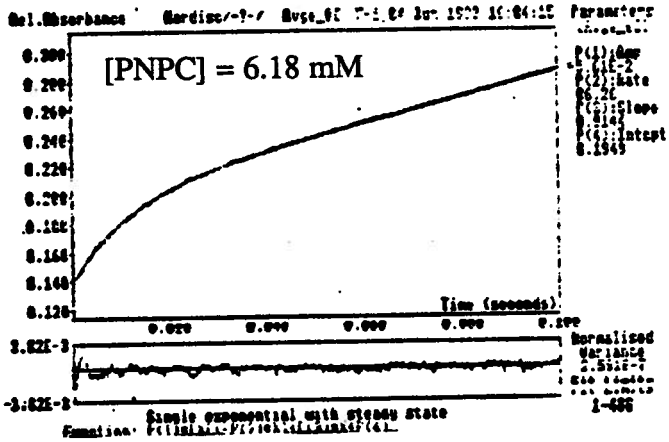


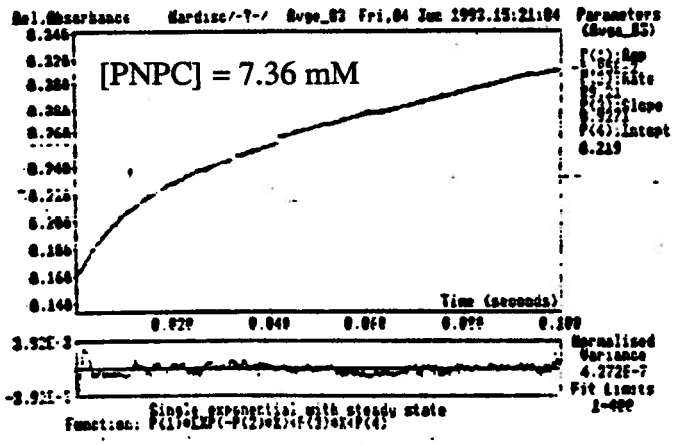


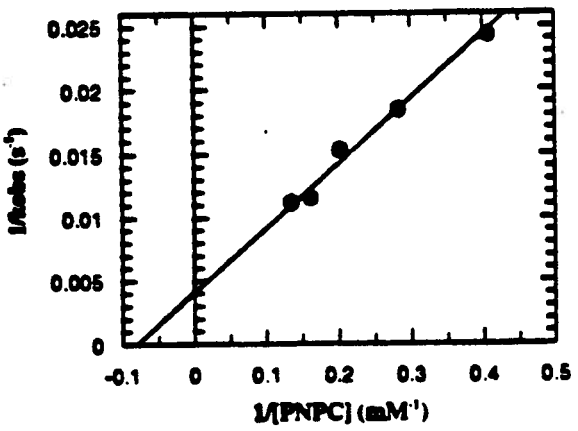

## A-5 Lineweaver-Burk Plots of the Pre-Steady State Analysis of Aryl β-Cellobiosides with Native *C. fimi* Exoglycanase.

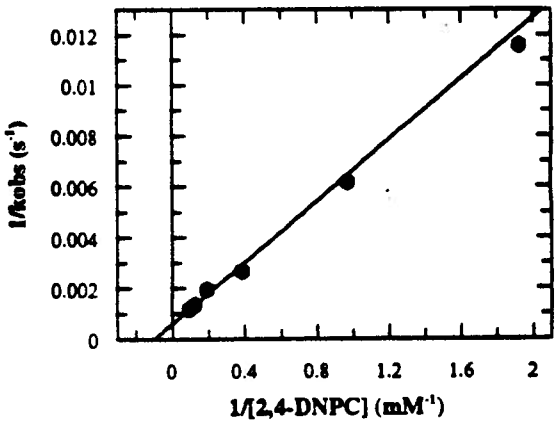


[E] = 0.28 mg/ml
λ = 400 nm; Δε = 10.91 $mM^{-1}$ $cm^{-1}$

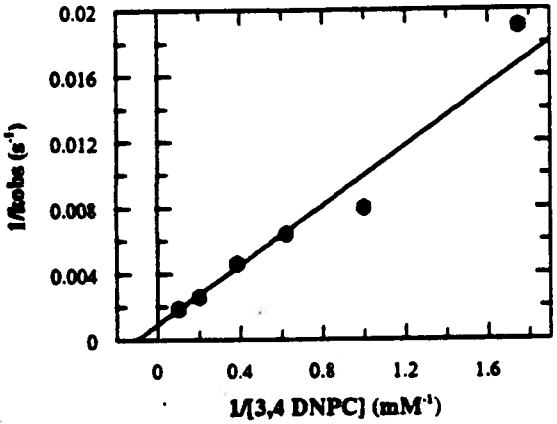


[E] = 0.28 mg/ml
λ = 400 nm; Δε = 11.05 $mM^{-1}$ $cm^{-1}$

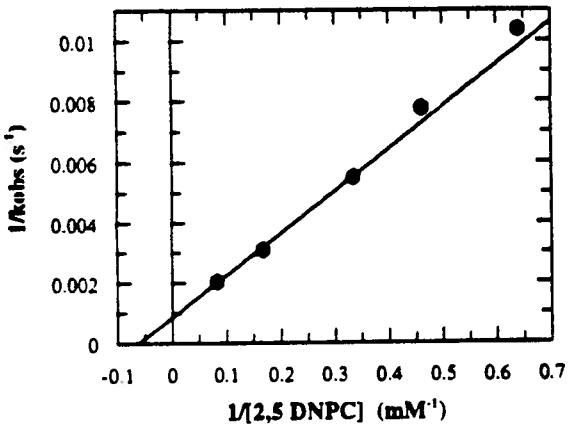


[E] = 0.71 mg/ml
λ = 440 nm; Δε = 4.29 $mM^{-1}$ $cm^{-1}$

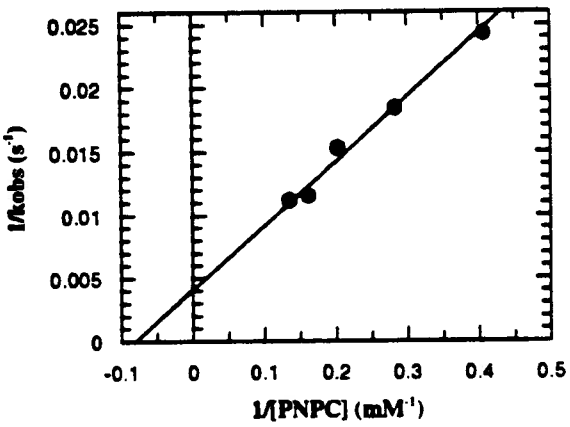


[E] = 0.40 mg/ml
λ = 400 nm; Δε = 7.28 $mM^{-1}$ $cm^{-1}$

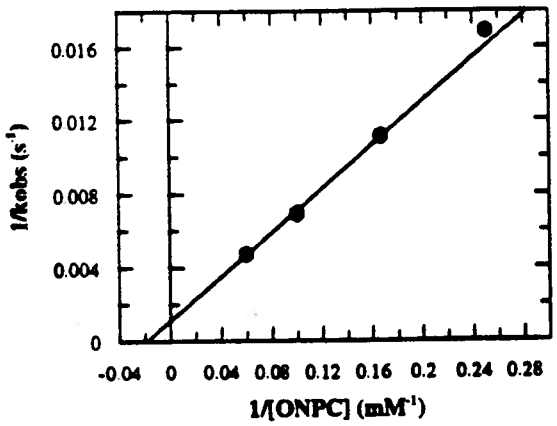


[E] = 1.30 mg/ml
λ = 400 nm; Δε = 2.17 $mM^{-1}$ $cm^{-1}$

## A-6 Lineweaver-Burk Plots for the Hydrolysis of Aryl β-Glucosides and $PNPX_2$ by the Glu233Asp Mutant of *C. fimi* Exoglycanase.

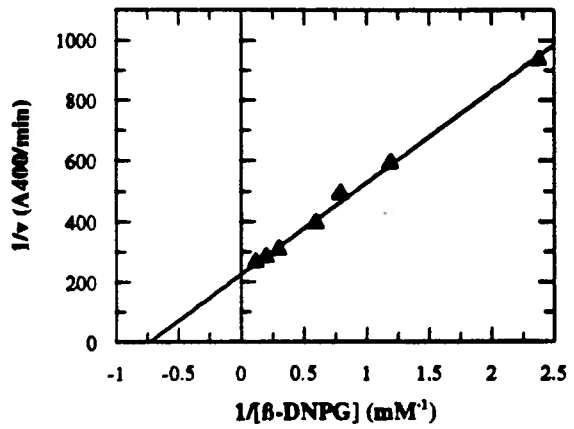


[E] = 0.31 mg/ml
λ = 400 nm, Δε = 10.91 $mM^{-1}$ $cm^{-1}$

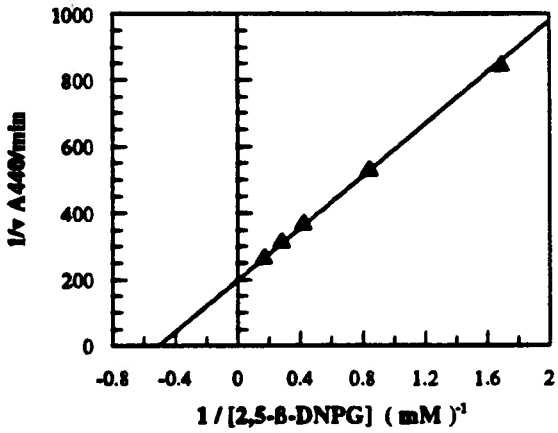


[E] = 0.14 mg/ml
λ = 440 nm, Δε = 4.29 $mM^{-1}$ $cm^{-1}$

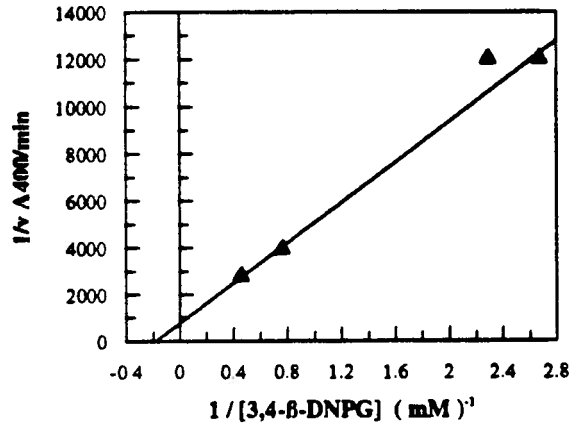


[E] = 0.20 mg/ml
λ = 400 nm, Δε = 11.05 $mM^{-1}$ $cm^{-1}$

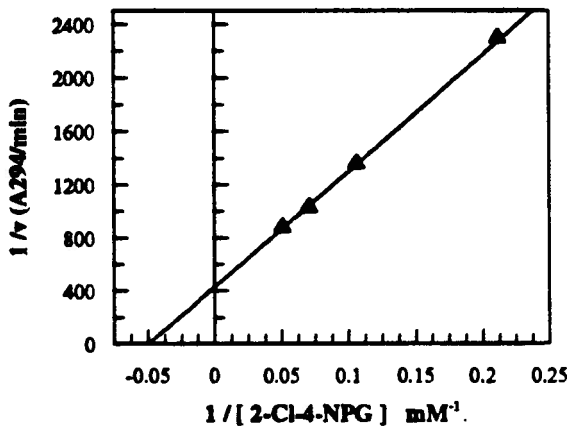


[E] = 0.20 mg/ml
λ = 400 nm, Δε = 7.52$mM^{-1}$ $cm^{-1}$

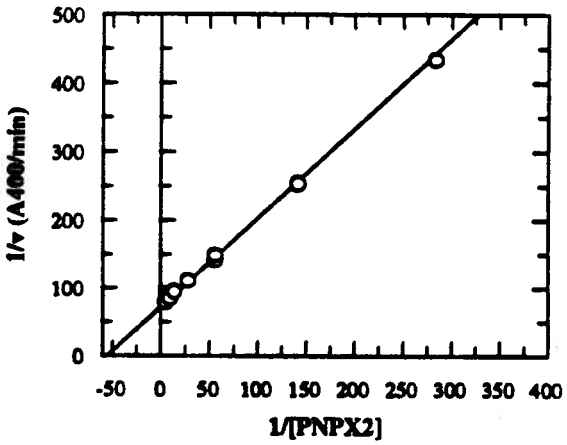


E] = 0.083 mg/ml
λ = 400 nm, Δε = 7.28 $M^{-1}$ $cm^{-1}$

## A-7 Lineweaver-Burk Plots for the Hydrolysis of Aryl β-Cellobiosides by the Glu233Asp Mutant of *C. fimi* Exoglycanase.

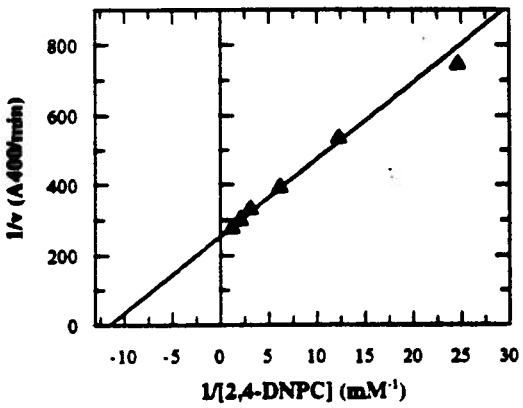


[E] = 0.16 mg/ml
λ = 400 nm, Δε = 10.91 $mM^{-1}$ $cm^{-1}$

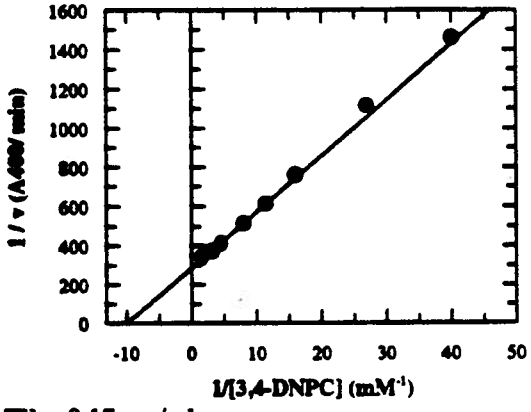


[E] = 0.17 mg/ml
λ = 400 nm, Δε = 11.05 $mM^{-1}$ $cm^{-1}$

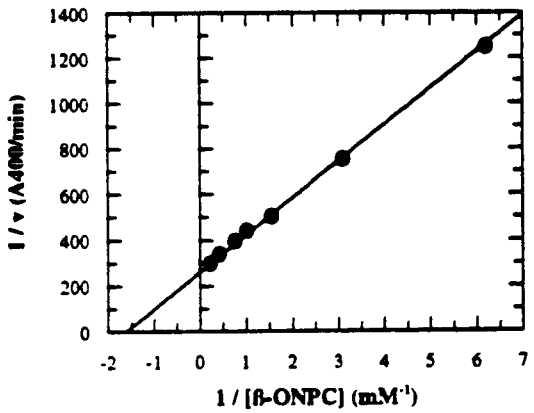


[E] = 0.12 mg/ml
λ = 400 nm, Δε = 2.17 $mM^{-1}$ $cm^{-1}$

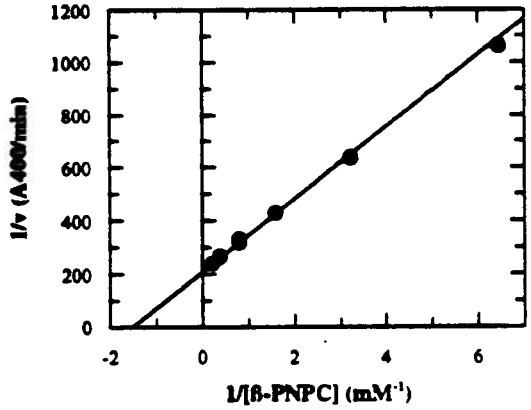


[E] = 0.305 mg/ml
λ = 400 nm, Δε = 7.28 $mM^{-1}$ $cm^{-1}$

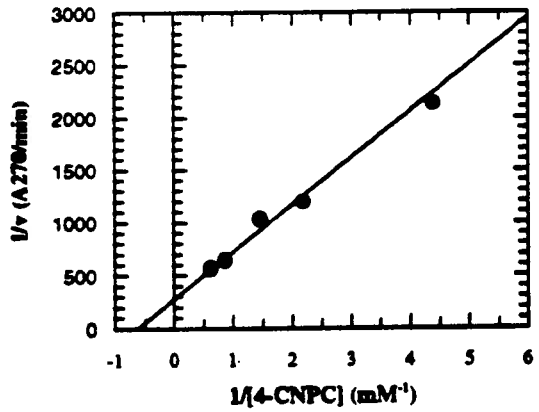


[E] = 0.12 mg/ml
λ = 270 nm, Δε = 3.10 $mM^{-1}$ $cm^{-1}$

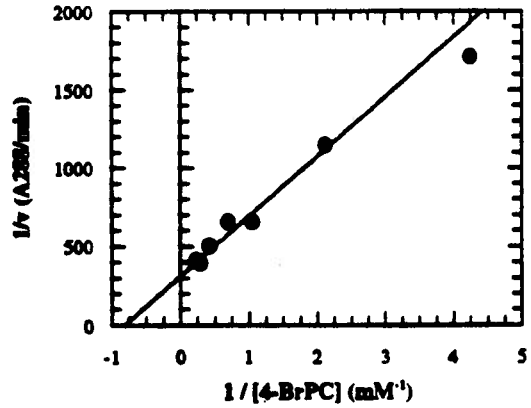


[E] = 0.12 mg/ml
λ = 288 nm, Δε = 0.68 $mM^{-1}$ $cm^{-1}$

## A-8 Lineweaver-Burk Plots for the Hydrolysis of Aryl β-Cellobiosides by the Glu127Ala Mutant of *C. fimi* Exoglycanase.

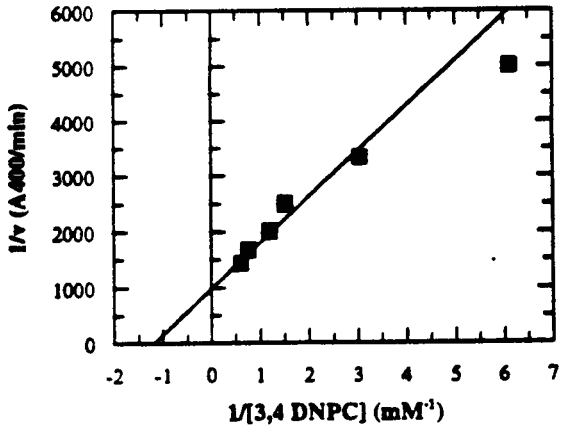


[E] = 0.0010 mg/ml
λ = 400 nm; Δε = 11.05 $mM^{-1}$ $cm^{-1}$

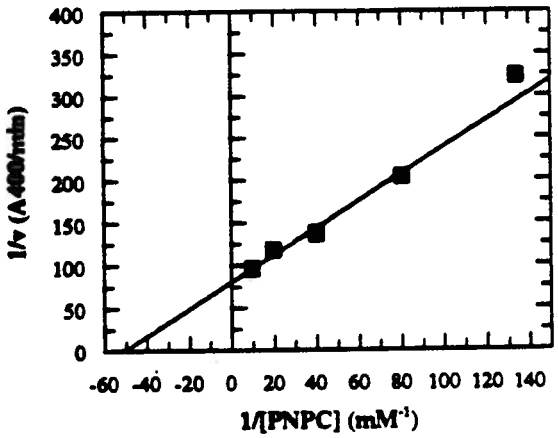


[E] = 0.040 mg/ml
λ = 400 nm; Δε = 7.28 $mM^{-1}$ $cm^{-1}$

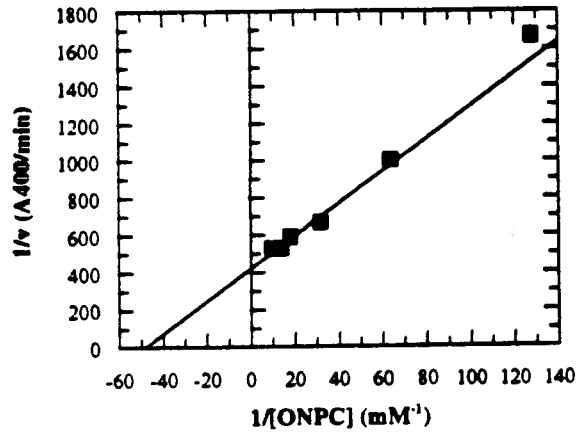


[E] = 0.040 mg/ml
λ = 400 nm; Δε = 2.17 $mM^{-1}$ $cm^{-1}$

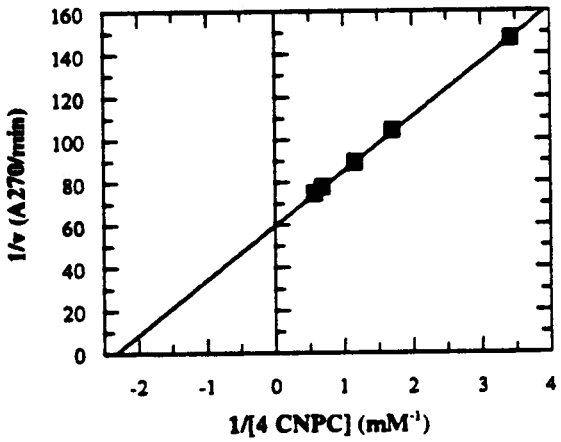


[E] = 0.20 mg/ml
λ = 270 nm; Δε = 3.10 $mM^{-1}$ $cm^{-1}$

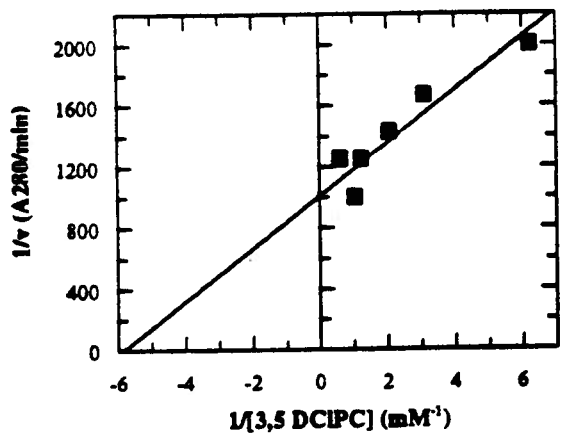


[E] = 0.20 mg/ml
λ = 280 nm; Δε = 0.732 $mM^{-1}$ $cm^{-1}$

## A-9 Lineweaver-Burk Plots of the Pre-Steady State Analysis of Aryl β-Cellobiosides with the Glu127Ala Mutant of *C. fimi* Exoglycanase.

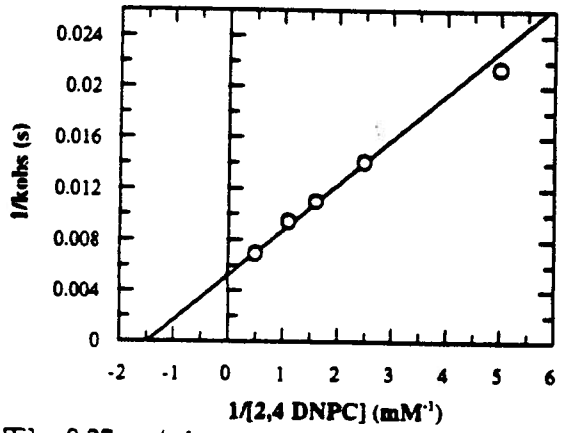


[E] = 0.27 mg/ml
λ = 360 nm; Δε = 14.0 $mM^{-1}$ $cm^{-1}$

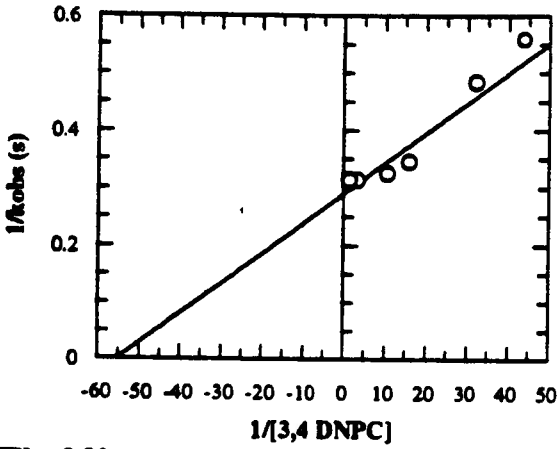


[E] = 0.20 mg/ml
λ = 400 nm; Δε = 11.09 $mM^{-1}$ $cm^{-1}$

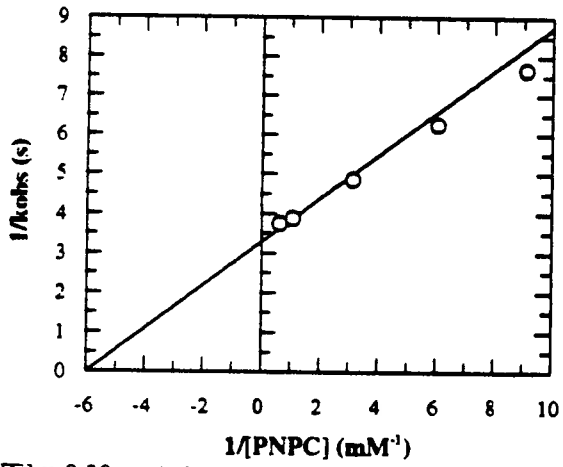


[E] = 0.39 mg/ml
λ = 400 nm; Δε = 7.28 $mM^{-1}$ $cm^{-1}$

## A-10 Inactivation-Reactivation Kinetics of *C. fimi* Exoglycanase.

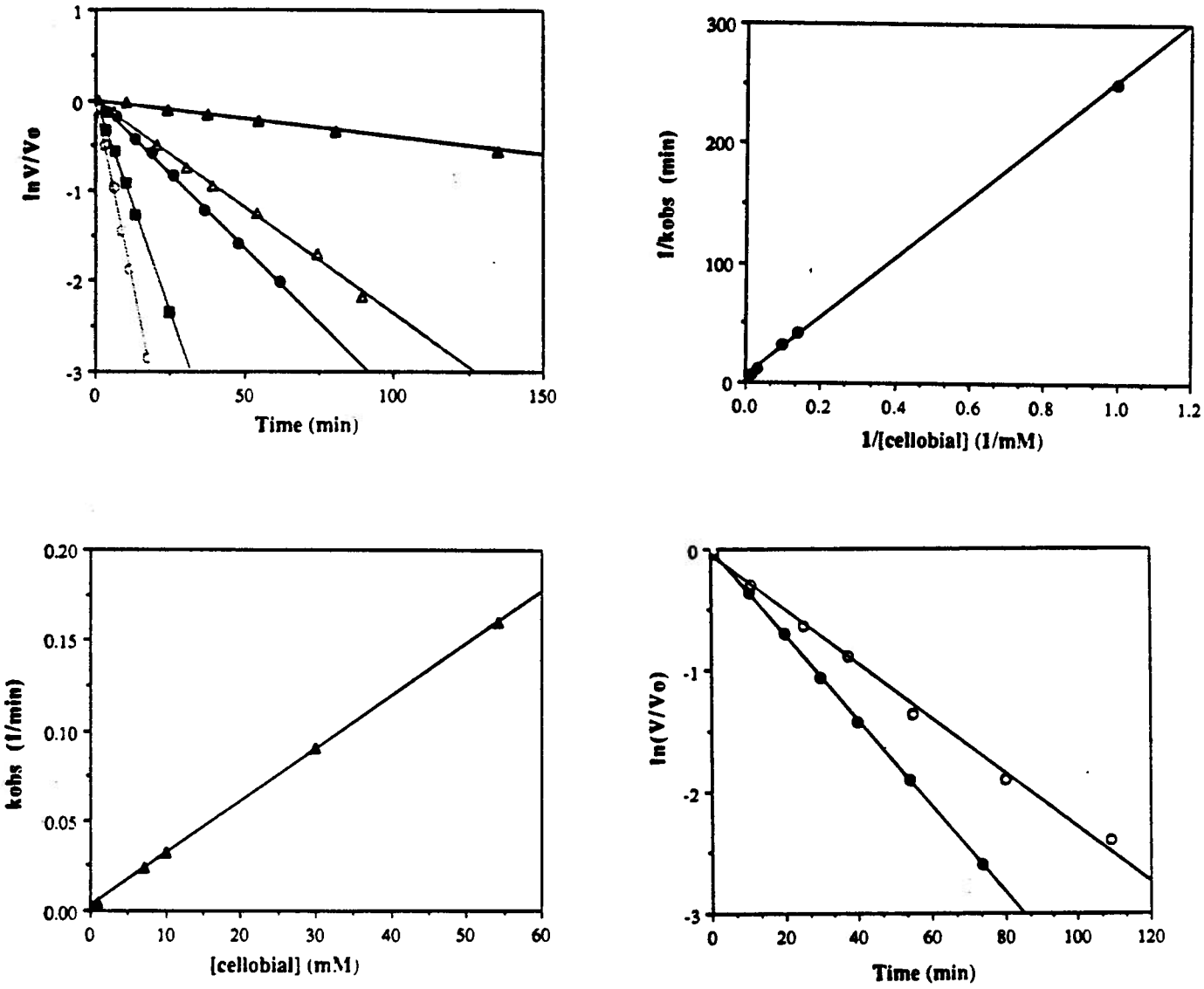


*Figure A-10-1 Inactivation of C. fimi exoglycanase by cellobial. (A) Semi-logarithmic plot of residual activity versus time ((▲), 1.0 mM; (◆) 7.1 mM; (●) 10.0 mM; (■) 29.9 mM; (○) 54.2 mM), (B) double reciprocal plot of pseudo-first order rate constants from the upper plot; (C) plot of the pseudo-first order rate constants versus cellobial concentration; and (D) protection against cellobial inactivation in the presence of GTBX ((●) 0 mM and (○) 2 mM).*

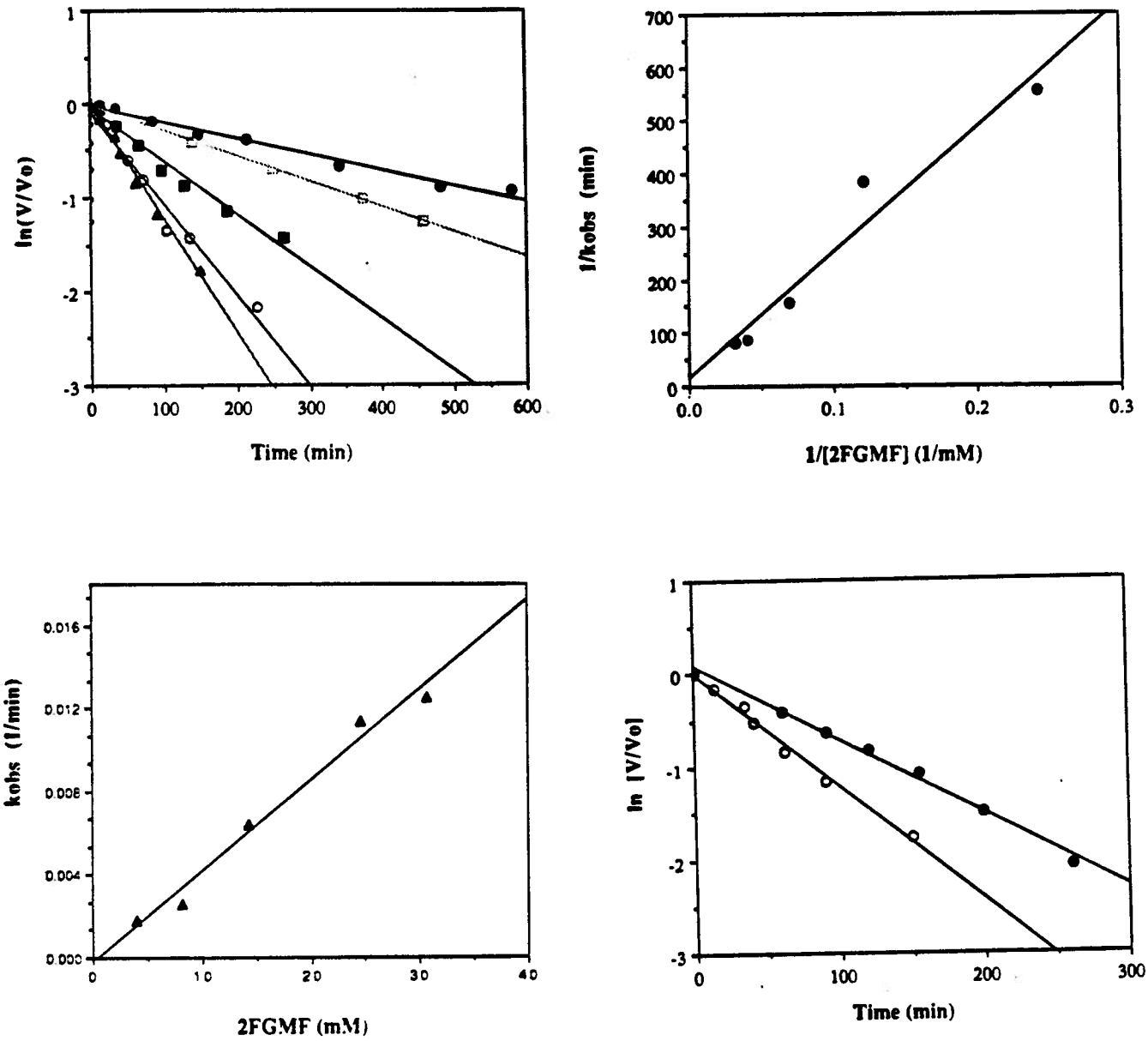


*Figure A-10-2 Inactivation of C. fimi exoglycanase by 2F-GMF. (A) Semi-logarithmic plot of residual activity versus time ((●), 4.1 mM; (□) 8.2 mM; (■), 14.4 mM; (○), 24.6 mM; (▲), 30.82 mM); (B) double reciprocal plot of pseudo-first order rate constants from the upper plot; (C) plot of the pseudo-first order rate constants versus 2F-GMF concentration; and (D) protection against 2F-GMF inactivation in the presence of GTBX ((●) 0 mM and (○) 2 mM).*

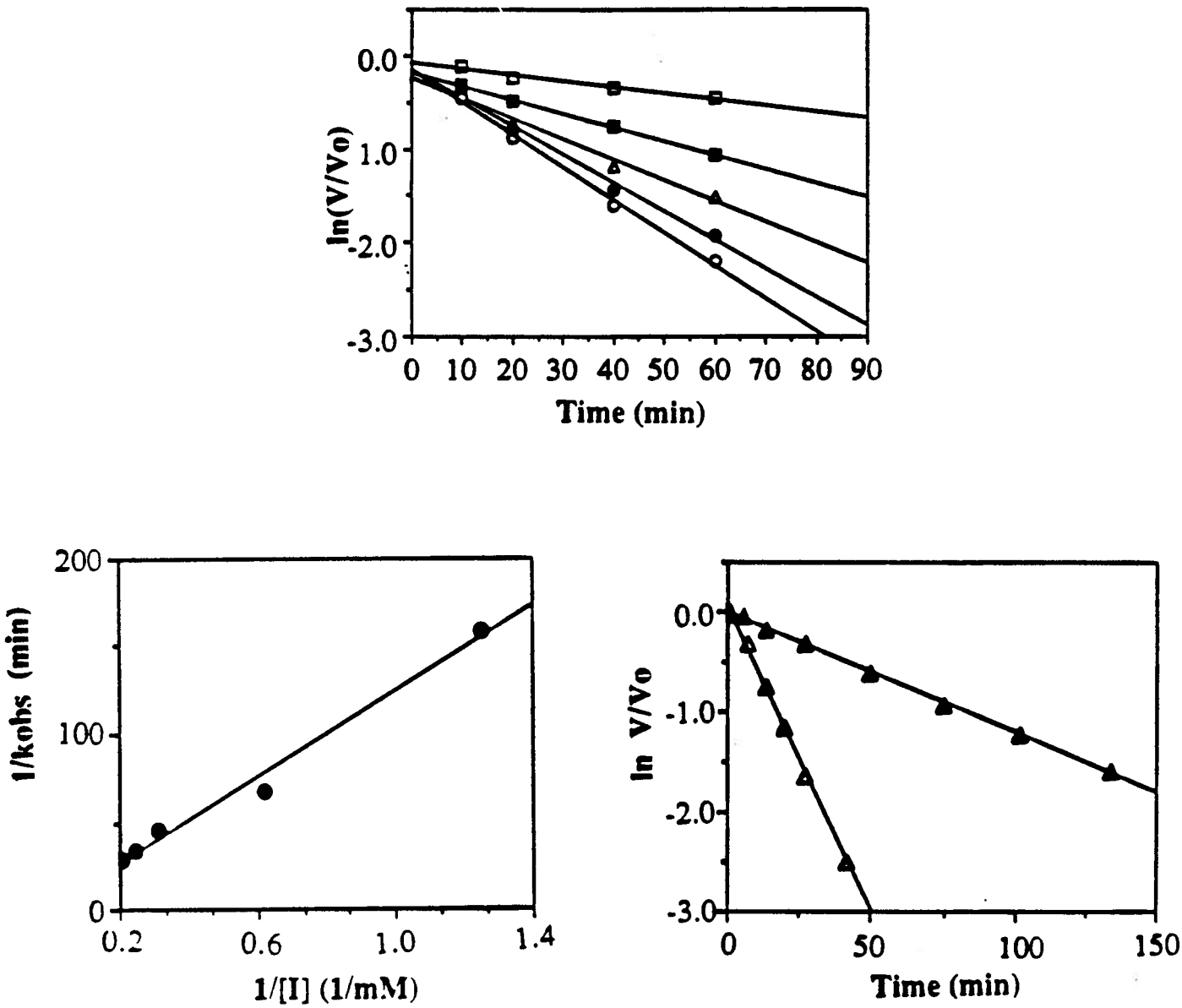


*Figure A-10-3 Inactivation of C. fimi exoglycanase by N-bromoacetyl cellobiosylamine. (A) Semi-logarithmic plot of residual activity versus time ((□),0.8 mM; (■) 1.6 mM; (Δ), 3.2 mM; (●), 4.0 mM; (○), 4.8 mM) (Black et al., 1993); (B) double reciprocal plot of pseudo-first order rate constants from the upper plot; and (C) protection against N-bromoacetyl cellobiosylamine inactivation in the presence of GTBX ((Δ) 0 mM and (▲) 2 mM).*

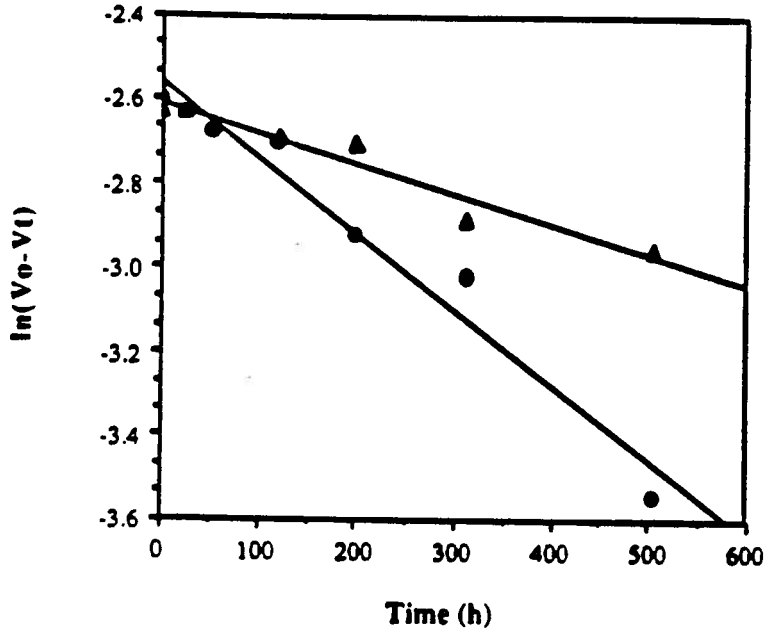


*Figure A-10-4 Reactivation of 2F-DNPX$_2$-inactivated C. fimi Exoglycanase. Plots of ln(full rate - observed rate) versus time. Buffer (▲) only and 50 mM cellobiose (●).*

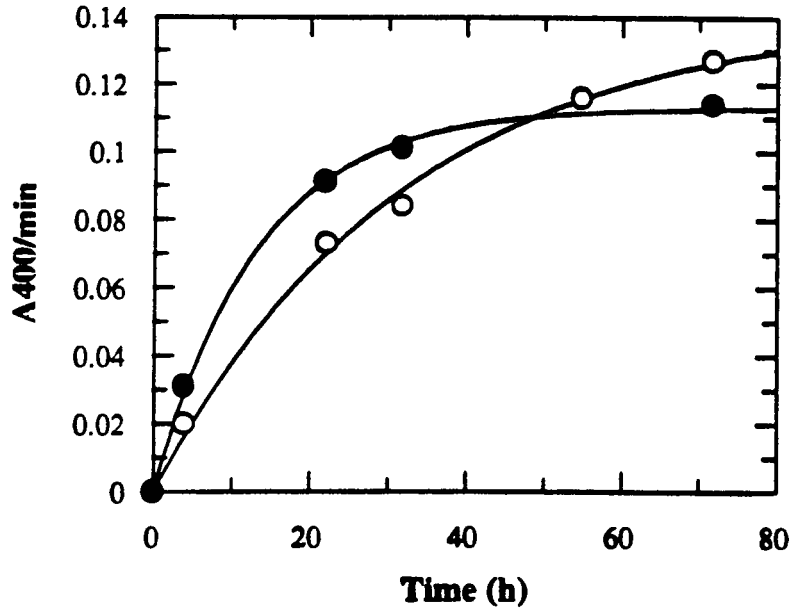


*Figure A-10-5 Reactivation of cellobial-inactivated C. fimi Exoglycanase. Plots of rate versus time. Buffer only (○) and 50 mM cellobiose (●).*

# APPENDIX B

# BASIC CONCEPTS OF ENZYME CATALYSIS

## B-1 Basic Enzyme Kinetics

The basic equation of enzyme kinetics is the Michaelis-Menten equation where v is the velocity of the reaction measured either as the initial rate of formation of the products or depletion of the substrates; [E] is the total concentration of the enzyme; [S] is the substrate concentration; $k_{cat}$ is the catalytic constant; and $K_m$ is the Michaelis constant.

$$v = \frac{[E_o]\,[S]\,k_{cat}}{K_m + [S]}$$

In the Michaelis-Menten equation two assumptions are made; the enzyme concentration is negligible compared to that of the substrate which is generally true since enzyme catalyse reactions with a high efficiency, and the velocity measured is the initial rate of product formation, thus there is no significant accumulation of product (or depletion of substrates) hence, the reverse reaction can be ignored. Therefore, the change in substrate concentration is generally linear with time.

The $K_m$ is the substrate concentration when $v = V_m/2$ ($V_m$ = maximum velocity). It may be treated as an apparent dissociation constant of all the bound enzyme species and as such is expressed as:

$$K_m = \frac{[E]\,[S]}{\Sigma\,[ES]}$$

The value of $K_m$ can be a measure of the enzyme affinity for the substrate, for example, a low $K_m$ means that the enzyme has a high affinity for the substrate.

At low substrate concentration ($[S] << K_m$) the Michaelis-Menten equation becomes

$$v = \frac{[E_o]\,[S]\,k_{cat}}{K_m}$$

whereas at saturating concentrations ([S] >> $K_m$) the equation becomes:

$$v = V_m = k_{cat}\,[E_o]$$

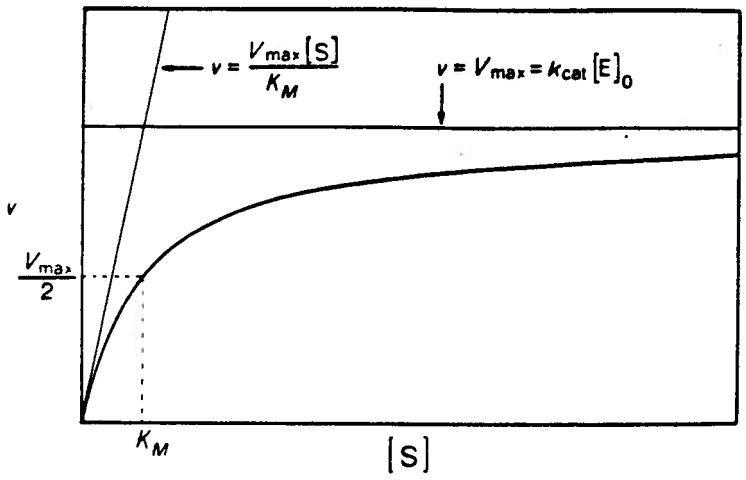


*Figure B-1-1 Plot of velocity versus substrate concentration for a typical enzymatic reaction (Fersht, 1985).*

At low [S] most of the enzyme is unbound such that the total enzyme concentration, which is a sum of the concentration of the free and bound enzyme, can be approximated to the concentration of the free enzyme, [E]. The Michaelis-Menten equation under these conditions is expressed as

$$v = \frac{[E]\,[S]\,k_{cat}}{K_m}$$

The $k_{cat}/K_m$ from the above equation is an apparent second-order rate constant which relates the reaction rate to the concentration of the free enzyme and free substrate. This kinetic parameter is also referred to as a specificity constant which is a measure of the catalytic efficiency for the substrate.

The Michaelis-Menten equation is often changed to a linear form which is useful for graphical analysis of the data and detection of deviations from the expected values. An example of the Michaelis-Menten equation transformed is where both sides of the Michaelis-Menten equation have been inverted.

$$\frac{1}{v} = \frac{1}{V_m} + \frac{K_m}{V_m [S]}$$

Plotting 1/v as a function of 1/[S] gives the Lineweaver-Burk plot (Figure B-1-2) where the y-intercept is $1/V_m$, the x-intercept is $-1/K_m$ and the slope is $K_m/V_m$.

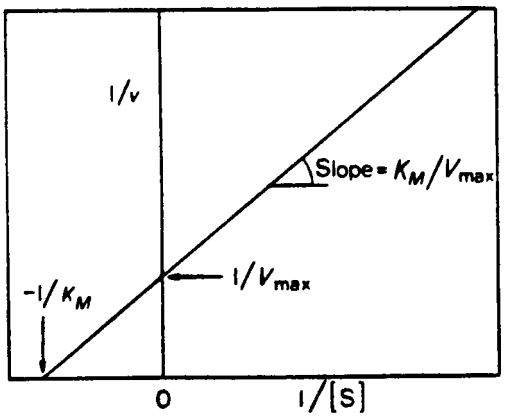


*Figure B-1-2 A typical Lineweaver-Burk plot for an enzymatic reaction (Fersht, 1985)*

## B-2 Interpretation Of $k_{cat}$ And $k_{cat}/K_m$

The rate constant $k_{cat}$ which equals $V_m/[E]_o$ is a reflection of the rate determining step and the rate constant, $k_{cat}/K_m$ reflects the rate of the first irreversible step in the reaction (Schowen, 1978). In order to show this, first consider the general mechanism shown below, where the formation of ES is referrred to as the association step, the interconversion of the ES and EP as the chemical step and the final step as product-release.

$$E + S \underset{k_{-1}}{\overset{k_1}{\rightleftharpoons}} ES \underset{k_{-2}}{\overset{k_2}{\rightleftharpoons}} EP \xrightarrow{k_3} E + P$$

The corresponding free energy diagram for this mechanism is shown in Figure B-2-1 where the energy levels are arbitrarily chosen. It can be shown that the kinetic parameters, $k_{cat}$, $K_m$ and $k_{cat}/K_m$, for the reaction are give by

$$k_{cat} = \frac{k_2 k_3}{k_{-2} + k_2 + k_3} \qquad (1)$$

$$K_m = \frac{k_3(k_{-1} + k_2) + k_{-1}k_{-2}}{k_1(k_{-2} + k_2 + k_3)} \qquad (2)$$

$$\frac{k_{cat}}{K_m} = \frac{k_1 k_2 k_3}{k_3(k_{-1} + k_2) + k_{-1}k_{-2}} \qquad (3)$$

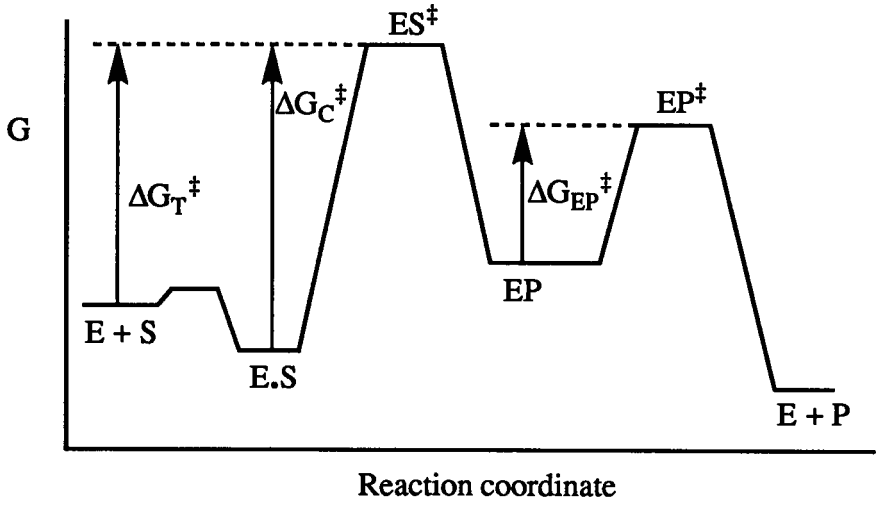


*Figure B-2-1 Reaction coordinate diagram for an enzymatic reaction involving the interconversion of intermediates.*

Now, consider the above reaction where there is a rapid, reversible association step followed by a rate determining chemical step. The kinetic relationships that describe this situation are $k_{-1} >> k_2$, $k_3 >> k_{-2}$ and $k_3 >> k_2$. When these conditions are applied to equations 1 and 3, the kinetic parameters are reduced to

$$k_{cat} = k_2$$

$$\frac{k_{cat}}{K_m} = \frac{k_1 k_2}{k_{-1}}$$

which expressed in Eyring form become:

$$k_{cat} = \frac{kT}{h} e^{[-(G_{ES}^{\ddagger} - G_{ES})]/RT}$$

$$= \frac{kT}{h} e^{-\Delta G_C^{\ddagger}/RT}$$

$$\frac{k_{cat}}{K_m} = \frac{\mathbf{k}T}{h} e^{[-(G_{ES}^{\ddagger} - G_{E+S})]/RT}$$

$$= \frac{\mathbf{k}T}{h} e^{-\Delta G_T^{\ddagger}/RT}$$

where **k** is the Boltzmann constant and h is Planck's constant. Thus, under these conditions, $k_{cat}$ and $k_{cat}/K_m$ both give information pertaining to the transition state of the chemical step. However, the initial reference point for $k_{cat}$ is the ES complex and for $k_{cat}/K_m$, it is free enzyme (E) and free substrate (S).

If however, the restrictions on the reaction were rapid, reversible association followed by an irreversible chemical step and then rate determining product release, the kinetic relationships would be $k_{-1} >> k_2$, $k_2 >> k_3$ and $k_3 >> k_{-2}$. The kinetic constants then can be reduced to

$$k_{cat} = k_3$$

$$\frac{k_{cat}}{K_m} = \frac{k_1 k_2}{k_{-1}}$$

and the Eyring equations are

$$k_{cat} = \frac{\mathbf{k}T}{h} e^{[-(G_{EP}^{\ddagger} - G_{EP})]/RT}$$

$$= \frac{\mathbf{k}T}{h} e^{-\Delta G_P^{\ddagger}/RT}$$

$$\frac{k_{cat}}{K_m} = \frac{\mathbf{k}T}{h} e^{-\Delta G_T^{\ddagger}/RT}$$

In this case, $k_{cat}$ refers to the transition state for release of the product, with the enzyme-product complex as the initial reference point, and $k_{cat}/K_m$ refers to the transition state of the chemical step with E and S as the initial reference points.

Thus, these examples, show that $k_{cat}$ refers to the rate determining step while $k_{cat}/K_m$ corresponds to the first irreversible step in the reaction with E and S as the reference states.

These general concepts can be extended to the hydrolysis of β-glycosides by *C. fimi* exoglycanase where the chemical step corresponds to glycosylation, and product release to deglycosylation. Thus, the first example of rapid, reversible association followed by a rate determining chemical step is equivalent to the situation when glycosylation is the rate determining step and the second example of rapid reversible association, an irreversible chemical step and then rate determining product release corresponds to the situation when deglycosylation is rate determining.

## B-3 Binding Energy And Enzyme Catalysis

The function of any catalyst, including enzymes, is to lower the activation energy of a reaction, thus leading to rate acceleration. Enzymes are known to bind specifically to their substrates and the binding energies involved may be quite large. However, since the structure of the substrate changes as it is converted to product via a transition state, the enzyme can only be fully complementary to one form of the substrate. It will be shown that it is catalytically advantageous for the enzyme to be complementary to the transition state structure rather than to the ground state of the substrate.

Consider a typical enzymatic reaction consisting of a binding step and a catalytic step such as that shown below.

$$E + S \overset{K_m}{\rightleftharpoons} E.S \xrightarrow{k_{cat}} E + P$$

The energy diagram for this reaction is illustrated in Figure B-3-1 where $k_{-1} >> k_2$, so that $K_m = K_d$ and the kinetic parameters may be expressed as the following.

$$K_m = e^{-\Delta G_{ES}/RT}$$

$$k_{cat} = \frac{kT}{h} e^{-\Delta G_C^{\ddagger}/RT}$$

$$\frac{k_{cat}}{K_m} = \frac{kT}{h} e^{-\Delta G_T^{\ddagger}/RT}$$

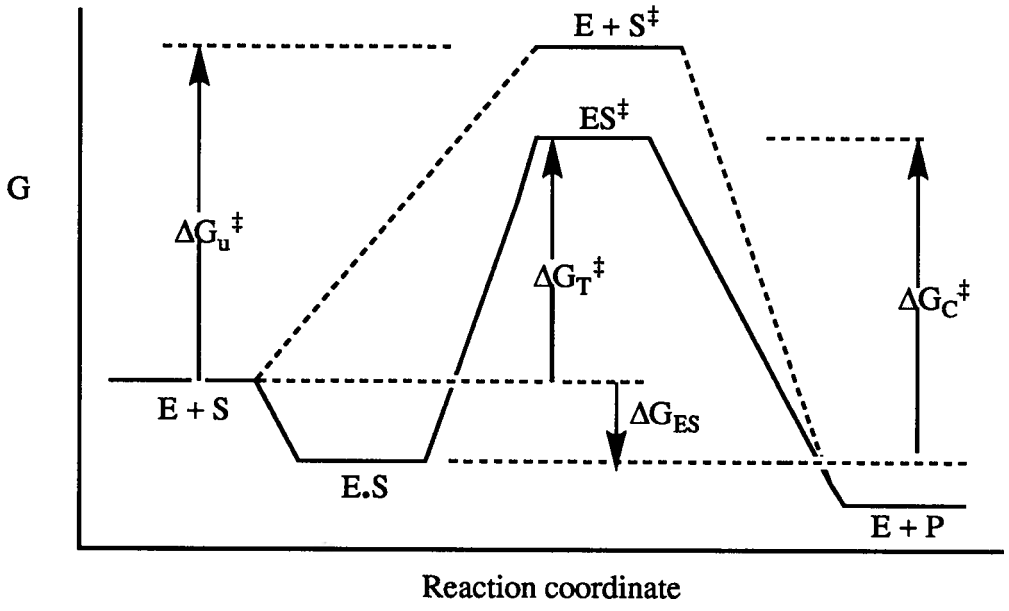


*Figure B-3-1 The reaction coordinate diagram for a typical reaction (solid line) and the corresponding uncatalysed reaction (dashed line).*

Now, consider the above situation when an extra amount of binding energy, $\Delta G_R$, has become available, for example a hydrogen bond between the enzyme and the substrate. If

that extra binding energy is realised at the ground state (Figure B-3-2 (left plot)) rather than the transition state, then the ground state is stabilised and $\Delta G_{ES}$ increases by $\Delta G_R$, thus $K_m$ is decreased. The value of $k_{cat}$ is also reduced since $\Delta G_C^{\ddagger}$ (Michaelis complex (ES) proceeding to the transition state ($ES^{\ddagger}$)) is increased by the ground state stabilisation, $\Delta G_R$. However, $k_{cat}/K_m$ is unaffected as this is the rate constant for free enzyme (E) and free substrate (S) proceeding to the transition state ($ES^{\ddagger}$). This shows that if the enzyme is complementary to the ground state, then there is tighter substrate binding but slower reaction rate, $k_{cat}$. Alternatively, if the extra binding energy, $\Delta G_R$, is realised at the transition state (Figure B-3-2 (right plot)), then the transition state is stabilised and $\Delta G_C^{\ddagger}$ and $\Delta G_T$ will be lowered by $\Delta G_R$, thus, $k_{cat}$ and $k_{cat}/K_m$ will be increased. The value of $\Delta G_{ES}$ is unchanged, and hence, $K_m$ remains the same. This shows that when the enzyme is complementary to the transition state rather than the ground state, then the rate of the reaction and the enzyme efficiency ($k_{cat}/K_m$) is increased.

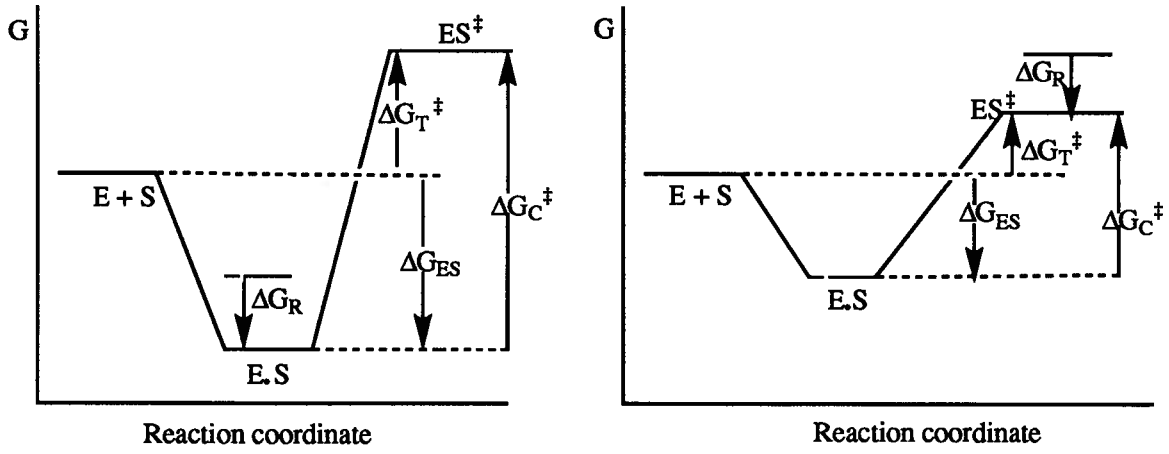


*Figure B-3-2 The reaction coordinate diagram illustrating complementarity of the enzyme to (left) the ground state, and (right) the transition state of the substrate.*

## B-4 Inactivation Kinetics of *C. fimi* Exoglycanase

A schematic representation of the mechanism of the exoglycanase-catalysed hydrolysis of substrates is the following where $k_2$ corresponds to glycosylation and $k_3$ to deglycosylation.

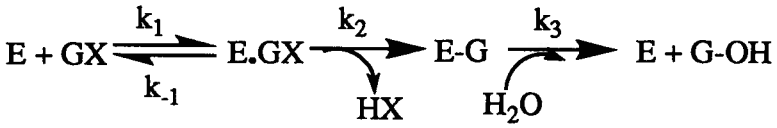


For the inactivators used, $k_3 << k_2$ and $k_1 >> k_2$, thus the covalent glycosyl-enzyme intermediate accumulates. The kinetic equation for this inactivation, is the following variation of the Michaelis-Menten equation,

$$v = \frac{k_i [E_o] [GX]}{K_i + [GX]}$$

where $k_i$ is the inactivation rate constant, and $K_i$ is the apparent dissociation constant for all bound enzyme species.

If $[GX] >> [E_o]$, then [GX] appears constant throughout the inactivation process and the kinetics are pseudo-first order with respect to the enzyme concentration. Thus, the Michaelis-Menten equation can be expressed as

$$v = k_{obs} [E_o]$$

$$k_{obs} = \frac{k_i [GX]}{K_i + [GX]}$$

The value of $k_{obs}$ can be calculated by directly fitting the data to a first-order function or from the slope of the natural logarithm of the residual enzymatic activity plotted as a

function of time. That is, since the rate of formation of HX is equal to the rate of inactivation of the enzyme then

$$v = \frac{d[HX]}{dt} = - \frac{d[E_o]}{dt}$$

The rate can then be expressed as

$$- \frac{d[E_o]}{dt} = k_{obs} [E_o]$$

$$- \frac{d[E_o]}{[E_o]} = k_{obs}\, dt$$

Therefore,

$$\ln [E_o] = -k_{obs}\, t$$

Values of $k_i$ and $K_i$ can then be calculated by direct fit of values of $k_{obs}$ to the equation

$$k_{obs} = \frac{k_i [GX]}{K_i + [GX]}$$